# MOLECULAR MECHANISMS OF CELLULAR IMMUNE RESPONSES IN MARINE INVERTEBRATES

**Dissertation**

zur Erlangung des Doktorgrades

der Mathematisch-Naturwissenschaftlichen Fakultät

der Christian-Albrechts-Universität zu Kiel

vorgelegt von

**Julia Saphörster**

Kiel, 2013

Erster Gutachter: Prof. Dr. Philip Rosenstiel

Zweiter Gutachter: Prof. Dr. Matthias Leippe

Tag der mündlichen Prüfung: 15.04.2013

Zum Druck genehmigt: 15.04.2013

*gez. Prof. Dr. Wolfgang J. Duschl, Dekan*

Meinen Eltern

TABLE OF CONTENTS

## ABBREVIATIONS

| | |
|---|---|
| # | Number |
| °C | Degree Celsius |
| µg | Microgram |
| µl | Microliter |
| *A. islandica* | *Arctica islandica* |
| aa | Amino acids |
| *ad.* | (lat.) *addere* (fill-up to) |
| AMP | Antimicrobial peptide |
| ATP | Adenosine triphosphate |
| BAPTA-AM | 1,2-bis(o-aminophenoxy)ethane-N,N,N',N'-tetraacetic-acid tetra(acetoxymethyl)este |
| BLAST | Basic Local Alignment Search Tool |
| bp | Base pairs |
| cDNA | Complementary DNA |
| CFU | Colony forming units |
| cm | Centimeter |
| Ct-value | Cycle threshold-value |
| ddNTP | Dideoxynucleoside triphosphate (Dideoxynucleotide) |
| DEPC | Diethylpyrocarbonate |
| DMF | Dimethylformamid |
| DMSO | Dimethylsulfoxid |
| DNA | Deoxyribonucleic acid |
| dNTP | Deoxyribonucleoside triphosphate (Deoxynucleotide) |
| DPBS | Dulbecco's phosphate-buffered saline |
| DPI | Diphenyleneiodonium |
| dsRNA | Double-stranded RNA |
| DUOX | Dual oxidase |
| E | Efficiency |
| E value | Expect value |
| *E. coli* | *Escherichia coli* |
| EDTA | Ethylenediaminetetraacetic acid |
| emPCR | emulsion PCR |
| FAD | Flavin adenine dinucleotide |
| g | Gram |

| | |
|---|---|
| *g* | *g-force* = Relative centrifugal force (RCF) |
| GAPDH | Glyceraldehyde 3-Phosphate dehydrogenase |
| GO | Gene Ontology |
| HEPES | 4-(2-hydroxyethyl)-1-piperazineethanesulfonic acid |
| ICMB | Institute for Clinical Molecular Biology |
| IL-17 | Interleukin-17 |
| IκB | Inhibitor of NF-κB |
| kg | Kilogram |
| l | Liter |
| *L. anguillarum* | *Listonella anguillarum* |
| *L. elliptica* | *Laternula elliptica* |
| LB | Luria-Bertani |
| LBP/BPI | Lipopolysaccharide-bining protein/bactericidal-permeability increasing protein |
| LITAF | Lipopolysaccharide-induced tumor necrosis factor-alpha factor |
| LPS | Lipopolysaccharide |
| m | Meter |
| *M. edulis* | *Mytilus edulis* |
| MAMP | Microbe associated molecular pattern |
| min | Minute |
| ml | Milliliter |
| mM | Millimolar |
| mOsm kg$^{-1}$ | Milliosmol per kilogram |
| mRNA | Messenger RNA |
| NADPH | Nicotinamide adenine dinucleotide phosphate |
| NCBI | National Center for Biotechnology Information |
| NF-κB | Nuclear factor kappa-light-chain-enhancer of activated B cells |
| ng | Nanogram |
| NLR | NOD-like receptor |
| nm | Nanometer |
| NOX | NADPH oxidase |
| OD$_{612}$ | Optical density at 612 nm |
| PCR | Polymerase chain reaction |
| PMA | Phorbol 12-myristate 13-acetate |
| PPi | Inorganic pyrophosphate |

| | |
|---|---|
| PRR | Pattern recognition receptor |
| p-Value | Probability value |
| qRT-PCR | Real-time quantitative RT-PCR |
| RAC | Ras-related C3 botulinum toxin substrate |
| RACE | Rapid amplification of cDNA ends |
| RFU | Relative fluorescence units |
| RISC | RNA-induced silencing complex |
| RLR | RIG-I-like receptor |
| RNA | Ribonucleic acid |
| RNAi | RNA interference |
| ROS | Reactive oxygen species |
| rpm | Rounds per minute |
| rRNA | Ribosomal RNA |
| RT | Room temperature |
| RT-PCR | Reverse transcription polymerase chain reaction |
| S | Svedberg |
| siRNA | Small interfering RNA |
| SMART | Simple modular architecture research tool |
| SMART™ | Switching mechanism at 5' end of RNA transcript |
| sstDNA | Single-stranded template DNA |
| T-ACE | Transcriptome analysis and comparison explorer |
| $T_{anneal}$ | Annealing temperature |
| $t_{elong}$ | Elongation time |
| TIMP | Tissue inhibitor of metalloproteinases |
| TLR | Toll-like receptor |
| TRIS | Tris(hydroxymethyl)-aminomethane |
| X-gal | 5-Brom-4-chlor-3-indolyl-β-D-galactopyranosid |

## 1. INTRODUCTION

### 1.1 The immune system

All living organism are constantly exposed to foreign bodies and substances. Even though most of these foreign objects do not pose a threat, a small subset of these can be harmful causing damage in the affected organism. Infectious agents including prions, viruses, bacteria, fungi and even eukaryotic parasites, which lead to disease in their host organisms, are commonly termed pathogens. As a consequence, organisms have developed a multitude of structures and processes to defend themselves against infections and disease; the entity of these protective mechanisms is known as the immune system. In vertebrates the immune system can be divided into two different but interwoven systems, referred to as the innate and the adaptive or acquired immune system.

#### 1.1.1 Innate versus adaptive immunity

In 1908 the Nobel Prize was awarded to Elie Metchnikoff (1845–1916) und Paul Ehrlich (1854–1915) for their fundamental scientific contributions enhancing the understanding of the immune system itself, which is regarded as the birth of the field of immunology (Kaufmann 2008). Both researchers had a very different view on immune system processes, which was seen as a huge controversy and contradiction at the beginning. Today we know that they were just looking from different angles at the immune system. While Ehrlich's research by describing the side-chain theory of antibody formation dealt with the adaptive arm of the immune system, Metchnikoff's work depicting phagocytosis as a defense mechanism centered mainly on the innate immune system. Nowadays it is widely accepted that innate and adaptive immunity go hand in hand, since various innate immune system processes are able to 'shape' further adaptive immune responses (Hoebe *et al.* 2004).

The adaptive immune system in jawed vertebrates relies mainly on cells of lymphatic origin, the lymphocytes. Major types of these cells are either T cells or B cells. Their primary function lies in the detection of foreign structures (=antigens), which can, for example, be invading pathogens or even abnormal, endogenous cells. Antigens can be internalized by antigen-presenting cells (APC), which will in turn expose a part of the antigen on their cell surface with aid of the major histocompatibility complex (MHC). Intracellular antigens, such as peptides from viruses or abnormal, endogenous proteins, can be presented by every nucleated cell of the human body using MHC class I. The displayed peptide/MHC class I complex can then be recognized by a cytotoxic T cell (CTL; CD8$^+$ cell) via its specific T cell receptor (TCR) leading to killing of the presenting cell by the activated CTL. APCs, such as dendritic cells, monocytes and macrophages, are called professional APCs, because they are able to present

extracellular antigens via MHC class II. As a consequence, the recognition of exposed antigen/MHC class II complexes by specific TCRs results in the activation of T helper cells (CD4$^+$ T cells). Antigens can also be bound by antibodies present on a specific B cell leading to its activation and antigen presentation, which are therefore also referred to as B cell receptors (BCRs). The recognition of a wide variety of antigens is based on several complex genetic mechanisms, as for example the rearrangement of genetic elements, producing numerous types of receptors with each lymphocyte possessing its own specific receptor (Alberts *et al.* 2007). If the antigen/MHC class II complex on an activated B cell is further recognized by a T helper cell, the B cell is stimulated to proliferate and mature to plasma cells producing and secreting a huge amount of antibodies against the particular antigen. As a consequence, the secreted antibodies lead to specific immune responses against the antigen, such as e.g. direct inactivation by binding, labeling the antigen for phagocytes (=opsonization), activation of the complement system and agglutination. Therefore, one advantage of the adaptive immune system is the highly specific detection and elimination of foreign structures mostly without damaging the body's own healthy cells. Furthermore, the adaptive immune system can develop a post-infectious immunological memory leading to an efficient and rapid clearance of the target upon repeated encounter with the antigen and, therefore, inhibiting repeated infection. Despite these great attainments, the adaptive immune system is yet not able to function on its own, relying strongly on the innate immune system as a first line of defense and to mediate further adaptive immune responses (Medzhitov & Janeway Jr 1998).

The innate immune system consists of physiological barriers as well as cell-mediated immune-responses, such as phagocytosis by macrophages or reactive oxygen species (ROS) production by granulocytes. Even though, the innate immune response is not exclusively specific for a particular pathogen, it is directed against a broad spectrum of invaders and occurs much faster than the adaptive immune response. One of the major obstacles of the immune system, which also resembles one of the greatest differences between adaptive and innate immunity, is how the organism can distinguish normal healthy cells from foreign or abnormal, endogenous cells. To separate 'self' from 'non-self' the adaptive immune system uses the antigen-antibody reaction, while the innate immune system mainly relies on germ-line encoded pattern recognition receptors (PRRs).

### 1.1.2 Innate pattern recognition receptors

Pattern recognition receptors (PRRs) recognize specific structures on pathogens. Therefore, these structures were initially named pathogen-associated molecular patterns or PAMPs. Since the innate immune system is not able to differentiate between pathogenic, neutral or beneficial microbes (Casadevall & Pirofski 2002), nowadays the term microbe-associated molecular pattern (MAMP) is

increasingly used. Structures characterized as MAMPs, which can be found on microbes in the broader sense such as bacteria, viruses, protozoa and fungi, are for instance flagellin, zymosan A, LPS, dsRNA, peptidoglycan, unmethylated CpG islands and many more. In addition to MAMPs, PRRs can also recognize endogenous molecules from damaged cells, consequently referred to as damage-associated molecular patterns or DAMPs, such as heat shock proteins or DNA. Mammalian PRRs are mainly divided into four different classes (Figure 1-1) consisting of cytoplasmic receptors such as NOD-like receptors (NLRs, see 1.1.2.1) and the RIG-I-like receptors (RLRs, see 1.1.2.2), as well as membrane-bound receptors such as Toll-like receptors (TLRs, see 1.1.2.3) and C-type lectin receptors (CLRs, see 1.1.2.4) (Takeuchi & Akira 2010).
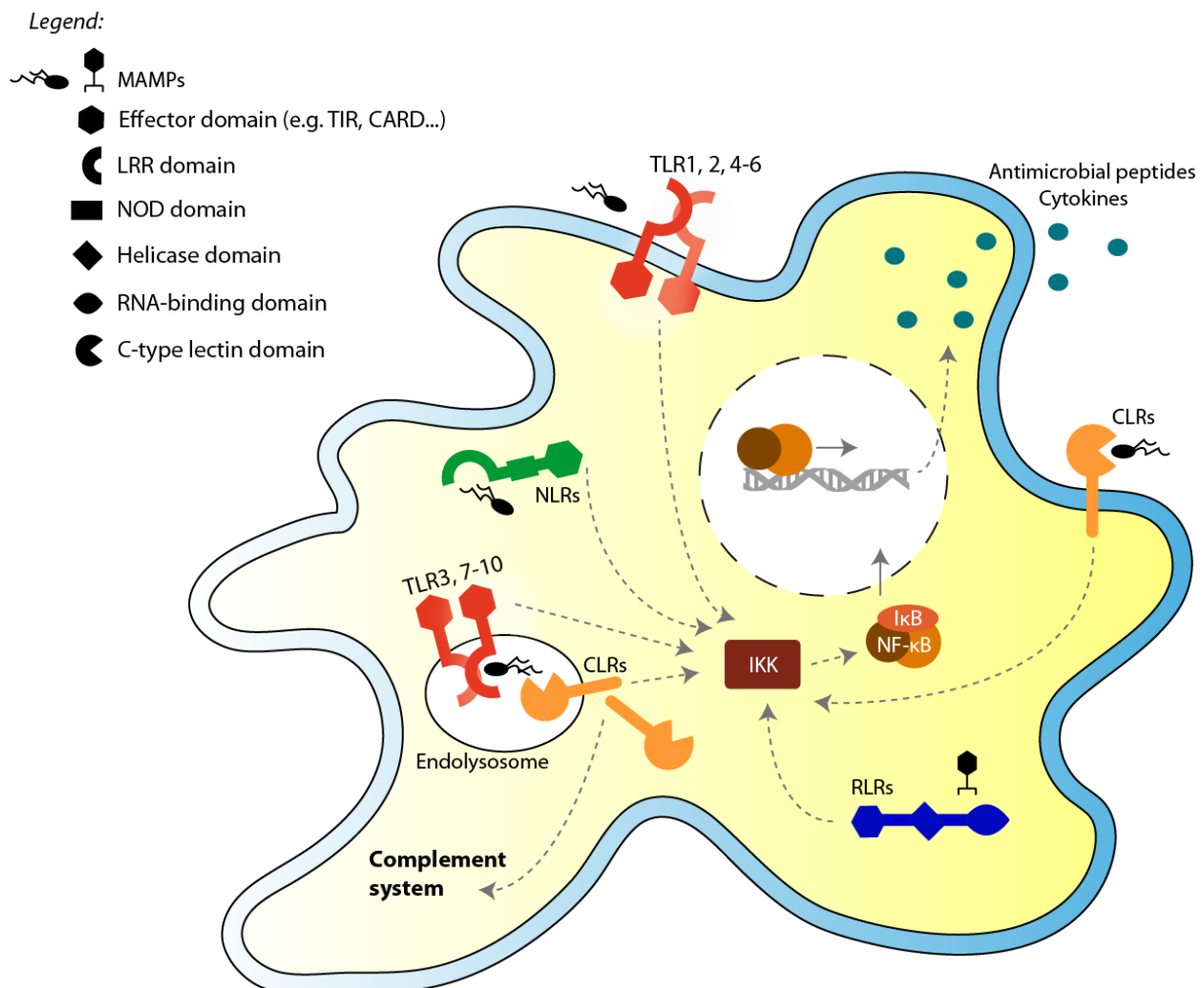


**Figure 1-1: Overview of important innate immune receptors and processes in an eukaryotic cell.** Recognition of MAMPs by NLRs, RLRs, TLRs and CLRs leading to the activation of the complement system or induction of antimicrobial peptide and cytokine gene expression via the NF-κB signaling pathway is depicted in a roughly schematic manner. See text for details.

### 1.1.2.1   NOD-like receptors

The family of intracellular NOD-like receptors (NLRs) was named according to their common central nucleotide-binding and oligomerization domain, short NOD. The NOD domain can be further differentiated into the N-terminal NACHT (named after the proteins it was first found in, namely NAIP, CIITA, HET-E und TP1) and the C-terminal NACHT-associated domain (NAD). On their C-terminal end all NLR proteins possess a domain of several leucin-rich repeats (LRR domain). According to their N-terminal effector domain determining the specialized function of each NLR, the NLR family can be divided into five classes of proteins so far: 1) NLRC proteins containing the caspase activation and recruitment domain (CARD) (e.g. NLRC2 also known as NOD2); 2) NLRP proteins containing a pyrin domain (PYD) (e.g. NLRP1 also known as NALP1); 3) NLRB proteins containing the baculoviral inhibitor of apoptosis repeat (BIR) domain (e.g. NLRB1 also known as BIRC1); 4) NLRA proteins containing an additional activation domain (AD) between their CARD and their NACHT domain (e.g. CIITA); and 5) NLRX proteins, which exhibit no strong homology to the N-terminal domain of any other NLR (e.g. NOD9) (Ting *et al.* 2008).

Despite their differing effector domain, all NLR proteins belong to the signal transduction ATPases with numerous domains (STAND) supposedly acting as molecular switches upon nucleotide binding (Leipe *et al.* 2004). In the conventional activation pathway in plants this means that upon MAMP recognition by the LRR domain a conformational change is thought to occur abolishing the negative regulation on the NACHT domain, which enables the nucleotide ADP to be exchanged for the nucleotide ATP. This 'active state' of the protein leads to the activation of downstream signaling pathways and also ATP-hydrolysis, which subsequently inactivates the protein again. The same mechanism is hypothesized to be conserved in mammals. Furthermore, active proteins can also undergo homo- or heterodimerization with accessory proteins or other NLRs, which is supposed to attract additional components necessary for further signaling cascades (Bonardi *et al.* 2012).

Activation of NLRs by MAMPs, such as flagellin (NLRB and NLRC4) and peptidoglycan (NLRC1 and NLRC2) as well as DAMPs (NLRP1 and NLRP3) is thought to result mainly in inflammatory immune responses via the activation of several signaling pathways. These can be the activation of the nuclear factor kappa-light-chain-enhancer of activated B cells (NF-κB) and the mitogen-activated protein kinase (MAPK) pathways via the receptor-interacting protein kinase 2 (RIPK2) CARD-containing adaptor protein (by NLRC1 and NLRC2), inflammasome formation (by NLRC4, NLRP1 and NLRP3) or c-Jun N-terminal kinase (JNK) activation (by NLRB). But recently functions other than immune-related responses are also increasingly recognized. It is reported that NLRs seem to play an important role in apoptosis, tissue homeostasis and early developmental processes as well (Kufer & Sansonetti 2011). But studies on NLRs are limited and the exact functioning of many NLR proteins is still subject of on-going research.

### 1.1.2.2 RIG-I-like receptors

The second group of cytosolic innate PRRs is the family of virus sensing RIG-I-like receptors (RLRs). Members of the RLR family are RNA helicases comprised of the retinoic-acid-inducible gene I (RIG-I) protein, the melanoma differentiation-associated protein 5 (MDA5) and the Laboratory of Genetics and Physiology 2 (LGP2) protein. The common feature of all RLRs is their central helicase domain and their C-terminal RNA-binding domain. But in contrast to LGP2, RIG-I and MDA5 possess tandem repeats of a CARD-like effector domain at their N-terminal end. At their C-terminal end RIG-I and LGP2 also contain an additional repression domain (Yoneyama & Fujita 2012).

The repression domain seems to directly interact with the functional tandem CARD domain inhibiting further CARD-mediated signaling. Even though LGP2 lacks the CARD effector domain, overexpression of LGP2 can result in the repression of other RLRs. Although the exact mechanisms upon double-stranded RNA (dsRNA) binding to RLRs are still unclear, it has been suggested for RIG-I that the helicase domain can unwind dsRNA using ATP-hydrolysis, which initiates further downstream signaling via its tandem CARD domain. Since dsRNA binding seems to be weak for MDA5, LGP2 has been suggested to act as a positive regulator upon dsRNA binding especially for MDA5 (Satoh *et al.* 2010).

A diverse class of viruses uses dsRNA for replication. dsRNA with a length of up to 1,000 nucleotides can be recognized by RIG-I, while longer dsRNA with over 2,000 nucleotides can be bound by MDA5. Furthermore, it has been proposed that RIG-I is also able to sense RNA/DNA duplexes. Upon binding, the CARD domains of both, RIG-I and MDA5, interact with a CARD-containing adaptor protein, the IFN-β-promoter stimulator 1 (IPS-1) located at the mitochondrial membrane. This leads to the induction of type I interferon (IFN) expression and NF-κB-mediated expression of further cytokines (Takeuchi & Akira 2010). Cytokines such as interferons (IFNs) are highly important for the communication between cells to trigger synergistic defense mechanisms (see also 1.5). Interferons, named after their ability to interfere with viral replication in the host, particularly activate immune cells to elicit anti-viral responses.

### 1.1.2.3 Toll-like receptors

Toll-like receptors (TLRs) are membrane-bound receptors, which occur at the cell membrane (TLR1, 2, 4, 5 and 6) and also intracellular in the membrane of endosomes, lysosomes and endolysosome (TLR3, 7/8, 9, 10). They are characterized by an N-terminal, semicircular-formed stretch of leucin-rich repeats (LRRs) facing outward, a central transmembrane domain and a C-terminal toll/interleukin-1 receptor homology (TIR) domain facing inward into the cell.

The receptors form homodimers (e.g. TLR5) or heterodimers (e.g. TLR2 with TLR1 or TLR6) with each other. Upon ligand binding to the LRR domain, they undergo a conformational change, which brings the TIR domains in close spatial proximity and results in the recruitment of TIR-domain containing adaptor molecules for further downstream signaling. Binding to the LRR domain by the ligand can occur directly or with aid of further accessory components. In the case of TLR4, for instance, binding to lipopolysaccharides (LPS) depends on the receptor forming a complex with the myeloid differentiation factor 2 (MD2) prior to receptor dimerization (Monie *et al.* 2009). Furthermore, LPS can also be bound and delivered to TLR4 by the lipopolysaccharide-binding protein (LBP).

In humans, TLRs can recognize a wide variety of MAMPs and DAMPs including triacyl lipoproteins (by TLR1 with TLR2), dsRNA (by TLR3), LPS (by TLR4), flagellin (by TLR5), diacyl lipoproteins (by TLR6 with TLR2), ssRNA (by TLR 7/8) and CpG DNA (by TLR9). TLRs can activate different signaling pathways according to their TIR domain-containing adaptor molecule. There are four known adaptor proteins: 1) the Myeloid differentiation primary response gene 88 (MyD88), 2) the TIR-domain-containing adaptor-inducing interferon-β (TRIF), 3) the TIR domain containing adaptor protein (TIRAP) and 4) the TRIF-related adaptor molecule (TRAM). MYD88 is used by all TLRs except TLR3, whereas TRIF is used by TLR3 and also TLR4. Since TIRAP is used to attract either MyD88 to TLR2 or TLR4 and TRAM leads TRIF to TLR4, the TLR signaling pathways are mainly divided into MyD88-dependent pathways, which induces the production of inflammatory cytokines, and TRIF-dependent pathways, which also induces the production of inflammatory cytokines as well as type I interferons (Monie *et al.* 2009; Kawai & Akira 2010; Takeuchi & Akira 2010). A major role in this process is attributed to the activation of the transcription factor NF-κB.

### 1.1.2.4  *C-type lectins*

C-type lectins belong to the lectin domain-containing family of carbohydrate-binding transmembrane and soluble proteins, which were initially characterized due to the dependency on calcium by some family members. In addition to their homologous C-type lectin-like domain, they possess various other protein domains and a diverse overall protein structure (Drickamer 1999). In line with this, they possess a wide variety of functions in innate as well as in adaptive immunity including cell-cell adhesion, cell migration, antigen uptake, apoptosis and immune responses to pathogens (Cambi *et al.* 2005).

C-type lectin receptors (CLRs) involved in pathogen sensing are also able to detect MAMPs, which in this case are mostly specific carbohydrate patterns on the surface of bacteria (Weis *et al.* 1998; Zelensky & Gready 2005). Recognition of microbes by CLRs can lead to a wide variety of immune responses (Geijtenbeek & Gringhuis 2009), such as modulating TLR signaling or the direct induction of gene expression by NF-κB activation.

In this manner, mannose-binding lectins (MBL) belonging to the collectin subfamily of soluble C-type lectins can lead to the activation of the complement system upon binding of carbohydrates with 3- and 4-hydroxyl groups in the pyranose ring, such as mannose or N-acetyl-glucosamine. The subsequent activation of MBL-associated serine proteases (MASPs) leads to a proteolytic cascade resulting in the accumulation of the C3 molecule, the central molecule of the complement system. This activation pathway is referred to as the lectin pathway of complement system activation (Figure 1-1). In vertebrates, the induction of the complement system results mainly in three major immune responses: opsonization of pathogens; chemotaxis and activation of leukocytes; as well as direct killing of pathogens (Fujita 2002).

### 1.1.3  The complement system

The complement system in mammals comprises three distinct activation pathways: the classical, the lectin and the alternative pathway. Whereas the classical pathway is induced by binding of the complement C1-complex to antigen-antibody complexes, the alternative and lectin pathway are involved in innate immunity.

In the classical pathway, binding of the C1q protein to antibodies complexed with their target leads to a conformational change in the protein inducing two serine proteases to cleave the C4 and C2 molecules. The C4b and C2a cleavage products then form the C3 convertase (C4b2a) resulting in the cleavage of C3 to C3a and C3b, which later on joins the C4b2a complex, thereby creating the C5 convertase (C4b2a3b) that cleaves C5 to C5a and C5b (Fujita 2002; Sarma & Ward 2011).

The lectin pathway can be activated by binding of carbohydrate patterns on the surface of bacteria to ficolins, which possess a fibrogen-like domain instead of the C-type-lectin-like domain, and MBLs, as described in the section before (1.1.2.4). The induction of MASPs then leads to cleavage of C4 and C2 resulting in the formation of the C3 convertase as described for the classical activation pathway.

In case of the alternative pathway, C3b is continuously formed by hydrolyzation of C3 at a low level. Upon binding of C3b to its target, such as carbohydrates, lipids and proteins found on foreign surfaces, Factor B is attracted to the complex. As a result, Factor D cleaves Factor B leading to the formation of the alternative C3 convertase (C3bBb), which is stabilized by properdin. Properdin is a plasma protein secreted by activated immune cells, such as neutrophils and macrophages, which prevents the cleavage and inactivation of C3b by complement factors H and I (Fujita 2002; Sarma & Ward 2011).

All activating pathways involve the sequential cleavage of zymogens and their subsequent activation resulting in the accumulation of the C3 molecule, the central molecule of the complement system and the, subsequent, formation of the activation products: C3a, C3b, C5a and the membrane

attack complex (C5b-9). Despite its function in the C5 convertases (C4b2a3b and C3bBbC3b), C3b can also act as an opsonin, facilitating the phagocytosis of foreign particles and supporting further amplification of the complement activation. The membrane attack complex (MAC), formed by binding of C6, C7 to C5b followed by C8 and C9, inserts itself into membranes of pathogens resulting in pore formation and cell lysis. The activation products C3a and C5a are known as anaphylatoxins and exhibit a wide variety of inflammatory responses, e.g. they can attract phagocytes to the site of inflammation or injury, activate the oxidative burst in neutrophils and are involved in TNF-α production (Sarma & Ward 2011).

### 1.1.4 The NF-κB signaling pathway

The nuclear factor kappa-light-chain-enhancer of activated B cells (NF-κB) is a transcription factor and the central member of the NF-κB signaling pathway, which plays a crucial part in innate and adaptive immune responses (Hayden *et al.* 2006). The NF-κB protein family is divided into the NF-κB (also known as Class I) and the Rel (Class II) subfamily. These proteins are characterized by a common DNA-binding and dimerization domain, the Rel homology domain. But whereas Rel proteins, such as RelA (also known as p65), RelB and c-Rel, possess C-terminal transactivation domains, NF-κB proteins, such as p100 and p105, contain long C-terminal stretches of ankyrin repeats. For activation, p100 is transformed into the shorter and active p52 molecule, similarly as p105 is transformed into p50. Mostly all NF-κB proteins are able to form either homo- or heterodimers, but can only activate transcription when dimerized with Rel proteins (Gilmore 2006). In unstimulated cells NF-κB complexes are generally kept in an inactive state by bound inhibitor of κB (IκB) proteins.

As discussed in the sections before, most PRRs seem to be able to induce the expression of major immune genes by activation of the canonical NF-κB signaling pathway (Figure 1-1). In vertebrate cells it was shown that for instance TLRs (Hayden & Ghosh 2004) and C-type lectins (Kingeter & Lin 2012) are able to induce the IκB kinase complex (IKK), which then phosphorylates IκB proteins leading to their degradation as well as the release and activation of the transcription factor NF-κB (Scheidereit 2006). In turn, NF-κB induces the transcription of IκB, amongst many other important immune genes (Hoffmann *et al.* 2002; Hoffmann & Baltimore 2006). Therefore, prolonged exposure to the stimulus can lead to repeated degradation and expression of IκB, corresponding to cycles of activation and inactivation of NF-κB. As a consequence, the expression of some genes is dependent on this oscillatory behavior (Nelson *et al.* 2004).

Since NF-κB is constitutively present in most unstimulated cells in an inactive state, it allows the NF-κB pathway to be among the first to respond to a harmful stimuli. Thus, binding of NF-κB to its target DNA sequences induces the transcription of many important immune genes, such as genes encoding

cytokines and antimicrobial peptides (Figure 1-1). Therefore, the NF-κB pathway is one of the most important signaling pathways in immunity, playing not only a role in the direct innate defense response against pathogens but also in the development of immune cells, lymphoid organs, inflammation and also adaptive immune responses (Hayden *et al.* 2006).

### 1.1.5 Antimicrobial peptides

Antimicrobial peptides are effector molecules, used to defend the organism against a wide variety of different microbes, such as viruses, bacteria, fungi and protozoa. Furthermore, also cytotoxic activity against cancer cells has been reported (Hoskin & Ramamoorthy 2008). Due to the huge diversity of antimicrobial peptides (>500 identified sequences in the year 2002), they can only be broadly categorized into different groups depending on their secondary structure. But the underlying mechanism common to all antimicrobial peptides is the formation of an amphipathic conformation, in which hydrophobic and cationic amino acids of the protein cluster spatially separated from each other (Zasloff 2002).

Most antimicrobial peptides are present as inactive prepropeptides. After cleavage of the signal peptide, the still inactive propeptide can be further cleaved into the active peptide upon stimulation. Most antimicrobial peptides possess a similar mode of action, which is based on the negatively charged outer surface of bacteria. Since bacteria possess various outward-facing, anionic polymers on their exterior, such as lipopolysaccharides and lipoteichoic acids, the cationic part of the antimicrobial peptide can bind, leading to the destabilization of lipids and intrusion of the peptide. Upon interaction with the negatively charged head group of some phospholipids, the peptide can further enter the plasma membrane and alter the membrane structure due to its amphipathic design (Zasloff 2002).

The exact mechanisms underlying the killing of microbes by antimicrobial peptides are still unclear, but various processes are implied including the depolarization of the bacterial membrane; the formation of lytic pores and, subsequent, leakage of intracellular contents; induction of harmful processes, such as the degradation of the cell wall by hydrolases; disturbance of membrane functions; and in some cases even the internalization of the peptide causing intracellular damage (Zasloff 2002).

### 1.2 Invertebrates as model organisms

Even simple unicellular organisms such as bacteria exhibit rudimentary innate immune mechanisms to defend themselves, as for instance against bacteriophages (Garneau *et al.* 2010). But whereas the innate immune system seems to be a part of all living organisms, the adaptive immune system, as

known in mammals, is thought to exist solely since the evolution of jawed vertebrates (Flajnik & Kasahara 2001) (Figure 1-2). But the boundaries between adaptive and innate immunity are, however, blurred (Boehm 2012). Hence, it has been shown that agnathans (jawless fish) are also able to produce a wide variety of lymphocytes each possessing its unique antigen receptor, quite similar to the lymphocytes in gnathostomes (jawed vertebrates). But in contrast to the immunoglobulin domain-containing T and B cell receptors in gnathostomes, these variable lymphocyte receptors (VLRs) contain various LRR domains instead (Pancer *et al.* 2004).
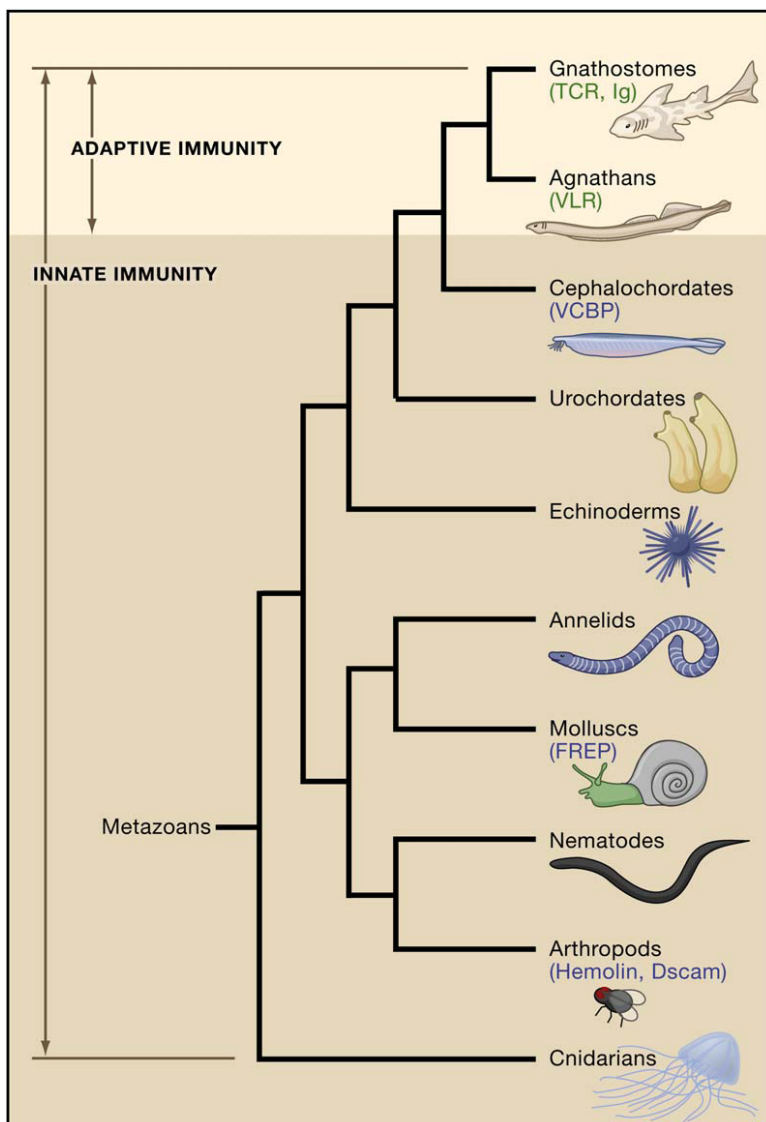


**Figure 1-2: Phylogenetic tree depicting the emergence of adaptive immunity and putative evolutionary relationships of metazoans.** Invertebrate immune molecules belonging to the immunoglobin superfamily are indicated in blue: V type Ig domains and chitin binding domain containing proteins (VCBP), fibrinogen-related proteins (FREPs), hemolin, and Down's syndrome cell adhesion molecule (Dscam). The recombinatorial-based immune receptors are indicated in green: T cell receptors (TCR), immunoglobulins (Ig), and variable lymphocyte receptors (VLR). Graphic taken from Cooper & Alder (2006).

Even though in invertebrates long-lived lymphocyte-like cells, including their clonally diverse anticipatory receptors, have not been found, some striking members of the immunoglobin superfamily, the key element in the adaptive immune response of Gnathomstomata, have already been identified (Cooper & Alder 2006). These include variable region-containing chitin binding proteins (VCBPs) in lancelets;

Down's syndrome cell adhesion molecules (Dscams) and hemolins in insects; and the fibrinogen-related proteins (FREPs) in molluscs (Figure 1-2). All of these proteins are involved in immune responses and are characterized by hypervariable sequences (Flajnik & Du Pasquier 2004; Cooper & Alder 2006).

Many molecules and principles of the innate immune system, however, seem to be highly conserved throughout the eukaryotes. In this context, various major proteins and pathways involved in innate immunity, as outlined before (section 1.1), exist not only in vertebrates but also in various invertebrates, ranging from phylogenetic ancient organisms, such as sponges, to early deuterostomes, including sea urchins and lancelets. Evolutionary conserved components of the innate immune system are, for instance pattern recognition receptors, such as TLRs and NLRs, as well as NF-κB pathway members (Rosenstiel *et al.* 2008; Rosenstiel *et al.* 2009), complement system components (Dodds & Matsushita 2007; Dodds 2008) and a multitude of antimicrobial peptides (Sperstad *et al.* 2011). Since invertebrates do not possess an adaptive immune system in the 'classical' sense and rely solely on their innate immune responses, they are often regarded as a simplified model of the vertebrate innate immune system.

Investigations of the immune system in invertebrates may also give insights into innate immune mechanisms from an evolutionary perspective, which might provide valuable information for disease-relevant immune processes in humans. During the last decade the occurrence of most inflammatory diseases drastically increased (Bach 2002), especially those connected with dysfunctions of TLR and NLR signaling in barrier organs, such as inflammatory bowel disease (Baumgart & Carding 2007). Interestingly, these diseases are thought to have arisen mainly under today's living conditions due to increased hygiene or altered nutrition (Schreiber *et al.* 2005). Therefore, insights obtained from phylogenetic older animals might help to elucidate the original purpose of conserved immune genes in more basal animals. This might lead to a better understanding of the molecular function of the respective genes in humans and may even contribute to a more efficient treatment of diseases in the future.

Marine organisms are especially suited to study the innate immune system from an evolutionary perspective, because they are constantly exposed to the various biotic (e.g. dense microbial communities and trophic conditions) and abiotic (e.g. light and salinity) stresses of the aquatic habitat exerting selective pressures (Rosenstiel *et al.* 2009). Particularly the investigation of sessile, filter-feeding marine invertebrates seems to be an interesting topic, since they have no means to escape adverse conditions. In this context, it is especially surprising that the longest-lived, non-colonial animal is a sessile, filter-feeding bivalve of the species *Arctica islandica* (>400 years) (Wanamaker Jr *et al.* 2008). Therefore, it is of great interest to understand how these animals so successfully cope with harmful conditions by relying solely on their innate immune system.

Invertebrate animals comprise 95 % of all animal species and are characterized by the absence of a vertebral column. Most invertebrates belong to the group of Bilateria, which can be subdivided into three major clades: basal Deuterostomia (e.g. lancelets, tunicates, sea urchins), Ecdysozoa (nematodes, arthropods) and Lophotrochozoa (annelids, molluscs). The use of Ecdysozoa as model organisms for the evolution of the innate immune system may not be useful for many genes, since extensive genome analyses has revealed a major loss of genes, which were otherwise conserved from Deuterostomia to Cnidaria (Kortschak *et al.* 2003). Lophotrochozoa, on the other hand, seem to be more suitable as model organisms, because their immune system depicts a higher degree of conservation and is more closely related to that of deuterostomes (Altincicek & Vilcinskas 2007; Philipp *et al.* 2012a). Furthermore, gene loss occurred probably at a much lower rate than in the Ecdysozoa (Kortschak *et al.* 2003). But, as also noted by other authors (Altincicek & Vilcinskas 2007; Takahashi *et al.* 2009), research on the innate immune system at molecular level is still under-represented in the Lophotrochozoa in contrast to the other clades. This is probably partly due to the fact that Ecdysozoa are hitherto more accessible for research by a large variety of already established molecular methods than Lophotrochozoa. Therefore, "this imbalance needs to be redressed in order to obtain a more balanced understanding of animal genome evolution and comparative biology" (Takahashi *et al.* 2009).

### 1.2.1   Short introduction into the taxonomy of Lophotrochozoa

The superphylum Lophotrochozoa was determined based on DNA sequence data obtained from 18S rRNA (Halanych *et al.* 1995). It comprises the former groups of the Lophophorata, such as Bryozoa and Brachiopoda, and the Trochozoa, such as molluscs and annelids. The Lophotrochozoa are regarded as a sister taxon to the Ecdysozoa within the clade of Protostomia, which stands in contrast to the superphylum Deuterstomia. Even though most studies recognize the Lophotrochozoa as a monophyletic superphylum within the protostomes (Philippe *et al.* 2005; Brinkmann & Philippe 2008; Dunn *et al.* 2008; Helmkampf *et al.* 2008), some studies are still controversial (Mallatt *et al.* 2012) and its internal relationships are yet not fully resolved. Therefore, this section will focus mainly on the largest group of Lophotrochozoa, the molluscs, whose species number with 100,000 extant species is only exceeded by the diversity of arthropods (Ponder & Lindberg 2008; Kocot *et al.* 2011).

The Mollusca are thought to be a sister taxon to the Annelida (Figure 1-3), which consists of segmented worms, such as polychaetes or leeches. Recent evidence strongly supports the 'Aculifera hypothesis', which suggests the Aculifera as a sister taxon to the Conchifera (Kocot *et al.* 2011; Smith *et al.* 2011). The Conchifera are conch- or shell-bearing molluscs, whereas the Aculifera comprise the Polyplacophora (=molluscs bearing shell plates) and the Aplacophora (=worm-like molluscs without a

shell). In addition to the taxon Scaphopoda, many economically important taxa used as food source or pearl producers belong to the Conchifera, such as Cephalopoda (octopuses, squid and cuttlefish), Gastropoda (snails) and Bivalvia (clams, oysters, mussels, scallops). The latter two classes can be further merged into the clade of Pleistomollusca (Kocot *et al.* 2011). Since bivalves are mostly sessile, filter-feeding aquatic invertebrates belonging to the Lophotrochozoa, they seem to possess all the desired features, discussed in the last sections, to be a suitable model to gain deeper insights into evolution of the innate immune system.
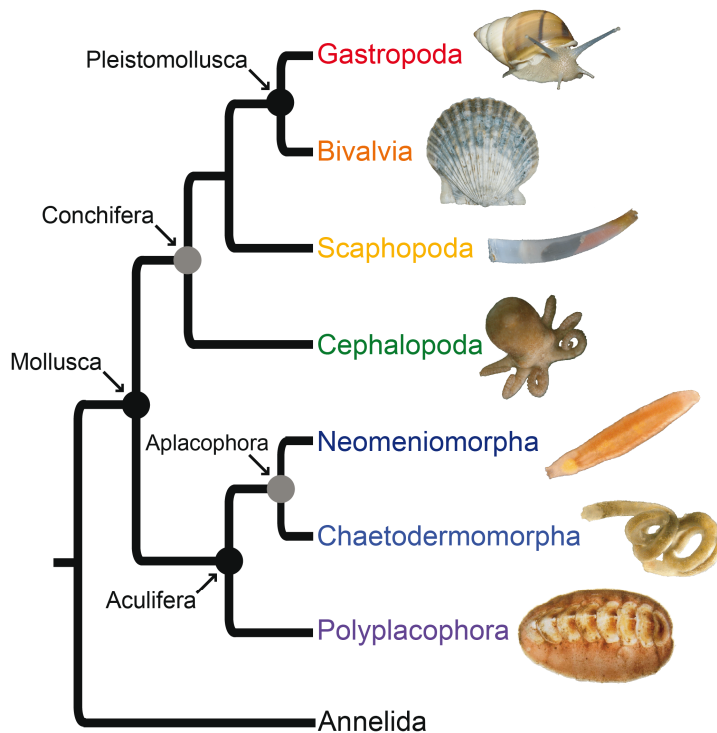


**Figure 1-3: Phylogenetic relationships within molluscs.** Bayesian inference topology with several clades collapsed for clarity. Photos depicting examples for each taxon are not to scale. Image modified after Kocot *et al.* (2011).

Diverse phylogenetic hypotheses centering on different species lineages within the Bivalvia were proposed during the recent decades as graphically summarized by Sharma *et al.* (2012) (Figure 1-4). Most recent evidence suggests that bivalves can be separated into Protobranchia and Autobranchia, the latter consists of all bivalves with ctenidia modified for filter-feeding. The Autobranchia can be further split into Pteriomorphia, which possessed byssal attachment at least at some time in their geological history, and Heteroconchia, which in turn can be split into two sister groups. The first group contains the clades of Archiheterodonta and Palaeoheterodonta, while the second contains the Euheterodonta, which is made up of the clade Anomalodesmata, e.g. including the Antarctic bivalve *Laternula elliptica*, as well as a cluster of all other Euheterodonta, putatively also including the long-lived ocean quahog, *Arctica islandica* (Sharma *et al.* 2012). The Pteriomorpha comprises economically important species of oysters, scallops and mussels, such as for instance the blue mussel *Mytilus edulis.*
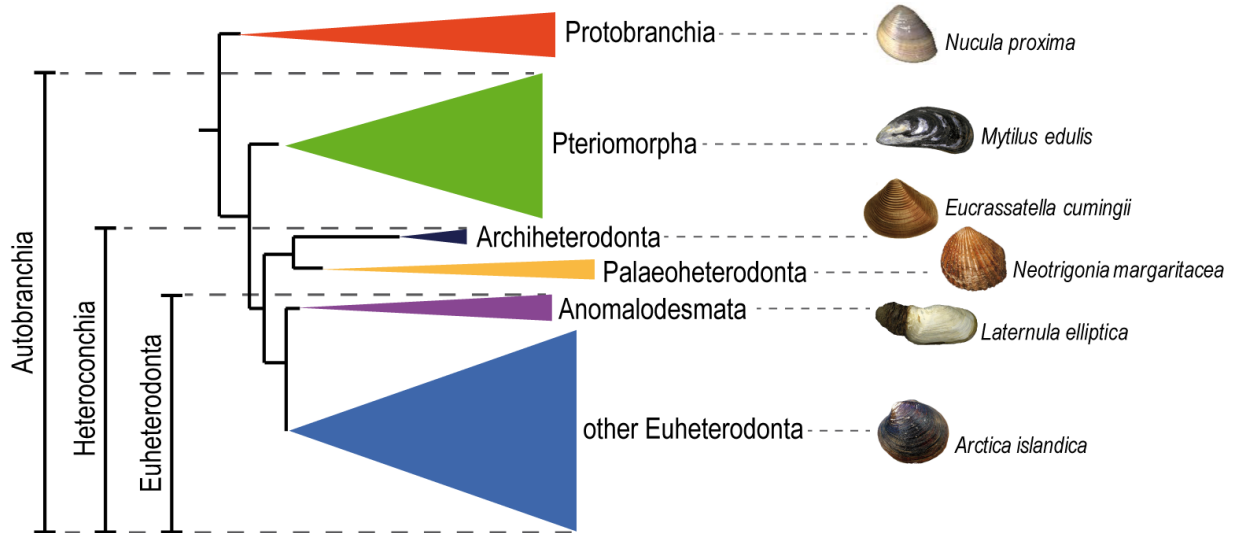
**Figure 1-4: Schematic summary of evolutionary relationships among bivalves.** Phylogenetic tree modified after Sharma *et al.* (2012). Example organisms not drawn to scale. Copyright: *Nucula proxima* by Bill Frank (http://www.jaxshells.org), *Mytilus edulis* by Rainer Zenz (Creative-Commons-License CC-BY-SA 3.0), *Eucrassatella cumingii* by W. H. Baily (public domain), *Neotrigonia margaritacea* by Engeser (CC-BY-SA 3.0), *Laternula elliptica* by the Smithsonian National Museum of Natural History (http://invertebrates.si.edu) and *Arctica islandica* by Hans Hillewaert (CC-BY-SA 3.0).

### 1.2.2 The blue mussel *Mytilus edulis*

#### 1.2.2.1 General importance of M. edulis

Mussels of the genus *Mytilus* sp. are among the most common marine molluscs world-wide (Gosling 1992). In line with this, the common blue mussel *Mytilus edulis* (Linné 1758) (Figure 1-5A), is the dominant benthic organism covering the hard-bottom benthos in the Baltic Proper, making up 95% of the total animal biomass (Kautsky 1982; Kautsky & Van der Maarel 1990). Furthermore, *M. edulis* is an important ecosystem engineer. It provides a habitat for other animals due to its hard shell and also by forming dense mussel beds (Gutiérrez *et al.* 2003). This is especially important in areas, which most other animals cannot access, such as the Wadden Sea. Due to their filter-feeding behaviour, they produce a constant flow of seawater through their body cavity using their gills and, hence, are constantly exposed to the surrounding microbiota while ingesting phytoplankton and suspended particles. Thereby they change the inorganic nutrient pool available for phytoplankton through regeneration and storage of nutrients in the mussel biomass (Prins *et al.* 1997). Hence, mussels were found to be a natural eutrophication control as has been shown for the San Francisco bay (Officer *et al.* 1982) and the Bay of Brest (Hily 1991). As a result, they produce faeces and pseudofaeces, which settle to the seafloor. This important process, known as biodeposition, accounts for 1.8 g shell free dry mass (SFDM), 0.33 g ash free dry mass (AFDM), 0.13 g carbon, $1.7 \cdot 10^{-3}$ g nitrogen and $2.6 \cdot 10^{-4}$ g phosphorus per g mussel and year in the Baltic Proper (Kautsky & Evans 1987). This increased deposition has a significant impact on

benthic fauna (Ragnarsson & Raffaelli 1999) and can reduce erosion by a factor of 10 (Widdows & Brinsley 2002). In addition, blue mussels also play a major role in the global aquaculture production accounting for 207,918 t and 349,072 US$ in 2010 (FAO 2012). On the other hand, it can also have negative economical impacts by being one of the major contributors of biofouling (Woods Hole Oceanographic Institution & United States Navy's Bureau of Ships 1952). Therefore, *Mytilus edulis* is not only an interesting putative model organism to study the evolution of the innate immune system, results obtained from these studies could also have considerable economical and ecological impacts, for instance by improving aquaculture conditions or anti-fouling measures.
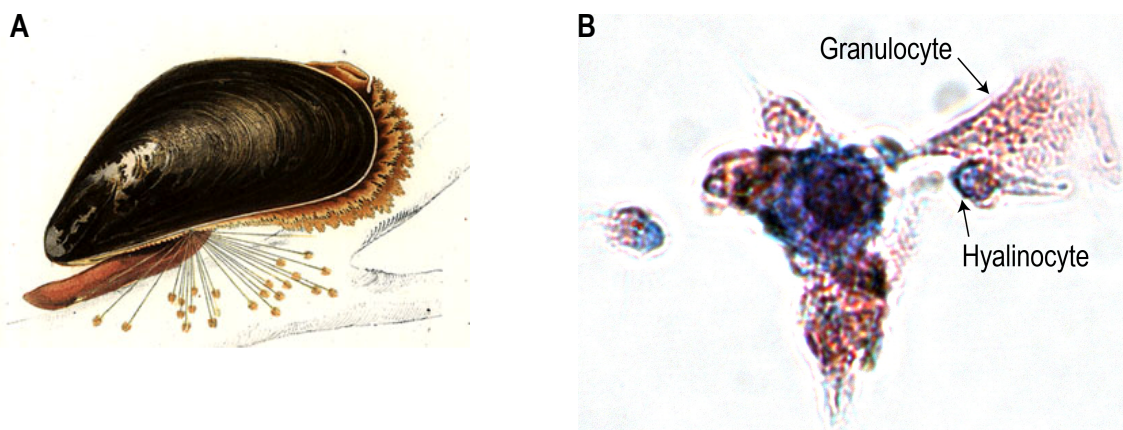


**Figure 1-5: The blue mussel *Mytilus edulis*. A**) Habitus of *M. edulis* adopted from Meyer & Möbius (1872). **B**) Microscopic image of aggregating *M. edulis* hemocytes stained with May-Grünwald/Giemsa dye (also known as Pappenheim staining). Basophile granules are depicted by a purple color and acidic granules are bright red, while the cytoplasm displays a light blue color. Two types of hemocytes can be observed: the mostly red to purple granulocytes containing a high amount of granules and the blue, mostly agranular hyalinocytes.

### 1.2.2.2 Basic physiology of the M. edulis immune system

*Mytilus edulis* and other bivalves possess circulating immune cells, called hemocytes (Figure 1-5B), which are capable of immune responses quite similar to the ones in mammals. In this context, hemocytes are for instance capable of encapsulation and phagocytosis of foreign particles (Nöel *et al.* 1993), such as macrophages (Aderem & Underhill 1999), and can generate reactive oxygen species (ROS) (Winston *et al.* 1996), such as neutrophils in humans (Nathan 2006). In addition, they also play an important role in wound healing in bivalves, which has been studied to a great extend in oysters so far (DesVoigne & Sparks 1968; Brereton & Alderman 1979).

In bivalves, the colourless plasma containing the hemocytes, which is referred to as hemolymph, serves as 'blood' and does not contain a respiratory pigment in most species. Therefore, the oxygen-carrying capacity of the hemolymph is equal to that of seawater. The blood system of *Mytilus edulis* is an open circulatory system, meaning that the hemolymph is collected in three different sinuses after the

hemolymph left the heart ventricle via a single anterior aorta and was further carried to the rest of the body through different arteries. From these sinuses hemolymph is distributed to the kidneys, then the gills and back to the heart by a major vein (Song *et al.* 2010).

The characterization of hemocytes into different types is still controversial. But two major categorizations based on morphology and histochemistry are generally accepted today: the granule containing granulocytes and the mostly agranular hyalinocytes (Figure 1-5B). The granules seem to possess a variety of hydrolytic enzymes. Different immune function have also been implicated for both cell types, but remain a topic of current investigations (Song *et al.* 2010).

In case of a microbial invasion hemocytes are able to migrate through the connective tissue to the site of infection exhibiting chemotactic and chemokinetic behavior towards molecules of bacterial origin, such as LPS (Schneeweiß & Renwrantz 1993). In addition to cellular defense mechanisms, such as phagocytosis and destruction of pathogens via lysosomal enzymes (Canesi *et al.* 2002), they also possess humoral immune responses against pathogens. These include the production and release of antimicrobial proteins, reactive oxygen and nitrogen species, complement-like molecules (Zänker 2001), as well as the secretion of agglutinating and cytotoxic molecules (Leippe & Renwrantz 1985; Leippe & Renwrantz 1988). Hence, the immune response in *M. edulis* is the combined effect of cellular and humoral processes, even though the exact molecular mechanisms for most of these defense responses still need to be elucidated and for which new next-generation sequencing approaches could provide a useful tool.

## 1.3 Hemocyte transcriptome analysis as a tool for the identification of conserved immune gene orthologs

An outdated and quite simplified dogma in molecular biology was that a gene, which is a sequence of deoxyribonucleic acid (DNA) comprising the information for a protein, is transcribed into ribonucleic acid (RNA) and then translated into the corresponding amino acid sequence. However, the term genome applies to the entirety of DNA in a cell or a population of cells, which includes genes and also other, noncoding DNA sequences. Similarly, the term transcriptome refers to all RNA molecules produced in a cell or a set of cells at a given time, which includes not only messenger RNA (mRNA) as template for proteins, but also ribosomal RNA (rRNA) and transfer RNA (tRNA) used for protein biosynthesis, as well as other, mostly regulatory RNAs. In contrast to the genome, the analysis of the transcriptome enables the direct investigation of active and, hence, expressed genes in response to a specific stimulus at a specific time point. Because mature mRNA is already processed for translation, these transcripts provide more information about the putative protein sequence than the corresponding gene, as they

include additional information, e.g. about alternative splicing and other post-transcriptional modifications. While the genome is thought to be more or less static, the transcriptome is highly variable due to several internal and external stimuli affecting gene expression, such as cell differentiation processes or immune challenges. Therefore, the transcriptome represents a dynamic link between genetic information and the physical condition of a cell (Velculescu *et al.* 1997).

To rapidly identify nucleic acid sequences at genome and transcriptome level, the Sanger sequencing method was established in the 1970s (Sanger *et al.* 1977). This method allowed for the identification of whole genomes and transcriptomes for the first time. In recent years, the need for an even higher sequencing throughput and shorter run times together with more economical sequencing technologies was the driving force behind the development of ultra-fast and low-cost next-generation sequencing technologies (Schuster 2008). The high output obtained by these technologies, for instance, enabled researchers to obtain 13 million base pairs of sequence information from a 28,000 year old mammoth only with one single run on the GS FLX Genome Sequencer from Roche (Poinar *et al.* 2006). Together with the Genome Analyzer by Illumina (sequencing by synthesis) and the SOLiD system by Life Technologies (sequencing by ligation), the FLX Genome Sequencer (454 pyrosequencing) is one of the leading next-generation sequencing systems.

All three systems produce short fragments of sequence information (=reads), which need to be merged to a much longer sequence afterwards (=assembly) in order to reconstruct the original nucleic acid sequence. The assembly results in sets of overlapping nucleotide sequences representing consensus cDNA sequences (=contigs) and left over reads (=singletons). The current FLX version (FLX+) is characterized by relatively long read lengths (~700 bp) in comparison to other next-generation sequencing systems such as the 5500xl SOLiD with ~75 bp; even though it produces with 700 megabases a much smaller amount of sequence information than any other system, e.g. the SOLiD system can produce up to 300 gigabases per run. Therefore, with the advantage of longer read lengths, the FLX system is especially suited for the transcriptional investigation of organisms, whose genomes have not been described yet.

During the recent years, genomes and transcriptomes of many important invertebrate organisms have already been deciphered, including the common fruit fly *Drosophila melanogaster* (Adams *et al.* 2000); the medical leech *Hirudo medicinalis* (Macagno *et al.* 2010); the amphioxus *Branchiostoma floridae* (Putnam *et al.* 2008); the sea quirt *Ciona intestinalis* (Dehal *et al.* 2002); the fresh water polyp *Hydra magnipapillata (*Chapman *et al.* 2010*)*; and the purple sea urchin *Strongylocentrotus purpuratus* (Sea Urchin Genome Sequencing Consortium *et al.* 2006). Furthermore, these studies were often used to gain insights into conserved immune genes at molecular level. In line with this, a diverse immune repertoire of invertebrates was identified in the genome analyses of

*Branchiostoma floridae* (Huang *et al.* 2008), *Hydra magnipapillata* (Miller *et al.* 2007) and *Strongylocentrotus purpuratus* (Hibino *et al.* 2006; Rast *et al.* 2006).

In this context, the transcriptome analysis by Philipp *et al.* (2012a) using the 454 pyrosequencing technology identified a wide variety of putatively conserved and important immune gene orthologs in the blue mussel *Mytilus edulis*. A wide variety of pattern recognition receptors were discovered including at least 27 TLRs in contrast to only 2 transcripts in the transcriptome analysis of *Mytilus galloprovincialis*, using a non-next-generation sequencing approach (Venier *et al.* 2011). Further PRRs found in *M. edulis* include putative RLR orthologs for RIG-I and MDA-5. Interestingly, NLR orthologs were not detected in a bivalve so far, hence it might be speculated that other molecules serve as intracellular DAMP and PAMP receptors in *M. edulis* (Philipp *et al.* 2012a). Not only PRRs, also orthologs of downstream transcription factors such as NF-κB family members and the expansion of interferon regulatory factors (IRFs) were identified in the transcriptome analysis of *M. edulis*, even though no interferon-like cytokine could be detected (Philipp *et al.* 2012a). On the other hand, orthologs of cytokines such as interleukin-17 (IL-17), macrophage migration inhibitory factors (MIF) and TNF-related transcripts as well as the corresponding JAK/STAT pathway members seem to be present in the transcriptome of the blue mussel. The presence of a diverse and wide repertoire of antimicrobial peptides has not only been thoroughly shown for *Mytilus galloprovincialis* (Mitta *et al.* 2000b), but was also verified for *M. edulis* using transcriptome analysis by Philipp *et al.* (2012a). Complement system components were also found in *M. edulis*, but their number and diversity appeared to be reduced compared to the cnidarian or vertebrate system as outlined by Philipp *et al.* (2012a), lacking for example C2, C4 and C5 orthologs. On the other hand, complex apoptosis and autophagy mechanisms similar to pathways in vertebrates are thought to be already present at molecular level in the blue mussel (Philipp *et al.* 2012a).

In the present study, transcriptome datasets with emphasis on mRNA of unstimulated *M. edulis* hemocytes and hemocytes challenged with an immune-stimulating compound were developed and investigated for putatively conserved orthologs with relevance for the immune system. Therefore, by extending the transcriptome analysis by Philipp *et al.* (2012), the present study directly enables the comparison between unstimulated and immune-stimulated hemocytes and, hence, allows for direct identification of putative immune gene orthologs involved in the defense response against flagellin. In contrast to other methods investigating mRNA expression, such as microarrays and quantitative Real-time PCR (qRT-PCR), an *a priori* selection of genes is unnecessary, providing a non-biased analysis of cellular processes. This is especially important in the case of non-model organisms, such as *M. edulis*, for which only limited sequence information, as a requirement for approaches such as microarrays and qRT-PCR, is available.

Furthermore, genome and transcriptome analyses also provide the molecular background to search and characterize specific target genes; as for example a surprisingly rich variety of conserved sequences potentially encoding NLR-like proteins was revealed by specific search for NLRs in the EST database of the basal eukaryote *Hydra* sp. (Lange *et al.* 2011). Therefore, the transcriptome datasets obtained in the present study were not only used to identify immune gene orthologs involved in flagellin-induced defense responses, but also to investigate two phylogenetic ancient and conserved families of immune gene orthologs in detail at transcript level. These comprised transcripts putatively coding for NADPH- and dual oxidases as well as IL-17-like cytokines. Both families were chosen because they also fulfill a considerable role in the immune response in humans, as described in the following sections.

## 1.4    The NOX and DUOX family of ROS producing enzymes

The generation of reactive oxygen species (ROS) is known to be a widespread immune response among various marine invertebrates (Philipp *et al.* 2011). The term reactive oxygen species collectively describes highly reactive molecules containing oxygen, including superoxide, hydrogen peroxide, nitric oxide, peroxynitrite, hypochlorous acid, singlet oxygen and the hydroxyl radical (Murphy *et al.* 2011). In humans, it has been shown that ROS can be formed by several different mechanisms including the interaction of ionizing radiation with biological molecules; the generation of unfavorable byproducts in cellular respiration; and the production by specialized enzymes, such as myeloperoxidases, NADPH oxidases (NOX) and dual oxidases (DUOX). Due to their high reactivity, ROS can interact with a wide variety of inorganic molecules, proteins, lipids, carbohydrates, and nucleic acids, thereby destroying or altering the function of the corresponding molecule (Bedard & Krause 2007). Therefore, ROS can cause a great deal of cellular damage, which is, for instance, postulated to play a role in the aging process (Harman 1956). In order to regulate the level of ROS and prevent cellular damage, cells employ several antioxidant molecules, such as vitamin E, vitamin C and uric acid, as well as protective enzymes. These comprise superoxide dismutases (SOD), which convert superoxide into hydrogen peroxide; as well as catalases and glutathione peroxidases, both of which use hydrogen peroxide to produce water amongst others. On the contrary, ROS causing cellular damage is also used beneficially as an important part in host defense, where it leads to the elimination of pathogens. But how ROS lead to an efficient clearing of pathogens, e.g. by direct killing of microbes and/or by initiation of further important signaling cascades resulting in the release of other toxic molecules, such as antimicrobial peptides, is not clarified at the moment (Bedard & Krause 2007). ROS have also been observed to lead to inactivation of virulence factors; increases in phagosomal pH and ion concentration; modifications of signal transduction pathways e.g. by inhibition of phosphatases; as well as alterations of gene

expression by interaction with transcription factors; and many more (Bedard & Krause 2007). In the snail *Biomphalaria glabrata* it was shown that snails with resistance to the parasite *Schistosoma mansoni* produce more ROS than susceptible snails (Bender *et al.* 2005), indicating a direct importance of ROS for immune functioning even in molluscs.

**Table 1-1: Human NOX and DUOX orthologs.** The corresponding minor subunits and cofactors needed for their activation are listed. It has to be noted that Rac enzymes are not exclusively specific for NADPH oxidases, but are also involved in many other cellular processes. DUOXA is not directly needed for activation of ROS production but for the maturation of DUOX proteins. Tissue(s) exhibiting the highest expression as well as the function of the respective NOX/DUOX orthologs are given.

| Ortholog | Minor subunits and cofactors[1] | Major expression[2,3] | Functions[3] |
|---|---|---|---|
| NOX1 | $p22^{phox}$, Rac, NOXO1, NOXA1 | Colon, blood vessels | Angiotensin II-mediated hypertension, inflammatory pain, cell proliferation & differentiation |
| NOX2 | $p22^{phox}$, Rac, $p47^{phox}$, $p67^{phox}$, $p40^{phox}$ | Phagocytes | Host defense, Angiotensin II-induced cardiac hypertrophy, hippocampal synaptic plasticity |
| NOX3 | $p22^{phox}$, NOXO1 | Inner ear | Otoconia formation, gravity perception, cisplatin ototoxicity |
| NOX4 | $p22^{phox}$, *constitutively active* | Kidney, blood vessels | Apoptosis, cell proliferation, hypertrophy, survival, & differentiation |
| NOX5 | $Ca^{2+}$ | Lymphoid tissue, testis | Apoptosis, signaling in cancer cells, cell growth & proliferation, spermatogenesis[4], pregnancy[4] |
| DUOX1/2 | $Ca^{2+}$, (DUOXA) | Thyroid | Host defense, thyroid hormone biosynthesis |

[1] Aguirre & Lambeth 2010
[2] Bedard & Krause 2007
[3] Katsuyama 2010
[4] Bedard *et al.* 2012

The major source of ROS in humans is the family of NADPH- (NOX) and dual (DUOX) oxidases (Rada & Leto 2008). ROS production by these enzymes plays a major role in the killing of pathogens and triggering of further immune responses. Hence, lack or mutations in any of the NOX and DUOX subunits and, consequently, inhibited ROS production can have severe effects leading e.g. to the chronic granulomatous disease (CGD) (Heyworth *et al.* 2003). The NOX and DUOX family of enzymes comprises seven major orthologs in humans (Table 1-1), namely NOX1-5 and DUOX1-2, which possess the same basic building block: a homolog of the flavocytochrome $gp91^{phox}$ (NOX2) (Lambeth 2004). For proper functioning the major transmembrane subunit ($gp91^{phox}$) requires further minor subunits. In the case of NOX enzymes these can be the additional membrane bound subunit $p22^{phox}$; the cytosolic subunits $p40^{phox}$; $p47^{phox}$ or its ortholog NOXO1; and $p67^{phox}$ or its ortholog NOXA1; as well as the Ras-related C3 botulinum toxin substrate (Rac). The composition of required subunits varies between the different NADPH oxidase family members (Table 1-1). DUOX enzymes seem to rely solely on the DUOX maturation factor (DUOXA) and calcium as regulatory factors (Sumimoto 2008).
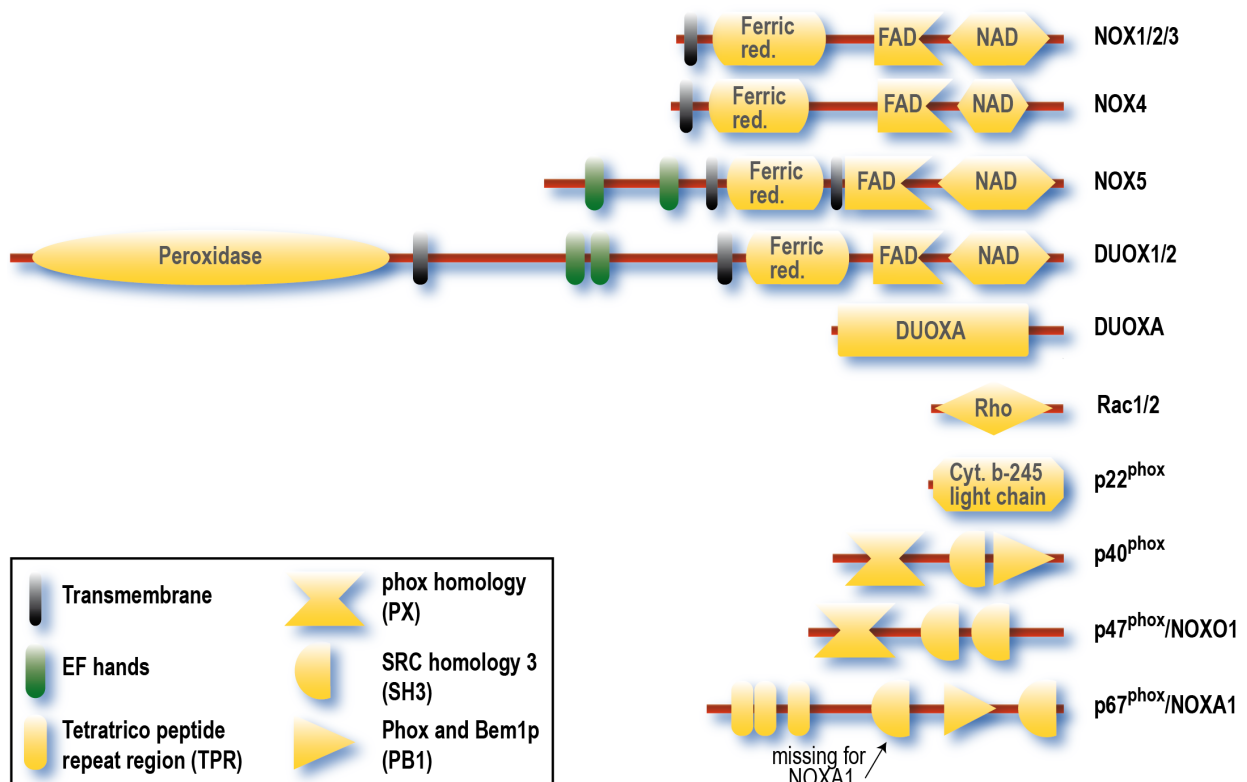
**Figure 1-6: Domain structure of human NOX and DUOX enzymes and their minor subunits.** Human orthologs are depicted as obtained by UniProt/Swiss-Prot and subsequent SMART (including PFAM) domain database search. Ferric red. = Ferric reductase, Rho = Ras homology domain, Cyt. b-245 = Cytochrome b-245.

In humans, all major subunits belonging to this enzyme family contain the unifying characteristic domain structure of the heavy chain of the flavocytochrome b-245 (gp91phox) (Figure 1-6): an N-terminal transmembrane ferric reductase component followed by cytoplasmic binding sites for flavin adenine dinucleotides (FAD) and nicotinamide adenine dinucleotide phosphates (NADPH) (Lambeth 2004; Sumimoto 2008). Furthermore, major subunits of NOX5 and DUOX possess additional N-terminal EF hands, which are preceded by a transmembrane peroxidase domain in DUOX orthologs (Kawahara *et al.* 2007) (Figure 1-6).

Most NOX enzymes rely on the membrane-bound p22phox minor subunit for ROS production, which forms the light chain of the flavocytochrome b-245 (also called *b588*) complex. For NOX2 it has been shown that upon cell activation, for instance due to bacterial invasion, the p47phox subunit and possibly other subunits become phosphorylated and Rac bound GDP is converted to GTP. This triggers the assembly of the cytoplasmic subunits, p47phox and the complexed subunits p40phox and p67phox, at the plasma membrane (Figure 1-7). Binding to the major membrane-bound subunit is achieved for instance via the SRC homology 3 (SH3) domains of p47phox, while the phox homology (PX) domain targets the plasma membrane for binding. The activation domain of bound p67phox is used to transfer the electrons

from NADPH to FAD (Lambeth 2004; Lambeth *et al.* 2007; Rada & Leto 2008), which can then be further transferred to the ferric reductase domain containing two heme groups (cytochrome b-245) including iron as an electron carrier (Figure 1-7). The heme groups then reduce molecular oxygen to produce superoxide (Vignais 2002), which can be transformed into the more stable hydrogen peroxide.
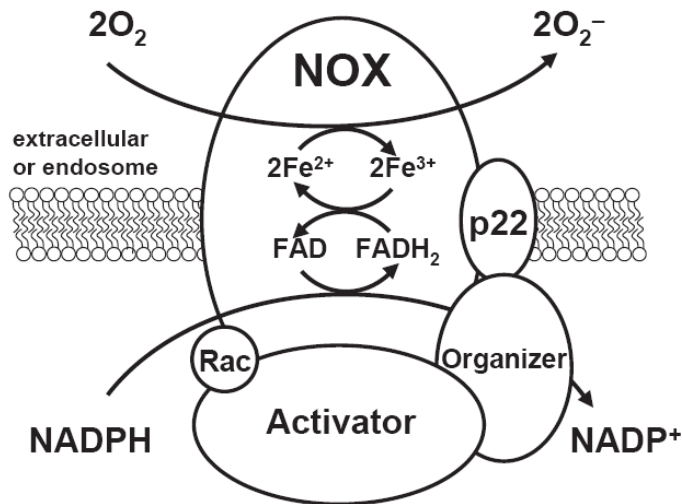


**Figure 1-7: Simplified scheme of oxygen radical generation by NADPH oxidases.** After assembly of a Rac homolog, a NOX activator (which can be p67[phox] or NOXA1) and a NOX organizer (which can be p47[phox] or NOXO1) with p22[phox] and the corresponding major NOX subunit at the plasma or endosome membrane, NADPH is oxidized to NADP$^+$. Using the conversion of FAD to FADH$_2$ and $2Fe^{3+}$ to $2Fe^{2+}$ and vice versa, molecular oxygen ($2O_2$) can then be reduced to oxygen radicals ($2O_2^-$). Requirement of the respective subunits and other components depends on the NOX isoform. Image taken from Katsuyama (2010).

For NOX1 and 3 as well as their subunits similar activation mechanisms have been reported (Lambeth 2004). The subunits of NOX4 have not been identified so far and in some studies it is even assumed that NOX4 is constitutively active (Lambeth *et al.* 2007). DUOX enzymes are fully synthesized in the endoplasmatic reticulum (ER), where they are retained. Using the DUOX maturation factor (DUOXA), they can overcome the ER retention and assemble at the plasma membrane (Grasberger & Refetoff 2006). Like NOX5, they putatively only require calcium as a regulatory factor instead of other minor subunits, even though a possible involvement of p22[phox] is still strongly debated. Binding of calcium is thought to result in a conformational change in the EF-hand domain and allows it to bind to the ferric reductase domain. This supposedly activates the electron transfer from NADPH (Bánfi *et al.* 2004). In addition to the EF-hand domain, DUOX enzymes also contain an N-terminal peroxidase domain.

Kawahara *et al.* (2007) depicted that members of the NOX/DUOX enzyme family are present in lower eukaryotes, such as the cellular slime mold, *Dictyostelium discoideum*, up to basal deuterostomes such as the sea urchin, *Strongylocentrotus purpuratus.* The authors concluded that the extraordinarily

high conservation of these enzymes suggest a common biological function, which remained throughout the evolutionary history. In addition, highly conserved phox-regulated subunits have also been identified in a variety of phylogenetic ancient organisms, such as the choanoflagellate, *Monosiga brevicollis,* and the sea anemone, *Nematostella vectensis*, (Kawahara & Lambeth 2007); therefore the authors concluded that the regulatory subunits have probably evolved together with their corresponding NOX/DUOX ortholog. Investigations of NOX and DUOX activity in invertebrate organisms have already provided important insights and valuable topics for future studies about the role of these enzymes in mammals (Aguirre & Lambeth 2010). In this context, the role of the DUOX peroxidase domain in the modification of the extracellular matrix by tyrosine cross-linking could be shown for the first time in *Caenorhabditis elegans*, which has been hypothesized to have similar functions in the mammalian lung (Edens *et al.* 2001). This mechanism is also used for cross-linking of the fertilization envelope by the sea urchin DUOX ortholog Udx-1 (Wong *et al.* 2004), which is proposed to be conserved throughout the eukaryotes, even though an increase in ROS production or a DUOX ortholog has not been observed during fertilization in mammals so far (Aguirre & Lambeth 2010). All of these studies do not include Lophotrochozoan organisms, except the snail, *Lottia gigantea*, for which NOX/DUOX sequences have been identified but no functional studies have been conducted. Therefore, it is especially interesting to gain further insight into the evolution and function of NOX and DUOX enzymes by investigating the most basal clade of the three major invertebrate clades (Lophotrochozoa, Ecdysozoa and basal deuterostomes) more closely.

## 1.5   The IL-17 family of cytokines

Cytokines are small signaling proteins, which play a major role in intracellular and cell-to-cell communication exhibiting autocrine, paracrine and/or endocrine activities. A cytokine can have a multitude of functions, which strongly depends on the specific cell type and other cytokines involved. Furthermore, cytokine pathways can be redundant and overlapping. Therefore, in vertebrates cytokines can only be broadly divided into five major types: Interferons, chemokines, colony-stimulating factors, tumor necrosis factors (TNF) and interleukins (Tisoncik *et al.* 2012). Interferons are highly important for the innate immune response towards viral infections (Fensterl & Sen 2009). After recognition by RLRs, as discussed in 1.1.2.2, they induce anti-viral responses in the host, such as for instance the induction of RNaseL destroying all RNA within the cell. Chemokines are named short for chemotactic cytokines, because of their ability to induce cell migration. In addition, some chemokines have also the ability to activate leukocytes, which can, amongst others, lead to an induction of NOX-coupled ROS production (Thelen 2001). Colony-stimulating factors influence the differentiation and proliferation of hematopoietic

progenitor cells, but may also play a role in immune pathways or mature myeloid cells (Hamilton 2008). TNFs are multifunctional proinflammatory cytokines, which are able to activate T-cells and seem to play a major role in human diseases such as inflammatory bowel disease and rheumatoid arthritis (Locksley *et al.* 2001). As the name implies, interleukins are responsible for signaling between leukocytes, but also other cell types. Like all cytokines, interleukins have a wide variety of functions. The interleukin family is a large family of anti- and proinflammatory proteins with paracrine or autocrine activity, binding to their corresponding receptors. Due to their non-homologous structure together with their, in some cases, even opposing function, further characterization into four major groups of interleukins is based mainly on gene and protein characteristics. Hence, interleukins (IL) can be divided into IL-1-like cytokines, class I helical cytokines (including IL-4, IL-6/12), class II helical cytokines (including IL-10 and IL-28) and the IL-17-like cytokines (Brocker *et al.* 2010).

Cytokines belonging to the interleukin-17 (IL-17) group are especially unique, since they are structurally very different from other interleukins and proteins (Aggarwal & Gurney 2002). These proteins exhibit a cystein-knot fold (Hymowitz *et al.* 2001), a structural motif also common for the neurotrophin growth factors. It is assumed that dimerization of IL-17 proteins is needed for receptor binding. In humans, six IL-17-like cytokines have been identified, IL-17A to F (Table 1-2); their function and corresponding receptors, however, have not been fully elucidated yet (Cua & Tato 2010).

**Table 1-2: The IL-17 family of cytokines in humans.** Their corresponding receptors and tissue-wide distributions are given. Information for this table was obtained from Cua & Tato (2010) and Gaffen (2009b).

| Cytokine | Receptor | Sources |
|---|---|---|
| IL-17A | IL-17RA & IL-17RC | αβ T cells, γδ T cells, NK cells, iNKT cells and LTi-like cells |
| IL-17B | IL-17RB | Intestine, pancreas and neurons |
| IL-17C | IL-17RE | Thymus, spleen, prostate and fetal kidney |
| IL-17D | Undefined | Secreted by T cells, muscles, epithelial cells, brain, heart, lung, pancreas and adipose tissue |
| IL-17E (also known as IL-25) | IL-17RA & IL-17RB | Mast cells, epithelial cells, alveolar macrophages, eosinophils, basophils, NKT cells and intestine |
| IL-17F | IL-17RA & IL-17RC | T helper cells, NK cells, iNKT cells and LTi-like cells |

Up- and downstream signaling seem to be dependent on different transcription factors, but the exact mechanisms still have to be elucidated. Involved in upstream signaling are most probably the signal transducer and activator of transcription 3 (STAT3), the retinoic acid receptor‑related orphan receptor‑γt (RORγt) and the aryl hydrocarbon receptor (AHR) (Cua & Tato 2010). It is now widely

accepted, that even though IL-17 transcription is not directly dependent on IL-23 production, IL-23 is probably needed for the survival and differentiation of naïve CD4 T helper cells into IL-17-producing T cells ($T_H17$ cells) (Cua & Tato 2010; Hirota *et al.* 2012). After binding of secreted IL-17 by IL-17 receptors (IL-17R), downstream signaling is proposed to occur in a similar way as in the TLR pathway by binding of an adaptor protein, such as CIKS (also known as ACT1) by IL-17RA, and, subsequent, activation of the NF-κB and MAPK signaling pathways (Gaffen 2009b).

Interestingly, IL-17 can be secreted by cells of the innate and the adaptive immune system alike. While the adaptive response is relatively well studied, innate IL-17 production is only poorly understood (Hirota *et al.* 2012). One way of inducing IL-17 production in innate lymphatic cells, such as γδT cells, is supposed to be the activation of RORγt via the induction of NF-κB transcription factors in response to *E.coli* infection (Powolny-Budnicka *et al.* 2011).

Numerous functions in host defense have been proposed for IL-17 family members. Production of IL-17 is thought to induce the release of various other cytokines and molecules, which in turn can trigger further important immune reactions. In line with this, innate IL-17 producing cells can rapidly trigger the secretion of granulopoietic factors of epithelial cells to recruit a large amount of neutrophils to the site of infection. IL-17 can also cooperate with other cytokines to activate tissue-infiltrating neutrophils. Furthermore, increased IL-17 production can lead to an enhanced generation of antimicrobial peptides (Cua & Tato 2010). The above were just a few features of host defense responses by innate IL-17 producing cells. Recent studies also suggest that IL-17 producing cells are essential for the interaction with the commensal microbiota and, hence, the regulation of mucosal homeostasis, for instance, by enhancing the integrity of the intestinal cell wall (Cua & Tato 2010). On the other hand, a harmful effect is caused by the overproduction of IL-17 leading to drastic inflammatory responses in many disorders such as inflammatory bowel disease (Fujino *et al.* 2003) and rheumatoid arthritis (Gaffen 2009a).

The sequencing of the sea urchin genome revealed the absence of many cytokine families present in vertebrates, an exception to this were numerous TNF and IL-17 encoding sequences (Hibino *et al.* 2006). Further studies revealed the existence of IL-17 orthologs also in other invertebrates, such as amphioxi (Wu *et al.* 2011; Dishaw *et al.* 2012) and oysters (Roberts *et al.* 2008). On the basis of these studies, IL-17 is regarded as a putative evolutionary conserved cytokine connecting adaptive and innate immune responses, whose existence in phylogenetic more ancient organisms than vertebrates has only recently been shown. Therefore, further studies are needed to investigate the function and presence of IL-17 orthologs in lower eukaryotes in more detail.

## 1.6    Aims of the study

The blue mussel *Mytilus edulis*, belongs to the superphylum of Lophotrochozoa, being the least studied clade of the three major bilaterian clades. However, studies focusing mainly on the bilaterian clades Ecdysozoa and Deuterostomia provide only an incomplete view on the evolution of the innate immune system. In this context, it has for example been suggested that the earliest NOX2 ortholog is existent in a basal deuterostome, the purple sea urchin, *Strongylocentrotus purpuratus* (Kawahara *et al.* 2007), since no NOX2-like ortholog had been discovered in protostomes or even lower taxa. The increasing amount of available genomic sequence information during the recent years, however, led to a revision of this finding and the earliest NOX2 orthologs were nowadays identified in even more ancient organisms such as the snail *Lottia gigantea* and the sea anemone *Nematostella vectensis* (Kawahara & Lambeth 2007). This especially exemplifies how genomic insights obtained from organisms other than the known Ecdysozoan model organisms can shape our understanding of the evolution of the innate immune system. Blue mussels are useful as potential model organisms for studying immune functions, since they are sessile, marine filter-feeders and, therefore, are continuously in direct contact to the surrounding microbiota. Hence, it is especially interesting to investigate, which components of the innate immune system evolved in these animals to deal with the constant microbial exposure within the marine ecosystem. In the present study, flagellin, a major virulence inducing factor of many microbes (Ramos *et al.* 2004), is used to create transcriptome datasets of unstimulated and immune-stimulated hemocytes, to provide insights into the transcriptional response of putative immune pathways and immune gene orthologs upon flagellin challenge in *M. edulis*. The extensive transcriptome database at the Institute for Clinical Molecular Biology (ICMB, Kiel, Germany), including also other tissues of *M. edulis* (Philipp *et al.* 2012a), will also provide the molecular background for the more detailed investigation of highly conserved and phylogenetic ancient immune gene orthologs, coding for NOX/DUOX and IL-17 family members. In addition, transcriptome databases of *Laternula elliptica* (Husmann *et al.* in revision) and *Arctica islandica* (Philipp *et al.* 2012c), which were also established at the ICMB in Kiel, offer the opportunity to validate the results obtained from *M. edulis* in other bivalves. Moreover, the findings obtained in the present study are discussed in comparison to findings from other Lophotrochozoan and invertebrate organisms, to provide a more complete view on the phylogeny of the selected immune gene orthologs. Hereby it will contribute to the understanding of the evolution of the innate immune system itself. Therefore, the focus of the present study can be summarized as outlined on the following page.

Focus of the present study:

- Identification of conserved processes and pathways in hemocytes, the immune cells of *M. edulis,* will be conducted with the aid of newly established hemocyte transcriptome datasets.

- Furthermore, the transcriptional profile of potential immune gene orthologs in *M. edulis* hemocytes will be determined in response to flagellin.

- The existence of NOX and DUOX enzymes, their role in ROS production and their function in bivalve hemocytes will be elucidated in detail. Moreover, the presence and evolution of NOX and DUOX orthologs throughout animal phylogeny will be specified with an emphasis on Lophotrochozoan organisms.

- In addition, to identify the presence and characteristics of IL-17 orthologs in bivalves, transcripts encoding IL-17 will be investigated more closely. The transcriptional response of IL-17 orthologs upon immune stimulation will be further observed in *M. edulis* hemocytes providing hints about a potential regulation during immune stress.

## 2. METHODS

A full list of the employed materials can be found in section 8 on page 153 and following.

### 2.1 Organisms and handling

#### 2.1.1 Collection and acclimation of mussels

Blue mussels, *Mytilus edulis,* ranging from 5-9 cm in size were collected from populations (depth approximately 2 m) in front of the west-shore building of the GEOMAR (Helmholtz Centre for Ocean Research, Germany) at Kiel Fjord (54°20`N; 10°9`E) between June 2009 and August 2011. Shells were cleaned from epifauna and byssus threads were removed. Animals were kept in a maintenance tank (~80 l) in a temperature-constant room at the GEOMAR and acclimated to a temperature of 15 °C over a period of 2-4 weeks, unless otherwise stated. A constant flow-through of Fjord seawater (salinity 12-19 g kg$^{-1}$) from below the sampling site (4-6 m depth) was ensured. Mussels were fed at least once a week with approximately 800 ml of a fresh *Rhodomonas* sp. culture. During feeding flow-through was stopped allowing sedimentation of algae to the ground. Prior experimentation, a certain amount of mussels was transferred from the aquaria to the laboratory and kept in an incubator at 15 °C for 1-2 days to recover from handling stress. Survival rate was above 99% during the acclimation phase.

Antarctic bivalves of the species *Laternula elliptica* were sampled, reared and dissected for tissue panel analysis by G. Husmann *et al.* (in revision). Animals of 7-8 cm shell length were sampled at 7-15 m depth in Potter Cove, King George Island, Antarctic Peninsula (62°14´S, 58°40´W), in November 2008. Bivalves were kept at 1 °C in aerated, regularly renewed seawater from Potter Cove at the Dallmann Laboratory of the Alfred-Wegener Institute at the Argentinean Calini Station for 10 days prior dissection.

*Arctica islandica* individuals were collected in March 2010 from 20 m water depth at the station "Süderfahrt" (54°33`N 10°42`E) in the Baltic Sea using a hydraulic dredge from the Research Vessel Littorina (GEOMAR). Animals of 4-6 cm shell length were transported to the GEOMAR and kept at 10 °C under stable conditions as described above for *Mytilus edulis*.

#### 2.1.2 Hemolymph extraction and tissue panel generation

To collect hemolymph of *M. edulis*, a blunt, fixed blade knife was gently inserted at the location of the byssus threads and the valves were slightly prised apart without injuring the animal, thereby thoroughly draining the seawater from the animal. A pipette tip prevented the shell halves from closing, while hemolymph was withdrawn from the posterior adductor muscle using a syringe and collected in falcon

tubes on ice. Hemocytes were counted using an automatic cell counter (Cellometer Auto T4, Nexcelom). *A. islandica* individuals were prepared in the aquaria before sampling by inserting a pipette tip between the already open valves. For further analysis, hemocytes were either plated directly in tissue culture plates or pelleted by centrifugation (1000 g [~820 rpm], 10 min, 15 °C), frozen in liquid nitrogen and stored at -80 °C.

For tissue panel analyses foot, gill, adductor muscle, mantle, mantle rim and digestive gland tissue as well as hemocytes of five *M. edulis* individuals were collected and stored at -80 °C. For *A. islandica* and *L. elliptica*, foot, gill tissue and hemocytes of five and three individuals, respectively, were collected for tissue specific analysis. Since the amount of hemocytes per *M. edulis* or *A. islandica* individual is too low for subsequent RNA isolation (2.2), hemocytes of five animals were pooled for each replicate.

Hemocytes and tissues of *L. elliptica* were prepared by G. Husmann *et al.* (in revision).

### 2.1.3   Cultivation of *Rhodomonas* sp.

*Rhodomonas* sp. as food source for *M. edulis*, was obtained from the working group of Dr. F. Melzner (GEOMAR, Kiel). Cultures were kept in 5 l Erlenmeyer flasks containing 2.5 l of artificial seawater enriched with Provasolis medium (Provasoli 1963, modified by U. Sommer, GEOMAR, Kiel, see 8.3), phosphate (final concentration: 0.036 mM $KH_2PO_4$) and nitrate (final concentration: 0.550 mM $NH_4NO_3$). Artificial seawater was obtained by adjusting sterile distilled water to a pH of 7.8, using HCl, and a salinity of 8.5 g $kg^{-1}$, using artificial sea salt. An air pump ensured sufficient mixing of the algae suspension. After one week of culture, algae were fed to the mussels.

### 2.1.4   Cultivation and preparation of *Listonella anguillarum*

*Listonella anguillarum* (DSM No. 11323, glycerol stocks obtained from Dr. Fedders from the Department of Zoophysiology at CAU-Kiel, Germany) used for immune stimulation experiments was cultured in medium 101 suitable for marine bacteria by addition of 3% NaCl. Two days prior experimentation 20 µl of the glycerol stock was suspended in 5 ml medium and cultured overnight in an incubator at 160 rpm and 28 °C. The next morning 1 ml of the culture was transferred to 4 ml medium and in the afternoon again transferred to 50 ml medium in a 100 ml culture flask to keep bacteria in the exponential growth phase. The following morning the optical density (OD) of 100 µl bacteria culture was measured in triplicate at 612 nm. The culture was then adjusted to 0.1 $OD_{612}$ in 10 ml DPBS, which corresponds to a concentration of 2.3 $10^7$ CFU $ml^{-1}$ (Fedders 2008). After centrifugation at 3,000 rpm (~1,950 *g*) for 10 min, the pellet was resuspended in 1 ml DPBS and involved in further experimentation (see 2.14).

## 2.2 RNA isolation

### 2.2.1 Isolation of RNA from *M. edulis*

Tissue samples were ground in liquid nitrogen and ~50 mg of the ground powder were lysed in RLT buffer containing 1% 2-mercaptoethanol. Hemocytes were either lysed in wells of a 24-well plate using 300 µl of RLT buffer per well or the frozen pellet of centrifuged hemocytes was resuspended in RLT buffer directly. The lysates were then homogenized using the QIAshredder columns (Qiagen) and RNA was extracted employing the RNeasy Mini Kit (Qiagen) following the manufacturer's protocol, carrying out the on-column DNase I (Qiagen) digestion twice to avoid contaminations by genomic DNA. The kit functions by RNA binding to silica membranes allowing the removal of most contaminants. In the end, pure and concentrated RNA was eluted in 30-50 µl RNase-free water. Before further use, quality and concentration of the extracted RNA was investigated at 260 nm using a NanoDrop spectrophotometer (ND-1000, Thermo Scientific).

### 2.2.2 Isolation of RNA from *L. elliptica* and *A. islandica*

RNA extraction of *L. elliptica* and *A. islandica* was improved by using a modified TRI Reagent protocol beforehand (RNA of *L. elliptica* was kindly provided by G. Husmann *et al.* (in revision). Samples (frozen ground powder or pellets) were homogenized in 600 µl TRI reagent by intense vortexing and subsequently using QIAshredder columns. The extraction, as described in Clark *et al.* (2010) but omitting the lithium chloride precipitation step, was followed by a washing step with ethanol (75%). The air dried pellet was then resolved in 100 µl DEPC-treated water mixed with 350 µl RLT buffer (without 2-mercaptoethanol) and 250 µl of 96% ethanol. RNA was further purified using the Qiagen RNeasy Mini Kit as described above (2.2.1).

### 2.2.3 Isolation of messenger RNA (mRNA)

After extraction of total RNA from *M. edulis* (2.2.1) subsequent mRNA extraction for the generation of the transcriptome datasets (2.3.2) and RACE-ready cDNA libraries (2.5.1) was carried out with the Oligotex mRNA Mini Kit (Qiagen), which functions by binding the polyadenylated tails of mRNAs to a special resin. The concentration of mRNA was adjusted by carefully diminishing the volume of mRNA using a centrifugal vacuum concentrator without heat (Concentrator 5301, Eppendorf). RNA quality before and after mRNA extraction was evaluated by spectrophotometric observation using the NanoDrop spectrophotometer (ND-1000, Thermo Scientific) and, additionally, a BioAnalyzer 2100 (Agilent) including the RNA 6000 Nano LabChip Kit (Agilent).

## 2.3    cDNA generation

### 2.3.1    Generation of single-stranded cDNA from total RNA

A prerequisite for further analysis of transcripts is the conversion of rather unstable RNA (2.2) into more stable complementary DNA (cDNA) by using the enzyme reverse transcriptase, which is also referred to as RNA-dependent DNA polymerase. 200 ng to 1 µg total RNA were used directly as template for the generation of single-stranded cDNA using the Advantage RT-for-PCR Kit (Clontech) and the RevertAid Premium First Strand cDNA Synthesis Kit (Fermentas) according to the manufacturer's protocol.

### 2.3.2    Generation of double-stranded cDNA from mRNA

Double-stranded cDNA for the generation of the transcriptome datasets was prepared from 500 ng mRNA of *M. edulis* (2.2.3) using the SMARTer cDNA Synthesis Kit (Clontech). During first strand synthesis the SMART II™ Oligonucleotide was added to the 3' end of the cDNA as described in 2.5.1. The included SMART™ sequence was then recognized by the 5' PCR Primer II A (Clontech) during subsequent second strand synthesis. Afterwards, products were purified using the QIAquick PCR Purification Kit (Qiagen). DNA quality and concentration was examined on a NanoDrop spectrophotometer (ND-1000), by gel electrophoresis as well as with a Bioanalyzer 2100 (Agilent).

## 2.4    Polymerase chain reaction (PCR)

### 2.4.1    Reverse transcription polymerase chain reaction (RT-PCR)

Specific nucleic acid sequences can be amplified for further analysis by using the polymerase chain reaction (PCR) method. In a RT-PCR the first step is the transcription of RNA into DNA as described in 2.3.1. In the next step the obtained cDNA is used as template for PCR including gene-specific oligonucleotides as a starting point for the DNA polymerase. The PCR method is depending on three distinct steps: After cDNA denaturation two opposing gene-specific oligonucleotides bind to their complementary cDNA sequence at an oligonucleotide-specific temperature (annealing phase) and the defined region of cDNA is elongated by a thermostable DNA-polymerase for a certain amount of time (Saiki *et al.* 1985; Mullis & Faloona 1987). The specific target cDNA sequence is amplified exponentially by repeated denaturation, annealing and elongation for several cycles. PCR was performed using the Advantage 2 PCR Kit (Clontech) containing the Advantage 2 Polymerase Mix, which included a small amount of proof-reading *Taq*-polymerase, and further components as displayed in Table 2-1. Employed PCR conditions are described in the following: Initial denaturation of the template at 95 °C for 5 min and

25 to 40 repetitions of the subsequent steps including denaturation at 95 °C for 1 min, annealing of oligonucleotides at $T_{anneal}$ for 1 min as well as elongation at 68 °C for $t_{elong}$. $T_{anneal}$ indicates the oligonucleotide-specific annealing temperature and $t_{elong}$ refers to the elongation time, which is determined by the length of the target sequence (~1 min per 1000 bp). A terminal longer elongation period of 5-7 min was added to ensure complete synthesis of all DNA strands. Afterwards, expected fragment lengths were investigated by agarose gel electrophoresis (2.6).

**Table 2-1: Standard PCR components.**

| Component | Volume (µl) |
|---|---|
| PCR-grade water | 20.0 |
| Advantage 2 PCR Buffer (10x) | 2.5 |
| dNTP mix (10 mM each) | 0.5 |
| Oligonucleotide mix (10 µM each) | 0.5 |
| cDNA template (20-100 ng µl$^{-1}$) | 1.0 |
| Advantage 2 Polymerase Mix (50x) | 0.5 |
| Sum | 25.0 |

## 2.4.2 Real-time quantitative RT-PCR (qRT-PCR) using SYBR Green

The relative quantity of RNA transcripts in comparison to the transcription of a reference gene can be assessed using real-time quantitative RT-PCR (qRT-PCR). After generation of single-stranded cDNA (2.3.1), the amount of template cDNA is evaluated by qRT-PCR using gene-specific oligonucleotides (8.5.2) and a fluorescent intercalating dye, i.e. SYBR Green (Applied Biosystems). The rise in fluorescence above background level, which marks the onset of the exponential phase, is described as the Ct-value (Cycle threshold value). Hence, the Ct-value is negatively correlated to the abundance of the target transcript, since a higher initial amount of the target requires fewer PCR cycle to reach the exponential amplification phase. Prior to qRT-PCR measurements, the target-specificity of oligonucleotides was investigated in a RT-PCR reaction (2.4.1). Obtained PCR products were evaluated by gel electrophoresis (2.6) to confirm the presence and length of transcripts. Subsequent qRT-PCR was carried out according to Table 2-2. PCR cycling conditions were 50°C for 2 min, 95°C for 10 min, followed by 40 cycles of 95°C for 15 s and 60°C for 1 min.

**Table 2-2: qRT-PCR components.**

| Component | Volume (µl) |
|---|---|
| cDNA (1.0-2.5 ng µl$^{-1}$) | 5.0 |
| Oligonucleotide mix (10 µM each) | 0.5 |
| Power SYBR Green PCR Master Mix | 4.5 |
| Sum | 10.0 |

Samples were run in duplicates or triplicates. A melting curve of the PCR product for each primer was also performed to ensure the absence of artifacts. The amount of target DNA is expected to double every cycle during the exponential amplification phase. However, the amplification efficiency (E) often varies greatly among oligonucleotides and templates. Therefore, the efficiency of each oligonucleotide pair (as stated in 8.5.2) was calculated using the Ct-values of a cDNA dilution series. Efficiencies were then determined using the slope of the linear regression employed in the following equation (1):

**Equation 1:**

$$E = 10^{\frac{-1}{m}}$$

E = Efficiency of amplification
m = Slope of the linear regression

Furthermore, the optimal starting amount of cDNA located in the linear phase was derived from the dilution series. The relative quantity of the respective transcript was calculated according to the comparative Ct method (delta Ct) as described by Livak and Schmittgen (2001). At first efficiencies were used to linearize Ct-values and afterwards the amount of target transcript was normalized against the amount of a constitutively active gene (=reference gene) according to the following equation (2):

**Equation 2:**

$$Relative\ mRNA\ expression = \frac{E_{target}^{-Ct}}{E_{reference\ gene}^{-Ct}}$$

E = Efficiency of amplification
Ct = Cycle threshold

The fold change of qRT-PCR expression data is calculated by using the absolut value of relative mRNA expression values above 1 and the reciprocal value of mRNA expression values below 1. Reference genes are used as endogenous controls to compensate for variations in expression caused by external

factors, e.g. due to differences in the amount of initially employed cDNA. Appropriate reference genes should, therefore, not depict a change in expression caused by the experiment. Since further quantification relies on an adequate reference gene, choosing suitable candidates was carried out with great care. 18S rRNA, 28S rRNA, elongation factor 1 alpha and the ribosomal protein S18 were investigated as putative reference genes for *M. edulis* using the program Normfinder (http://www.mdl.dk/publicationsnormfinder.htm). 18S rRNA was selected as the most suitable gene for tissue panel analysis, whereas 28S rRNA was most suitable for expression analysis between different hemocyte treatments in *M. edulis*. Later on during this thesis, an additional suitable reference gene, GAPDH (glyceraldehyde 3-phosphate dehydrogenase), was identified and a reference gene index composed of 28S rRNA and GAPDH was used for normalization of the hemocyte transcriptome dataset expression analysis. Investigation of 18S rRNA and GAPDH as reference genes for *A. islandica* depicted 18S rRNA as most suitable reference gene. 18S rRNA was also the most appropriate reference gene in the DUOX tissue panel and ß-actin in the IL-17 tissue panel for *L. elliptica.*

## 2.5 Rapid amplification of cDNA ends (RACE)

### 2.5.1 RACE-ready cDNA generation using the SMART™ technology

A RACE-PCR (Rapid Amplification of cDNA Ends) can be used to gain knowledge about the full-length nucleotide sequence of transcripts. In order to carry out a RACE-PCR, RACE-ready cDNA was prepared beforehand using the SMARTer RACE Kit (Clontech) according to the manufacturer's manual. To supply a sufficient amount of mRNA, gill tissue of five and hemocytes of ten *M. edulis* individuals were pooled and processed for RNA extraction as described before (2.2.1 and 2.2.3). Subsequent, 3' and 5' RACE-ready cDNA construction was performed with 200 ng mRNA each. During 5' RACE-ready cDNA construction, as depicted in Figure 2-1, using the SMART™ (Switching Mechanism At 5' end of RNA Transcript) technology, the reverse transcriptase binds to the 3' end of the RNA with aid of an oligo(dT) primer (5'-RACE CDS Primer A). Upon reaching the 3' end of the cDNA (corresponding to the 5' end of the RNA) the enzyme adds multiple cytosine residues to the cDNA. These serve as an anchor point for the SMART II™ Oligonucleotide, containing the SMART™ sequence (AAGCAGTGGTATCAACGCAGAGT) and a terminal stretch of guanine residues. This causes the reverse transcriptase to switch the template strand from the mRNA molecule to the SMART™ oligonucleotide adding the SMART™ sequence to the cDNA. During 3' RACE-ready cDNA generation, the 3' SMART™ CDS Primer II A is used as an oligo(dT) primer containing the SMART™ sequence at its terminal end and, hence, adding it to the 5' end of the cDNA (corresponding to the RNA 3' end).

5' RACE-ready cDNA construction    3' RACE-ready cDNA construction
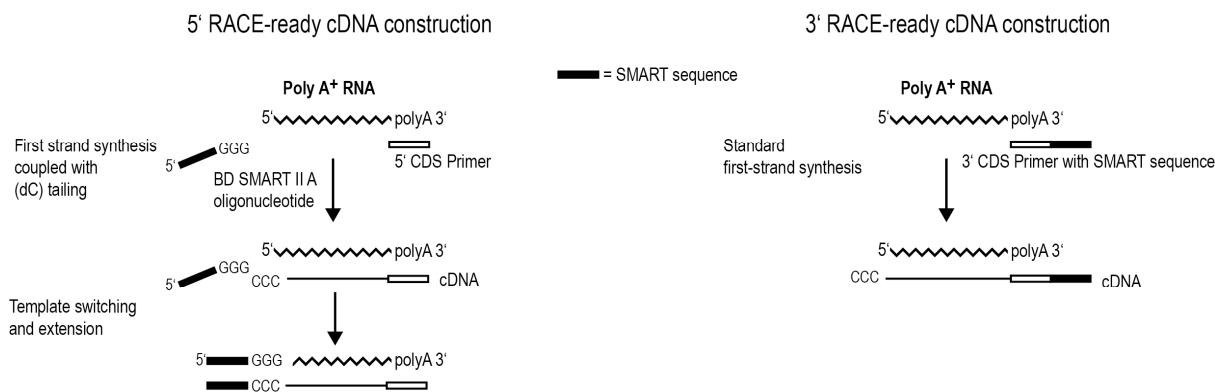


**Figure 2-1: Flow chart of 5' and 3' RACE-ready cDNA generation.** For further details see text section 2.5.1. Graphic modified after the manufacturer (Clontech).

## 2.5.2   RACE-PCR

Full length cDNA sequences can be identified by RACE-PCR, even if only a small fragment of the sequence is known. Therefore, a known sequence (the SMART™ sequence) was added to the 5' and 3' ends of the cDNA during reverse transcription as described in 2.5.1. The 5' and 3' RACE-ready libraries were utilized in RACE-PCR (Table 2-3) together with the universal primer mix (UPM, Clontech) binding to the SMART™ sequence; and a gene-specific primer especially designed for RACE-PCR with its binding sequence located in the known fragment of cDNA (8.5.1). The orientation and expected sequence length of the cDNA sequence was assessed beforehand by comparing the known sequence against verified protein sequences of other organisms in NCBI (tBLASTx). RACE-PCR was carried out according to Table 2-3 using one of the following programs. If the annealing temperature of the gene-specific primer was more than 70 °C, a touchdown PCR program was used to increase PCR specificity including five cycles of 94 °C for 30 sec and 72 °C for $t_{elong}$, five cycles of 94 °C for 30 sec, 70 °C for 30 sec and 72 °C for $t_{elong}$ as well as 20 cycles of 94 °C for 30 sec, 68 °C for 30 sec and 72 °C for $t_{elong}$. If the annealing temperature of the gene-specific primer was between 60-70 °C, a different PCR program was chosen including 20-40 cycles of 94 °C for 30 sec, 68 °C for 30 sec and 72 °C for $t_{elong}$. To remove any unspecific RACE-PCR products, for some fragments a nested PCR was carried out afterwards using a nested gene-specific primer and the nested RACE primer (NSP) from the SMARTer RACE kit (Clontech) in the second PCR program. Control reactions using only the UPM, the NSP or the gene-specific primer were carried out respectively. Acquired PCR products were cloned and Sanger sequenced. After the full-length sequence was obtained, standard PCR oligonucleotides covering the whole length of the transcript were designed for validation of the nucleotide sequence via cloning (2.7) and Sanger sequencing (2.8).

**Table 2-3: RACE-PCR components**

| Component | Volume (µl) |
|---|---|
| PCR-grade water | 34.5 |
| Advantage 2 PCR Buffer (10x) | 5.0 |
| dNTP mix (10 mM each) | 1.0 |
| 3' or 5' RACE gene-specific primer (10 µM) | 1.0 |
| Universal primer mix (10x) | 5.0 |
| 3' or 5' RACE-ready cDNA (~1 ng µl$^{-1}$) | 2.5 |
| Advantage 2 Polymerase Mix (50x) | 1.0 |
| Sum | 50.0 |

## 2.6 Agarose gel electrophoresis

The length of PCR products was determined by separation on agarose gels. The movement of negatively charged DNA fragments through an agarose matrix is triggered by applying an electric field. In this process the velocity of the electrophoretic movement is negatively correlated to the length of the nucleic acid sequence. To cast an agarose gel, 1% (w/v) agarose was dissolved in 1x TAE buffer (Tris-acetate-EDTA buffer, Roth) and heated until completely in solution. After cooling down to approximately 60 °C, 0.3 % (v/v) of the intercalating dye SYBR safe (Invitrogen) was added and the mixture was poured into a gel caster containing a UV-transparent gel tray with a comb. After polymerization for 30 min, the comb was removed and the gel tray holding the solid gel was placed into a horizontal gel chamber containing 1x TAE buffer as running buffer. DNA-loading-buffer (8.3) was added to the samples (1:5) before transferring 10-20 µl of sample or 5 µl of DNA ladder into the gel pockets. Electrophoresis was performed at 95-105 V for 45-75 min. Afterwards, PCR products were visualized under UV light using a molecular imaging system (ChemiDoc XRS with Quantity One 4.6.8, Bio-Rad). Sizes of fragments were estimated via a DNA ladder (see 8.6). If fragments were subjected to further experimental procedures, cDNA bands were cut-out under UV light using a clean disposable scalpel and purified from the gel using the Wizard SV Gel and PCR Clean-Up system (Promega) according to the manufacturer's instructions.

## 2.7 Cloning of PCR products

### 2.7.1 Ligation

PCR products can be amplified in large amounts by cloning to facilitate further sequence analysis. The first step is to ligate cut-out and cleaned PCR products from 2.6 into a plasmid (=vector). Since the Advantage 2 Polymerase Mix used for PCR (2.4) adds adenosine residues to the 3' ends of the double-stranded PCR product, it can be inserted into the pCR2.1-TOPO vector (Invitrogen) via its complementary thymine residues by a ligase. Ligation was carried out at 14 °C in a thermocycler overnight using the TA Cloning Kit (Invitrogen).

### 2.7.2 Transformation

The vector containing the ligated target DNA (2.7.1) can then be incorporated in competent bacteria in a process known as transformation. For this purpose, One Shot TOP10 chemically competent *E. coli* bacteria (Invitrogen) were carefully thawed on ice and 1 µl of the ligation product was added to 15 µl bacteria suspension immediately after melting. The mixture was incubated for 30 minutes on ice to make the bacterial cell wall more permeable before bacteria were heat shocked at 42 °C allowing the plasmid to enter the cell. After an additional 2 min on ice, 150 µl of pre-heated (37 °C) S.O.C. medium (Invitrogen) was added and bacteria were incubated at 37 °C under constant subtle shacking for 1 hour. Afterwards, 100 µl of the suspension was plated on an ampicillin-containing LB (lysogeny broth)-agar plate prepared with 50 µl X-gal (stock: 0.2 % (w/v) in DMF) and grown overnight at 37 °C. Only bacteria, which incorporated the pCR2.1-TOPO vector, were able to survive on the ampicillin-containing agar plate due to expression of the ampicillin resistence gene included in the sequence of the plasmid. Furthermore, positive bacterial clones containing the vector with the ligated target DNA were selected using the blue-white screening technique. Normally, One Shot TOP10 chemically competent *E. coli* express the enzyme β-galactosidase, which can use X-gal as a substrate leading to a blue color of the bacterial colony. If DNA is inserted into the vector, the gene coding for β-galactosidase is interrupted and the colony remains white. Four white colonies per plate were picked with a small pipette tip and transferred to 3 ml of LB-medium containing 100 µg/ml ampicillin. Bacteria were grown overnight at 37 °C under constant shaking (200-220 rpm) thereby also amplifying the amount of plasmids.

### 2.7.3    Extraction of plasmids

Incorporated and amplified vectors were isolated from the bacteria by using the GeneJet Plasmid Miniprep Kit (Fermentas) according to the manufacturer instructions. Therefore, bacterial suspensions were centrifuged for 1 min at 10,000 rpm (~9,300 *g*). After cell lysis and binding of the plasmid using the kit components, pure plasmid DNA was eluted in 50 µl of nuclease-free water. Quantity and quality of the extracted DNA was observed on a NanoDrop spectrophotometer (ND-1000, Thermo Scientific).

## 2.8    Sanger DNA sequencing

The specific nucleic acid sequences can be determined using the dye-terminator sequencing technique, a modification of the Sanger sequencing method originally described by Sanger *et al.* (1977). This technique requires, in addition to the standard PCR components such as template DNA, a gene-specific primer, DNA polymerase and a low amount of modified nucleotides, called dideoxynucleoside trisphosphates (ddNTPs), which terminate the DNA elongation when they are incorporated into the nucleic acid chain. This results into DNA fragments of different length, which can be separated by electrophoresis through capillaries (capillary sequencing). Since the ddNTPs are labeled with fluorescent dyes according to their corresponding nucleobase, the nucleotide sequence can be inferred from the succession of sequence fragments using a laser and a fluorescence detector. To investigate nucleotide sequences of PCR products, best results are obtained, if the target cDNA is firstly cloned and amplified as described before (2.7). Therefore, 300 ng of purified plasmid DNA were employed in the BigDye Terminator v1.1 Cycle Sequencing Kit (Applied Biosystems) according to Table 2-4.

**Table 2-4: DNA sequencing reaction components.**

| Component | Volume (µl) |
| --- | --- |
| Plasmid DNA (300 ng) | x |
| PCR-grade water | *ad.* 10.0 |
| SB buffer (5x) | 1.0 |
| M13 forward **or** reverse (5 µM) | 1.0 |
| BigDye-Mix | 1.5 |
| Sum | 10.0 |

For each plasmid two reactions were carried out, including either the M13 forward or M13 reverse oligonucleotide. M13 oligonucleotides (8.5.3) are complementary to the vector DNA directly adjacent to the side of target DNA insertion. Since the ends are often of bad quality during Sanger sequencing, using these oligonucleotides instead of gene-specific oligonucleotides ensures that the whole target sequence remains identifiable. PCR was conducted according to the following conditions: Denaturation for 1 min at 95 °C, 29 cycles of 95 °C for 10 sec, 50 °C for 5 s and 60 °C for 4 min. Afterwards, samples were sequenced on an ABI PRISM 3700 Genetic Analyzer (Applied Biosystems) and visualized using Sequencher version 4.5 (GeneCodes).

## 2.9 Sequence analyses involving the Basic Local Alignment Search Tool (BLAST)

The Basic Local Alignment Search Tool (BLAST) can be used to calculate the statistical significance of matches (Altschul *et al.* 1990) by comparison of unknown nucleotide or inferred protein sequences to established sequence databases, such as the nucleotide collection (nr/nt) of the National Center for Biotechnology Information (NCBI) or the UniProt protein database of the Universal Protein Resource Knowledgebase (UniProtKB) (see also 8.11). Furthermore, the UniProt/Swiss-Prot database, within the UniProt database only includes reviewed protein sequences. The statistical parameters usually taken from the analysis consist of the score, E value and identity as well as coverage. The score is a quantitative evaluation of the similarity of the query sequence with its corresponding BLAST hit and is calculated by BLAST using a substitution matrix and gap penalties. A higher score indicates a higher homology of the query sequence to the respective BLAST hit sequence. The E value is calculated using the alignment score and indicates the probability to obtain matches with the same score in the database. Therefore, a lower E value represents a higher significance of the distinct BLAST hit meaning that the match is not obtained randomly. The coverage represents the percentage of the query, which could be aligned to the matching BLAST hit. Similarly, the identity gives the percentage of the query sequence, which is identical to the BLAST hit. To examine nucleotide sequences, various BLAST programs were used including BLASTn, BLASTp, BLASTx and tBLASTx. Nucleotide sequences were compared to other nucleotide sequences via BLASTn. Using BLASTp or BLASTx (x=all six reading frames) amino acid sequences were compared to a protein database such as UniProt. Since the current study dealt with nucleotide sequences, these were translated beforehand using for instance ORF Finder (NCBI). If the nucleotide sequence was directly translated and blasted against other translated nucleotide sequences the involved BLAST parameter was tBLASTx (involving all six reading frames). BLAST analyzes were used to infer functional and evolutionary relationships between sequences as well as help identify members of gene families.

## 2.10   Generation of *M. edulis* hemocyte transcriptome datasets

### 2.10.1   Preparation of control and flagellin-challenged hemocytes

In order to gain insight into the immune repertoire of the immune cells of the blue mussel *M. edulis*, transcriptome datasets of control and immune-challenged hemocytes were created. For this purpose, 32 mussels (6-9 cm, ~19 g) were collected in February 2010 and acclimated to 4 °C. As described before (2.1.2), 50 ml hemolymph were extracted and centrifuged gently at 200 g and 4 °C for 5 min. The hemocyte concentration was adjusted to approximately 2,000,000 cells ml$^{-1}$ by removing 26 ml of hemolymph and resuspending the pellet in the remaining 24 ml hemolymph. Afterwards, 1 ml of the cell suspension was plated in each well of two 12-well tissue culture plates. To allow hemocytes to adhere to the culture dish, they were incubated at 4 °C for 1 h and adherence was checked under an inverted microscope (Wilovert H500, Helmut Hund GmbH). Afterwards, the two plates were treated differently by exchanging 25 µl hemolymph per well against 25 µl DPBS (control) or 25 µl flagellin (final concentration: 2.5 µg ml$^{-1}$) (flagellin isolate of *Salmonella typhimurium* strain 14028 obtained from Enzo Life Sciences). A stock solution of 100 µg flagellin per ml was prepared beforehand using distilled water, since the flagellin was already supplemented with PBS. After 4 h of incubation at 4°C, the tissue culture plates were centrifuged at 200 g for 3 min and cells were lysed. Total RNA and subsequent mRNA were extracted as described under 2.2 and double-stranded cDNA was synthesized as described in paragraph 2.3.2, resulting in a cDNA pool of each plate (control or flagellin-stimulated). Subsequent library preparation, emulsion PCR and 454 pyrosequencing were carried out by the sequencing platform of the ICMB (CAU-Kiel, Germany).

### 2.10.2   Library preparation

Double-stranded cDNA from control and flagellin-stimulated hemocytes was further processed into libraries of single-stranded DNA fragments for subsequent 454 pyrosequencing using the Rapid Library Preparation Kit (Roche) according to the manufacturer's manual. At first, double-stranded cDNA was fragmented by nebulization, during which the DNA is forced through a small hole thereby creating a fine mist with fragments of 400 to 800 bp length. Afterwards, blunt ends were ligated to adaptors, which were composed of two different double-stranded oligonucleotides (Adaptor A and B) containing sequences for amplification and nucleotide sequencing. These adaptors were supplied in great excess to the fragments to minimize the formation of cDNA fragment concatemers. Using the biotin moiety on one strand of Adaptor B, the cDNA was immobilized onto magnetic streptavidin-coated beads. Single-stranded template DNA (sstDNA) was produced by melting the non-biotinylated strand off the immobilized bead. As a result, the sstDNA libraries only possessed sequences containing Adaptor B on

merely one end. During the following steps only fragments containing also Adaptor A on the other end could be amplified. Quality and quantity of the obtained libraries were examined and sstDNA was also investigated for fragment size range and average size as well as contaminations with adaptor dimers using an Agilent 2100 BioAnalyzer.

### 2.10.3  Emulsion PCR (emPCR)

sstDNA fragments were further linked to specifically designed DNA Capture Beads and amplified in a emulsion PCR using the GS FLX Titanium SV emPCR Kit Lib-L (Roche) according to the manufacturer's instructions. The optimum library to bead concentration was determined by titration beforehand to obtain the highest possible amount of DNA Capture Beads each bound to only one single sstDNA fragment. Afterwards, the library-bound beads were emulsified in a water-in-oil mixture together with the components needed for amplification; each droplet thereby serving as its own microreactor containing one bead only. During subsequent massively parallel amplification, beads acquired multiple copies of their specific DNA fragment. These clonal colonies remained linked to their corresponding beads even after dispersion of the emulsion by isopropanol. By binding to Enrichment Beads and subsequent centrifugation, beads carrying DNA fragments were separated from beads without a bound DNA fragment. Enriched sstDNA containing beads were then annealed to the Sequencing Primer and sequenced the next day.

### 2.10.4  454 pyrosequencing

Captured, enriched and annealed sstDNA from control and flagellin-stimulated hemocytes was sequenced using the 454 pyrosequencing method (FLX, Roche) according to the GS-FLX-Titanium-Sequencing-Method-Manual (November 2010, Roche). This method, belonging to the second-generation sequencing techniques, allows for high-throughput screening at a low-cost but with shorter read lengths than the Sanger sequencing method described before (2.8). Samples were sequenced on a quarter of a PicoTiterPlate (PTP, Roche) each. The PTP was loaded firstly with a layer of enzyme carrying beads (Enzyme Beads, Roche), before the DNA Beads (Roche) containing the sample DNA or control DNA (internal control for the sequencing reaction) were supplied together with Packing Beads (Roche), which stabilized and immobilized the components in the well. At last another layer of Enzyme Beads was added and covered with a layer of PPiase Beads (Roche), which served as scavengers for inorganic pyrophosphate (PPi) to avoid background noise and interference during sequencing. After loading the beads onto the PTP with mostly only one DNA Bead per well due to its specific surface design, plates were sequenced using the GS FLX Sequencer (Roche). During sequencing the non-

template strand (coding strand) was synthesized by supplying nucleotides in a fixed order. Therefore, amplification reagents were delivered across the wells through a stream of fluid containing only one kind of the four possible nucleotides at a time. Incorporation of a complementary nucleotide led to the release of PPi, which in turn was used by a sulfurylase to produce ATP in the presence of adenosine 5´ phosphosulfate. The obtained ATP was then employed in the conversion of luciferin to oxyluciferin by a luciferase, thereby producing a detectable light signal proportional to the number of nucleotides incorporated. Unincorporated nucleotides and ATP were then degraded by an apyrase, and the procedure was repeated with the next nucleotide. Using the 454 Sequencing Data Analysis software, all wells were recorded in parallel and the nucleotide sequence was inferred by detecting each incorporation event via a CCD (charge-coupled device) camera.

### 2.10.5  Transcriptome dataset assembly and annotation

Assembly and annotation of the resulting sequences was conducted by Dr. Eva Philipp and Lars Kraemer as described in detail in Philipp *et al.* (2012a). After processing by a standardized in-house bioinformatic pipeline, nucleotide sequences were extracted from the 454 output files via the 454 command sffinfo (Roche). Using the tool SeqClean (TGI), SMART™ primer and 454 adaptor sequences as well as polyadenylated tails were trimmed because they would interfere with the assembly. Furthermore, reads with less than 40 bp left after the trimming were removed from further processing. Trimmed reads were firstly assembled with the GS De novo Assembler 2.3 (NEWBLER, Roche) using a minimum overlap length of 40 bp and a minimum overlap identity of 90 %. This was followed by several rounds with TGICL (CAP3) using a minimum overlap length between 40 and 460 bp and a minimum overlap identity between 80 and 98 %. A detailed list of the assembly process is given in Philipp *et al.* (2012a) resulting in the final transcriptome datasets.

To identify putative genes and protein orthologs, contigs and singletons of the final transcriptome dataset were investigated by BLAST (Basic Local Alignment Search Tool) analyses (described in detail in 2.9). These comprise the BLASTx algorithm in the UniProtKB/Swiss-Prot database of the UniProt Knowledgebase (UniProtKB) with a cut off E value (Expect value) of $\leq 10^{-3}$, as well as the tBLASTx (E value $\leq 10^{-3}$) and the BLASTn (E value $\leq 10^{-10}$) algorithm in the NCBI nt database. Furthermore, putative conserved domains, deduced from translated nucleotide sequences, were investigated via InterProScan. Gene Ontology (GO) terms were inferred from the NCBI BLAST and InterProScan results and categorized into 'molecular function', 'cellular component' and 'biological process'. In addition, KEGG (Kyoto Encyclopedia of Genes and Genomes) terms were derived from GO terms and BLAST hits. After the results were assigned to their corresponding contigs and singletons, transcriptome dataset analysis (2.11) was carried out as part of the present study using the Transcriptome Analysis

and Comparison Explorer (T-ACE, http://www.ikmb.uni-kiel.de/tace).The software is described in detail in Philipp *et al.* (2012b). The completed hemocyte database (Run numbers 283 for control and 284 for the flagellin-stimulated transcriptome dataset) can be found as part of the transcriptome database Mytilus_edulis_20100630 at the ICMB (CAU-Kiel, Germany).

## 2.11 Hemocyte transcriptome dataset analysis

### 2.11.1 Pathway analysis

A first overview of conserved and potentially important pathways in immune cells of mussels was obtained by investigating the existing pathways in the hemocyte transcriptome dataset and comparing them between different treatments and tissues. Using the annotations made before (2.10.5) pathway analyses were carried out via the 'RunCompare' tool in the transcriptome analysis software T-ACE. The 'RunCompare' tool compares transcriptome datasets on the basis of different parameters such as KEGG terms and their corresponding classification into different KEGG pathways. The total number of contigs and the number of contigs present in each KEGG pathway in the selected datasets together is detected (reference dataset). Based on these numbers, the number of expected contigs for each KEGG pathway within each datasets can be deduced from the total contig number within each dataset. By comparing the expected number to the number of contigs present in each dataset, p-values for significantly ($p < 0.05$) enriched, i.e. over-represented, or depleted, i.e. under-represented, KEGG pathways were calculated using the Fisher's exact test (not corrected for multiple testing). The obtained p-values were plotted using the -log (p-value). Negative values indicate depletion whereas positive values indicate enrichment. To identify enriched or depleted pathways in bivalve immune cells in general, the unstimulated hemocyte dataset (run ID 283 in the Mytilus_edulis_20100630 database) was compared to combined datasets of unstimulated tissues, including mantle, mantle rim, digestive gland, gill, foot and adductor muscle tissue (run IDs 272, 273, 115, 138, 152, 186, 222 and 231).

Furthermore, for analyses within the hemocyte transcriptome dataset, contigs were separated beforehand according to whether they were up- or down-regulated after flagellin stimulation. For this classification the 'Database statistics' module in T-ACE was employed as explained in detail below (2.11.2). Contigs with a minimum length of 100 bp, ≥20 reads per contig and with at least a two-fold change in expression were used for the analysis. The resulting two cohorts, one containing up- and the other down-regulated contigs, were then compared to the whole hemocyte transcriptome dataset using the 'RunCompare' tool. The entire hemocyte dataset was used as a reference (containing even the non-regulated contigs), which provided the total number of contigs for each KEGG pathway and, hence, the basis for the calculation of the expected number of contigs for each cohort.

### 2.11.2  Screening for contigs of putative immune gene orthologs

Contigs and their respective annotations were further analyzed using the software T-ACE. To identify conserved and potentially important immune-relevant contigs, transcripts were filtered according to selected parameters to narrow down the number of suitable candidate genes. An overview of the filtering steps is given in Figure 2-2. Fold change refers in the following to a negative or positive change in expression respectively. At first contigs displaying at least a 1.4 fold change in expression, a minimum contig length of 100 bp and a minimum read number of 3 reads per contig were derived from the database. The list of up- and down-regulated contigs and their corresponding annotations was then extracted from T-ACE and further processed in Windows Excel (Microsoft). Contigs with more than 50 reads were investigated for their possible function in more detail by literature search and/or re-blasting. This was also conducted for the 30 highest up- or down-regulated contigs (sorted by the extent of their fold change). In addition, contigs with ≥10 reads existing only in the control or flagellin-stimulated database as well as contigs present only in the transcriptome dataset of hemocytes in comparison to other tissues (fold change=∞) were examined in more detail as well. The same procedure was also carried out for the 50 highest up- or down-regulated contigs with >500 reads comparing the hemocyte dataset against all other *M. edulis* tissue transcriptome datasets existing at our institute (Philipp *et al.* 2012a). Setting cut-off values for the number of reads reduced the risk of false positive results.
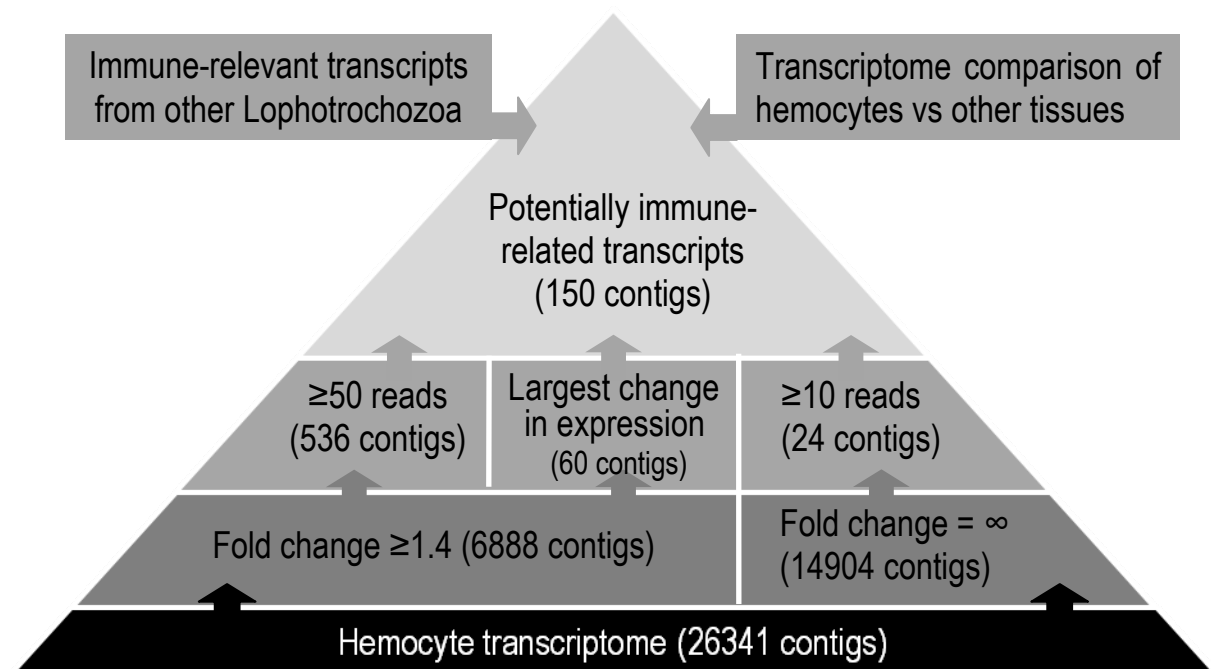


**Figure 2-2: Schematic drawing of hemocyte transcriptome dataset screening for the selection of potentially immune-relevant transcripts.** This figure provides only a brief overview; further details are given in the text. Only transcripts with a putative relevance for the immune system were included in the last step. Information about the immune-relevance of orthologs was mainly obtained from literature search.

**Table 2-5: Lophotrochozoan transcriptome datasets used to identify unifying immune-relevant transcripts.**
*Vibrio splendidus = V. splendidus, Vibrio* sp. *= V.* sp., *Micrococcus luteus = M.luteus, Echinostoma caproni = E. caproni.*

| Reference | Organism | Tissue | Stimulus | Method |
|---|---|---|---|---|
| Venier *et al.* (2011) | *Mytilus galloprovincialis* | Hemocytes | *V. splendidus* | Immunochip |
| de Lorgeril *et al.* (2011) | *Crassostrea gigas* | Hemocytes | *V.* sp. | DGE |
| Mitta *et al.* (2005) | *Biomphalaria glabrata* | Hemocytes | *E. caproni* | random cDNA Library |
| Hanelt *et al.* (2008) | *Biomphalaria glabrata* | Whole animal | *M. luteus, E. coli* | ORESTES sampling |
| Hou *et al.* (2011) | *Patinopecten yessoensis* | Mixed tissues | none | 454, FLX |
| Bettencourt *et al.* (2007) | *Bathymodiolus azoricus* | Gill | none | 454, FLX |
| Altincicek & Vilcinskas (2007) | *Platynereis dumerilii* | Whole animal | LPS | enriched cDNA Library |

As a next step, contigs potentially coding for none or even distant immune-related functions such as for instance β-actin were omitted. Putative immune-relevant contigs being related to each other were combined into pathways or functional clusters (e.g. Toll-like receptors pathway or apoptosis cluster) to facilitate further investigations.

To find unifying principles among the immune-responses in Lophotrochozoa, the hemocyte transcriptome dataset was compared to transcriptome analyses of other authors involving different immune stimuli (see Table 2-5). Transcriptome datasets were investigated for similarities and only those contigs were included in further analyses, which were present in our transcriptome database and in at least two of the other hemocyte transcriptome datasets from Table 2-5. A detailed file of the filtering process can be found in the supplements (see section 9.3).

To gain deeper insight into the expression of a few selected immune-relevant contigs from the obtained list, 19 candidate genes putatively important for the immune responses in bivalves were chosen. Their time-dependent expression was examined by investigating different durations of flagellin stimulation (described in detail in 2.15.1) in qRT-PCR analyses.

## 2.12 Investigation of selected immune gene orthologs

### 2.12.1 Identification and validation of NOX and DUOX as well as IL-17 transcripts

Transcripts of common immune gene orthologs were investigated in depth during the course of this thesis, which comprised transcripts potentially coding for NADPH- (NOX) and dual oxidases (DUOX) as well as interleukin-17-like (IL-17) cytokines. In addition, the minor subunits of NOX and DUOX, DUOXA and p22$^{phox}$, were included in the analysis as well. To identify contigs and singletons coding for the corresponding ortholog, key word and protein structure searches were carried out in the entire *M. edulis*

transcriptome database as well as in the transcriptome databases of the bivalves *L. elliptica* (Laternula_elliptica_2010110 database) and *A. islandica* (Arctica_islandica_20110826 database) using the T-ACE software. Databases of bivalves were generated at the ICMB and are described in detail for *L. elliptica* in Husmann *et al.* (in revision) and for *A. islandica* in Philipp *et al.* (2012c). The *A. islandica* transcriptome database was, however, extended after this first study and now comprises 116,375 contigs. The respective reads of each contig or singleton, putatively coding for the desired protein, were extracted from T-ACE and assembled with at least 20 bp overlap and 80% identity using the program Sequencher 4.5. This procedure distinctly decreased the number of base ambiguities in comparison to the transcriptome assembly and in some cases connected multiple contigs/singletons with each other. Afterwards, the newly assembled contigs were blasted by hand via nr/nt (tBLASTx, NCBI) to verify their annotations. Fragments were validated via PCR and Sanger sequencing (2.8). To obtain the nucleic acid sequence of full length transcripts, information about an unknown sequence fragment, separating two known sequence fragments (contigs or singletons) putatively coding for the same protein ortholog, was obtained using oligonucleotides spanning the missing sequence in a standard RT-PCR. In addition, nucleotide sequences for *Me* DUOX-a, *Me* DUOX-b and *Me* DUOXA were extended by RACE-PCR (2.5). In the end, sequences verified by Sanger sequencing were blasted in NCBI (nr/nt) and open reading frames were obtained using the program ORF Finder (NCBI). Domain and protein homologies were investigated using the simple modular architecture research tool (SMART, NCBI) and UniProt/Swiss-Prot (BLASTp, UniProtKB).

### 2.12.2 Identification of NOX and DUOX orthologs in other Lophotrochozoa

To validate the presence of NOX and DUOX orthologs at gene and transcript level among the superphylum of Lophotrochozoa, publicly available transcriptome and genome databases of other species were searched by key word search. These databases consisted of the MolluscDB by Mark Blaxter, DBGET from KEGG, Mytibase (a joint research project) and databases by the US Department of Energy Joint Genome Institute (JGI). Web addresses are given in the Materials section (8.11). The identified translated nucleotide sequences were blasted in UniProt/Swiss-Prot for a more detailed insight into the degree of conservation. Since in most cases only fragments of transcripts were available, sequences were further investigated in SMART for their putative domain architecture to identify which part of the enzyme they most probably resemble. Only fragments with ≥99 aa (amino acids) were included, because domains of shorter fragments could not successfully be predicted.

## 2.13 Construction of phylogenetic trees

The evolutionary relationship of NOX and DUOX orthologs from *M. edulis*, *L. elliptica* and *A. islandica* was further investigated using phylogenetic analysis. Therefore, the amino acid sequences of NOX and DUOX of other animals were extracted via key word search from the NCBI protein database. Sequences of plants and amoeba as well as algae and fungi were included as phylogenetic distant control groups (=out-groups). It was aimed to obtain around three orthologs per taxonomic group and, if possible, sequences, which were already reviewed in UniProt/Swiss-Prot (sequences are listed in Table S 2 and following). Mostly amino acid sequences inferred from the complete open reading frame (except otherwise stated) were included. Protein sequences were aligned using the MUSCLE tool (Edgar 2004) implemented in MEGA 5.05 (Tamura *et al.* 2011) (alignment files see supplements). Preliminary phylogenetic trees were calculated using the Maximum Likelihood, the Neighbor-Joining and the Minimum Evolution method. The succession of species and the corresponding information about their evolutionary relationship was very similar among the different methods. Therefore, the Maximum Likelihood method, displaying the best bootstrap values in this study and, hence, the highest reliability, was used to construct phylogenetic trees. The optimal amino acid substitution model was calculated beforehand using MEGA 5.05: Trees containing orthologs of NOX5 were therefore created using the Jones-Taylor-Thornton (JTT) (Jones *et al.* 1992) model, whereas trees for DUOX and NOX2 were generated via the Whelan and Goldman model (WAG) (Whelan & Goldman 2001). In every case, gamma distribution was used to model evolutionary rate differences among sites. Sequence sites with gaps were only partially deleted with the Site Coverage Cutoff set to 95 %, which means that the site was excluded from tree construction if it possessed more than 95 % ambiguous amino acids. The reliability of internal branches was calculated using 100 bootstrap pseudo-replicates (Felsenstein 1985).

## 2.14 Reactive oxygen species (ROS) detection in *M. edulis*

### 2.14.1 Time and dose dependent extracellular ROS production

Reactive oxygen species (ROS) production in hemocytes was investigated using the extracellular Amplex Red reagent (Invitrogen). Via a horse radish peroxidase (HRP Type II, Sigma-Aldrich) Amplex Red is converted to the fluorescent compound resorufin in the presence of reactive oxygen, i.e. hydrogen peroxide. To examine time and dose dependent ROS production upon immune stimulation, *M. edulis* individuals were collected in February 2011 and the hemolymph of 4-5 mussels per experiment was extracted and pooled as described before (2.1). Afterwards, hemocytes were plated in a 24-well culture plate at a density of 659,000 (±44,000) cells ml$^{-1}$ (1 ml hemolymph per well). Cells were allowed to adhere for 30 min before checking the attachment under an inverted microscope (Wilovert

H500, Helmut Hund GmbH). Afterwards the media was withdrawn and replaced with mussel-isosmotic DPBS, obtained by adjusting the osmolality to 500 mOsm kg$^{-1}$ with sodium chloride and checked with an Osmomat 030 (Gonotec). Osmoconformers, such as blue mussels, possess nearly the same osmolality as the seawater with a yearly average of approximately 500 mOsm kg$^{-1}$ at the sampling site in the Kiel Fjord. Note, that all analyses involving DPBS in this study were conducted using mussel-isosmotic DPBS. For extracellular ROS assays, DPBS was supplemented with 17 µM Amplex Red reagent as well as 100 mU horse radish peroxidase beforehand. After the solution was added to the wells, 100 µl supernatant per well was transferred immediately to wells of a black 96-well plate (Becton Dickson) and quantified at 530-560 nm excitation and 590 nm emission (Gain 25) in a GeniosPro Plate reader (Tecan) serving as the zero-point measurement. Cells were then stimulated using 100 µl isosmotic DPBS with 0, 25, 50 or 100 µg ml$^{-1}$ zymosan A (Sigma-Aldrich) or with 0.7, 1.3, 2.6 x 10$^7$ CFU ml$^{-1}$ *Listonella anguillarum* (prepared beforehand as explained in 2.1.4) for 0, 5, 15, 30, 60, 120 and 240 min. All incubations were carried out at 15 °C and after the respective periods of time 100 µl supernatant was transferred to the black 96-well plate and quantified using the plate reader as described before. Results were given in relative fluorescent units (RFU). For each treatment five replicate experiments were carried out (n=5). For every experiment positive controls, consisting of 100 µM hydrogen peroxide in DPBS, and negative controls, containing each stimulus without cells, were conducted.

### 2.14.2  ROS production upon NOX/DUOX activating or inhibiting compounds

More insight into the origin of ROS production was obtained by employing specific activators and inhibitors of the NOX and DUOX family of ROS generating enzymes. NOX and DUOX are thought to be stimulated by PMA (phorbol 12-myristate 13-acetate). PMA activates the protein kinase C, which in turn phosphorylates and activates subunits of NOX and DUOX enzymes. NOX and DUOX can also be inhibited by DPI (diphenyleneiodonium), which supposedly interacts with the catalytic core of the enzyme complex, the flavocytochrome b$_{558}$. The Amplex Red assay was conducted in a similar way as described before (2.14.1) including plating of hemocytes (880,000 ±380,000 cells per well) obtained from mussels caught in February 2011 and addition of the Amplex Red assay components. At first, 10 µM DPI (Sigma-Aldrich) or isosmotic DPBS (control) were added to each well. Cells were incubated at 15 °C for 45 min. Secondly, 100 µl stimulus or isosmotic DPBS (control) were added to the corresponding wells and incubated at 15 °C for 2 hours. This way, cells exposed to either DPBS or DPI in the first step were either stimulated with DPBS, 10 µg ml$^{-1}$ PMA (Sigma-Aldrich) or 50 µg ml$^{-1}$ zymosan A (Sigma-Aldrich) in the second step. As a consequence, stimulated cells were either incubated with an activator or an inhibitor alone, or incubated with both an inhibitor and an activator together. Five replicate experiments were conducted (n=5). For every experiment positive controls,

consisting of 100 µM hydrogen peroxide with or without DPI in DPBS containing Amplex Red, were included. Negative controls comprised each stimulus, i.e. PMA and zymosan A, without cells in DPBS containing Amplex Red. At the end of each experiment, 100 µl per well was transferred to a black 96-well plate and measured at 530-560 nm excitation and 590 nm emission in a GeniosPro Plate reader (Tecan).

NOX5 and DUOX enzymes additionally possess two or more EF-hand calcium binding motifs. Therefore, ROS production can also be inhibited by using a calcium chelator, such as 1,2-bis(o-aminophenoxy)ethane-N,N,N',N'-tetraacetic-acid (BAPTA). The membrane permeable form BAPTA-tetra(acetoxymethyl)ester (BAPTA-AM) can easily penetrate the membrane and, therefore, specifically trap intracellular calcium. To investigate the influence of BAPTA-AM on ROS production in hemocytes, hemolymph was withdrawn and pooled from 2-3 animals collected in October 2011 according to the procedure described before (2.1). Using a 96-well cell culture plate, 100 µl hemolymph per well were plated in triplicates at a density of 703,000 (±85,000) cells ml$^{-1}$. After 30 min of incubation at 15 °C, 1 mM BAPTA-AM (Calbiochem) or DPBS as a control were added to the wells and incubated for another 30 min. Afterwards 100 µg ml$^{-1}$ zymosan A or DPBS as a control were added and the supernatant was quantified after 2 hours in a black 96-well plate using the GeniosPro Plate reader (Tecan) as described before. Three replicate experiments were conducted (n=3). As positive controls 100 µM hydrogen peroxide was added to Amplex Red-containing DPBS with or without BAPTA-AM. Negative controls consisted of zymosan A without cells.

### 2.14.3  The role of phagocytosis in ROS production

To access the function of phagocytosis in ROS production, further ROS tests were carried out using carboxylated latex beads (1 µm, Polysciences). Overnight, beads were coated either with DPBS (control beads) or an immune challenging component, such as 2.5 µg ml$^{-1}$ flagellin, 30 or 50 µg ml$^{-1}$ LPS. The next day, 1 ml hemolymph per well was plated in a 24-well plate and after 30 min incubation the hemolymph was exchanged for the Amplex Red assay compounds in DPBS. After 2 hours, 100 beads per hemocyte were added. Corresponding negative and positive controls were included. After additional 2 hours, ROS production (n=3 technical replicates) was evaluated using the GeniosPro Plate reader (Tecan).

### 2.14.4  Intracellular ROS production

To localize oxygen radical production within hemocytes, intracellular generation of ROS was visualized by microscopic observation (EVOS fl, PeqLab) of the 2', 7'-dichlorfluorescein-diacetate (cDCFH-DA) dye (Sigma-Aldrich) and its ROS-coupled conversion to green fluorescent DCF. Therefore, hemocytes were

plated in 24-well plates as described before (2.1.2) and incubated with 10 µM DCFH-DA for 30 min. *L. anguillarum* bacteria were prepared as described in 2.1.4 and labeled for microscopic observation using the red fluorescent dye BacLight (Molecular Probes). 10 ml of bacteria ($OD_{612}$ = 0.1) were incubated with 100 nM BacLight in a shaking incubator at 160 rpm and 28 °C for 30 min. Afterwards, the suspension was centrifuged at 3,000 rpm (~1,950 *g*) for 10 min and the pellet was resuspended in 1 ml DPBS. Pure DPBS (as a control), zymosan A (50 µg $ml^{-1}$) or labeled *L. anguillarum* (1.3 x $10^7$ CFU $ml^{-1}$) were added to the wells containing DCFH-incubated hemocytes and ROS production was investigated under the microscope. Captured images were analyzed using the program Image J.

## 2.15 Immune-stimulation of hemocytes for the expression analysis of selected immune genes

### 2.15.1 Short-, mid- and long-term expression analysis

A more detailed insight into the regulation of selected immune gene orthologs was obtained by investigating the expression of hemocytes at transcript level upon immune-challenge. Therefore, experiments were conducted consisting of different stimuli and different durations of stimulation (see Table 2-6). However, the same workflow was applied for each experiment. At first mussels were reared and hemolymph was collected as described before (2.1). Hemocytes were plated in triplicates for each treatment and time point using 1 ml hemolymph per well (see Table 2-6 for details).

**Table 2-6: Overview of experiments incubating hemocytes of *M. edulis* with immune-challenging components.** The stimulants used in the respective experiment and their corresponding duration of exposure are given. For zero exposure DPBS was added as a control. The biotic parameters of each experiment such as the sampling date and the amount of mussels used as well as their particular hemocyte concentration is stated. 6-8 replicate experiments were performed for every analysis. *L. a.* = *Listonella anguillarum*.

| Experiment | Stimulant | Time of exposition to stimulant | Mussels | | Hemocyte concentration [cells $ml^{-1}$] | Number of replicate experiments |
|---|---|---|---|---|---|---|
| | | | Date of collection | Number of individuals | | |
| Short-term analysis | 50 µg $ml^{-1}$ zymosan A<br>1.3 x $10^7$ CFU *L. a.* | 0, 5, 15, 30 and 60 min | August, 2010 | 11-20 | 605,000 (±187,000) | 8 |
| Mid-term analysis | 2.5 µg $ml^{-1}$ flagellin<br>1.3 x $10^7$ CFU *L. a.* | 0, 1, 2, 4 and 8 hours | August, 2010 | 15-21 | 580,000 (±110,000) | 7 |
| Long-term analysis | 50 µg $ml^{-1}$ LPS<br>1.3 x $10^7$ CFU *L. a.* | 0, 3, 6, and 24 hours | February, 2011 | 12-16 | 513,000 (±985,000) | 6 |

After hemocytes adhered to the 24-well plate, 50 µl of hemolymph was replaced by the respective stimuli at the corresponding time point. All wells in an experiment were incubated for the same duration; only the exposition to the respective stimuli was varied by adding the stimuli at particular times before the end of the experiment. For example wells stimulated with LPS for 6 hours during the 24 hours long-term experiment were supplemented with LPS 18 hours after the start of the experiment, hence being exposed to LPS for the remaining 6 hours. This experimental setup decreased the variability, which may otherwise be caused by the different time spans of general handling stress, and also made only one control treatment necessary. To obtain unstimulated controls, DPBS was added to control wells at the beginning of each experiment. In the end, the supernatant was removed and attached cells were lysed directly in the wells. The remaining supernatant was centrifuged (400 g, 2 min) and the pellets were also lysed using RLT buffer (RNeasy Kit, Invitrogen). Lysates of three replicate wells with the same treatment were pooled and RNA was extracted as described before (2.2.1). The RNA was used to synthesize single-stranded cDNA (2.3.1), which was employed in further qRT-PCR expression analysis according to 2.4.2.

In addition, 100 µl hemolymph per well was also plated in triplicates in wells of a 96-well plate. This plate was used to investigate ROS production of the corresponding stimuli simultaneously to the subsequent expression analysis. Since the time dependent ROS production was already investigated in detail before (2.14.1), only one time point was involved in the analysis. For the short- and the mid-term expression analysis the longest time points were chosen (1 or 8 hours respectively). The long-term analysis incubated up to 24 hours, which led to autoxidation of the Amplex Red dye and, therefore, the 6 hour time point was selected for the ROS production assays. The Amplex Red test was carried out as discussed above (2.14).

### 2.15.2  Heat-killed bacteria

Most analyses in this thesis involving bacteria were carried out with living *Listonella anguillarum*. Since bacteria supposedly alter the immune response of their hosts to ensure their own survival, the influence of heat-killed *Listonella anguillarum* on the expression of selected immune genes orthologs was further investigated. Therefore, *Listonella anguillarum* bacteria were prepared as described before (2.1.4) and a part of the suspension was inactivated at 60 °C for 1 hour. The efficiency of heat-killing was 99 % as confirmed by plating triplicates on agar plates made from medium 101. DPBS, living or killed bacteria ($1.3 \times 10^7$ CFU ml$^{-1}$) were added to the attached hemocytes in a 24-well plate respectively as described above (2.15.1). After 2 hours hemocytes were lysed and processed for further qRT-PCR analysis. The experiment was carried out twice (n=2).

## 2.16  RNA interference (RNAi)

### 2.16.1  Hemocyte *in vitro* RNAi assays using small interfering RNA (siRNA)

Further insights into the function of transcripts and their corresponding proteins can be obtained using the RNAi (RNA interference) pathway resulting in the knock-down of specific transcripts. To take advantage of this pathway, short sequences (~20 bp) of double-stranded small interfering RNA (siRNA) complementary to a specific target transcript were synthesized. These can be recognized by the intracellular RNA-induced silencing complex (RISC), which incorporates the guide strand resulting in the degradation of the second strand (passenger strand). As a consequence, the guide strand can bind to its complementary target RNA transcript leading to its cleavage in a process called post-transcriptional gene silencing.

Preliminary experiments were conducted to determine the best method for the delivery of RNAi molecules into hemocytes. Therefore, fluorescently labeled control siRNA (Alexa Fluor 647, Invitrogen) was added to the cells in presence or absence of different transfection reagents. The transfer of siRNA into hemocytes was examined under a confocal laser scanning microscope (TCS SP5, Leica) at 650 nm absorption and 665 nm emission. As depicted in Figure 2-3 hemocytes appear to "ingest" the siRNA molecules by themselves, which seemed to be captured in phagocytic vacuoles. This response was indifferent whether a transfection reagent was present or not, making chemical transfection unnecessary. This is consistent with observations that ingestion of bacteria expressing dsRNA can also lead to a RNAi mediated knock-down of target mRNA in *Caenorhabditis elegans* (Timmons & Fire 1998; Timmons *et al.* 2001).
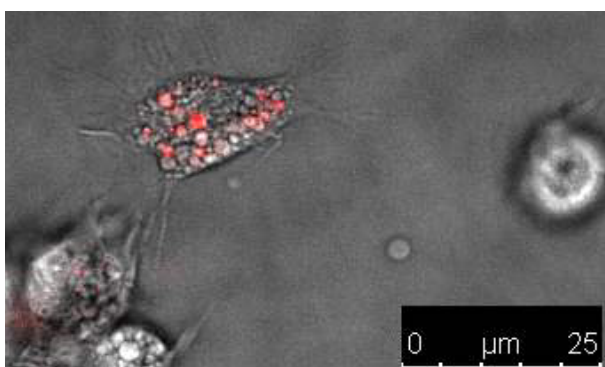


**Figure 2-3: Labeled siRNA (red) ingested by a hemocyte.** The picture was taken with a 40x objective on a confocal laser scanning microscope. A scale bar is depicted on the lower right side.

The verified sequence of *Me* DUOX-b was used as a template for siRNA synthesis in the RNAi Designer (Ambion). siRNA sequences containing more than two repetitive bases in a row were omitted, since they can act as a termination signal. Furthermore, the GC content was limited to a range of 30-50 % GC. By blasting obtained siRNA target sequences against the *M. edulis* transcriptome database in T-ACE (BLASTn), targets with more than 16-17 bp homology to other sequences were also

discarded. Even though it is known that the efficiency of siRNA transfection is not depending on the location within the corresponding transcript, two siRNAs located within the functional domains of *Me* DUOX-b were chosen as displayed in Table 2-7.

Hemocytes were incubated with a pool of both siRNAs (60-120 nM) for 24-72 hours (n=2-3). After RNA extraction (2.2.1) and cDNA generation (2.3.1) *Me* DUOX-b expression was analyzed using semi-quantitative RT-PCR (2.4.1) and normalized against the expression of the 28S rRNA reference gene. ROS generation was supervised using the Amplex Red test including zymosan A (50 µg ml$^{-1}$) stimulation as described before (2.14) in a 96-well plate.

**Table 2-7: *Me* DUOX-b siRNA target sequences.** All siRNAs were obtained from Ambion.

| Target sequence | Target domain |
|---|---|
| AACAGGACAATCACCTAATAA | Peroxidase |
| AACTGTCTGATTCTTCATTGG | EF-hand |

### 2.16.2 *In vivo* RNAi injection assays using long double-stranded RNA (dsRNA)

In some eukaryotes, such as the nematode *Caenorhabditis elegans* (Fire *et al.* 1998), target transcripts can be silenced by injecting longer (<500 bp) double-stranded RNA (dsRNA) molecules directly into the organism. Inside the cell, these molecules are cleaved into small fragments of around ~20 bp by an enzyme called Dicer, which leads to a similar response as the siRNA induced knockdown described above.

As a second approach for RNAi, DUOX family specific dsRNAs, targeting *Me* DUOX-b and *Me* DUOXA, were created employing the MEGAscript High Yield Transcription Kit (Applied Biosystems). Therefore cDNA templates of the target sequences containing the annealing sequence for a T7 polymerase on one end were produced in a standard RT-PCR (2.4.1) using specific oligonucleotides and conditions (Table 2-8). For details on primer construction see 8.5. The obtained PCR products were purified via the Wizard SV Gel and PCR Clean-Up System (Fermentas) and their quality and quantity investigated on a spectrophotometer (NanoDrop 1000, Thermo Scientific).

Employing a polymerase of the phage T7, 1 µg of each template cDNA was transcribed into single-stranded RNA. Transcription was carried out at 37 °C for 16 hours using the components of the kit according to the manufacturer's instructions. Afterwards, the template cDNA was digested by a DNase at 37 °C for 15 min, before the reaction was stopped using ammonium acetate (both included in the kit). The remaining RNA was extracted by adding one volume of phenol/chloroform/isoamyl alcohol

(25:24:1) and then one volume of pure chloroform (both Sigma). After mixing, the aqueous phase was transferred to a new tube to remove any unincorporated nucleotides, enzymes and salts. Using one volume of isopropanol (Merck) the RNA (incubation: 15 min, -20 °C) was precipitated after centrifugation at 4 °C and 16,000 g for 15 min. The RNA pellet was resuspended in RNase-free water and both the sense and the antisense reaction were mixed.

**Table 2-8: Oligonucleotides used for template cDNA generation for subsequent dsRNA synthesis.** PCR was performed for 35-37 cycles using 60 °C annealing temperature and 1 min elongation time. Starting sequence for T7 polymerase is written in italics.

| Target | Strand | Sequence 5' → 3' | Amplicon length (bp) |
|---|---|---|---|
| *Me* DUOX-b | Sense | *CCAAGCTTCTAATACGACTCACTATAGGGAGA*TTGTTGGGGGATTGATTGAG TGTGTGTGGTTCCTTGGTCTT | 560 |
| | Antisense | TTGTTGGGGGATTGATTGAG *CCAAGCTTCTAATACGACTCACTATAGGGAGA*TGTGTGTGGTTCCTTGGTCTT | |
| *Me* DUOXA | Sense | *CCAAGCTTCTAATACGACTCACTATAGGGAGA*CATTTTGACTGGAGATGGGAAC ACGCTCTTTGGTGTGCTTG | 567 |
| | Antisense | CATTTTGACTGGAGATGGGAAC *CCAAGCTTCTAATACGACTCACTATAGGGAGA*ACGCTCTTTGGTGTGCTTG | |

The RNA product is denatured by heating for 5 minutes at 75 °C and then immediately placed at room temperature for 3-4 hours to allow formation of dsRNA while the mixture cools down slowly. Quantity and quality was investigated via the intercalating dye PicoGreen (Quant-iT PicoGreen dsDNA reagent, Invitrogen Invitrogen) using a fluorospectrophotometer (NanoDrop ND-3300, Thermo Scientic). Since PicoGreen is primarily designed for double-stranded DNA, a standard curve was created at first using known concentrations of commercially obtained siRNA (Ambion, see 2.16.1). In addition, RNA concentration was investigated on a spectrophotometer (NanoDrop 1000, Thermo Scientific) and agarose gel electrophoresis was carried out as described in 2.6 estimating the approximate size and quantity by a DNA ladder. If all the information gathered about dsRNA quantity and quality were consistent, 30 µg of dsRNA were dissolved in 200 µl of sterile seawater (filtered through a 0.22 µm syringe filter, Rotilabo, Roth). Four treatments were prepared consisting of (1) pure sterile seawater or seawater with (2) *Me* DUOX-b or (3) *Me* DUOXA, respectively, or (4) *Me* DUOX-b/*Me* DUOXA together.

Mussels (26.2 ± 0.6 g, 64.1 ± 0.3 cm) were collected in October 2011 and treated as described before (2.1). Four mussels each were placed into four 6 l plastic aquaria (one for every treatment) located within the temperature-constant room (15 °C) and acclimated for a day. Water with an average salinity of 13.1 g kg$^{-1}$ (supervised daily using a PH/COND Instrument from WTW, VWR) was renewed every day. At the end of each experiment, accumulation of ammonia and nitrite in the aquaria was examined using the $NH_4$-Ammonium-Test-Set and the $NO_2$-Nitrite-Test-Set (both JBL) and potential harmful accumulation of neither ammonia (~0.6) nor nitrite (~0.3) was observed. For each treatment, 200 µl of either sterile seawater or the respective dsRNA in seawater were injected directly into the adductor muscle and incubated for four days. On the fifth day hemocytes were extracted according to the procedure described before (2.1.2) and 100 µl of the hemolymph was plated in triplicates in a 96-well plate. After adherence for 30 min, cells were stimulated with zymosan A (50 µg ml$^{-1}$) or *L. anguillarum* (1.3 10$^7$ CFU ml$^{-1}$) for 2 hours and the Amplex Red ROS detection assay was carried out as indicated before (2.14). The remaining hemolymph was centrifuged and further processed for qRT-PCR analyses (2.4.2). Experiments were conducted in triplicates.

## 2.17  Statistics

Data was tested for normality using the Kolmogorov-Smirnov test, which provides the basis for the following statistical analysis. If data passed the test, the analysis of variance (ANOVA) or the Student's t-test were employed accordingly. ANOVA was followed by the Bonferroni post-hoc test. If the normality test failed, data was log transformed and if it failed again the non-parametric Mann-Whitney test (U-test) or the Kruskal-Wallis-Test (H-test) including the Dunns post-hoc test were applied respectively. Data was additionally checked for equal variances using the Bartlett's test and the F-test. In case of unequal variances, an unpaired t-test with Welch's correction was performed. For time and dose dependent ROS production a two-way ANOVA, using stimulus concentration and duration as factors, was carried out. Included significance levels were 99.5 %, 99.0 % and 99.9 %. The software Prism 5.03 (Graph Pad software Inc.) was used for statistical analyses and generation of figures. General calculations were conducted in Excel (Microsoft).

A standard deviation threshold of 0.5 for three technical replicates from qRT-PCR was used to exclude samples with substantial measuring inaccuracies. Furthermore, outliers were removed from the expression analysis using the Grubbs' test (http://graphpad.com/quickcalcs/Grubbs1.cfm). Since fold changes of qRT-PCR expression data do not contain numbers between 1 and -1, statistical tests were carried out using the relative mRNA expression data for Figure 3-16.

## 3.  RESULTS

### 3.1  Immunotranscriptome analysis in *M. edulis*

#### 3.1.1  General characteristics of the generated hemocyte transcriptome data sets

Hemocytes can be regarded as the immune cells of bivalves exhibiting various humoral and cellular defense responses (Canesi *et al.* 2002). To gain a deeper insight into the immune repertoire of the blue mussel *Mytilus edulis*, transcriptome datasets of control and flagellin-challenged hemocytes were generated on a Genome Sequencer FLX system (454, Roche). 181,117 reads were obtained from control hemocytes and 208,947 reads from flagellin-treated hemocytes (Table 3-1). 92-93 % of these reads were assembled into contigs resulting in 169,061 assembled reads of the control treatment and 192,909 assembled reads of the flagellin treatment. 7-8% of the reads could not be assembled and, therefore, 12,056 reads remained as singletons in the control dataset as well as 16,038 in the dataset received from flagellin-stimulated hemocytes. Altogether, datasets were not distinctly different at this level, displaying similar numbers of reads, assembled reads and singletons.

**Table 3-1: Overview of read numbers in the control and flagellin-stimulated hemocyte transcriptome datasets.** The total number of transcriptome reads in relation to the number of assembled reads and singletons (in %) is given.

| Transcriptome dataset | Total reads | Assembled reads | Singletons |
|---|---|---|---|
| Control hemocytes | 181,117 | 169,061 (93 %) | 12,056 (7 %) |
| Flagellin-stimulated hemocytes | 208,947 | 192,909 (92 %) | 16,038 (8 %) |

For the assembly of reads the collective hemocyte transcriptome dataset, comprising the control and flagellin-treated dataset, was included into the *M. edulis* transcriptome database at the ICMB (CAU-Kiel, Germany), which includes transcriptome datasets of various tissues and treatments, creating the final *M. edulis* transcriptome database (ID=Mytilus_edulis_20100630, for more details see Philipp *et al.* 2012a). Using the *M. edulis* transcriptome database as a reference, the number of bases as well as the number of contigs covered by reads of each hemocyte dataset was determined (Table 3-2). The proportion of covered bases by reads of control and flagellin-stimulated hemocytes was similar with 24 and 29 %, respectively. Both hemocyte datasets together covered 38 % of all transcriptome bases, which was more than the individual datasets alone. A similar result was obtained at contig level, including also contigs being only partially covered by reads of each dataset. 35 % of the contigs in the *M. edulis* transcriptome database were covered by reads of the collective hemocyte transcriptome dataset in comparison to 23 % coverage by the control and 27 % coverage by the flagellin-treated

dataset. Since the coverage values in the individual datasets were not entirely added up in the cumulative dataset, it can be concluded that some parts of the *M. edulis* hemocyte transcriptome dataset are covered by both the control and the flagellin-challenged hemocytes, whereas other parts are covered treatment-specific.

**Table 3-2: Number of bases and contigs of the *M. edulis* transcriptome database covered by hemocyte transcriptome datasets.** The length of the final *M. edulis* transcriptome database (as discussed in more detail in Philipp *et al.* 2012a), as a reference, covered by the collective hemocyte transcriptome dataset as well as the control and the flagellin-stimulated hemocyte transcriptome dataset is depicted in basepairs (bp) and percentage of the reference transcriptome database (%). In addition, the number and percentage of contigs of the *M. edulis* transcriptome database covered by each dataset is shown.

| Transcriptome dataset | Covered transcriptome bases | Covered contigs (also partially) |
|---|---|---|
| *M. edulis transcriptome database (Philipp et al. 2012a)* | *48,139,203 bp (100 %)* | *74,622 (100 %)* |
| Collective hemocyte transcriptome dataset | 18,375,723 bp  (38 %) | 26,341   (35 %) |
| Control hemocytes | 11,478,365 bp  (24 %) | 17,463   (23 %) |
| Flagellin-stimulated hemocytes | 13,820,427 bp  (29 %) | 20,258   (27 %) |

### 3.1.2    Overview of conserved signaling pathways by pathway analysis

#### 3.1.2.1    *Over- or under-represented pathways in hemocytes of M. edulis*

A general overview of over- or under-represented pathways in hemocytes, independent of any specific immune stimulation, was gained by comparing the transcriptome dataset of control hemocytes versus datasets of unstimulated tissues via pathway analysis. For a better overview, only those pathways are discussed, which are highly significantly ($p<0.001$) enriched, i.e. over-represented, or depleted, i.e. under-represented, in hemocytes.

Pathway analysis of hemocytes was carried out using KEGG annotations and corresponding pathways. To limit the number of non-sense results, pathways of human diseases were omitted from the analysis. In order to facilitate further analyses, KEGG pathways were further arranged into related groups of pathways (e.g. pathways related to immune system or metabolic processes) according to information obtained from literature, as seen in Figure 3-1.
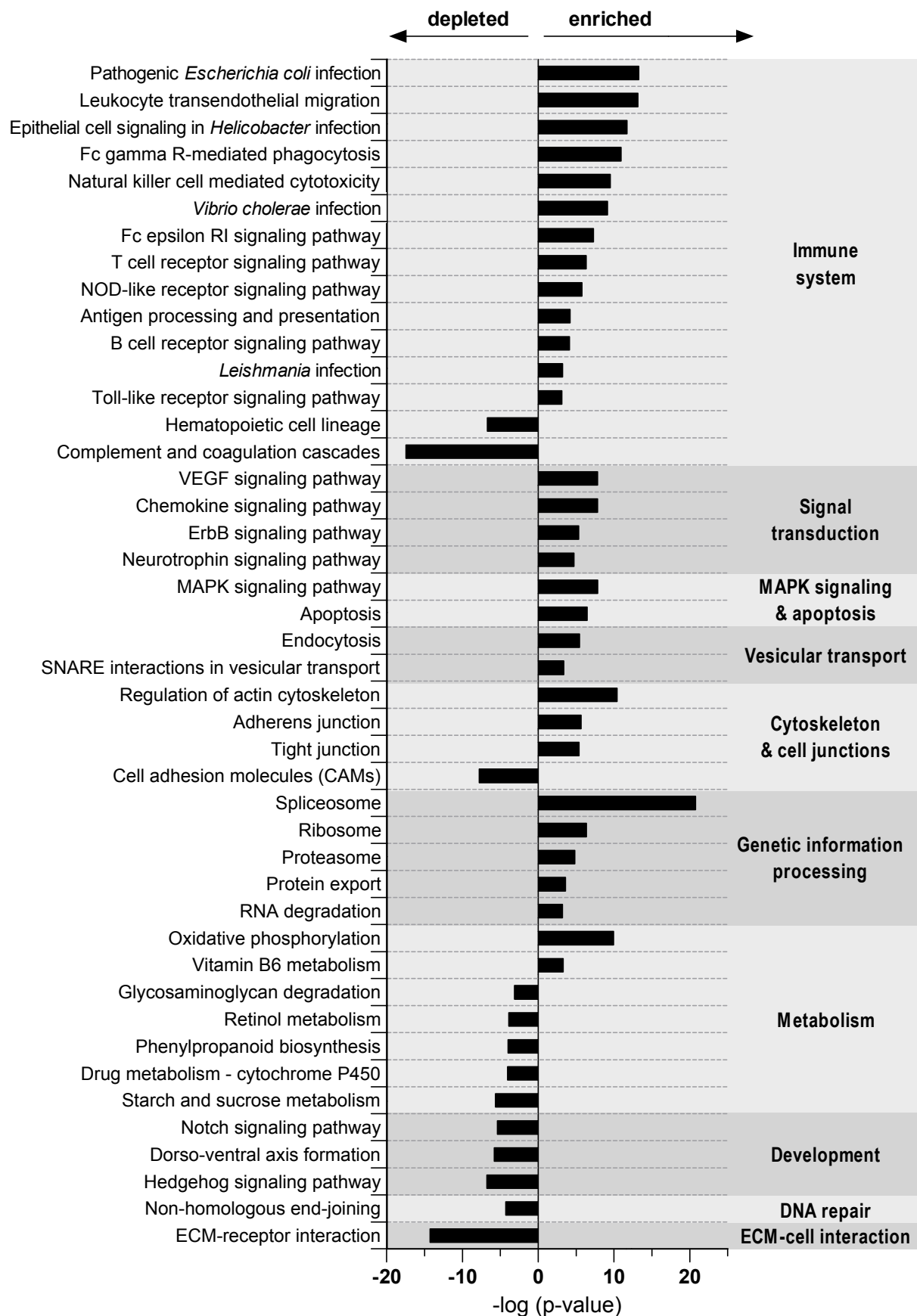
**Figure 3-1: KEGG pathway analysis of unstimulated hemocytes.** Significant enrichment (positive values) and depletion (negative values) of KEGG pathways are depicted as -log (p-value) with a threshold of 3 and -3 respectively (p<0.001). Results were obtained using unstimulated hemocytes and tissues (including mantle, mantle rim, digestive gland, gill, foot and adductor muscle). Pathways of human diseases were omitted.

Most of the pathways enriched in hemocytes were directly relevant for the immune system (Figure 3-1), e.g. the Toll-like receptor signaling pathway. In addition to directly immune-relevant pathways, pathways contributing to the immune response under certain circumstances were enriched in hemocytes as well. These include pathways involved in signal transduction, vesicular transport, apoptosis and MAPK signaling. Further, pathways contributing to genetic information processing, the cytoskeleton and cell junctions were also mainly enriched in hemocytes. The majority of pathways being significantly depleted in hemocytes were related to the metabolism and development. But pathways affiliated with DNA repair and extracellular matrix (ECM) to cell interactions were depleted as well.

During this analysis a general overview of relevant pathway groups in hemocytes was obtained. To gain a more detailed insight into which pathways may potentially be important in presence of an immune-challenging component, pathway analysis involving control and flagellin-stimulated hemocytes was carried out as described in the next section.

### 3.1.2.2 *Pathway analysis in hemocytes upon immune challenge*

For a closer look at pathways present in differentially regulated hemocyte contigs after immune challenge, pathway analysis, as described in the section before, was further elaborated. Therefore, contigs of the hemocyte transcriptome dataset were characterized beforehand as being either up- or down-regulated after flagellin stimulation and compared to the whole hemocyte database.

Only the KEGG pathway "focal adhesion", participating in ECM to cell interactions, was found to be enriched in up-regulated contigs and depleted in down-regulated contigs at the same time after flagellin stimulation (Figure 3-2). This was also the only pathway found to be significantly depleted at all in this analysis. All other KEGG pathways were enriched either in up-regulated or down-regulated contigs. In up-regulated contigs, especially pathways directly involved in the immune system as well as pathways distinctly related to immune system functions, such as signal transduction and MAPK signaling pathways were enriched. Further, pathways involved in development, the regulation of the cytoskeleton and cell junctions were enriched in up-regulated contigs as well. In down-regulated contigs, mainly pathways related to metabolic processes or involved in the processing of genetic information were enriched. Pathways contributing to vesicular transport processes were enriched in both, up- and down-regulated, contigs after flagellin treatment, and therefore yielded no uniform result.

This analysis provided a rough overview of over- and under-represented pathway groups during immune responses in hemocytes. To further investigate immune-relevant processes selected orthologs were examined more closely at transcript level as depicted in the next section.
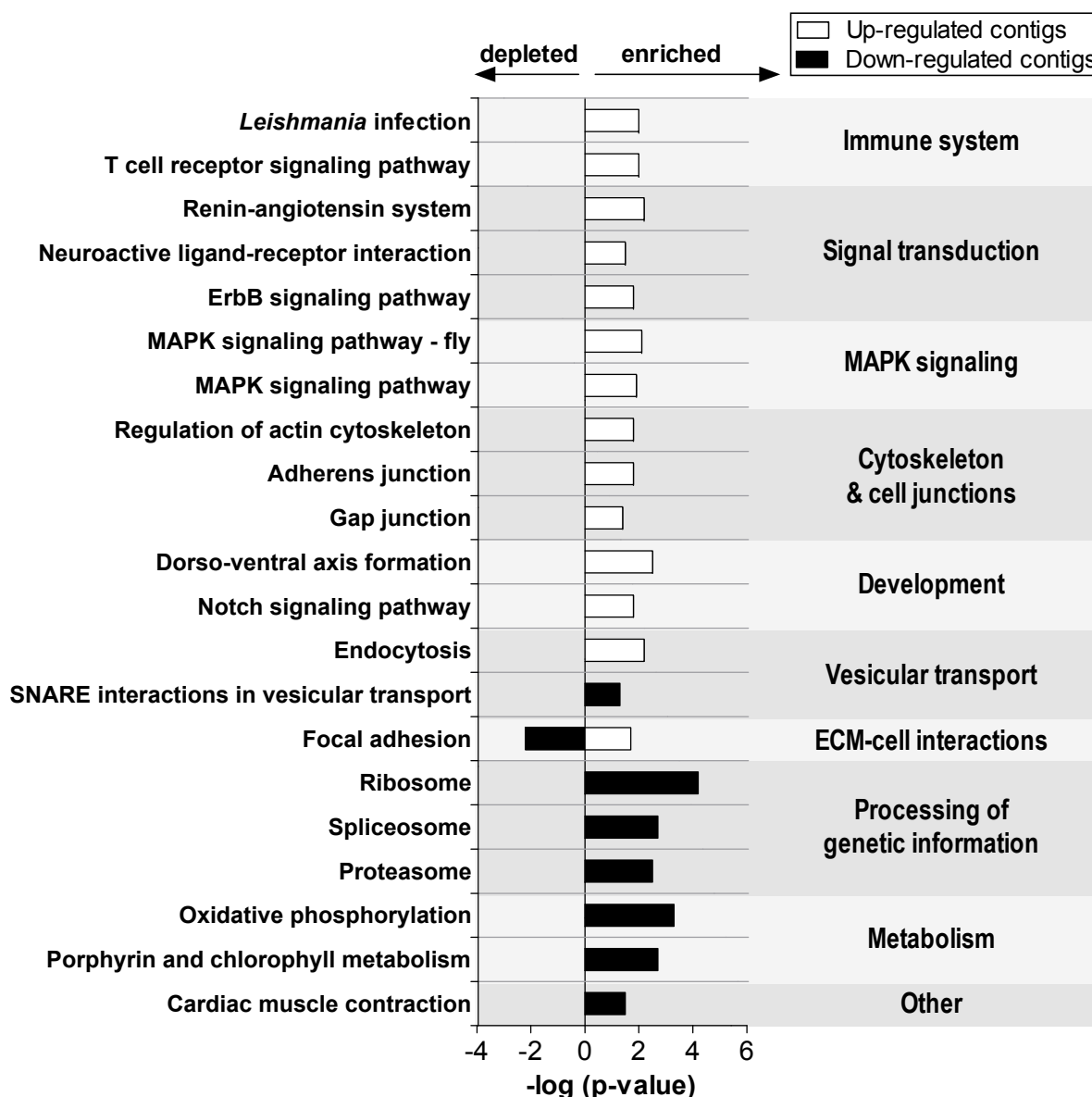
**Figure 3-2: KEGG pathway analysis of up- and down-regulated contigs in hemocytes upon flagellin-stimulation.** Contigs with a fold change of >2 were characterized as up-regulated and <2 as down-regulated. Significant enrichment (positive values) and depletion (negative values) of KEGG pathways are depicted as -log (p-value) with a threshold of 1.3 and -1.3 respectively (p<0.05). Note that only KEGG pathways enriched in hemocytes and depleted in the corresponding tissue, and *vice versa*, are displayed. Pathways of human diseases were omitted.

### 3.1.3 Investigation of putatively immune-relevant contigs

#### 3.1.3.1 Selection of transcripts for further investigation

To gain a deeper insight into the *M. edulis* immune system, the expression pattern of a few putatively important immune gene orthologs was examined. Therefore, 19 transcripts (=contigs) were chosen for subsequent expression analysis upon immune challenge via qRT-PCR analysis (Table 3-3). Orthologs were picked according to a high expression change upon immune stress in *M. edulis* and other bivalves

as well as a high read coverage in the *M. edulis* hemocyte transcriptome database, as will be discussed in the following (for annotations and further information see supplements Table S 1). Candidates were characterized as possible receptors, regulators and effectors of putative immune pathways in *M. edulis*.

**Table 3-3: Putatively important immune-relevant orthologs in *M. edulis* selected for further analysis.** Orthologs and their respective contigs (hemocyte database ID and, if already available, ENA accession number are stated) were arranged into three major functional groups, namely receptors, regulators and effectors of immune pathways. The number of reads for each contig as well as the fold change obtained by comparing the number of reads from the control dataset to reads from the flagellin-treated dataset is given.

| Functional group | Ortholog | Contig ID (if existing ENA accession number) | Reads | Fold change |
|---|---|---|---|---|
| *Receptors* | *Me1* TLR | Mytilus_edulis_20100630_66395 (HE609238) | 6 | 2.0 |
| | *Me2* TLR | Mytilus_edulis_20100630_26463 (HE609227) | 1 | Inf |
| | *Me3* TLR | Mytilus_edulis_20100630_20401 (HE609225) | 106 | 1.6 |
| | *Me4* TLR | Mytilus_edulis_20100630_72076 (HE609242) | 111 | 2.2 |
| | *Me1* LBP/BPI | Mytilus_edulis_20100630_53859 (HE609065) | 47 | 1.5 |
| | *Me1* C-type lectin | Mytilus_edulis_20100630_3828 + _49170 | 248 | 1.8 |
| | *Me1* C3a-receptor | Mytilus_edulis_20100630_49208 | 87 | 3.4 |
| | *Me2* C3a-receptor | Mytilus_edulis_20100630_69548 | 32 | 5.4 |
| *Regulators* | *Me1* IκB | Mytilus_edulis_20100630_50465 (HE609059) | 58 | 1.1 |
| | *Me2* IκB | Mytilus_edulis_20100630_73988 (HE609060) | 245 | 2.1 |
| | *Me2* LITAF | Mytilus_edulis_20100630_17485 (HE609139) | 32 | 4.3 |
| | *Me3* NF-κB p50 | Mytilus_edulis_20100630_72440 | 56 | 2.3 |
| *Effectors* | *Me1* TIMP | Mytilus_edulis_20100630_6837 | 685 | 1.6 |
| | *Me2* TIMP | Mytilus_edulis_20100630_52435 | 158 | -1.9 |
| | *Me1* Ependymin | Mytilus_edulis_20100630_2314 + _3913 | 2119 | 1.7 |
| | *Me2* Ependymin | Mytilus_edulis_20100630_7396 | 1218 | -1.9 |
| | *Me1* Defensin | Mytilus_edulis_20100630_73329 (HE609174) | 833 | -1.1 |
| | *Me1* Myticin A | Mytilus_edulis_20100630_74205 | 350 | -3.7 |
| | *Me1* Mytilin D | Mytilus_edulis_20100630_16574 (HE609180) | 106 | 1.7 |

*Receptors*

Selected receptors included orthologs of four different Toll-like receptors (TLRs), a lipopolysaccharide-binding protein (LBP) or the very similar bactericidal/permeability-increasing protein (BPI), a C-type lectin and two complement component 3a (C3a) receptors. Within the group of TLRs in the hemocyte transcriptome dataset, *Me3* TLR and *Me4* TLR were both covered by a high number of reads (>100 reads) and were up-regulated after 4 hours of flagellin stimulation. *Me1* TLR and *Me2* TLR, on the other hand, were covered only by 1-6 reads, but a study, conducted in parallel to the present study

depicted a significant increase in *Me1* and *Me2* TLR after LPS stimulation, but no increase in *Me3* TLR (Saphörster, Findeisen, Rosenstiel, Philipp unpublished data, see 9.7). Thus, these orthologs were selected to gain an even deeper insight into TLR pathway induction in *M. edulis*.

Other proteins involved in the recognition of LPS include the LBP and BPI proteins. Four orthologs for LBP/BPI have been identified in the overall transcriptome database of *M. edulis* so far (Philipp *et al.* 2012a). The contig coding for *Me1* LBP/BPI was up-regulated upon flagellin stimulation and, with 47 reads, covered by a distinctly higher number of reads in the hemocyte dataset than any other LBP/BPI ortholog, which were covered by less than 8 reads. In addition, LBP/BPI orthologs were identified as immune-relevant in all other Lophotrochozoan transcriptome analyses investigated for the selection of candidate genes as listed in Table 2-5.

The contig coding for the *Me1* C-type lectin was up-regulated upon flagellin exposure and covered by a high amount of reads (248 reads) in the *M. edulis* hemocyte transcriptome dataset. Furthermore, hemocyte transcriptome dataset analyses of the bivalves *M. galloprovincialis* and *C. gigas* depicted also an up-regulation upon immune challenge (de Lorgeril *et al.* 2011; Venier *et al.* 2011).

During the general analysis of the hemocyte transcriptome database, overall expression changes were not particularly high. Only 21 contigs, covered by more than 50 reads, exhibited an expression change of more than 3 fold. Therefore, the high expression changes of the *Me1* C3a receptor (3.4 fold change) and the *Me2* C3a receptor (5.4 fold change) were outstanding. In addition, a C3a receptor ortholog was also up-regulated in the oyster transcriptome dataset analysis by de Lorgeril *et al.* (2011).

*Regulators*

Regulators chosen for further analysis comprised orthologs of two inhibitor of κB alpha (IκBα) proteins, a lipopolysaccharide-induced tumor necrosis factor-alpha factor (LITAF) and a nuclear factor kappa-light-chain-enhancer of activated B cells (NF-κB) subunit p50. For *Me3* NF-κB p50 and *Me2* IκB a distinct increase in expression upon flagellin stimulation was observed in the *M. edulis* hemocyte dataset. In addition, IκB orthologs were also up-regulated in immuno-transcriptome datasets of *M. galloprovincialis* and *C. gigas* (de Lorgeril *et al.* 2011; Venier *et al.* 2011). *Me1* IκB on the other hand depicted no distinct expression change after flagellin challenge and also possessed fewer reads than *Me2* IκB (58 to 245 reads). But since *Me1* IκB displayed a significant increase in hemocytes of *M. edulis* after 24 hours of LPS incubation (Saphörster, Findeisen, Rosenstiel, Philipp unpublished data, see 9.7), it was included in further analysis to gain more insight into the regulation of IκB orthologs in *M. edulis* during MAMP-induced NF-κB activation.

In addition to the NF-κB transcription factor, the identified ortholog of the DNA-binding lipopolysaccharide-inducible tumor necrosis factor-alpha factor (LITAF) was further investigated as well. In the *M. edulis* hemocyte transcriptome dataset, *Me2* LITAF depicted an extraordinarily high change in

expression of 4.3 fold after flagellin exposure. Transcriptome dataset analyses of other authors also revealed an up-regulation upon immune stimulation in *M. galloprovincialis* and *C. gigas* (de Lorgeril *et al.* 2011; Venier *et al.* 2011).

*Effectors*

Orthologs acting as putative effectors in the immune response against flagellin included orthologs of tissue inhibitor of metalloproteinases (TIMP), ependymin and the antimicrobial peptides defensin, myticin A and mytilin D. *Me1* TIMP was up-regulated upon flagellin challenge and with 685 reads among the contigs covered by the highest amount of reads in the dataset. TIMP orthologs were also up-regulated in the transcriptome analyses of *M. galloprovincialis* and *C. gigas* (de Lorgeril *et al.* 2011, Venier *et al.* 2011). Furthermore, TIMP orthologs were also among the highest expressed immune genes in the oyster hemocyte transcriptome dataset (de Lorgeril *et al.* 2011). Another TIMP ortholog of the blue mussel, *Me2* TIMP, was down-regulated in the flagellin-stimulated hemocyte dataset. To investigate the opposing behavior of TIMP orthologs in *M. edulis* more closely, both orthologs were subjected to further analysis.

*Me1* Ependymin and *Me2* Ependymin were covered by >1000 hemocyte reads each and were, therefore, among the contigs covered by the highest amount of reads in the hemocyte transcriptome dataset. In addition, they were also extremely high expressed in hemocytes in comparison to all other tissue transcriptome datasets being up to 21 times higher expressed in hemocytes. Hence, despite little information available about a possible immune function of ependymin (see discussion section 4.1.2.4), they were subjected to further analysis. To obtain a more differentiated insight into ependymin expression during flagellin challenge, an up-regulated (*Me1* Ependymin) and a down-regulated ortholog (*Me2* Ependymin) were chosen for further investigations.

In mussels, and specifically also in the *M. edulis* transcriptome database (Philipp *et al.* 2012a), a vast amount of diverse antimicrobial peptides were identified, which can be divided into four major groups: (i) defensins, (ii) mytilins, (iii) myticins and strictly antifungal (iv) mytimycins (Li *et al.* 2011). Therefore, one ortholog from each of the first three groups was chosen to be examined in further detail. *Me1* Myticin A depicted a distinct down-regulation in the hemocyte transcriptome dataset upon flagellin stimulation with a -3.7 fold decrease in expression. In contrast to this, *Me1* Mytilin D was up-regulated in flagellin-challenged hemocytes. The change in expression of *Me1* Defensin upon flagellin stimulation was initially too low to be included in our analysis (cut off |fold change| ≥1.4). However, it displayed a high abundance in hemocytes (833 reads), even when compared to other tissues (55 reads), since the hemocyte dataset contained 15 times more reads than datasets of other tissues. In contrast to the present study transcriptome dataset analyses of other bivalves displayed a distinct down-regulation

upon immune challenge (de Lorgeril *et al.* 2011; Venier *et al.* 2011). Therefore, *Me1* Defensin was included in further analysis to elucidate its role in flagellin-triggered immune responses.

These potentially immune-relevant receptors, regulators and effectors were investigated at various time points upon flagellin exposure providing a higher temporal resolution and a higher number of biological replicates in the next section (3.1.3.2).

### 3.1.3.2 Expression analysis of candidate transcripts

Transcription of selected candidate genes (see previous section 3.1.3.1), which were characterized as putative receptors (Figure 3-3a-h), regulators (Figure 3-3i-l) or effectors (Figure 3-3m-s) of possible immune-relevant pathways in *Mytilus edulis,* were examined in more depth by quantitative RT-PCR (qRT-PCR). To obtain a deeper insight into the time-dependent expression pattern of the candidates, hemocytes of *M. edulis* were incubated with flagellin for 1-8 hours (n=5-7) and unstimulated cells were included as a control.

### Receptors

Expression of *Me1* and *Me2* TLR did not significantly change (p>0.05, ANOVA), while *Me3* and *Me4* TLR depicted a strong increase after 4 hours of flagellin stimulation in comparison to control cells (p<0.01, ANOVA, Bonferroni). The expression level of *Me3* TLR returned to the expression level of control cells at 8 hours of prolonged flagellin stimulation, whereas *Me4* TLR remained increased (p<0.01). In contrast to the steep increase of *Me3* and *Me4* TLR, transcript levels of *Me1* LBP/BPI were gradually increasing until they were significantly elevated after 4 hours of flagellin stimulation (p<0.05, ANOVA, Bonferroni). After 8 hours, the expression levels were slightly decreased again exhibiting the same expression level as observed at 4 hours. The C-type lectin ortholog *Me1* C-type lectin displayed a slightly increased trend in expression during flagellin stimulation being significant only at 1 (p<0.05) and 8 hours (p<0.001, ANOVA, Bonferroni) of stimulation. In addition to MAMP binding proteins, such as TLRs, LBP/BPI and lectins, expression of two orthologs of the complement component 3a binding receptor were assessed. While the expression of the *Me1* C3a receptor was not significantly altered upon exposure to flagellin (p>0.05, ANOVA, Bonferroni), the expression of the *Me2* C3a receptor was markedly increased after 2-8 hours of flagellin stimulation (p<0.05, ANOVA, Bonferroni).

### Regulators

Orthologs of the inhibitor of NF-κB, *Me1* and *Me2* IκBα, were the highest inducible genes in these experiments. Expression levels increased significantly during flagellin challenge in comparison to the control. Especially at 4 hours expression levels were strongly elevated up to 3 fold (p<0.001, ANOVA,

Bonferroni; or t-test with Welch's correction respectively) and remained significantly increased at all other time points throughout the experiment in comparison to the control ($p<0.05$ to $p<0.001$). Similarly, expression levels of the NF-κB transcription factor ortholog *Me3* NF-κB p50 were also significantly elevated during 1-8 hours of flagellin stimulation in comparison to the control. However, the increase was not as steep, it rather depicted an incremental increase from 1 hour ($p<0.05$ in comparison to the control, ANOVA, Bonferroni) over 2 hours ($p<0.01$ in comparison to the control) to 4 hours ($p<0.001$ in comparison to the control) and after 8 hours decreased again to the expression level seen also at 1 hour of stimulation ($p<0.05$ in comparison to the control). In contrast to the high induction of NF-κB pathway members, *Me2* LITAF depicted a significant but less pronounced increase in expression level ($p<0.01$, ANOVA, Bonferroni) in comparison to the control only after 2 hours of flagellin incubation.

*Effectors*

Two orthologs of TIMP and ependymin proteins were analyzed each. But whereas *Me1* TIMP and *Me2* Ependymin displayed a significant increase at transcript level after 4 hours of flagellin challenge in comparison to the control ($p<0.05$ and $p<0.01$, ANOVA, Bonferroni), no expression changes were investigated for *Me2* TIMP and *Me1* Ependymin ($p>0.05$, ANOVA). In addition, no change in expression was observed for all antimicrobial peptides investigated including *Me1* Defensin, *Me1* Myticin A and *Me1* Mytilin D ($p>0.05$, ANOVA or t-test with Welch's correction respectively).

Taken together, many orthologs investigated further in qRT-PCR experiments displayed a major response at transcript level upon immune challenge in hemocytes, suggesting a possible role in the defense response of *M. edulis*. In summary, upon flagellin challenge selected regulators exhibited the highest increase in expression, followed by receptors and then effectors of putative immune pathways in *M. edulis*. In addition to the general hemocyte transcriptome dataset analyses, as discussed in this section, the hemocyte transcriptome was also used to identify and examine specific target transcripts putatively encoding proteins, which are of particular interest from an evolutionary perspective. Hence, the first part of the following sections deals with the production of reactive oxygen species (ROS) and putatively contributing NOX and DUOX enzymes (page 67), while the last part deals with the phylogenetic ancient interleukin IL-17 (page 91) in *M. edulis* and other bivalves.
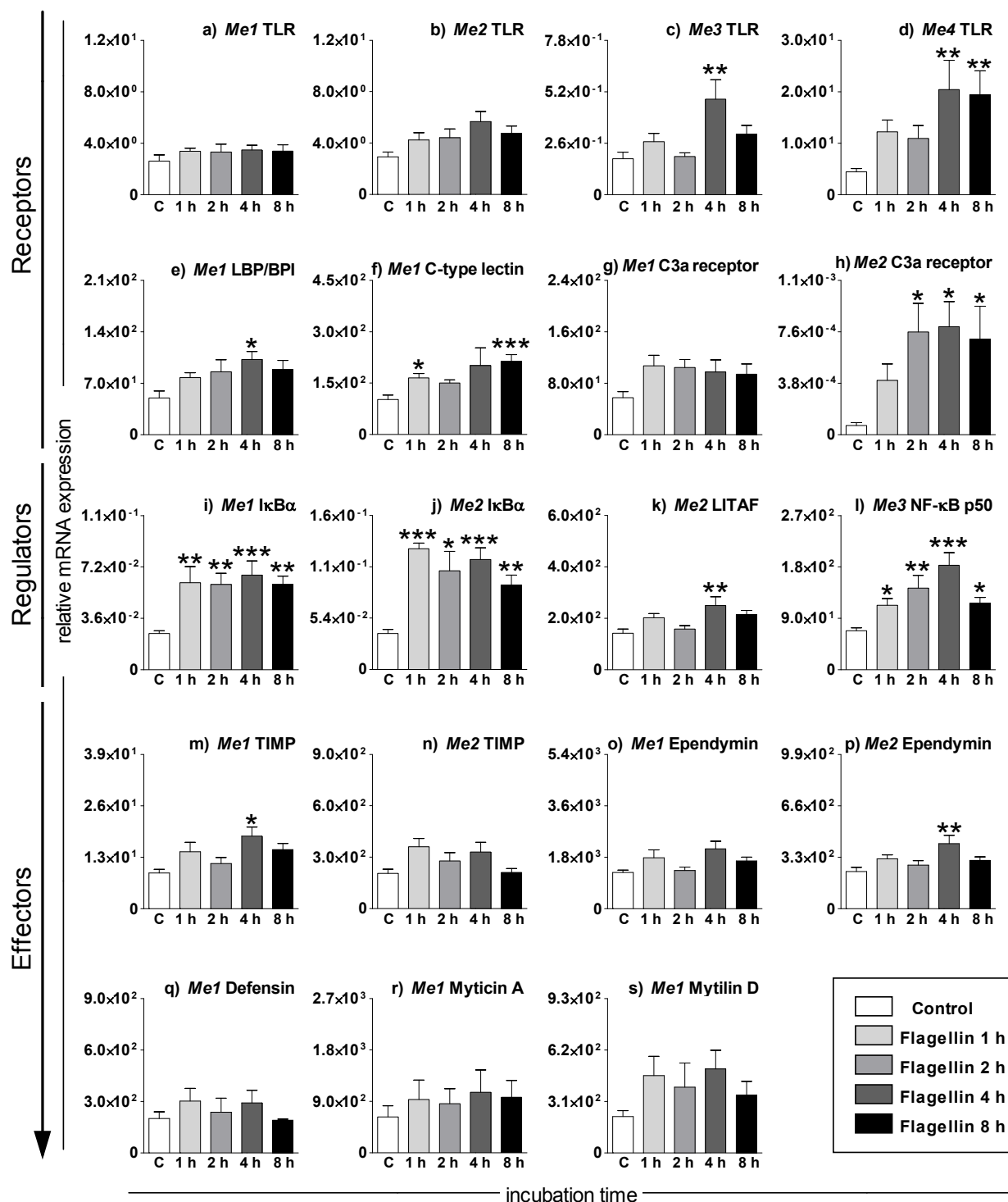
**Figure 3-3: Expression analysis of putative immune-relevant receptors, regulators and effectors in hemocytes of *M. edulis* upon flagellin stimulation.** Using qRT-PCR the relative mRNA expression of receptors (**a-h**), regulators (**i-l**) and effectors (**m-s**) was determined in relation to the *Me* GAPDH/28S rRNA index. Hemocytes were incubated with 2.5 µg ml$^{-1}$ flagellin for 1, 2, 4 and 8 hours. Unstimulated cells were used as control. Standard errors of 5-7 replicate experiments are displayed. Note that for a better graphical representation, asterisks depict significant differences compared only to the control (see text for further details of the statistic analyses involved).

## 3.2 The role of NOX and DUOX orthologs in ROS production of bivalve hemocytes

### 3.2.1 Generation of ROS in hemocytes of *M. edulis*

#### 3.2.1.1 ROS in hemocytes upon immune stress

The production reactive oxygen species (ROS) is regarded a conserved and widespread immune response in bivalves. To obtain deeper insights into the time- and dose-dependent generation of ROS in the blue mussel *Mytilus edulis*, ROS production (in relative fluorescent units; RFU) was examined over the course of time in hemocytes during an immune challenge (n=5). Therefore, hemocytes were incubated with different concentrations of zymosan A (Figure 3-4a), a component of the yeast cell wall, and marine bacteria of the species *Listonella anguillarum* (Figure 3-4c) in presence of an extracellular ROS-detecting dye (Amplex Red).

ROS production of *M. edulis* hemocytes was clearly stimulated by zymosan A and *L. anguillarum* and displayed a significant time- and dose-dependency on the selected stimuli ($p < 0.001$, two-way ANOVA, Figure 3-4). In both experiments ROS levels steadily increased within 5, 15, 30, 60, 120 and 240 min. In cells incubated with zymosan A, reactive oxygen species quickly increased during the first 60 min. In the highest treatment containing 100 µg ml$^{-1}$ zymosan A, the Amplex Red test reached a close-to saturation state during 120-240 min, whereas in treatments with lower concentrations, the assay still maintained a steeper increase (Figure 3-4a). Hence, the ROS assay in the 50 µg ml$^{-1}$ zymosan A treatment began to reach its plateau not until 240 min of incubation, while in hemocytes stressed with 25 µg ml$^{-1}$ zymosan A it did not reach its maximum during the experiment. In addition, different doses of zymosan A did not only affect the time required to reach a saturation of the ROS assay, but also on the amount of ROS produced in the first place. Therefore, cells stimulated with 100 µg ml$^{-1}$ zymosan A produced a higher amount of ROS than cells incubated with 50 µg ml$^{-1}$ zymosan A, which in turn generated more than cells challenged with 25 µg ml$^{-1}$.

Similarly, ROS production was higher in cells stimulated with 2.6 10$^7$ CFU ml$^{-1}$ *L. anguillarum* than in the treatment containing 1.3 or even 0.7 10$^7$ CFU ml$^{-1}$ *L. anguillarum*, respectively (Figure 3-4c). However, even though ROS levels increased over time, cells stimulated with *L. anguillarum* did not appear to reach a saturation state during the same length of incubation. By comparing zymosan A to *Listonella anguillarum* treated cells it becomes obvious, that within the chosen treatment concentrations ROS were generated faster in zymosan A-stimulated hemocytes than in *L. anguillarum*-treated cells.

**Zymosan A**

a)



b)



*Listonella anguillarum*

c)



d)
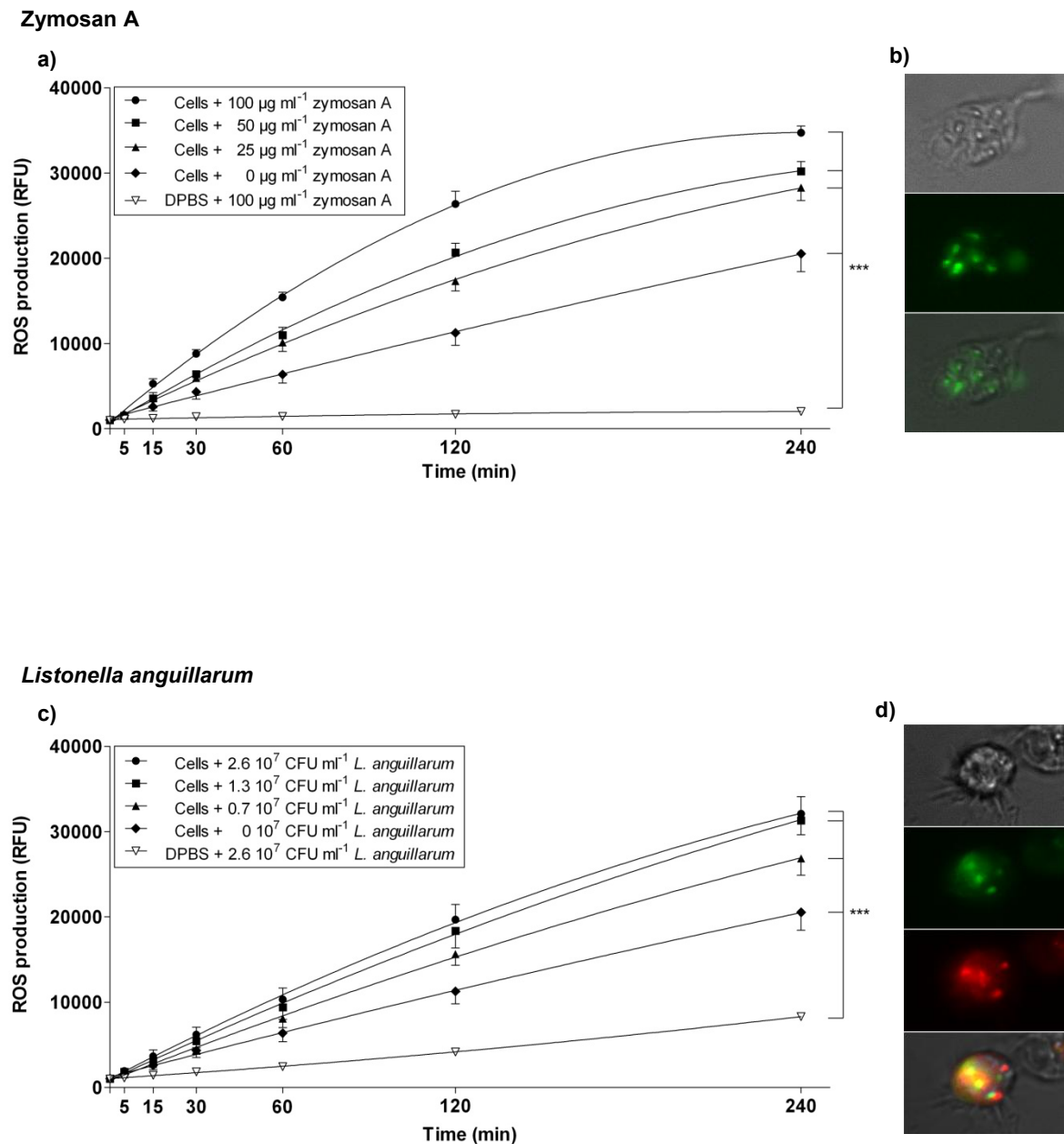


**Figure 3-4: ROS production in *M. edulis* hemocytes upon immune stimulation.** The graphs on the left side illustrate time dependent (min) ROS production (RFU) in hemocytes upon stimulation with different concentrations of **(a)** zymosan A (µg ml^{-1}) or **(c)** *Listonella anguillarum* (CFU ml^{-1}). ROS production is significantly dependent on incubation time and concentration of the stimulus ($p < 0.001$, two-way ANOVA). Mean values of n=5 experiments with standard errors are given. Microscopic images (40x objective), on the right side, depict ROS production (green fluorescence) by a hemocyte exposed to **(b)** zymosan A particles or **(d)** labeled *Listonella anguillarum* (red fluorescence). Transmission, fluorescence and overlaid images are shown in this order from top to bottom.

Unstimulated cells also continuously produced a small amount of ROS over the course of the experiment (up to approximately 20,000 RFU), which was, however, lower than in stimulated cells (up to approximately 30,000 RFU). Furthermore, the negative control treatment consisting of the stimulus without hemocytes was slowly increased over time reaching a relatively low ROS level (<10,000 RFU) after 240 min of *Listonella anguillarum* stimulation, whereas it remained constant using zymosan A. This increase in ROS production by living cells, whether they are bacteria or hemocytes, is most probably due to the enrichment of oxygen radicals as a metabolic by-product in the medium.

Further, localization of intracellular ROS production in hemocytes was investigated by employing the intracellular ROS-detecting dye cDCFH-DA in microscopic observations upon phagocytosis of zymosan A particles and labeled, red fluorescent *Listonella anguillarum* bacteria. In line with the experiment carried out before, both stimuli were able to trigger a distinct increase in ROS production after 2 hours of incubation, indicated by the green fluorescence of the oxidized intracellular DCF dye. Sites of encapsulated zymosan A particles closely correlated with spots of high ROS production in hemocytes (Figure 3-4b). The spatial proximity of immune stimulus and ROS production became even more apparent using labeled *Listonella anguillarum* bacteria. The fluorescence of phagocytosed bacteria and loci of ROS production clearly merge in the overlay image indicating a high degree of colocalization (Figure 3-4d).

These experiments depicted that ROS production upon immune stimulation is not only time and dose dependent, but the generation of ROS also takes place in close spatial proximity to the stimulus in phagocytotic vesicles of *M. edulis* hemocytes. To gain a deeper understanding of the underlying mechanisms of ROS generation in bivalve hemocytes, the role of ROS producing enzymes was investigated more closely at molecular level.

### 3.2.1.2    *ROS generation in hemocytes in relation to NADPH oxidase activators or inhibitors*

In many eukaryotes, membrane bound enzymes belonging to the NADPH oxidases (NOX) and dual oxidases (DUOX) family of enzymes seem to be mainly responsible for ROS production upon immune stimulation (Kawahara *et al.* 2007; Rada & Leto 2008). It is widely accepted that NADPH oxidases can be induced by activation of the protein kinase C(PKC) using phorbol-12-myristate-13-acetate (PMA) (Heyworth & Badwey 1990; Lambeth *et al.* 2007) and directly inhibited by DPI (diphenyleneiodonium) (Doussiére & Vignais 1992; Doussiére *et al.* 1999). Since NOX5 and DUOX enzymes additionally possess two or more EF hand calcium binding motifs, which promote ROS production upon interaction with calcium (Bánfi *et al.* 2004; Rigutto *et al.* 2009), ROS production can also be constrained using the calcium chelator BAPTA-AM (Kawahara & Lambeth 2008; Pacquelet *et al.* 2008; Damiano *et al.* 2012).

In respect to the knowledge gained from other model organisms, hints for the possible involvement of NOX and DUOX enzymes in ROS production in hemocytes of the blue mussel were obtained by tracking extracellular ROS production using NOX and DUOX activation and inhibition assays. Therefore, hemocytes were incubated with the inhibitor DPI and/or an inducer of ROS production such as PMA or zymosan A (n=5, Figure 3-5a). Zymosan A was included as a control for the induction of ROS production, since it has been verified as a proper trigger for ROS in the section before (3.2.1.1). In an additional experiment cells were treated with zymosan A in the absence or presence of the intracellular calcium chelator BAPTA-AM (n=3, Figure 3-5b).

A significant increase in ROS production was observed after 2 h upon stimulation with PMA (p<0.05, one-way ANOVA, Bonferroni) or zymosan A (p<0.01) in comparison to the control. Furthermore, cells pre-incubated with DPI or BAPTA, which were afterwards stimulated with zymosan A or PMA, exhibited a significant lower level of ROS than cells stimulated in the absence of an inhibitory compound (p<0.001). Hence, PMA and DPI or BAPTA were able to distinctly increase or decrease ROS production, respectively.
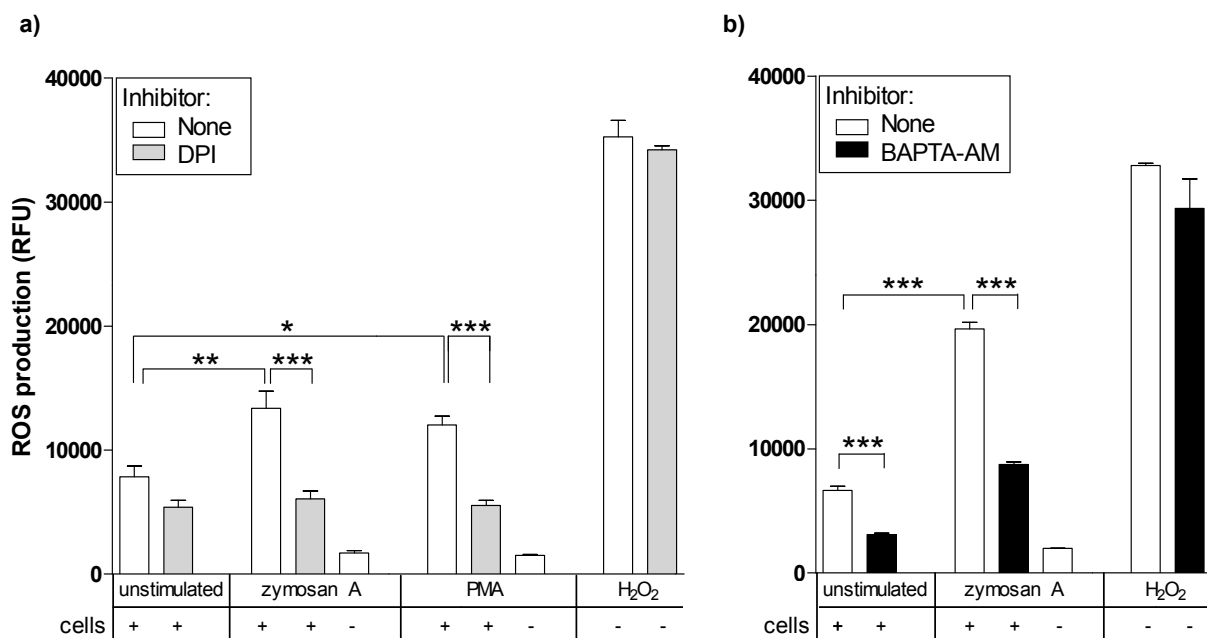


**Figure 3-5: ROS production (RFU) in hemocytes upon incubation with NOX/DUOX activating and inhibiting compounds.** Cells were stimulated for 2 hours with DPBS (unstimulated control), PMA or zymosan A in the absence or presence of **(a)** DPI (n=5 experiments), or **(b)** BAPTA (n=3 experiments). Data are shown as means with standard errors. Asterisks indicate significant differences (Bonferroni, one-way ANOVA). Positive controls ($H_2O_2$) and negative controls (cell-free stimuli) (significances not shown) indicated proper functioning of the assay.

Interestingly, all DPI treated cells seemed to exhibit the same basal level of ROS production and even unstimulated control cells decreased to this level upon DPI incubation (Figure 3-5a). This decrease in ROS production of unstimulated cells was more pronounced and even significant after BAPTA incubation (p<0.001, Figure 3-5b). Negative controls consisting of the stimuli without cells showed that the stimuli alone had no effect on the Amplex Red test. $H_2O_2$ was used to verify proper functioning of the ROS assay. In addition, when compared to $H_2O_2$ in combination with DPI or BAPTA, ROS production did not differ significantly. Thus, the decrease in ROS levels is evoked rather due to an inhibition of ROS producing enzymes by DPI or BAPTA than due to an inhibition of the Amplex Red test itself.

Activation and inhibition of ROS production by PMA and DPI or BAPTA, respectively, hints towards the presence of NOX and DUOX enzymes in the blue mussel *M. edulis*. In addition, since ROS production also decreased upon addition of BAPTA, special attention should be given to EF-hand containing NADPH oxidase family members. Based on these results indicating the involvement of NOX and DUOX enzymes in the generation of ROS in mussels, the occurrence of these enzymes was further investigated at transcript level.

### 3.2.2 ROS producing enzymes in bivalves and other Lophotrochozoa

*3.2.2.1 Identification of transcripts encoding NOX/DUOX enzymes and their co-factors in M. edulis*

The family of NADPH- (NOX) and dual (DUOX) oxidases comprises seven orthologs in humans, namely NOX1-5 and DUOX1-2 (Lambeth 2004). For proper functioning the orthologs of the major subunit gp91$^{phox}$ require further minor subunits, such as p22$^{phox}$, p47$^{phox}$ (or its ortholog NOXO1), p40$^{phox}$, p67$^{phox}$ (or its homolog NOXA1), DUOXA, and Rac.

As a consequence of the successful application of NOX/DUOX activating and inhibiting compounds influencing ROS production in hemocytes (3.2.1.2), the *M. edulis* transcriptome database was screened for transcripts coding for members of the NOX and DUOX family of ROS producing enzymes using keyword and domain searches. The obtained reads were aligned, sequenced and if possible elongated by RACE-PCR (see supplements pages 165-165 for initial contigs and singletons as well as information about the final sequences). As a result, various major and minor subunits of the NOX/DUOX family were identified in the *M. edulis* transcriptome database and verified via BLAST analyses in the UniProt/Swiss-Prot (BLASTp) and NCBI nt (tBLASTx) databases (Table 3-4). More specifically, two DUOX 1/2-like transcripts were identified, which were named *Me* DUOX-a and *Me* DUOX-b in order of their discovery.

**Table 3-4: NOX/DUOX orthologs and their co-factors in *M. edulis*.** Sequence length (bp) and ORF length (number of amino acids, aa) of the identified NOX/DUOX orthologs as well as the corresponding best BLAST hit are shown. The ORF length was obtained by ORF Finder. Fragments were blasted in NCBI (nr/nt; tBLASTx) as well as in UniProt/Swiss-Prot (BLASTp). Important parameters (E value, score, coverage (Cover.) and identity (both in %)) of the organism displaying the best BLAST hit are stated. Only reviewed orthologs from NCBI and UniProt/Swiss-Prot were included.

| | ID | Ortholog | Length (bp) | ORF (aa) | NCBI nt (tBLASTx) | | | | | UniProt/Swiss-Prot (BLASTp) | | | | | |
|---|---|---|---|---|---|---|---|---|---|---|---|---|---|---|---|
| | | | | | Cover. (%) | Score | E value | Organism | Accession number | Length (aa) | Identity (%) | Score | E value | Organism | Accession number |
| Major subunits | *Me*DUOX-a | DUOX1/2 | 5204 | 1571 | 68 | 2976 | 0 | *Strongylocentrotus purpuratus* | NM_001124765.1 | 1551 | 39 | 2866 | 0 | *Homo sapiens* | Q9NRD9 |
| | *Me*DUOX-b* | DUOX1/2 | 7456 | 1594 | 82 | 3366 | 0 | *Lytechinus variegatus* | AY747667.1 | 1545 | 39 | 2842 | 0 | *Sus scrofa* | Q8HZK2 |
| | *Me*NOX2 | NOX1-3 | 2101 | 574 | 79 | 1311 | 0 | *Bos taurus* | NM_174035.3 | 570 | 52 | 1593 | $10^{-175}$ | *Bos taurus* | O46522 |
| | *Me*NOX5 | NOX5 | 1031 | 309 | 73 | 711 | $10^{-97}$ | *Bos taurus* | NM_001101137.1 | 719 | 48 | 749 | $10^{-77}$ | *Homo sapiens* | Q96PH1-4 |
| Minor subunits | *Me*p22$^{phox}$ | p22$^{phox}$ | 572 | 174 | 70 | 293 | $10^{-35}$ | *Rattus norvegicus* | NM_024160.1 | 192 | 51 | 441 | $10^{-42}$ | *Rattus norvegicus* | Q62737 |
| | *Me*DUOXA | DUOXA | 1888 | 428 | 40 | 323 | $10^{-40}$ | *Homo sapiens* | NM_144565.2 | 483 | 36 | 467 | $10^{-44}$ | *Homo sapiens* | Q1HG43-2 |
| | *Me*Rac-a | Rac1/2 | 732 | 195 | 77 | 1038 | $10^{-116}$ | *Danio rerio* | AY682791.1 | 192 | 90 | 914 | $10^{-97}$ | *Rattus norvegicus* | Q6RUV5 |
| | *Me*Rac-b | Rac1/2 | 440 | 124 | 98 | 591 | $10^{-57}$ | *Caenorhabditis elegans* | XM_002676953.1 | 191 | 69 | 489 | $10^{-48}$ | *Caenorhabditis elegans* | Q03206 |

*only the ORF sequence of *Me*DUOX-b was blasted in NCBI due to problems with its size and the CPU usage limit of the BLAST server

In addition, a NOX1-3-like transcript, named *Me* NOX2 due to its greater resemblance to NOX2, and a NOX5 ortholog, named *Me* NOX5, were detected. These transcripts are all orthologs of the major subunit gp91$^{phox}$. Furthermore, some minor subunits were also discovered including p22$^{phox}$ (*Me* p22$^{phox}$), the DUOX maturation factor DUOXA (*Me* DUOXA) and two Rac orthologs (*Me* Rac-a and -b). Identification of the minor subunits p47$^{phox}$, p40$^{phox}$ and p67$^{phox}$ was inconclusive, since their characteristic functional domains are also present in a variety of other proteins. Except for *Me* NOX5, the complete open reading frames (ORFs) containing all functional domains were obtained (nucleotide and amino acid sequences with the detailed results of the SMART domain architecture analyses are given in the supplements in section 9.4). This was supported by the observation that ORF lengths of *M. edulis* orthologs greatly matched the expected ORF length obtained from orthologs displaying the best BLAST hit in UniProt/Swiss-Prot. As depicted in Table 3-4, the E values of the NCBI as well as of the UniProt/Swiss-Prot BLAST results are very low, their score and identities or coverage (both in %), on the other hand, are very high, which taken together indicates that the search results are highly significant and the likelihood for being NOX and DUOX family members is extraordinarily high.

### 3.2.2.2 Identification of NOX/DUOX orthologs in other Lophotrochozoa

Orthologs of the NADPH- and dual oxidase family of enzymes were identified in various eukaryote species, ranging from plants to mammals (Kawahara *et al.* 2007), but only little is known about Molluscs and even other Lophotrochozoa. Therefore, the occurrence of NOX and DUOX orthologs in the blue mussel *M. edulis*, as discovered in 3.2.2.1, led to further investigations of a possible broad distribution in the superphylum Lophotrochozoa.

To examine if NOX and DUOX orthologs are also widespread among various Lophotrochozoan species, publicly available sequence data bases were searched for major subunits of the corresponding orthologs. Their similarity to other NOX and DUOX proteins was analyzed in UniProt/Swiss-Prot (BLASTp) and their domain structure was investigated in SMART.

Table 3-5 displays fragments identified for Lophotrochozoa with a high similarity to NOX and DUOX enzymes and an ORF length of more than 99 aa. Similar orthologs as discovered in *Mytilus edulis*, namely at least two DUOX orthologs, a NOX1-3 and a NOX5 ortholog, were obtained in the transcriptome databases of the bivalves *Laternula elliptica* and *Arctica islandica*. Orthologs of NOX1, 2 or 3 could not be attributed to one distinct ortholog due to their similar domain structure and were therefore referred to as NOX1-3. Results even indicated a third DUOX ortholog (*Le* DUOX-c) in *Laternula elliptica*, which could not be assembled or elongated with one of the other DUOX orthologs (*Le* DUOX-a and -b).

**Table 3-5: Overview of NOX and DUOX sequences found in Lophotrochozoa.** The sequence type (T = transcriptome, G = genome) as well as the corresponding predicted protein length (in amino acids, aa) is indicated. If there are more than two orthologs for the same gene, they are marked with small letters in order of their discovery. Only the three longest sequence fragments of one source per ortholog and species have been used. And only fragments with ≥ 99 aa were included. The covered domains are stated. The sequences' source and accession numbers are also given. Sequences were blasted in UniProt/Swiss-Prot (BLASTp) and identity (Id., in %), score as well as the E value of the best Swiss-Prot hit are denoted.

| | Class | Species | Type | ORF (aa) | Covered domains | UniProt/Swiss-Prot Id. (%) | Score | E value | Accession no. | Source |
|---|---|---|---|---|---|---|---|---|---|---|
| **DUOX** | | *For comparison: Homo sapiens (DUOX1)* | Protein | 1551 | PeOx, EF, Ferric, FAD, NAD | | | | Q9NRD9 | 6 |
| | Bivalvia | *Mytilus edulis (a)* | T | 1571 | PeOx, EF, Ferric, FAD, NAD | 39 | 2866 | 0 | *Me* DUOX-a | 1 |
| | | *Mytilus edulis (b)* | T | 1594 | PeOx, EF, Ferric, FAD, NAD | 39 | 2842 | 0 | *Me* DUOX-b | 1 |
| | | *Arctica islandica (a)* | T | 1531 | PeOx, EF, Ferric, FAD, NAD | 41 | 2968 | 0 | *Ai* DUOX-a | 1 |
| | | *Arctica islandica (b)* | T | 1571 | PeOx, EF, Ferric, FAD, NAD | 38 | 2715 | 0 | *Ai* DUOX-b | 1 |
| | | *Laternula elliptica (a)* | T | 1498 | PeOx, EF, Ferric, FAD, NAD | 42 | 2937 | 0 | *Le* DUOX-a | 1 |
| | | *Laternula elliptica (b)* | T | 423 | Ferric, FAD, NAD | 54 | 1711 | $10^{-126}$ | *Le* DUOX-b | 1 |
| | | *Laternula elliptica (c)* | T | 1221 | PeOx, EF, Fer | 36 | 1979 | 0 | *Le* DUOX-c | 1 |
| | | *Crassostrea gigas (a)* | EST | 189 | FAD, NAD | 65 | 706 | $10^{-72}$ | CGC01263 | 2 |
| | | *Crassostrea gigas (b)* | EST | 308 | EF | 31 | 348 | $10^{-31}$ | 2724 | 3 |
| | | *Crassostrea gigas (c)* | EST | 322 | FAD, NAD | 62 | 1134 | $10^{-122}$ | 3751 | 3 |
| | | *Crassostrea gigas (d)* | EST | 234 | PeOx | 38 | 418 | $10^{-39}$ | 13724 | 3 |
| | | *Crassostrea virginica* | EST | 213 | PeOx | 41 | 378 | $10^{-34}$ | CVC02126 | 2 |
| | | *Mytilus galloprovincialis* | EST | 151 | PeOx | 44 | 284 | $10^{-24}$ | MGC04473 | 4 |
| | Gastropoda | *Lottia gigantea (a)* | G | 1519 | PeOx, EF, Ferric, FAD, NAD | 41 | 3055 | 0 | 71226 | 5 |
| | | *Lottia gigantea (b)* | G | 1576 | PeOx, EF, Ferric, FAD, NAD | 39 | 2784 | 0 | 112284 | 5 |
| | | *Lottia gigantea (c)* | G | 1519 | PeOx, EF, Ferric, FAD, NAD | 39 | 2837 | 0 | 71249 | 5 |
| | | *Biomphalaria glabrata (a)* | EST | 183 | PeOx | 40 | 338 | $10^{-30}$ | BGC01447 | 2 |
| | | *Biomphalaria glabrata (b)* | EST | 117 | PeOx | 49 | 252 | $10^{-20}$ | BGC02667 | 2 |
| | | *Aplysia californica (a)* | EST | 252 | PeOx | 38 | 449 | $10^{-42}$ | 5196 | 3 |
| | | *Aplysia californica (b)* | EST | 298 | FAD, NAD | 60 | 986 | $10^{-105}$ | 17140 | 3 |
| | | *Aplysia californica (c)* | EST | 211 | PeOx | 36 | 374 | $10^{-34}$ | 37921 | 3 |
| | Polychaeta | *Capitella teleta* | G | 1437 | PeOx, EF, Ferric, FAD, NAD | 39 | 2781 | 0 | 191097 | 5 |
| **NOX1-3** | | *For comparison: Homo sapiens (NOX2)* | Protein | 570 | Ferric, FAD, NAD | | | | P04839 | 6 |
| | Bivalvia | *Mytilus edulis* | T | 574 | Ferric, FAD, NAD | 52 | 1593 | $10^{-175}$ | *Me* NOX2 | 1 |
| | | *Arctica islandica* | T | 226 | FAD, NAD | 39 | 371 | $10^{-33}$ | *Ai* NOX2 | 1 |
| | | *Laternula elliptica* | T | 154 | Ferric | 55 | 373 | $10^{-34}$ | *Le* NOX2 | 1 |
| | | *Crassostrea gigas(a)* | EST | 99 | Ferric | 57 | 273 | $10^{-22}$ | 5938 | 3 |
| | | *Crassostrea gigas(b)* | EST | 168 | NAD | 55 | 511 | $10^{-50}$ | 23808 | 3 |
| | Gastropoda | *Lottia gigantea* | G | 563 | Ferric, FAD, NAD | 51 | 1558 | $10^{-170}$ | 175333 | 5 |
| | Cephalopoda | *Euprymna scolopes* | T | 571 | Ferric, FAD, NAD | 50 | 1441 | $10^{-157}$ | *Es* NOX2 | 1 |
| | Polychaeta | *Capitella teleta* | G | 579 | Ferric, FAD, NAD | 50 | 1532 | $10^{-167}$ | 223007 | 5 |
| | Clitellata | *Helobdella robusta* | G | 554 | Ferric, FAD, NAD | 39 | 1118 | $10^{-119}$ | 66368 | 5 |
| **NOX4** | | *For comparison: Homo sapiens (NOX4)* | Protein | 578 | Ferric, FAD, NAD | | | | Q9NPH5 | 6 |
| | Cephalopoda | *Euprymna scolopes* | T | 302 | Ferric, FAD | 38 | 486 | $10^{-54}$ | *Es* NOX4 | 1 |
| **NOX5** | | *For comparison: Homo sapiens (NOX5)* | Protein | 765 | EF, Ferric, FAD, NAD | | | | Q96PH1 | 6 |
| | Bivalvia | *Mytilus edulis* | T | 309 | FAD, NAD | 48 | 749 | $10^{-77}$ | *Me* NOX5 | 1 |
| | | *Arctica islandica* | T | 293 | FAD, NAD | 51 | 772 | $10^{-80}$ | *Ai* NOX5 | 1 |
| | | *Laternula elliptica (a)* | T | 156 | EF | 47 | 362 | $10^{-33}$ | *Le1* NOX5 | 1 |
| | | *Laternula elliptica (b)* | T | 403 | FAD, NAD | 52 | 1143 | $10^{-123}$ | *Le2* NOX5 | 1 |
| | Gastropoda | *Lottia gigantea (a)* | G | 743 | EF, Ferric, FAD, NAD | 49 | 1910 | 0 | 159226 | 5 |
| | | *Lottia gigantea (b)* | G | 744 | EF, Ferric, FAD, NAD | 48 | 1864 | 0 | 179958 | 5 |
| | Polychaeta | *Capitella teleta (a)* | G | 726 | EF, Ferric, FAD, NAD | 50 | 1880 | 0 | 147619 | 5 |
| | | *Capitella teleta (b)* | G | 745 | EF, Ferric, FAD, NAD | 48 | 1837 | 0 | 147607 | 5 |

1:  ICMB, Kiel (*E.scolopes* transcriptome dataset generated in cooperation with Prof. Dr. Margaret McFall-Ngai)
2:  MolluscDB, Mark Blaxter (http://www.nematodes.org/NeglectedGenomes/MOLLUSCA/
3:  DBGET, KEGG (http://www.genome.jp/dbget/)
4:  MytiBase (http://mussel.cribi.unipd.it/?p=search)
5:  JGI Database (http://genome.jgi-psf.org/)
6:  Uniprot/Swissprot (http://www. uniprot.org)
Domains:  PeOx: peroxidase, EF: EF-hands, Ferric: ferric reductase, FAD: FAD-binding, NAD: NADPH-binding

This is concordant with findings in the snail *Lottia gigantea*, where three full length DUOX orthologs were found. But not only in Bivalvia, also in the classes of Gastropoda and Polychaeta were orthologs of DUOX, NOX1-3 and NOX5 identified. In contrast, just one kind of the mentioned orthologs was detected in Cephalopoda and Clitellata, which exhibited only orthologs of NOX1-3. However, it has to be noted that these two classes also had the least sequence information available. Due to the limited sequence information, likely not all orthologs were identified in all species of a taxonomic class. Even though merely fragments of most orthologs were available, the obtained UniProt/Swiss-Prot parameters (low E values, high scores and identities) clearly indicate that these fragments belong to the NOX and DUOX family. Interestingly, there is no evidence so far for the occurrence of NOX4-like orthologs in any of the investigated Lophotrochozoa except for in *Euprymna scolopes* (see also Figure 4-1).

In the previous two sections, orthologs of the NOX and DUOX family of enzymes were identified in *M. edulis* and other Lophotrochozoa comprising mainly NOX1-3, NOX5 and DUOX orthologs. But moreover, the results indicate that NOX and DUOX orthologs seem to be highly conserved throughout the whole superphylum Lophotrochozoa. To further broaden the knowledge of NOX and DUOX in Lophotrochozoa I set the newly obtained NOX and DUOX orthologs in bivalves and other Lophotrochozoa in relation to NOX and DUOX orthologs of other eukaryotes using phylogenetic analysis as discussed in the next section (3.2.2.3).

### 3.2.2.3 *Phylogenetic analysis of NOX/DUOX orthologs*

The evolutionary relationship of NOX and DUOX orthologs can be assessed by phylogenetic tree generation. In phylogenetic trees species joined together are implied to have descended from a common ancestor represented by the corresponding node. The branch lengths indicate the number of amino acid substitutions per site. Bootstrap analysis (n=100) indicates the confidence for each node by re-sampling the original data matrix and giving the percentage of trees that also exhibit the respective clade.

Since DUOX1 and DUOX2 are only clearly defined in mammals, DUOX orthologs of invertebrate organisms were named in this study in order of their discovery a, b and c. The phylogenetic analysis (Figure 3-6) revealed that bivalve DUOX orthologs cluster with other molluscan DUOX enzymes as expected. But interestingly, DUOX orthologs of basal deuterostomes, consisting of Tunicates, Lancelets and Echinoderms, seem to be more closely related to Lophotrochozoa than to the Ecdysozoa, including other well known model organisms, such as *Caenorhabditis elegans* or *Drosophila melanogaster.* The phylogenetic most ancient DUOX-like ortholog in animals was found in Cnidaria, i.e.

*Hydra magnipapillata.* EF hand containing DUOX orthologs, NOX C in amoeba and Rboh D/B in plants, were included and validated as out-groups. Particularly interesting is the observation that bivalve DUOX orthologs cluster into three distinct groups, DUOX-a, -b and -c, according to their kind of ortholog rather than into species-specific groups, as can also be observed for mammalian DUOX1 and 2 orthologs. Especially *Le* DUOX-c seems to have a larger phylogenetic distance to other bivalve DUOX orthologs, clustering together with DUOX-c of *Lottia gigantea* and a DUOX ortholog of *Capitella teleta* in a clade between Ecdysozoa and the remaining Lophotrochozoa. This result shows for the first time the existence of distinctly different groups of DUOX orthologs in bivalves, similar to presence of DUOX1 and 2 in mammals.

The NOX5 tree (Figure 3-7) differed from the DUOX tree by depicting a more divergent evolution in basal deuterostomes such as *Saccoglossus kowalevskii* and *Strongylocentrotus purpuratus*. Basal deuterostomes displayed two differently evolved NOX5 orthologs, which clustered together with Ecdysozoa and Placozoa on one hand and with the Lophotrochozoa on the other hand. In contrast to the DUOX tree, the group Ecdysozoa in the NOX5 tree was solely comprised of NOX5 orthologs from arthropods, since up to date no NOX5 ortholog has been identified in Nematoda. EF hand containing NOX5 orthologs in amoeba (NOX C), plants (Rboh D/B), fungi (NOX C) and algae (NOX D) were included and validated as out-groups.

The phylogenetic analysis of NOX2 (Figure 3-8) yielded no distinct results providing low bootstrap values for protostomes and basal deuterostomes. Therefore, only a condensed tree could be calculated (cut-off bootstrap value: 50%), in which basal deuterostomes clustered together with Protostomes, Amoeba and Cnidaria in no specific order. Plant Rboh D and B orthologs were used as out-group. It has to be noted so far no NOX2 orthologs have been found in the Ecdysozoa.

Taken together, EF-hand containing orthologs, whether it is NOX5 or DUOX, seem to be present in all eukaryotes from plants and amoeba to vertebrates. In bivalves and other molluscs, three distinct DUOX ortholog clusters were identified, which are more closely related to the early ancestors of vertebrates than the Ecdysozoa. In addition, NOX5 and NOX2 were present in most analyzed Lophotrochozoan species, which is in contrast to well investigated Ecdysozoan model organisms, such as *Caenorhabditis elegans* or *Drosophila melanogaster.* So far only the presence, structure and evolutionary relationship of NOX and DUOX orthologs were examined. To gain more hints for their putative function in hemocytes of bivalves, orthologs were further investigated at mRNA expression level.
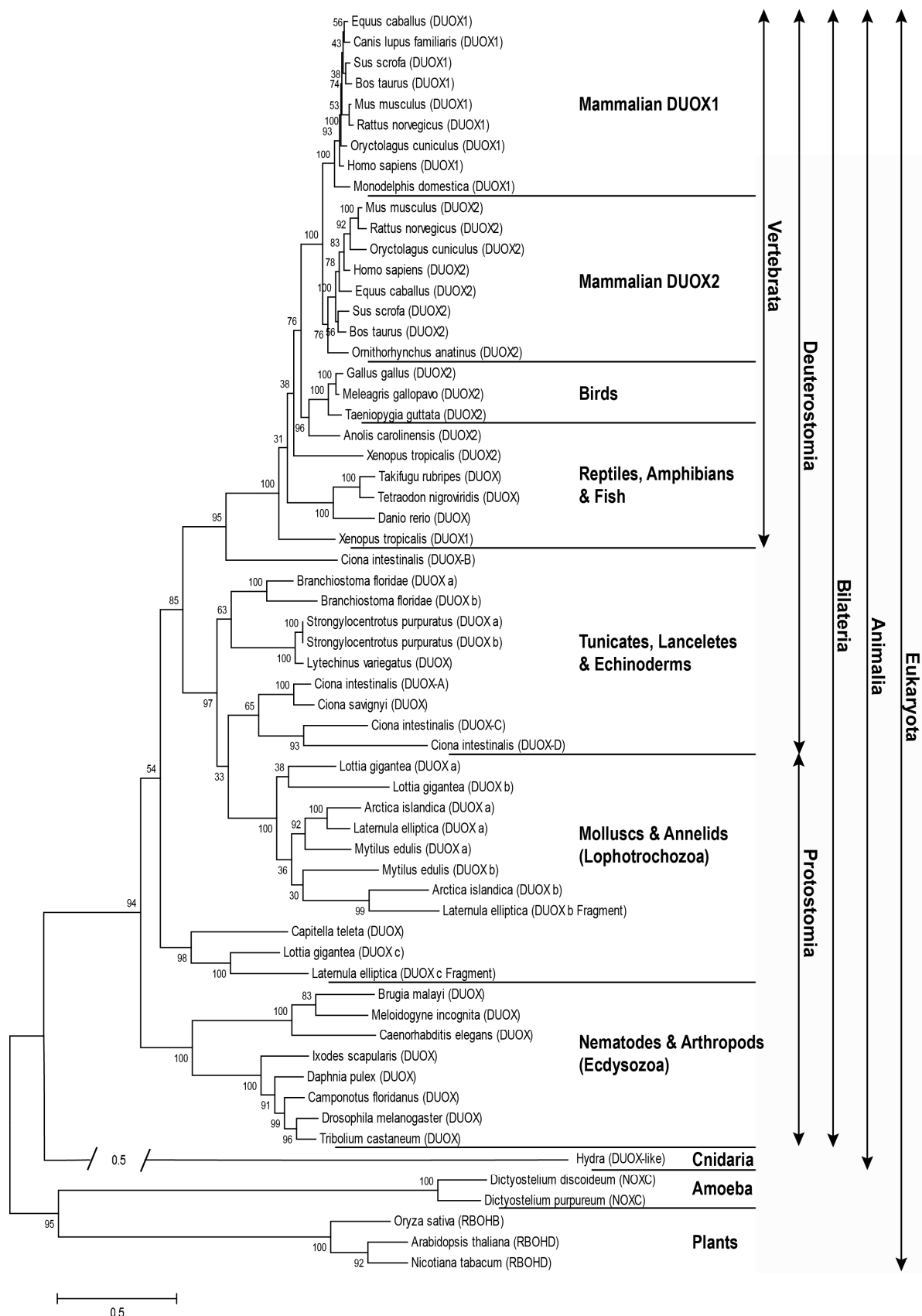
**Figure 3-6: Phylogenetic tree of DUOX orthologs obtained from molecular phylogenetic analysis.** The evolutionary history was inferred using the Maximum Likelihood method based on the WAG model. The tree with the highest log likelihood (-39867.0825) is shown. 100 bootstrap replicates were conducted. The percentage of trees in which the associated taxa clustered together is shown next to the branches. A discrete Gamma distribution was used to model evolutionary rate differences among sites (5 categories (+G, parameter = 2.0741)). The tree is drawn to scale with branch lengths measured in the number of substitutions per site. The analysis involved 61 amino acid sequences. There were a total of 714 positions.
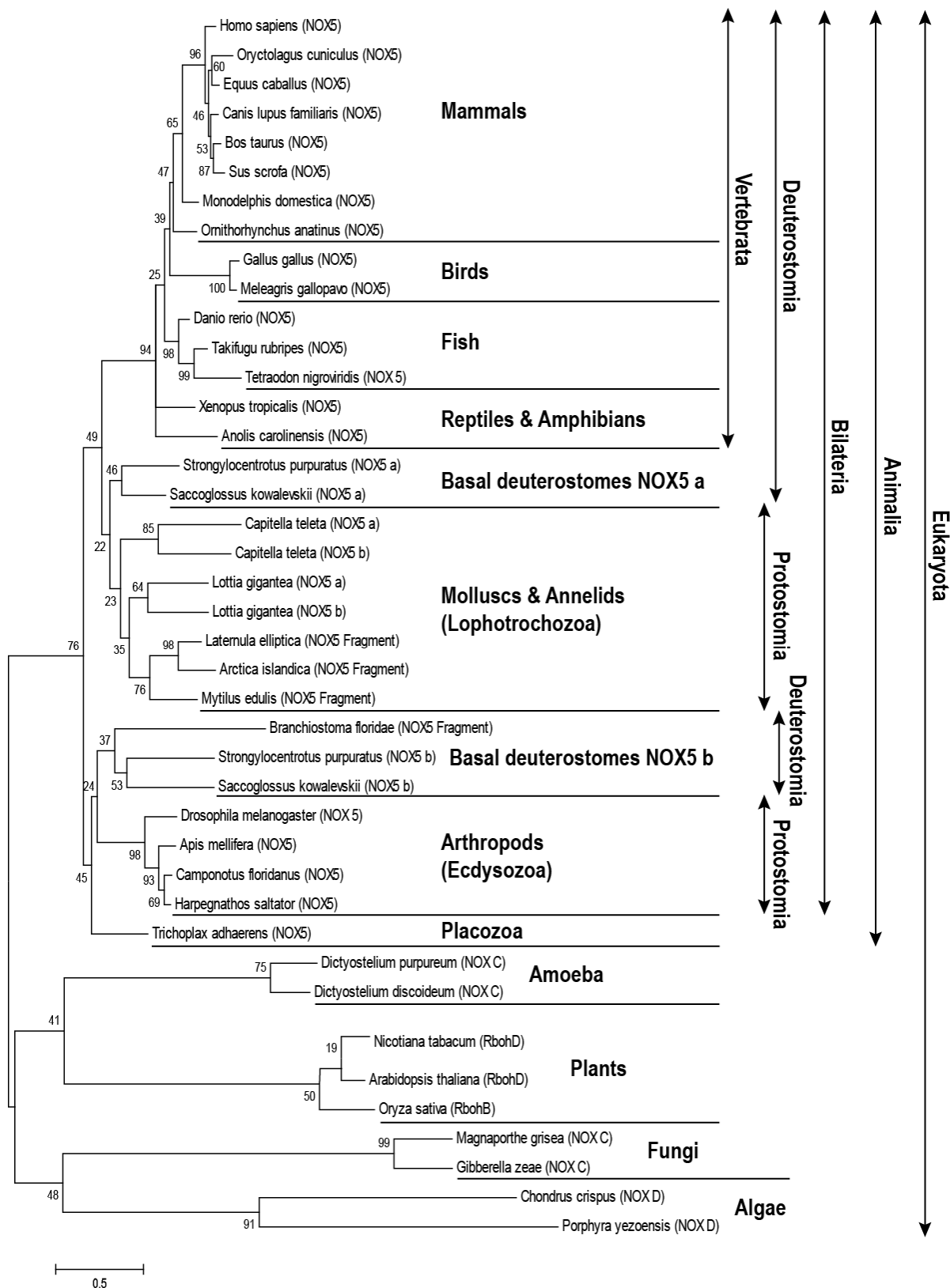
**Figure 3-7: Phylogenetic tree of NOX5 orthologs obtained from molecular phylogenetic analysis.** The evolutionary history was inferred by using the Maximum Likelihood method based on the JTT model. The tree with the highest log likelihood (-13564.6307) is shown. 100 bootstrap replicates were conducted. The percentage of trees in which the associated taxa clustered together is shown next to the branches. A discrete Gamma distribution was used to model evolutionary rate differences among sites (5 categories (+G, parameter = 1.8879)). The tree is drawn to scale with branch lengths measured in the number of substitutions per site. The analysis involved 42 amino acid sequences. There were a total of 275 positions in the final dataset.
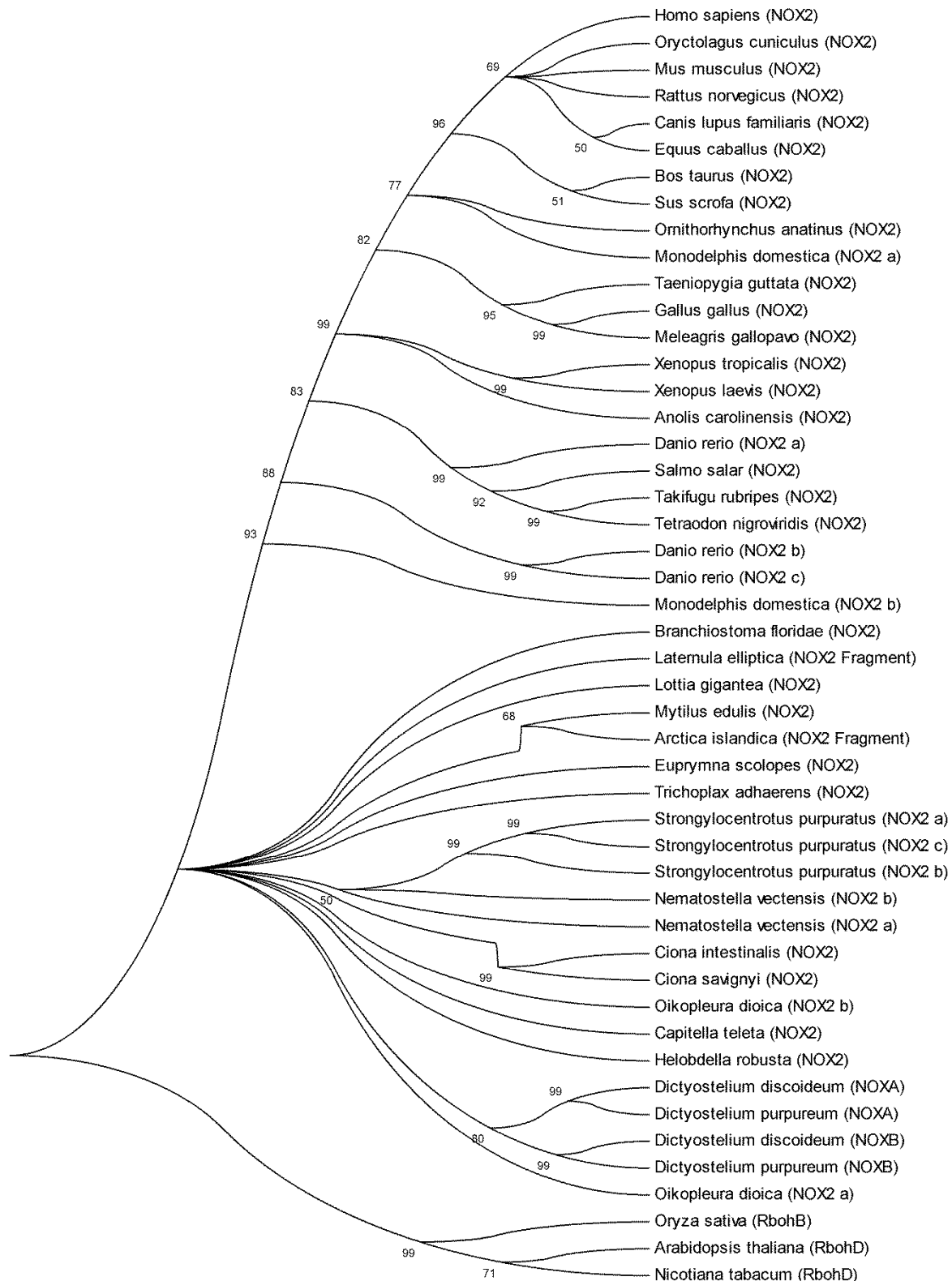
**Figure 3-8: Condensed phylogenetic tree of NOX2 orthologs obtained from molecular phylogenetic analysis.** The evolutionary history was inferred by using the Maximum Likelihood method based on the WAG model. The tree with the highest log likelihood (-15524.1874) is shown. 100 bootstrap replicates were conducted. The percentage of trees in which the associated taxa clustered together is shown next to the branches (cut-off: 50%). A discrete Gamma distribution was used to model evolutionary rate differences among sites (5 categories (+$G$, parameter = 1.9618)). The analysis involved 48 amino acid sequences. There were a total of 373 positions in the final dataset.

### 3.2.2.4 Tissue-specific mRNA expression of NOX/DUOX orthologs in M. edulis

To locate NOX and DUOX orthologs in different tissues of *M. edulis*, the expression of major subunits of NOX and DUOX orthologs was examined at mRNA level using qRT-PCR in a tissue panel consisting of digestive gland, gill, adductor muscle, foot, mantel and mantel margin tissue as well as hemocytes (n=3). The qRT-PCR analysis (Figure 3-10, normalized with 18S rRNA) revealed that *Me* NOX5 and *Me* DUOX-a exhibited a significantly higher expression in the gills than in any other tissues, whereas *Me* NOX2 was significantly increased in hemocytes only in comparison to muscular tissues, such as foot and adductor muscle. In contrast to *Me* NOX2, *Me* DUOX-b showed an extraordinary high (p<0.001, ANOVA, Bonferroni) expression in hemocytes not only compared to other tissues but also compared to other immune genes (Figure 3-9). The latter was observed in another expression analysis at mRNA level (n=7) consisting of major immune genes expressed in hemocytes (versus 28S rRNA), such as orthologs of LBP/BPI, antimicrobial peptides like mytilin C and myticin C, the antifungal peptide mytimycin, as well as IκB orthologs. Of all these genes, only *Me* Myticin C and *Me* Mytimycin depicted an equal or even higher expression than *Me* DUOX-b in hemocytes.

Due to its remarkably high expression in the immune cells of *M. edulis,* particularly *Me* DUOX-b may be involved in ROS production in hemocytes. To examine if this expression pattern can also be found in other bivalves, which would additionally support the obtained hypothesis, the tissue-specific expression of DUOX orthologs was examined in two further bivalves.
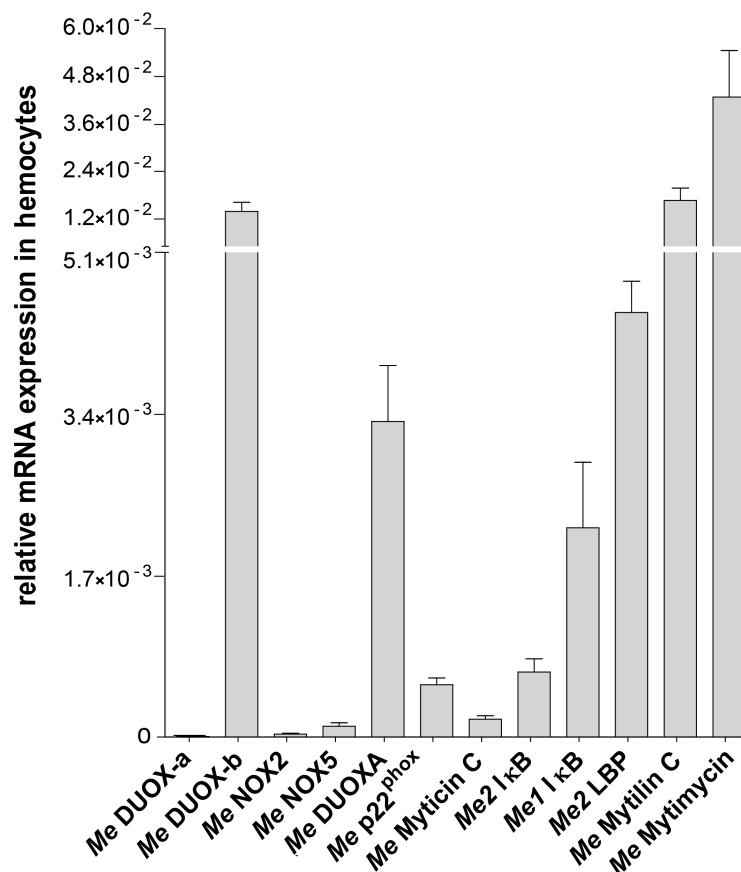


**Figure 3-9: Relative mRNA expression of major immune genes in hemocytes of *M. edulis*.** Results are obtained by normalizing against the 28S rRNA reference gene using qRT-PCR. The mean and standard error of 7 hemocyte pools are shown. Note the two segmented y-axis.
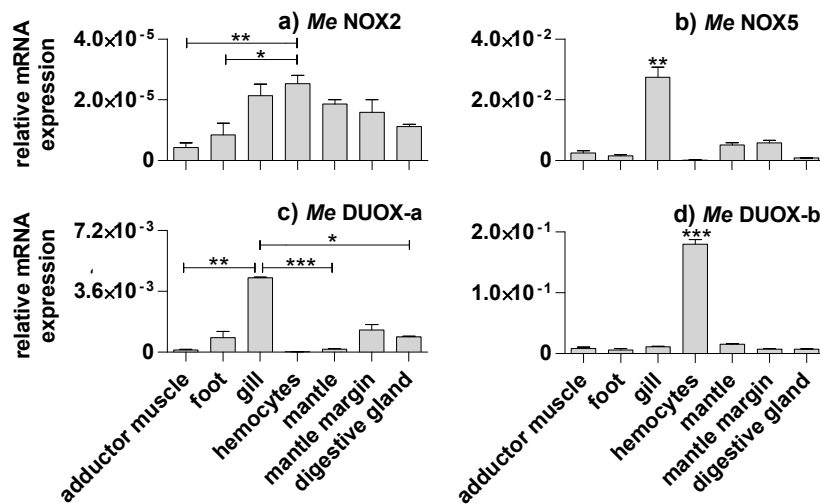
**Figure 3-10: Tissue panel analysis of NOX and DUOX orthologs in *M. edulis.*** The relative mRNA expression of *Me* NOX2 (**a**), *Me* NOX5 (**b**), *Me* DUOX-a (**c**) and *Me* DUOX-b (**d**) in relation to the expression of the 18S rRNA reference gene was investigated in different tissues including adductor muscle, foot, gill, hemocytes, mantle, mantle margin and digestive gland tissue using qRT-PCR (n=3). For a simplified graphical representation asterisks only indicate significant differences of the tissue depicting the highest expression in comparison to the other tissues (ANOVA, Bonferroni). Standard errors are displayed.
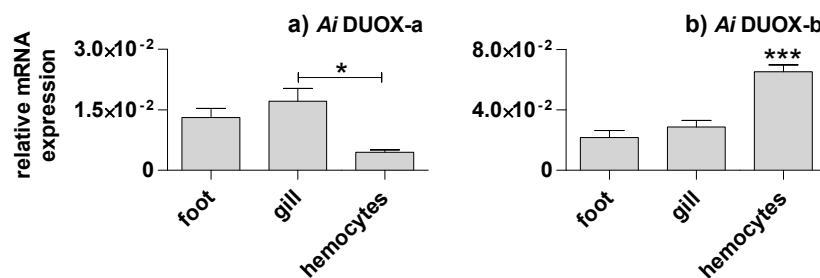


**Figure 3-11: Tissue panel analysis of NOX and DUOX orthologs in *A. islandica.*** The relative mRNA expression of *Ai* DUOX-a (**a**) and *Ai* DUOX-b (**b**) in foot, gill and hemocytes in relation to 18S rRNA expression was investigated using qRT-PCR (n=4). Asterisks indicate significant differences (ANOVA, Bonferroni). Standard errors are displayed.
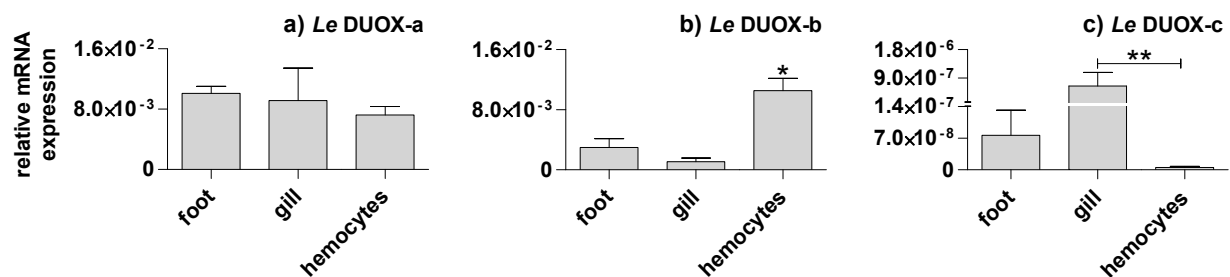


**Figure 3-12: Tissue panel analysis of NOX and DUOX orthologs in *L. elliptica.*** The relative mRNA expression of *Le* DUOX-a (**a**), *Le* DUOX-b (**b**) and *Le* DUOX-c (**c**, note the two segmented y-axes) in foot, gill and hemocytes in relation to 18S rRNA expression was investigated using qRT-PCR (n=4). Asterisks indicate significant differences (ANOVA, Bonferroni). Standard errors are displayed.

*3.2.2.5   Tissue-specific expression of NOX/DUOX orthologs in A. islandica and L. elliptica*

For validation of tissue panel findings (3.2.2.4) in *M. edulis* and to obtain a possible unifying expression pattern among bivalve tissues, expression of DUOX orthologs was further investigated in the Antarctic bivalve *Laternula elliptica* (n=3, Figure 3-12) and in the Islandic clam *Arctica islandica* (n=4, Figure 3-11). Therefore, qRT-PCR analyses were carried out using a tissue panel consisting of gill and foot tissue as well as hemocytes normalized versus the 18S rRNA reference gene. Similar to DUOX-a expression levels in *M. edulis*, *Ai* and *Le* DUOX-a displayed a higher expression in gill tissue in contrast to lower expression levels in hemocytes, which was even significant in *A. islandica* (p<0.05, ANOVA, Bonferroni). Nevertheless, this higher expression of DUOX-a in gills compared to other tissues was distinctly more pronounced in *M. edulis*; especially in relation to foot tissue, which possessed an equally high DUOX-a expression level than gill tissue in *L. elliptica* and *A. islandica*. In line with *Me* DUOX-b, *Ai* and *Le* DUOX-b showed a significantly elevated expression in hemocytes (p<0.001 and p<0.05 respectively) compared to any other tissues. A third ortholog, *Le* DUOX-c, depicted a similar tissue panel expression pattern to DUOX-a with a significantly increased (p<0.01) expression in gill tissue. However, in the phylogenetic analysis it was revealed that this ortholog was distinctly different from DUOX-a.

In summary, DUOX-b transcript levels were highly elevated in hemocytes of all three bivalve species. The different orthologs not only shared a DUOX-a- or DUOX-b-specific expression pattern among tissues, they also clustered together during phylogenetic analysis (3.2.2.3) building taxonomic and putative functional groups. After unraveling their tissue-specific distribution, the expression of NOX and DUOX encoding genes as possible immune genes involved in ROS production in hemocytes was further examined in response to immune stimulation.

### 3.2.3   Functional analysis of NOX/DUOX orthologs in *M. edulis*

*3.2.3.1   Expression analysis of NOX/DUOX orthologs in hemocytes after immune stimulation*

To investigate whether mRNA levels of major and minor NOX/DUOX subunits are regulated during immune stress in hemocytes of *Mytilus edulis*, stimulation experiments involving different stimuli and incubation times were conducted using qRT-PCR analysis. In addition to NOX and DUOX family members, the expression of the antimicrobial peptide *Me* Myticin C was assessed. Antimicrobial peptides are responsible for bacterial killing and presumably work complementary to ROS production by NOX and DUOX enzymes, as postulated for human phagosomes (Flannagan *et al.* 2009). Therefore, short- (5-60 min), mid- (1-8 h) and long-term (3-24 h) expression analyses, including various microbial associated molecular patterns (MAMPs), were carried out (normalized against 28S rRNA,

Figure 3-14). In addition to MAMPs, which resemble only a specific part of a microbe, living *Listonella anguillarum* were included in all three analyses as a more naturally occurring stimulus. Concomitantly, extracellular ROS production was measured after 1, 8 and 6 hours, respectively, employing the Amplex Red test. Unstimulated cells were used as a control.

For the short-term expression analysis, zymosan A (n=6-8) or *L. anguillarum* (n=4-8) were chosen as stimuli, since both stimuli depicted a significant increase in ROS production during this period of time as discovered in 3.2.1.1. No increase in the expression of all investigated transcripts was observed throughout the experiment neither in zymosan A nor *L. anguillarum* stimulated cells (Figure 3-14A). Furthermore, expression seemed to be decreased in all orthologs during stimulation, being even significant lower (ANOVA, Bonferroni) after 5 min of stimulation with *L. anguillarum* compared to the control in *Me* NOX2 ($p<0.05$), *Me* DUOX-b ($p<0.05$) and *Me* DUOXA ($p<0.01$) and also after 30 min in *Me* DUOXA ($p<0.05$). Zymosan A did not evoke a significant response in the expression of NOX and DUOX orthologs. Concomitant to a significant decrease in *Me* Myticin C expression after 5 min of *L. anguillarum* stimulation ($p<0.01$, t-test with Welch's correction), *Me* Myticin C depicted also a decreasing trend at transcript level during zymosan A stimulation in comparison to the control. On the other hand, a clear increase in simultaneous ROS production assays was observed for both stimuli ($p<0.001$, ANOVA, Bonferroni) during the course of this experiment (Figure 3-13A).

Parallel to *L. anguillarum* (n=4-7) stimulation, flagellin (n=5-7) was used as stimulus in the mid-term expression analysis (Figure 3-14B), to investigate the expression of NOX/DUOX orthologs simultaneously with other major immune gene orthologs in hemocytes (as described in 3.1.3.2). Comparing the transcript levels after 1 hour of *L. anguillarum* stimulation in the mid-term experiment to 1 hour transcript levels in the short term experiment, the decreased trend in expression for *Me* Myticin C in comparison to the control is verified. The expression levels even remained slightly decreased during the rest of the mid-term expression analysis. NOX and DUOX orthologs did not depict a decrease after 1 hour of *L. anguillarum* stimulation in the mid-term experiment as was observed in the short-term experiment. During the remaining 2 to 8 hours of incubation with *L. anguillarum,* also no significant changes in the expression levels of NOX and DUOX orthologs occurred ($p>0.05$, ANOVA). In contrast to the stimulation with *L. anguillarum*, incubation with flagellin resulted in significant elevated expression levels of major NOX and DUOX subunits. While all minor subunits and *Me* Myticin C displayed only an increased trend at mRNA level during the experiment, except the significant increase after 8 hours in *Me* DUOXA, all major subunits displayed a significant increase at least at some point during flagellin stimulation. Major subunits showed a significantly elevated expression level after 2 hours of incubation. In comparison to the control, this increase was particularly more noticeable in DUOX orthologs ($p<0.001$, ANOVA, Bonferroni) than in NOX orthologs ($p<0.05$, ANOVA, Bonferroni). In contrast to NOX

orthologs, DUOX orthologs were even significantly up-regulated after 1 and 4 hours of stimulation (p<0.01) in relation to the control. At 8 hours transcript levels of DUOX orthologs (p<0.05) and *Me* NOX5 were significantly (p<0.01) elevated. On the whole, DUOX orthologs showed a higher and faster induction in hemocytes upon immune challenge by flagellin than NOX orthologs. In contrast to this, only *L. anguillarum* but not flagellin was able to elicit a significant (p<0.01, ANOVA, Bonferroni) increase in ROS production during 8 hours of stimulation (Figure 3-13B).

In the long-term experiment (Figure 3-14C) stimuli employed were either *L. anguillarum* (n=4-6) or LPS (n=4-6), which is known to elicit immune-reactions by the induction of TLR pathway members at mRNA level (Saphörster, Findeisen, Rosenstiel, Philipp unpublished data, see 9.7). No significant changes were observed after 3 and 6 hours neither in LPS nor in *L. anguillarum* stimulated cells. But a significant down-regulation (p<0.01) was observed after 24 hours of stimulation with *L. anguillarum* in *Me* NOX2, *Me* DUOX-b (both ANOVA, Bonferroni) and *Me* p22phox (t-test with Welch's correction). In addition, expression of *Me* DUOX-b was also significantly down-regulated after 24 hours of stimulation with LPS (p<0.001, ANOVA, Bonferroni). In contrast, *Me* Myticin C was significantly up-regulated (p<0.05, ANOVA, Bonferroni) after 24 hours of *L. anguillarum* stimulation. LPS did not evoke a response in ROS production after 6 hours, but *L. anguillarum* stimulation did significantly increase ROS levels (p<0.001, ANOVA, Bonferroni), even though no significant increase in NOX/DUOX expression was measured (Figure 3-13C).
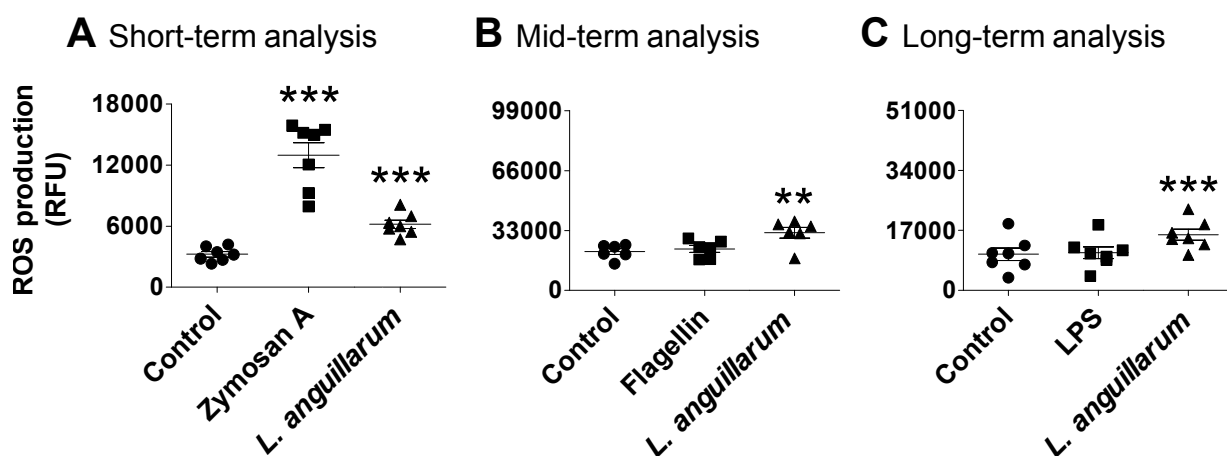


**Figure 3-13: ROS production in *M. edulis* hemocytes during immune-stimulation experiments.** Extracellular ROS production (in RFU) was assessed after **A**) 1 hour incubation with zymosan A for experiments involved in the short-term (n=8); **B**) after 8 hours incubation with flagellin in the mid-term (n=7); and **C**) after 6 hours incubation with LPS (p<0.001) in the long-term (n=6) expression analysis of NOX and DUOX. All analyses also included a *Listonella anguillarum* treatment. Control measurements consisted of unstimulated hemocytes. Individual experiments, as well as mean values and standard errors are displayed. Asterisks indicate significant differences (ANOVA, Bonferroni).
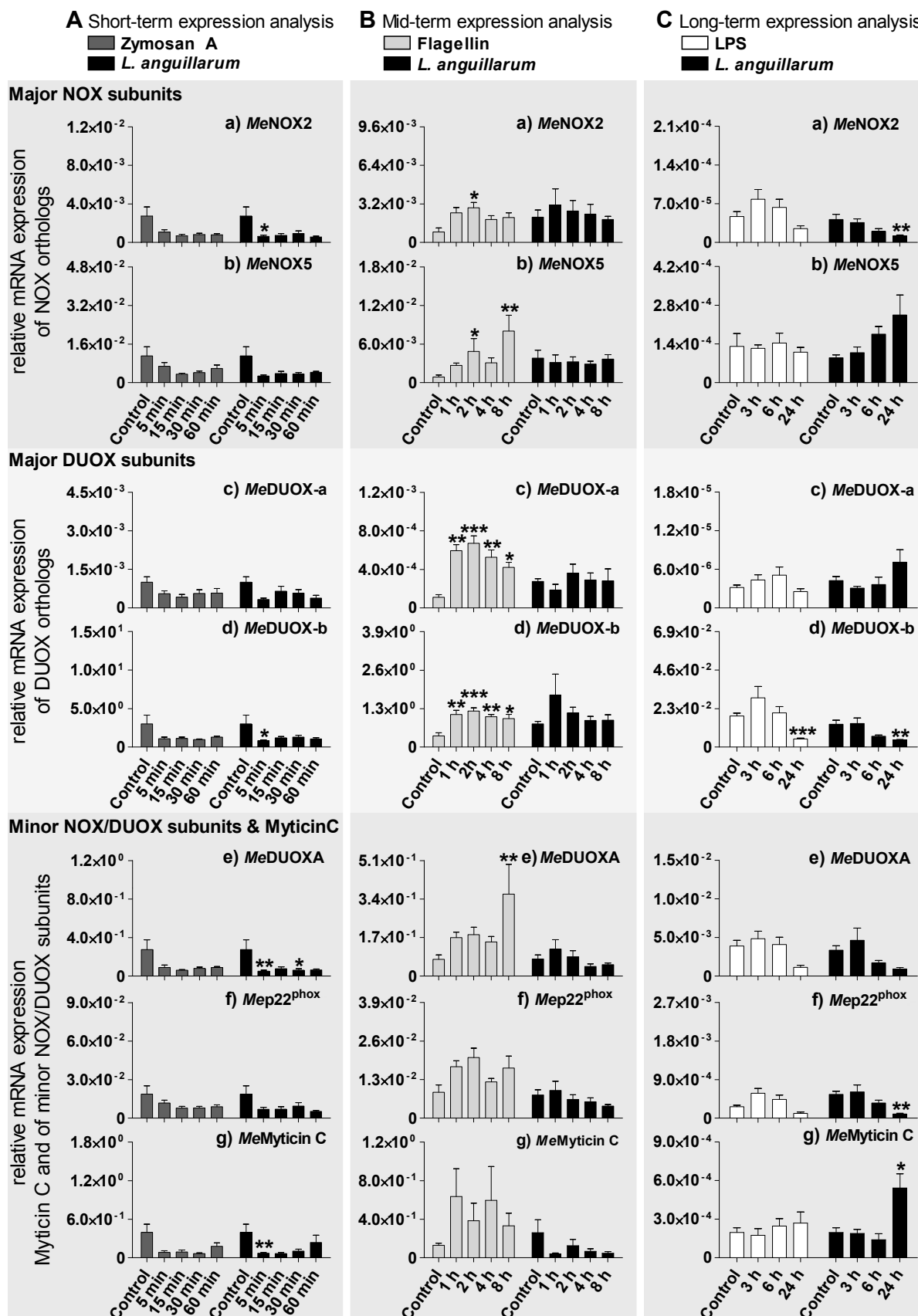
**Figure 3-14: Expression analysis of NOX/DUOX orthologs and myticin C in hemocytes of *M. edulis* after immune stimulation.** The relative mRNA expression of major NOX (**a-b**) and DUOX subunits (**c-d**), minor NOX/DUOX subunits (**e-f**) as well as *Me* Myticin C (**g**) in relation to the 28S rRNA reference gene is displayed. Expression was investigated using qRT-PCR in **A**) a short-term (5-60 min) analysis including zymosan A as stimulus; **B**) a mid-term (1-8 h) analysis including flagellin; as well as **C**) a long-term (3-24 h) analysis including LPS. All analyses also included a *Listonella anguillarum* treatment. Standard errors of n=4-8 experiments are displayed. Note that only significant differences compared to the control are depicted (see text for further details).

In summary, only zymosan A and *L. anguillarum* were able to induce ROS production in the experiments discussed above, but both stimuli failed to elicit a significant increase at transcript level of NOX and DUOX orthologs during the time periods investigated. On the other hand, flagellin was able to evoke a significant increase at mRNA level especially in DUOX orthologs, but no significant response in ROS production. Therefore, the following hypotheses arose: At first it might be concluded that phagocytosis, as observed for zymosan A and bacteria in microscopic images (Figure 3-4b and d), may be necessary for ROS production, which was further investigated in ROS measurements of hemocytes ingesting LPS- and flagellin-coated latex beads (see section 3.2.3.2). Secondly I was hypothesized, that living bacteria, such as *L. anguillarum,* may be able to alter the immune response of the host to increase their own survival, which was further examined using qRT-analysis after stimulation with heat-killed bacteria as discussed in section 3.2.3.3.

### 3.2.3.2    *ROS generation in relation to phagocytosis in hemocytes*

In humans it has already been shown that phagocytosis of MAMPs, such as zymosan A, is associated with the assembly of the phagocytic NADPH oxidase complex at the phagosome membrane and subsequent ROS production (DeLeo *et al.* 1999; Li *et al.* 2009). As described above for hemocytes of *Mytilus edulis* (3.2.3.1), *L. anguillarum* and zymosan A were the only stimuli, which were able to trigger significantly elevated extracellular ROS levels. Interestingly, these two particulate stimuli were also shown to be phagocytosed leading to intracellular ROS generation in phagosome-like vesicles as discussed in 3.2.1.1. To explore if usually soluble stimuli, such as LPS and flagellin, can also lead to increased ROS levels when phagocytosed, they were bound to latex beads and extracellular ROS production was investigated upon ingestion of beads by hemocytes.

ROS production of unstimulated control cells in presence and absence of un-coated latex beads was compared to the ROS production of cells ingesting flagellin- or LPS-coated beads (Figure 3-15). Neither phagocytosis alone nor the ingestion of coated beads were sufficient to provoke a significant change in ROS levels ($p > 0.05$, ANOVA), which remained distinctly constant throughout the experiment.

.
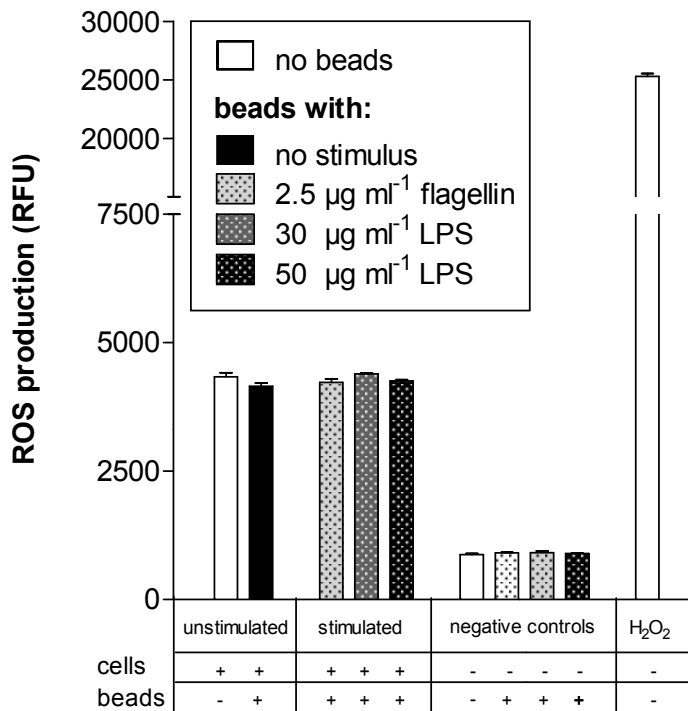
**Figure 3-15: ROS production in *M. edulis* hemocytes after the ingestion of coated latex beads.** Extracellular ROS production (in RFU) was determined after 2 hours incubation with latex beads, coated beforehand with pure DPBS (control), 2.5 µg ml$^{-1}$ flagellin, 30 µg ml$^{-1}$ LPS or 50 µg ml$^{-1}$ LPS. Cells without beads were included as an additional control. No significant regulation of ROS production occurred among all treatments ($p > 0.05$, ANOVA). Cell-free negative controls and positive controls ($H_2O_2$) verified the assay functioning (significances not shown). Means and standard errors of n=3 technical replicates are shown.

### 3.2.3.3  NOX/DUOX expression in relation to inactivated bacteria

The second hypothesis derived from the expression analysis in section 3.2.3.1 was based on the observation that flagellin was able to trigger a significant increase in the transcript levels of various NOX and DUOX orthologs after 2 hours, whereas flagella-containing bacteria of the species *Listonella anguillarum* were not. One way of inhibiting harmful host defense mechanisms by microbes can include the alteration of the host's gene expression (Hornef *et al.* 2002). It was hypothesized, therefore, that *L. anguillarum* might be able to interfere with NOX and DUOX expression in *M. edulis*.

This implication was examined more closely in hemocytes stimulated with living and heat-killed *L. anguillarum* bacteria using *Me* GAPDH as reference gene in qRT-PCR analysis (n=2). As already seen in section 3.2.3.1, there was no significant ($p > 0.05$, ANOVA) elevation of NOX and DUOX mRNA expression after 2 hours of incubation with living bacteria (Figure 3-16). Furthermore, this response was not altered when inactivated bacteria were utilized instead. Hence, a diminishing influence of living bacteria on the expression levels of NOX and DUOX orthologs could not be proven.

So far no functional connection between higher ROS levels and increased NOX and DUOX mRNA expression was obtained. Therefore, the following experiments dealt with the knock-down of DUOX orthologs and subsequent functional analysis via ROS production assays (3.2.3.4).
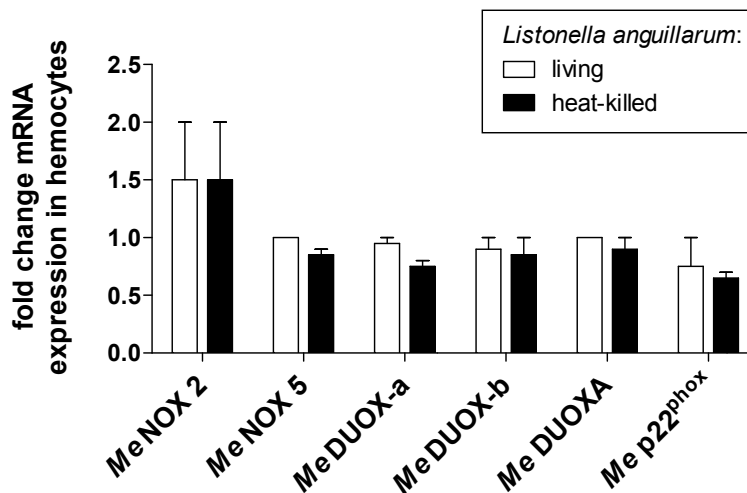


**Figure 3-16: NOX/DUOX expression at mRNA level in _M. edulis_ hemocytes after stimulation with living and heat inactivated bacteria.** The fold change in mRNA expression of NOX and DUOX orthologs using GAPDH as a reference gene was obtained by normalization against the expression of unstimulated control cells after 2 hours of stimulation. No significant differences were observed ($p > 0.05$, ANOVA of relative mRNA expression data). Standard errors of n=2 experiments are displayed.

### 3.2.3.4  Functional analysis of NOX/DUOX orthologs using RNA interference

To directly link ROS production and NOX/DUOX expression at transcript level, RNA interference (RNAi) experiments were conducted. It was hypothesized that a down-regulation of NOX and DUOX transcripts will impair generation of ROS in hemocytes. _Me_ DUOX-b was chosen as the most potential candidate influencing ROS production in mussels due to its extraordinary high expression in hemocytes and increased transcript levels upon immune stimulation.

Therefore, various hemocyte _in vitro_ experiments (each with n=2-3) were conducted using 60-120 nM of pooled siRNA (21 bp long) against the EF-hand domain and the peroxidase domain of _Me_ DUOX-b. After 24-72 hours semi-quantitative expression analysis was carried out using 28S rRNA as a reference. ROS production was assessed simultaneously investigating the effects of zymosan A stimulation in siRNA incubated cells. None of the experiments were able to elicit a significant change in ROS levels or a knock-down of _Me_ DUOX-b gene expression. As an example, one of the experiments involving 48 hours of incubation (n=2) is displayed in Figure 3-17. Further, _in vitro_ experiments involving longer (~500 bp) double-stranded RNA (dsRNA) did also not have an effect on ROS production or DUOX-b expression.
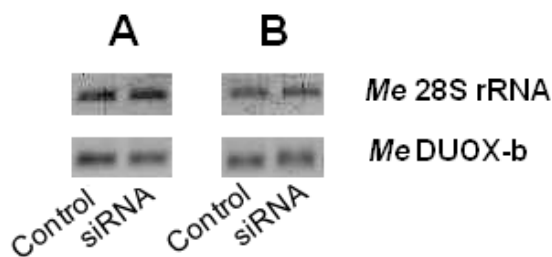
**Figure 3-17: *Me* DUOX-b expression of hemocytes incubated with siRNA.** Hemocytes were incubated for 48 h in the absence (control) or presence of siRNA against *Me* DUOX-b. In addition to the target transcript (*Me* DUOX-b), *Me* 28S rRNA expression was investigated in a semi-quantitative RT PCR analysis using agarose gel electrophoresis. Two replicate experiments (**A** and **B**) were assessed.

Since *in vitro* siRNA transfer into mussel hemocytes did not result in a knock-down of gene expression, *in vivo* experiments (n=3) were performed. These were carried out according to similar successful RNAi studies in bivalves dealing with the injection of longer dsRNA directly into the animal (Fabioux *et al.* 2009; Suzuki *et al.* 2009; Huvet *et al.* 2011; Wang *et al.* 2011). Therefore, longer dsRNA against DUOX-b (560 bp) and/or its activator DUOXA (567 bp) was injected directly into the posterior adductor muscle of *M. edulis*. Sham injections were conducted using sterile seawater. After 4 days the expression of the target transcripts in hemocytes was examined via qRT-PCR using *Me* GAPDH as reference gene (Figure 3-18). Karpala *et al.* (2005) suggested to investigate the transcription of general RNA-responsive genes to provide hints for possible off-target effects. Therefore, in order to investigate whether the innate immune system reacts in general to the specifically designed dsRNAs, gene expression of the RNA sensing 2'-5'-oligoadenylate synthetase (OAS) and retinoic acid inducible gene I (RIG-I) orthologs was additionally assessed.

*Me* DUOX-b expression displayed a slightly decreased trend in hemocytes when treated with dsRNA against *Me* DUOX-b alone or with *Me* DUOX-b & *Me* DUOXA together and remained constant in the anti-DUOXA dsRNA treatment (Figure 3-18). In contrast to this, *Me* DUOXA expression did slightly increase in all of these treatments. Furthermore, *Me* OAS and *Me* RIG-I displayed elevated transcript levels in cells treated with dsRNA against *Me* DUOX-b and/or DUOXA. However, variations at mRNA level were not significant in any of the orthologs involved. In addition to the transcription level, extracellular ROS production was observed 2 hours after hemocyte sampling from all treatments. Investigations included basal ROS production in unstimulated cells as well as ROS production in cells stimulated with zymosan A or *L. anguillarum*. Consistent with the above findings at transcript level, no significant alterations of ROS production were observed (data not shown). Therefore, *Me* DUOX-b transcription could not be linked to ROS production.

**DUOX family members**
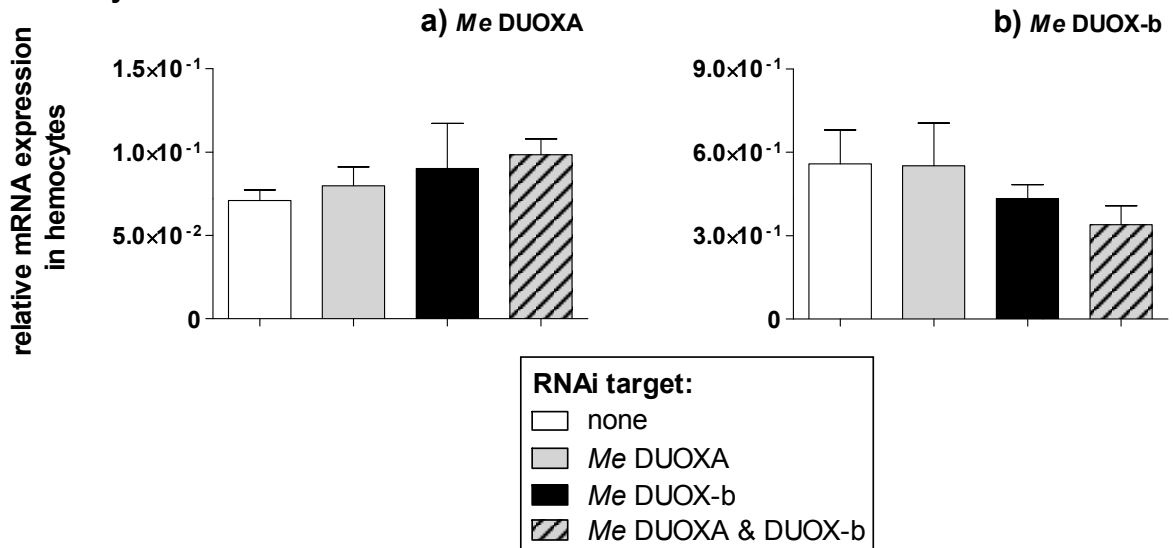


**Indicator transcripts for dsRNA recognition**
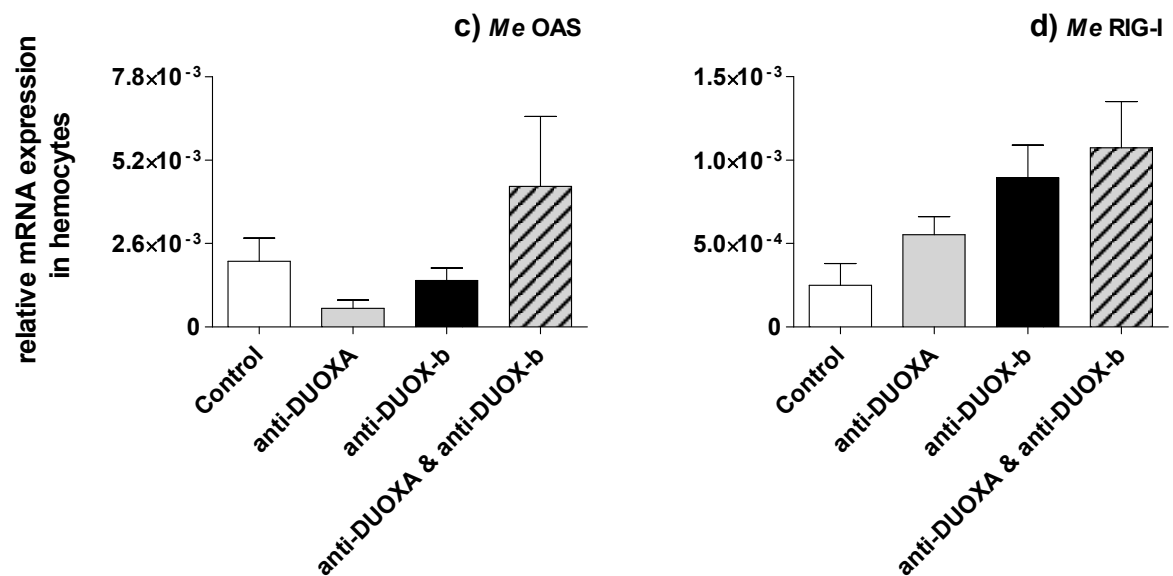


**Figure 3-18: Expression of DUOX-related orthologs and general RNA-responsive genes in hemocytes after *in vivo* injection of dsRNA (~500 bp).** The relative mRNA expression of *Me* DUOXA (**a**), *Me* DUOX-b (**b**), *Me* OAS (**c**) and *Me* RIG-I (**d**) in relation to *Me* GAPDH was determined in three replicate experiments via qRT-PCR analysis. Hemocytes were obtained from animals 4 days after injection with 30 µg dsRNA against *Me* DUOXA (anti-DUOXA), *Me* DUOX-b (anti-DUOX-b) or a pool of both (anti-DUOXA & anti-DUOX-b) into the posterior adductor muscle. Injections with filtered sterile seawater were used as a control. No significant differences were observed (p>0.05, ANOVA). Standard errors are displayed.

## 3.3 The role of IL-17 orthologs in the immune response of bivalves

### 3.3.1 Identification of potential IL-17 encoding transcripts in bivalves

Interleukin-17 (IL-17) is regarded an evolutionary conserved cytokine, since homologous sequences were found even in invertebrates, which otherwise lack many cytokines present in vertebrates. To further examine their existence in bivalves, transcriptome databases of *Mytilus edulis, Laternula elliptica* and *Arctica islandica* were examined for transcripts putatively encoding IL-17-like cytokines. Using key word and domain searches, I was able to identify sequences coding for IL-17 orthologs in all three bivalves. These were aligned, sequenced and if possible elongated (see supplements pages 169 for initial contigs and singletons as well as the final sequences). As a result, two IL-17 orthologs were identified in *M. edulis*, named *Me1* IL-17 and *Me2* IL-17, and in *L. elliptica,* named *Le1* IL-17 and *Le2* IL-17, whereas only one ortholog was found in *A. islandica,* named *Ai* IL-17 (Table 3-6). RACE-PCR for these orthologs could not be conducted successfully during the course of this study. Nevertheless, comparison of the identified ORF length to the ORF length of the corresponding best blast hit in UniProt/Swiss-Prot (BLASTp) indicated that at least more than half of the putative IL-17 sequence length was identified for all orthologs. SMART domain searches indicated a confidently predicted (E value < $10^{-3}$) IL-17 domain in all orthologs. Furthermore, except for *Le1* IL-17 (E value 1.6, score 70), all other orthologs possessed corroborative UniProt/Swiss-Prot BLASTp E values and scores (E values < $10^{-3}$ and score >110). On the other hand, *Le1* IL-17 depicted an identity of 34 % to its corresponding best BLAST hit, which was comparable to the identities of other IL-17 orthologs to their respective best BLAST hits (25-34%, see Table 3-6). Together these results indicate that the IL-17 family of cytokines is also present and conserved in the investigated bivalve species.

**Table 3-6: IL-17 orthologs in the bivalves *Mytilus edulis, Laternula elliptica* and *Arctica islandica*.** Orthologs in each bivalve species are represented by corresponding identifiers (ID). Sequence length (in bp) and ORF length (in amino acids (aa)) of each ortholog are depicted. E values for the IL-17 domain as obtained by SMART domain searches are displayed. Furthermore, the protein length (aa), Id. (Identity in %), score, E value and accession number of the best BLASTp hit in UniProt/Swiss-Prot are shown.

| Organism | ID | Length (bp) | ORF (aa) | IL-17 SMART domain (E value) | Protein (aa) | Id. (%) | Score | E value | Organism | Accession Number |
|---|---|---|---|---|---|---|---|---|---|---|
| | | | | | UniProt/Swiss-Prot (BLASTp) | | | | | |
| *M. edulis* | *Me1* IL-17 | 898 | 135 | $10^{-9}$ | 200 | 29 | 110 | $10^{-3}$ | *Crassostrea gigas* | A9XE49 |
| *M. edulis* | *Me2* IL-17 | 1454 | 194 | $10^{-9}$ | 200 | 25 | 128 | $10^{-5}$ | *Crassostrea gigas* | A9XE49 |
| *L. elliptica* | *Le1* IL-17 | 450 | 134 | $10^{-6}$ | 202 | 34 | 70 | 1.6 | *Homo sapiens* | Q8TAD2 |
| *L. elliptica* | *Le2* IL-17 | 561 | 110 | $10^{-16}$ | 200 | 31 | 123 | $10^{-5}$ | *Crassostrea gigas* | A9XE49 |
| *A. islandica* | *Ai* IL-17 | 416 | 106 | $10^{-21}$ | 163 | 34 | 120 | $10^{-5}$ | *Callithrix jacchus* | A6N6I9 |

### 3.3.2 Tissue-specific mRNA expression of bivalve IL-17 orthologs

Further insight into the mRNA expression of IL-17 orthologs in bivalves was gained by tissue panel expression analyses. Therefore, the expression of *Me1* IL-17 and *Me2* IL-17 was investigated in adductor muscle, digestive gland, foot, gill and mantle tissue as well as hemocytes of *M. edulis* in relation to the expression of the *Me* 18S rRNA reference gene using qRT-PCR (n=5, Figure 3-19A). The expression analysis depicted, that *Me1* IL-17 did not reveal any explicit tissue-specific expression. In contrast to this, *Me2* IL-17 transcripts were distinctly elevated in gill tissue, which was especially significant in comparison to digestive gland and adductor muscle tissue (p<0.05, ANOVA, Bonferroni).
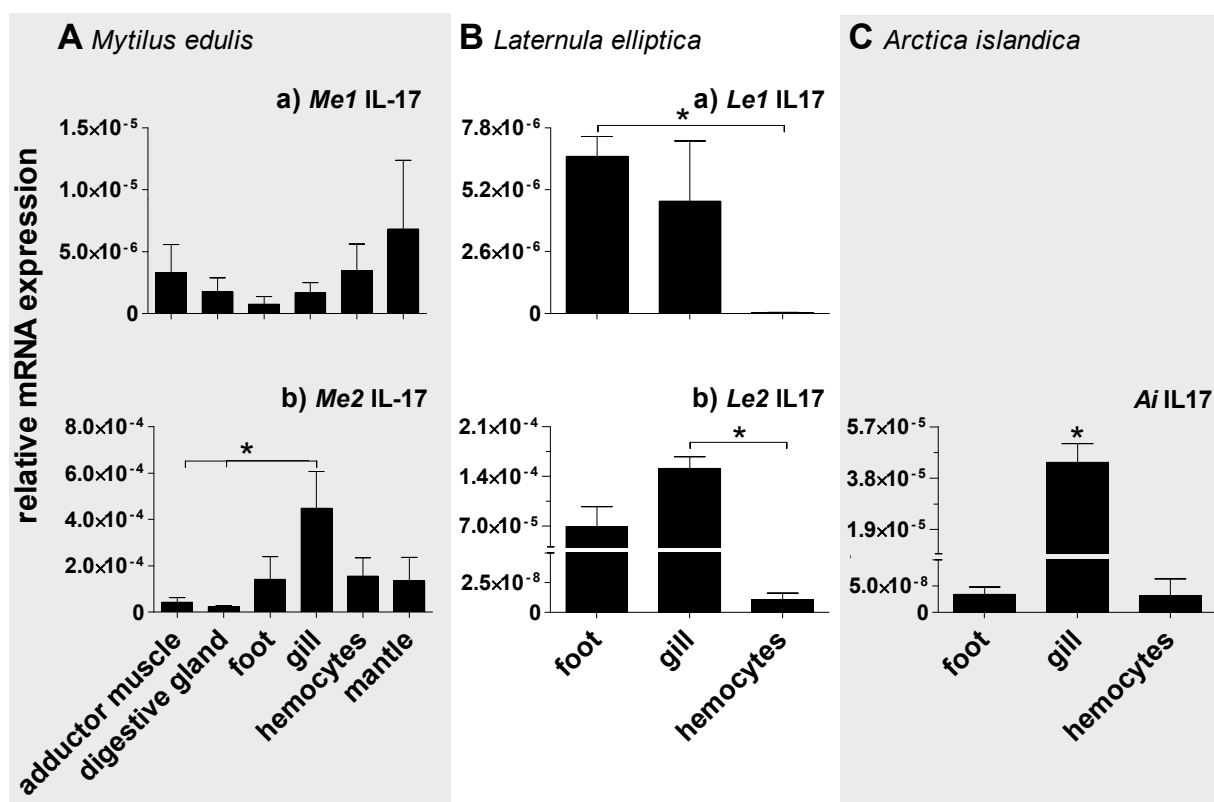


**Figure 3-19: Tissue panel analysis of IL-17 orthologs in *Mytilus edulis, Laternula elliptica* and *Arctica islandica*.** **A**: The relative mRNA expression of *Me1* IL-17 and *Me2* IL-17 in relation to the 18S rRNA reference gene expression (n=5, p<0.05, ANOVA, Bonferroni). **B**: The relative mRNA expression of *Le1* IL-17 and *Le2* IL-17 in relation to the ß-actin reference gene expression (n=3, p<0.05, t-test with Welch's correction). **C**: The relative mRNA expression of *Ai* IL-17 in relation to the 18S rRNA reference gene expression (n=3-5, p<0.05, Kruskal-Wallis-test, Dunn's) using qRT-PCR Standard errors are displayed. Note the two-segmented y-axes for *Le2* and *Ai* IL-17. Asterisks indicate significant differences

To verify these findings among bivalves, the expression of IL-17 orthologs was further investigated in foot, gill and hemocytes in relation to ß-actin in *L. elliptica* (n=3, Figure 3-19B) and in relation to 18S rRNA in *A. islandica* (n=3-5, Figure 3-19C). The *Le1* IL-17 ortholog exhibited a different tissue-specific expression pattern then all other orthologs, since it was not only highly abundant in gill

tissue but also in foot tissue being even significantly increased in comparison to hemocytes (p<0.05, t-test with Welch's correction). *Le2* IL-17 and *Ai* IL-17 depicted both the highest transcript level in gill tissue as was noted for *Me2* IL-17. This elevation was significant compared to hemocytes in *L. elliptica* (p<0.05, t-test with Welch's correction) and compared to foot and hemocytes in *A. islandica* (p<0.05, Kruskal-Wallis-test, Dunn's). Interestingly, a higher amount of cDNA was needed for proper quantification of IL-17 than for the other genes involved in qRT-PCR analysis during this study (15 ng in comparison to 5-10 ng). This indicates a very low basal transcription of IL-17 in unstimulated cells.

To summarize these findings, IL-17 orthologs were identified in *M. edulis, L. elliptica* and *A. islandica*. *Me2* IL-17, *Le2* IL-17 and *Ai* IL-17 all displayed the same tissue-specific expression pattern, being highly elevated in gill tissue in comparison to the other tissues. However, the overall basal expression of IL-17 orthologs in unstimulated cells was low in comparison to other genes investigated so far.

### 3.3.3  Expression analysis of IL-17 transcripts in hemocytes after immune stimulation

To elicit the regulation of IL-17 encoding genes during immune responses in *M. edulis*, immune stimulation experiments were conducted including flagellin (1-8 h), LPS (3-24 h) or living *Listonella anguillarum* bacteria (1-24 h) as stimuli. The expression of *Me1* IL-17 and *Me2* IL-17 was investigated in hemocytes in relation to the expression of the 28S rRNA reference gene using qRT-PCR (Figure 3-20).

During 1-8 hours of flagellin stimulation (n=5-7), the expression of *Me1* IL-17 and *Me2* IL-17 was significantly elevated (up to 30 fold) in comparison to the control treatment (p<0.001, ANOVA, Bonferroni). Whereas the amount of *Me1* IL-17 transcripts remained at a very high level throughout the stimulation lasting up to 8 hours, *Me2* IL-17 expression decreased about 3 fold after 4 hours, but still remained significantly above the expression level of control cells (Figure 3-20A). Stimulation of cells with LPS (n=5-6) resulted in a significant increase (p<0.01, ANOVA, Bonferroni) in gene expression of both IL-17 orthologs simultaneously in comparison to the control, but only after 24 hours (Figure 3-20B). At the same time as cells were incubated with MAMPs, subsets of hemocytes were stimulated with living *Listonella anguillarum* bacteria for 1-8 hours (n=4-7) and 3-24 hours (n=4-6). Even though a significant rise of *Me2* IL-17 mRNA levels above control cells was not detectable before 3 hours of stimulation with *L. anguillarum* (p<0.01, ANOVA, Bonferroni), an increased trend was already noticeable after 2 hours.
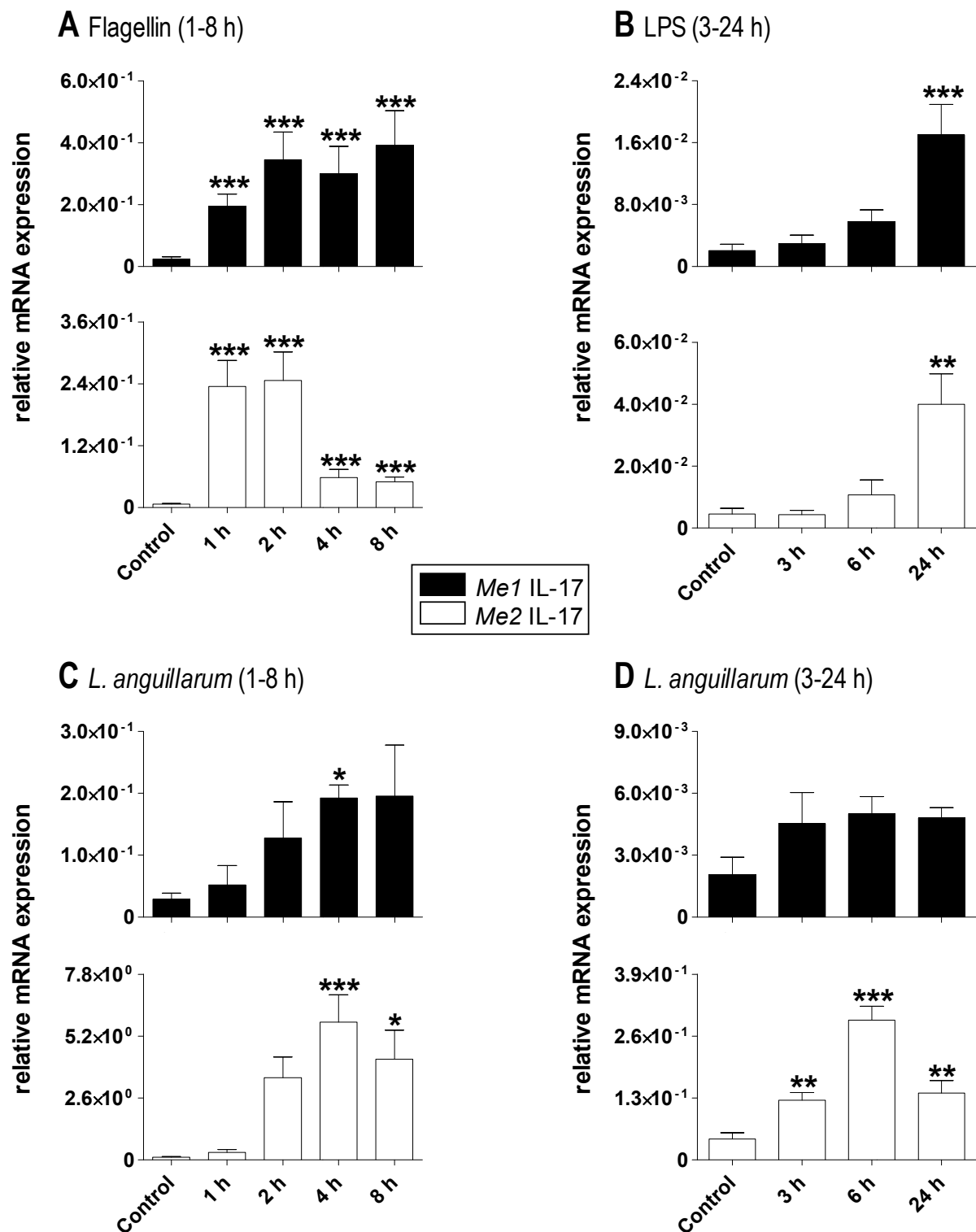
**Figure 3-20: Expression analysis of IL-17 orthologs in hemocytes of *M. edulis* after immune challenge.** The relative mRNA expression of *Me1* IL-17 (black bars) and *Me2* IL-17 (white bars) was determined in relation to 28S rRNA expression. qRT-PCR analysis was carried out after stimulation with 2.5 µg ml-1 flagellin (n=5-7, **A**) or 1.3 10[7] CFU *Listonella anguillarum* (n=4-7, **C**) for 1-8 h; as well as after stimulation with 50 µg ml-1 LPS (n=5-6, **B**) or 1.3 10[7] CFU *Listonella anguillarum* (n=4-6, **D**) for 3-24 hours. Unstimulated cells were included as a control. Asterisks indicate significant differences in comparison to control cells (ANOVA, Bonferroni). Data are shown as means with standard errors.

*Me2* IL-17 displayed the highest expression in comparison to control cells after 4 and 6 hours stimulation with bacteria (p<0.001), but transcripts are still highly elevated after 8 hours (p<0.05) and even 24 hours (p<0.01). On the other hand, *Me1* IL-17 exhibited significantly elevated transcript levels in comparison to the control (p<0.05) only at 4 hours of stimulation with bacteria. Nevertheless, an increased trend in *Me1* IL-17 expression was observed in cells stimulated with *L. anguillarum* for 2-24 - hours (Figure 3-20C-D).

In summary, responses of both *M. edulis* IL-17 orthologs to the selected stimuli differed markedly from each other. In response to flagellin stimulation both orthologs reacted to the stimulus by increasing their expression. But whereas *Me1* IL-17 expression remained increased during 1-8 hours, *Me2* IL-17 expression decreased after 4 hours. During LPS treatment both orthologs were affected in a similar way by the stimulus, since expression of both orthologs significantly increased not until 24 hours of stimulation. In experiments involving *L. anguillarum* mainly *Me2* IL-17 seemed to respond to the stimulus. These findings support the existence of two distinctly different IL-17 orthologs.

## 4. DISCUSSION

Aim of the present study was to identify conserved and putative important immune pathways and proteins in hemocytes of the blue mussel *Mytilus edulis*, and to verify these findings for other marine invertebrates. A first insight into putative immune gene orthologs was obtained by transcriptome dataset analysis. Two striking examples of phylogenetic ancient and highly conserved immune gene orthologs identified by their respective transcripts in bivalves, namely transcripts putatively coding for NOX and DUOX enzymes as well as IL-17-like cytokines, were investigated in more detail at molecular level.

## 4.1 Insights into innate immunity of *Mytilus edulis* obtained by hemocyte transcriptome dataset analysis

The present study represents the first comparison of control to immune-stimulated *M. edulis* hemocytes at the whole transcriptome level. The generated transcriptome datasets were successfully assembled, annotated and included in the *M. edulis* reference transcriptome database at the ICMB, Kiel, Germany (as described by Philipp *et al.* 2012a). Insights into conserved proteins and pathways were successfully obtained via pathway analysis (4.1.1) and qRT-PCR of selected transcripts (4.1.2).

Hemocytes are regarded as the immune cells of bivalves (e.g. reviewed by Humphries & Yoshino 2003) and consequently depict a high expression of various immune gene orthologs in comparison to most other tissues (Philipp *et al.* 2012a). Hence, to gain information about the regulation of genes at transcript level during immune responses, hemocytes were immune-challenged by flagellin treatment and compared to control cells. Flagellin was chosen as a stimulus because flagellin and not LPS has been shown to be a major factor for the virulence of the marine bacterium *L. anguillarum* (McGee *et al.* 1996; Milton *et al.* 1996), which was also commonly found in blue mussels (see also 4.2.1.2). However, for the development of the transcriptome dataset, flagellin of *Salmonella typhimurium* strain 14028 (Enzo) was used, since it was highly purified and, hence, did not contain other pathogenic substances. Therefore, observed immuno-stimulatory effects were clearly attributable to flagellin stimulation and not to a mixture of microbial-associated molecular patterns (MAMPs). As outlined in section 1.1.2, the recognition of flagellin by specialized pattern recognition receptors (PRRs) is a part of the innate immune system and seems to be conserved from plants to mammals (Gómez-Gómez & Boller 2002). In mammals, flagellin is recognized by TLR5, thereby inducing the transcription of many immune genes mainly via the NF-κB pathway (Hayashi *et al.* 2001). In the recent years, flagellin has gained considerable attention in regard to mucosal innate immune processes and especially inflammatory bowel disease in humans, where it is a dominant target of the immune system (Vijay-Kumar & Gewirtz

2009). Hence, it is especially interesting to examine immune responses of phylogenetic older organisms, such as *M. edulis*, to flagellin. In this manner, the newly created transcriptome datasets are a meaningful tool to gain deeper insight into the immune repertoire of *M. edulis* at a molecular level.

### 4.1.1 Conserved and putative important pathways in hemocytes

Pathway analysis is a useful tool to group lists of genes into cellular pathways and to examine which pathways are over- or under-represented. An increasing amount of tools and methods are available for this approach, which is sometimes also referred to as gene set analysis (GSA) (Nam & Kim 2008). In the present study, the RunCompare tool in T-ACE (Philipp *et al.* 2012b) was used to compare hemocytes and tissues in general as well as up- and down-regulated sets of contigs in hemocytes on the basis of their respective KEGG terms. The KEGG database (Ogata *et al.* 1999) provides functional annotations (terms) for the selected list of contigs and also defines the functional relationship between different terms, thereby sorting contigs according to their KEGG terms into categories or pathways. Therefore, this method can be used to analyze contigs not only on an individual level but also in a larger context related to the biological or molecular function of sets of contigs.

### 4.1.1.1 *Pathway analysis in hemocytes compared to other tissues supports their role as the immune cells of bivalves*

Pathways under-represented in unstimulated hemocytes in comparison to other tissues were mostly related to metabolic processes. Proliferating cells are known to possess a high metabolic rate to provide energy and sufficient organic macromolecules for their daughter cells, whereas non-proliferating, fully differentiated cells reduce their metabolism to the amount of energy needed for regular cellular processes (Vander Heiden *et al.* 2009). Therefore, a significant depletion of metabolic processes in hemocytes may support the hypothesis that hemocytes are slowly or even non-dividing cells and that the higher number of hemocytes, which is sometimes observed upon immune challenge, is related to an increased migration from non-inflamed tissues rather than proliferation of the hemocytes themselves (Pipe *et al.* 1999). In addition to this, the production of new hemocytes is thought to occur mainly in specialized tissues as reviewed by Ottaviani (2006). Furthermore, hemocytes potentially only play a minor role in the catabolism and anabolism of nutrients in contrast to many other tissues, such as mantle and digestive gland tissue, where the utilization and storage of nutrients and energy is assumed to be closely coupled to the reproductive cycle in order to meet the high costs of gonadal development (Zandee *et al.* 1980; de Zwaan & Mathieu 1992; Mathieu & Lubet 1993). Moreover, intracellular digestion of food into macromolecules, which in turn make up the metabolic pool, is mainly accomplished in the digestive gland tissue in bivalves (Deslous-Paoli 1986).

Further pathways significantly under-represented in hemocytes were pathways affiliated with DNA repair and development. The restricted proliferative ability of hemocytes, as described above, might be one reason for the depletion of these pathways. In vertebrates, it has been shown that DNA repair mechanisms are closely coupled to the cell cycle (Gupta & Sirover 1980; Jones & Petermann 2012). In comparison to hemocytes, pathways contributing to developmental processes are putatively especially important in the mantle tissue of *M. edulis,* where the gametes are produced (Gabbott & Peek 1991).

Additionally, a pathway involved in extracellular matrix (ECM) to cell interactions was also under-represented in hemocytes, which potentially underlines their behavior as freely-circulating cells.

Putative directly immune-relevant KEGG pathways, such as the TLR pathway, were mainly over-represented in hemocytes. This is in accordance with findings by Philipp *et al.* (2012a), who detected the highest expression of various immune gene orthologs, as expected, in tissues possessing immune functions, namely hemocytes and gill, rather than in tissues such as inner mantle, mantle rim and digestive gland using qRT-PCR. Other pathways mostly over-represented in hemocytes comprise pathways involved in signal transduction; apoptosis and MAPK signaling; vesicular transport processes; as well as the cytoskeleton and cell junctions. Even though these pathways play an important role in various cellular processes, they can take part in immune responses as well. In this manner, most signal transduction pathways can also influence and be influenced by immune stress. In vertebrates, this was shown, for instance, for some chemokines, which play an important part in the crosstalk between immune cells (Rot & von Andrian 2004). Similarly, VEGF signaling is thought to be involved in inflammation in the vertebrate lung (Lee *et al.* 2004). And in line with this, neurotrophin signaling is suggested to fulfill even various functions in macrophages (Vega *et al.* 2003). Furthermore, under certain circumstances MAPK signaling can lead to apoptosis, which, in molluscs, is "an indispensable [immune] process because it enables the adequate clearance of damaged, senescent and infected cells without inflammation" (Terahara & Takahashi 2008). Vesicular transport processes play also an important part in immune cells of mussels, since hemocytes possess a high amount of various types of vesicles such as endo- and phagocytic vesicles, which play an important role in the uptake of foreign particles and bacteria (Cajaraville & Pal 1995). In addition, in vertebrates it was shown that the rearrangement of the cytoskeleton is necessary for migration of these phagocytic vesicles and immune cell migration in general (Vicente-Manzanares & Sanchez-Madrid 2004), during which cell junctions may also play an essential part. Furthermore, cell junctions are involved in cell communication and, hence, are probably helpful in passing on and receiving immune signals between immune cells. In this manner, gap junctions, whose respective innexin and pannexin proteins seem to exist also in bivalves (Venier *et al.* 2011; Zhang *et al.* 2012), were shown to transfer danger signals upon immune challenge in vertebrate hepatocyte-derived cells (Patel *et al.* 2009) and immune cells (Rozental *et al.* 2000).

Therefore, it can be stated that most pathways over-represented in hemocytes are directly or at least remotely relevant for the immune system, which further underlines the assumed function of hemocytes as the immune cells of bivalves. Based on this, it can be hypothesized that genetic information processing pathways, contributing to a turnover of RNA and proteins, are also over-represented in hemocytes, because they may ensure sufficient amounts of readily-available defense molecules in case of an immediate immune threat.

### 4.1.1.2 *Pathways playing a putative role in the immune system are augmented and potentially energy consuming processes diminished upon immune challenge*

To gain deeper insight into relevant pathways upon immune challenge in hemocytes, pathway analysis was carried out comparing processes present in up- or down-regulated contigs after flagellin exposure against the complete hemocyte dataset as a reference. Groups of pathways involving directly immune-relevant processes as well as pathways playing only a remote role in the immune system, such as processes involved in signal transduction and MAPK signaling, were over-represented in up-regulated contigs. In this context, pathways affiliated with the cytoskeleton and cell junctions were over-represented as well. This reflects results obtained for pathways over-represented in unstimulated ('resting') hemocytes, when compared to other tissues, as discussed above (4.1.1.1). It can be concluded that over-representation of certain pathway groups in hemocytes is enhanced upon immune challenge, which highlights their importance for the bivalve immune system. On the other hand, pathways involved in metabolic processes and genetic information processing were over-represented in contigs being down-regulated upon flagellin exposure, which might be an energy saving mechanism during immune stress. This is further supported by the fact that immune functions, such as cell migration and phagocytosis, are known to require a high amount of energy in mammalian cells (Buttgereit *et al.* 2000). In humans, cells of the innate immune system have been reported to meet their energy supply nearly exclusively by glycolysis, whereas adaptive immune cells rely on oxidative phosphorylation (Kominsky *et al.* 2010). As a consequence, other metabolic processes not necessarily required for the immediate innate immune response might be reduced upon immune stimulation. Furthermore, genetic information processing, such as the turnover of DNA, RNA and proteins, is among the most energy-consuming mechanisms in mammalian cells (Buttgereit *et al.* 2000), and therefore probably among the first to be diminished in case of an immune threat. Hence, during immune challenge, processes identified as having a potential role in the immune system are augmented, as expected, whereas processes not directly involved in the early defense against pathogens are decreased, putatively in order to save energy and resources.

Interestingly, only the pathway "focal adhesion" was under-represented in contigs, whose expression was down-regulated upon flagellin challenge. And at the same time it was over-represented in contigs depicting an increased expression due to flagellin. In vertebrates, focal adhesions are large subcellular multiprotein complexes providing adhesion to the extracellular matrix as well as a means for intracellular signaling upon mechanical stimulation (Wehrle-Haller 2012). Focal adhesions are not only highly important in migrating cells (Ridley *et al.* 2003), such as leukocytes, they also possess various signaling molecules connecting the extracellular matrix with the cytoplasm. In this manner, the focal adhesion kinase (FAK) has recently been identified to play a crucial role in the RIG-I-mediated innate immune response against viruses in vertebrate cell lines (Bozym *et al.* 2012). Since hemocytes have been shown to excessively infiltrate infected tissues, as for example observed in adductor muscle tissue of *Mytilus galloprovincialis* after bacteria injection (Mitta *et al.* 2000a), focal adhesion pathways may also play a role in the migration of immune cells in bivalves.

Surprisingly, two KEGG pathways characterized as being involved in development, namely "Dorso-ventral axis formation" and "Notch signaling pathway", were enriched in up-regulated contigs. This is caused by an over-representation of Notch proteins, which constitute by far the majority of KEGG terms in both pathways in the present study (see supplements 9.2 for contigs of each pathway and their respective KEGG terms). Even though Notch proteins fulfill many roles during development (Bray 2006), diverse functions in immune cells were also identified. For instance, in macrophages an interaction between Notch and TLR pathways was shown to activate NF-κB target genes (Hu *et al.* 2008; Palaga *et al.* 2008; Foldi *et al.* 2010), e.g. leading to an elevated cytokine production. Therefore, it could be speculated that an enrichment of these pathways upon flagellin challenge may rather reflect their relevance in immune than developmental processes. The drastic over-representation of Notch proteins in the mentioned KEGG pathways also exemplifies how only one KEGG term can lead to an enrichment of the whole pathway and even affect several pathways at once, which depicts one of the major disadvantages of the pathway analysis, as discussed in the following.

### 4.1.1.3   *The pathway analysis method provides a rough overview at a more systemic level*

The pathway analysis method conducted in the present study has many draw backs. First of all it is based on the similarity of *M. edulis* sequences to orthologs obtained primarily from vertebrates. The mapping into the corresponding KEGG pathway is, therefore, based on this sequence similarity, even though the function of these orthologs could be different in bivalves. However, it has been proposed that a very large fraction of genes is structurally and functionally conserved throughout the eukaryotes (Ashburner *et al.* 2000). Secondly, even if we disregard the possibility of imprecise or missing annotations and incomplete transcriptome data, many contigs can belong to more than one pathway,

which may drastically influence the results, as seen for putative Notch proteins. This becomes especially obvious when looking at the NLR pathway or pathways involved in adaptive immune responses. These pathways have been identified as being over-represented in hemocytes, even though current knowledge proves, for instance, NLRs to be absent from bivalves (cf. discussion by Philipp *et al.* 2012a). The TLR pathway on the other hand, which was also significantly over-represented in hemocytes, is highly conserved in *M. edulis* (Philipp *et al.* 2012a, Saphörster, Findeisen, Rosenstiel, Philipp unpublished data, see 9.7). Therefore, an enrichment of the NLR pathway in *M. edulis*, despite the absence of NLRs, is due to an enrichment of common downstream targets, as for instance TLRs and NLRs can lead to the activation of MAPK and NF-κB signaling.

Nonetheless, pathway analysis is a useful tool to gain a rough overview of biological processes involved in hemocytes at a more systemic level rather than individual gene level, because most genes gain their importance not solely from a single action they fulfill, but from the gene network they are a part of. Therefore, various methods of pathway analysis have already become a "routine approach for the analysis of gene expression data" from microarrays (Emmert-Streib & Glazko 2011). As a result, in some studies dealing with human diseases, where the gain of knowledge by investigating the expression of individual genes was small, the analysis of genes grouped according to their biological function successfully revealed many important disease-associated pathways, as for instance in lung cancer, leukemia (Subramanian *et al.* 2005) and human diabetic muscle cells (Mootha *et al.* 2003).

### 4.1.2 Time-dependent expression of selected receptors, regulators and effectors at individual gene level

Since pathway analysis in *M. edulis* provides only a rough overview of biological processes in hemocytes as discussed above, a closer look was taken at individual gene level in order to elucidate the time-dependent expression of important receptors, regulators and effectors of immune pathways in hemocytes. And, therefore, a first hint for their involvement in the immune response of *M. edulis* was obtained. A detailed explanation for the selection of the chosen immune gene orthologs and some background information was given in the results section (3.1.3.1). Therefore immune gene orthologs will be discussed in the following mostly on the basis of their expression data.

#### 4.1.2.1 *Flagellin or LPS recognition by different TLRs putatively induces the NF-κB pathway*

The gene expression of four Toll-like receptor orthologs after flagellin stimulation was investigated in the present study. Whereas mRNA levels of *Me1* TLR and *Me2* TLR were not significantly altered during the course of the experiment, *Me3* TLR and *Me4* TLR transcripts levels were significantly increased after

4 hours of flagellin stimulation. Especially *Me4* TLR seems to play an important role in the immune response against flagellin, as it was still elevated even after 8 hours of stimulation. Interestingly, a parallel study by J. Saphörster, U. Findeisen, P. Rosenstiel and E. Philipp (unpublished data, see 9.7; *Me4* TLR was not assessed), exposing hemocytes for 3, 6 and 24 hours to LPS, depicted basically the opposite expression pattern, namely a significant increase of *Me1* TLR and *Me2* TLR transcripts, whereas *Me3* TLR was not significantly influenced. Evolutionary conserved Toll-like receptors are known to recognize microbial associated molecular patterns (MAMPs), as for example in humans flagellin is sensed by TLR5 (Hayashi *et al.* 2001) and LPS by TLR4 (Poltorak *et al.* 1998). Hence, it could be speculated that *Me1* TLR and *Me2* TLR are involved in LPS sensing, while *Me3* TLR and *Me4* TLR participate in flagellin recognition similar to TLR4 and TLR5 in humans.

Even though the transcription of TLR genes is not induced before 4 hours of prolonged flagellin stimulation in *M. edulis*, the recognition of flagellin by TLR proteins putatively occurs a lot faster, since the initial TLR protein levels have to be sufficiently high to be able to respond to a sudden and unexpected immune challenge. As a consequence, the observed delayed increase in TLR expression levels may prepare the cell for a prolonged microbial attack.

In fact, in vertebrate cells the recognition of microbial-associated molecular patterns (MAMPs) by TLRs has been shown to phosphorylate IκB kinases (IKK), which then phosphorylate inhibitor of κB (IκB) proteins leading to the release and activation of the transcription factor NF-κB. NF-κB in turn induces the transcription of IκB and may also stimulate its own expression (Sun *et al.* 1993; Hayden & Ghosh 2012). In vertebrates this autoregulatory process takes place mostly between 30-60 minutes upon immune stimulation. In the present study, a significant up-regulation of both IκB orthologs and NF-κB after 1 hour of flagellin stimulation was also depicted, lasting up to 8 hours. A closer look at the expression levels of NF-κB revealed a steady gradual increase in transcription up to 4 hours, which slowly decreased again after 8 hours. In humans the interplay of IκB release and NF-κB activation upon stimulation, followed by subsequent IκB transcription and renewed inhibition of NF-κB by IκB, as explained before, can lead to oscillations in NF-κB transcript levels (Hoffmann *et al.* 2002). Therefore, it is necessary to keep in mind, that the differences in the observed NF-κB expression levels between 1-8 hours could also have been influenced by different stages of this circular feedback process. Nevertheless, NF-κB and IκB depicted the earliest response at mRNA level of all assessed orthologs. The high increase especially in IκB orthologs after 1 hour of flagellin stimulation suggests that the induction of these orthologs occurs a lot earlier than 1 hour of flagellin stimulation. In addition, IκB expression upon MAMP-stimulation was also increased after LPS stimulation (Saphörster, Findeisen, Rosenstiel, Philipp unpublished data, see 9.7). The strong induction of NF-κB pathway members hints towards the importance of the NF-κB signaling pathway in the mediation of further immune responses in

bivalves. Similarly, in mammals the NF-κB pathway possesses an outstanding role in the immune gene network by regulating the expression of various important immune genes, as for instance due to TLR stimulation (Hayden *et al.* 2006).

Immune genes influenced by NF-κB in humans include for instance genes encoding NADPH oxidases (NOX) (Anrather *et al.* 2006; Gauss *et al.* 2007) and presumably also dual oxidases (DUOX). As discussed below in section 4.2.3, it was shown that DUOX transcripts are strongly and rapidly up-regulated already after 1 hour of flagellin stimulation, whereas NOX transcripts were elevated after 2 hours of stimulation. In humans, these reactive oxygen species (ROS) producing enzymes play not only an important part in killing invading bacteria, they are also crucial for the induction of further immune responses, as will be discussed in section 4.2. Other important genes inducible by NF-κB (Shen *et al.* 2006) and strongly up-regulated at an early stage during flagellin stimulation are genes encoding the IL-17 family of cytokines (see 4.3.2). In mammals, due to its notable role in inducing and mediating proinflammatory responses, various immune regulatory functions are implicated for the IL-17 family, as will be discussed in 4.3. Therefore, an early and strong induction of these orthologs may suggest a role in the mediation and propagation of further immune responses in hemocytes.

### 4.1.2.2   *The lectin pathway of the complement system*

Further assessed immune gene orthologs depicting an early increase in expression after 1-2 hours of stimulation were a *Me2* C3a receptor and a *Me1* C-type lectin encoding gene, which highlights their putative role in the early response against pathogens and the initiation of further immune cascades.

C-type lectins are known to bind carbohydrate patterns existing on microorganisms and thereby play an important role in recognizing MAMPs. In mammalian cells they have been shown to be able to influence TLR signaling or even NF-κB signaling directly, leading to a prolonged nuclear activity of NF-κB (Geijtenbeek & Gringhuis 2009). The recognition of MAMPs by pattern recognition receptors (PRRs) such as lectins, and also TLRs, can result in the cleavage of C3, the central molecule of the complement cascade, thereby producing the anaphylatoxin C3a amongst others. The critical role of the complement system in innate immunity is mainly defined by the variety of activities downstream of the complement components C3 and C5, which in turn depends on the engagement of specific complement receptors, such as the C3a receptor (Hawlisch & Köhl 2006). In human granulocytes these activities include for instance assembly of the NADPH oxidase complex (see 4.2) and also NF-κB activation (Pan 1998), which in turn leads to increased C3 expression. Therefore, the up-regulation of the *Me2* C3a receptor and the *Me1* C-type lectin may reflect the up-regulation of the lectin pathway of the

complement system (Fujita 2002). Interestingly, the *Me2* C3a receptor depicts one of the strongest responses, while the *Me1* C3a receptor remains unchanged hinting towards a different function of both orthologs.

Even though the complement pathway has been assumed to exist since the beginning of multicellularity itself, little is known about the complement system in bivalves. However, the available evidence hints towards the existence of at least the lectin pathway (Song *et al.* 2010) in bivalves, in contrast to the classical or the alternative activation pathway of the complement system. The central molecule of all three complement system activation pathways, the C3 molecule, has been widely investigated in invertebrates, but the existence of other vertebrate complement component orthologs is still obscure. It is, therefore, postulated that the complement system in protostomes putatively differs from the vertebrate or cnidarian system (Nonaka 2011). Interestingly, whereas this hypothesis was further supported by the recent transcriptome analysis of *M. edulis* (Philipp *et al.* 2012a), a current study by Moreira *et al.* (2012) reported most complement components to be existent in the transcriptome of the clam *Ruditapes decussata* for the first time. But these results were mainly inferred from transcriptome annotations and, therefore, a closer look at these sequences at molecular level is recommended. Together with the expression data in the present study, this would be an interesting topic for future work.

### 4.1.2.3 Up-regulation of LPS-inducible orthologs may prepare the cell for further challenge by Gram-negative bacteria

Contigs, potentially coding for proteins inducible by LPS, such as *Me1* LBP/BPI and *Me1* LITAF, are up-regulated a little delayed after 4 hours of flagellin stimulation. Nevertheless, the elevation at transcript level might prime the cell for further immune challenges by Gram-negative bacteria. LBP and BPI are both structurally closely related and seem to be conserved even in invertebrates (Krasity *et al.* 2011). Similarly, expression of LBP/BPI from the oyster *Crassostrea gigas* was induced in hemocytes after *E. coli* infection, where it depicted bactericidal and membrane-permeabilizing properties, hence it was suggested to be more closely related to BPI than LBP (Gonzalez *et al.* 2007).

LITAF mRNA levels have also been found to be up-regulated after 3 hours of bacterial challenge in the disk abalone, *Haliotis discus discus*, but in contrast to the present study the expression steadily increased up to 24 hours (De Zoysa *et al.* 2010), probably due to the continuous stimulation with LPS. Furthermore, in the same study a NF-κB/Rel ortholog of the abalone was assessed and no regulation was detected. In human cells, LITAF mediates TNF expression by direct binding to the promoter region of the TNF-α gene (Myokai *et al.* 1999). Therefore, De Zoysa *et al.* (2010) concluded, in accordance with other studies on putative class II NF-κB orthologs in bivalves, that NF-κB signaling and the LITAF

pathway in *Haliotis discus discus* are independent pathways and that subsequent putative TNF secretion relies solely on LITAF regulation. In contrast to this, in the present study, the expression of a putative class I NF-κB ortholog (*Me3* NF-κB p50) was assessed and a significant up-regulation was observed, even before the increase in LITAF expression was detected. Therefore, more studies on class I together with class II NF-κB orthologs in bivalves at transcripts and especially at protein level are recommended.

It is postulated that TNF orthologs are also important players in the immune system of invertebrates (Hibino *et al.* 2006; Zhang *et al.* 2008; De Zoysa *et al.* 2009). Since putative TNF-related contigs have also been identified in the *M. edulis* transcriptome database (Philipp *et al.* 2012a), further investigations in relation with LITAF and NF-κB expression in *M. edulis* might lead to more insights into TNF orthologs in invertebrates in general.

### 4.1.2.4 *Me1 TIMP and Me2 Ependymin are putative functional effectors of bivalve immune pathways*

Transcript levels of two investigated effector genes, *Me1* TIMP and *Me2* Ependymin, were significantly up-regulated during flagellin stimulation, whereas the expression of *Me2* TIMP, *Me1* Ependymin and antimicrobial peptides was unaltered. TIMP proteins are inducible protease inhibitors, which are also targets of NF-κB (Clark *et al.* 2008). Besides their function in tissue remodeling and extracellular matrix turnover, they possess potential roles in regeneration after injury, angiogenesis and immunity, playing for instance a presumed role in apoptosis due to interactions with TNF proteins (Brew *et al.* 2000). Invertebrate TIMP orthologs were already thoroughly investigated in the oyster *Crassostrea gigas,* where a TIMP ortholog was shown to be up-regulated upon immune challenge originating from *Vibrio* sp. exposure (Montagnani *et al.* 2001). Later on, a second TIMP ortholog was also identified in *Crassostrea gigas*, displaying a different expression pattern during development and also expressed by a different gene (Montagnani *et al.* 2005), which indicates a different function for each protein. This corresponds well with the findings in the present study, as *Me1* TIMP was significantly increased after 4 hours of flagellin stimulation, while *Me2* TIMP was not significantly influenced. However, this result has to be considered with care, since differences are not as pronounced as in other genes, e.g. the expression of the *Me1* C3a receptor versus the *Me2* C3a receptor.

The same holds true when comparing the unaltered expression of *Me1* Ependymin to the slightly but significantly increased *Me2* Ependymin transcript levels, indicating a different function for each ortholog. In vertebrates, ependymin proteins are thought to play a role in regeneration and neuroplasticity. They are apparently conserved in various animal clades. New molecular and phylogenetic analyses suggest four specific groups of ependymins: The first two groups are exclusively present in fish, while the third group seems to be deuterostome-specific, and the last group appears to

be more basal, existing in deuterostomes and protostomes (Suárez-Castillo & Garcia-Arraras 2007). Even though immune functions of ependymin proteins are still under investigation, a few studies already addressed this topic. In salmon, ependymin was found to be up-regulated in liver cells of head kidney infected with *Aeromonas salmonicida* (Tsoi *et al.* 2004). Furthermore, in echinoderms ependymin is thought to be involved in regeneration of organs after adverse stimuli (Suárez-Castillo *et al.* 2004). These findings together with the extraordinarily high basal expression of ependymin orthologs at transcript level in hemocytes of *M. edulis* might hint towards a possible immune function of ependymin. But since there is only a slight increase at transcript level and not much is known about the putative immune function of ependymin, further studies need to be conducted to validate and further elaborate these results.

Antimicrobial peptides (AMP) consisting of *Me1* Defensin, *Me1* Myticin A and *Me1* Mytilin D, as well as *Me* Myticin C (see section 4.2.3 for the latter) showed no significant expression changes within 8 hours of flagellin stimulation. Since mRNA levels of all measured AMPs so far depicted very high initial expression in hemocytes, transcript levels are supposedly high enough for the first line of defense. To further increase transcript levels, a longer stimulation period is probably needed. This can also be inferred from the stimulation of *Me* Myticin C with *L. anguillarum* for 5 min to up to 24 hours, where a significant transcriptional up-regulation is observed only after 24 hours of stimulation (see discussion in section 4.2.3).

Furthermore, in the discussed bivalve transcriptome datasets even a distinct down-regulation of AMPs, such as defensin and myticin A was detected, which was probably not strong enough to be resolved by qRT-PCR in the present study. Recent findings suggest that bivalve AMP transcript levels of freely circulating hemocytes are decreased, whereas they are increased at the site of infection (Schmitt *et al.* 2012). Since an increase of AMP-positive hemocytes has already been shown in infected gill and adductor muscle tissue (Mitta *et al.* 2000a), Schmitt *et al.* (2012) hypothesized that AMP-expressing hemocytes are associated with a different chemotactic ability resulting in a migration towards the area of infection and a decrease of AMP transcripts in the circulating hemocyte population. In the present study, on the other hand, hemocytes were stimulated *in vitro* and, hence, a loss of hemocytes due to a migration into tissues can be eliminated. Therefore, it can also be speculated that the observed elevation of AMP levels at the site of infection may potentially be related to an interaction of the hemocytes with the tissue itself. But this hypothesis still needs to be validated and would be an interesting topic for future research, providing insights into the functioning of hemocytes in barrier organs of bivalves.

*4.1.2.5   Expression analysis provided striking new insights into immune gene orthologs in bivalves*

In summary, the time dependent expression profile let to the identification of orthologs highly involved in the early transcriptional response to flagellin. These orthologs consist of the receptors *Me1* C-type lectin and *Me2* C3a receptor; the regulators *Me3* NF-κB p50, *Me1* and *Me2* IκB; as well as the effectors NOX/DUOX and IL-17, which may, therefore, have an important role in the first line of defense, supposedly by triggering further immune responses. Orthologs up-regulated later on and, therefore, serving also as possible important players in the immune response upon flagellin include the TLRs *Me3* TLR and *Me4* TLR; the LPS inducible proteins *Me1* LBP/BPI and *Me1* LITAF; as well as the effectors *Me1* TIMP1 and *Me2* Ependymin. It can be speculated that either these genes fulfill functions not immediately needed at the onset of an immune challenge and/or that their initial transcript (and proposed subsequent protein) levels are sufficiently high to confront pathogens in case of a sudden immune stimulation.

The present study depicted the differential expression of TLR orthologs in *M. edulis* in response to different MAMPs (LPS, flagellin) at transcript level. Furthermore, it was demonstrated that especially IκB was strongly inducible in *M. edulis* in response to MAMPs in correspondence with TLR up-regulation. In addition the present study is the first investigation of the complement system parameter C3a receptor together with a C-type lectin in bivalves.

Changes in expression of the selected candidate genes after 4 hours flagellin exposure, as predicted by the hemocyte transcriptome dataset, could not always be verified via qRT-PCR analysis. But 9 of 13 contigs (~70%) up-regulated in the hemocyte transcriptome dataset were also found to be significantly up-regulated in the qRT-PCR analysis. Furthermore, most contigs displayed at least the same trend in fold change induction in both analyses. For example, the *Me2* C3a-receptor possessed the highest change in expression in both the hemocyte transcriptome dataset and qRT-PCR experiments. Most probably these differences occur due to the different amount of biological replicates in the analyses.

On the whole these findings contribute to a first understanding of the flagellin-mediated transcriptional response in *M. edulis*. But deeper molecular analyses are needed to further characterize and validate orthologs as well as to further investigate their putative function.

The created transcriptome datasets were further used to identify and characterize specific target genes, with relevance for the immune system, at transcript level. Two gene families, consisting of NOX/DUOX and IL-17 encoding genes, were chosen due to their conservation throughout the animal kingdom and the importance of their respective proteins for the human immune system, as will be discussed in the following.

## 4.2 NOX and DUOX orthologs: Evolutionary conserved enzymes responsible for ROS production in bivalves?

### 4.2.1 A closer look at ROS production in marine invertebrates

#### 4.2.1.1 ROS generation as a ubiquitous immune response in invertebrate immune cells

The present study demonstrated that hemocytes of the blue mussel *Mytilus edulis* produce ROS in a distinct time- and dose-dependent manner in relation to zymosan A or *Listonella anguillarum* stimulation. This increase in reactive oxygen radical levels upon stimulation is in accordance with other studies in *Mytilus* sp. dealing with zymosan A (Pipe 1992; Torreilles & Guérin 1999; Ordás *et al.* 2000; Costa *et al.* 2009), *L. anguillarum* (Costa *et al.* 2009) or other bacteria of the family *Vibrionaceae* (Pipe & Coles 1995; Ciacci *et al.* 2010). Zymosan A was able to elicit a faster response than *L. anguillarum* within the applied concentration range and experimental conditions.

The production of reactive oxygen species (ROS) is regarded an important and widespread response of immune cells in marine invertebrates. Numerous studies are available dealing with elevated ROS levels upon immune challenge in hemocytes. In this manner, increased levels of ROS have already been observed upon stimulation with zymosan A and PMA in the hydrothermal vent mussel *Bathymodiolus azoricus* (Bettencourt *et al.* 2007), the oysters *Ostrea edulis* and *Crassostrea gigas* (Comesaña *et al.* 2012) as well as the Antarctic bivalve *Laternula elliptica* (Husmann *et al.* 2011). Similarly, enhanced ROS production in response to other adverse stimuli, such as for example laminarin or LPS amongst others, can be found in hemocytes of most bivalve species investigated so far, including *Patinopecten yessoensis, Pecten maximus, Crassostrea virginica, Mya arenaria, Mercenaria mercenaria* as well as *Mytilus edulis* and many more (for review see Roch 1999; Tiscar & Mosca 2004). But not only in bivalves also in other molluscs, ROS production in hemocytes triggered by immune-stimulation was observed. These include several gastropod species, such as the planorbid snail *Biomphalaria glabrata* (Hahn *et al.* 2000; Moné *et al.* 2011), the pond snail *Lymnaea stagnalis* (Dikkeboom *et al.* 1987; Adema *et al.* 1993) and abalone, *Haliotis* sp. *(Cheng et al. 2004; Donaghy et al. 2010)*; as well as cephalopods, as for instance the octopus *Eledone cirrhosa* (Malham *et al.* 2002). ROS production of circulating immune cells further contributes to the immune response in various other marine invertebrates, as for example in coelomocytes of echinoderms, as seen in the sea urchin *Paracentrotus lividus* (Coteur *et al.* 2001) and the sea star *Asterias rubens* (Coteur *et al.* 2002); or in the coelomocytes of crustaceans, as seen in the tiger shrimp *Penaeus monodon* (Song & Hsieh 1994). Therefore, it seems to be an ubiquitous immune-response in invertebrate immune cells.

### 4.2.1.2  The use of fluorescent dyes in ROS production studies

Even though, ROS production seems to be a wide-spread immune mechanism in marine invertebrates, Wootton & Pipe (2003) were unable to detect the release of ROS upon PMA, concanavalin A and LPS stimulation in the bivalve *Scrobicularia plana*. These contradictions in respect to the bivalve studies discussed before have been postulated to result mainly from less sensitive ROS detection methods in the past (Philipp *et al.* 2011). Nowadays highly sensitive fluorescent dyes, like cDCFH-DA and Amplex Red, overcome this obstacle and provide evidence for ROS production even in species formerly claimed to be incapable of ROS production, as for example seen in *Mercenaria mercenaria* (Buggé *et al.* 2007).

Employing these techniques, ROS production in hemocytes of *Mytilus edulis* in relation to the duration of incubation and concentration of the stimulus has been assessed using zymosan A and *Listonella anguillarum* as stimuli. Zymosan A is a component of the yeast cell wall, which contains several microbe-associated molecular patterns (MAMPs) including β-glucans, mannans, proteins, and lipids, and was therefore chosen as an appropriate stimulus. Furthermore, in mammalian macrophages zymosan A can induce immune responses by binding to TLR2 (Underhill *et al.* 1999; Sato *et al.* 2003). As discussed above, hemocytes of many bivalves depict an extraordinarily strong increase in ROS levels upon encounter with this stimulus (e.g. Anderson *et al.* 1994; Greger *et al.* 1995; Hégaret *et al.* 2003). The marine Gram-negative bacterium and fish pathogen *Listonella anguillarum*, belonging to the family of *Vibrionaceae*, was chosen as a natural stimulus occurring in the Baltic Sea (Eiler *et al.* 2006), the natural habitat of *M. edulis*. Moreover, *L. anguillarum* has been shown to directly infect *M. edulis* (Hariharan *et al.* 1995) leading to disintegration of gill tissue (Nottage & Birkbeck 1986), inhibition of filtration (McHenery & Birkbeck 1986) and toxic effects for hemocytes (Lane & Birkbeck 1999). In fact, the occurrence of *Vibrio* sp. has been observed to induce high mortalities in larvae of various bivalves (Anguiano-Beltrán *et al.* 2004).

Although numerous studies suggest that bivalve hemocytes are capable of a process similar to the oxidative or respiratory burst in human phagocytes, the question if the mechanism of ROS production in bivalves can really be compared to vertebrate phagocytic cells remains unsolved. It is postulated that the respiratory burst in vertebrate phagocytes occurs much faster (within a few minutes) and is much more pronounced than in invertebrate immune cells (Donaghy *et al.* 2009; Philipp *et al.* 2011). In contrast to this, a similar pattern or rate of reactive oxygen production, as examined over the course of time in the present study, was also observed in bovine neutrophils stimulated with zymosan A (Rinaldi *et al.* 2007) or by PMA stimulation in human granulocytes (Mohanty *et al.* 1997) using the Amplex Red assay. The discrepancy between these observations may be associated with the methods applied. By directly comparing luminol-enhanced chemiluminescence with Amplex Red fluorescence a distinct peak in ROS levels during the first 10 minutes was detected by Serrander *et al.* (2007) using the first method

in contrast to a steady time-dependent increase obtained with the latter method, as also seen in the present study. While the luminol based method detects a wide range of oxygen radicals (including $O_2^{\bullet-}$, intracellular $H_2O_2$, $HO^{\bullet}$, $HOCl$), Amplex Red is highly specific for extracellular $H_2O_2$. Therefore, it may be concluded that if differences in ROS production between vertebrates and invertebrates occur, they are supposedly not a result from variations in $H_2O_2$ generation, since rates in the present study did not appear to be different from that in granulocytes measured by the Amplex Red test.

In mammals, enzymes mainly responsible for ROS production upon immune stimulation belong to the family of NADPH oxidases. This enzyme family can be divided into orthologs of the superoxide anion ($O_2^{\bullet-}$) producing NADPH oxidases (NOX) and the hydrogen peroxide ($H_2O_2$) generating dual oxidases (DUOX). $O_2^{\bullet-}$ quickly converts to the more stable $H_2O_2$ either spontaneously or enzymatically (Bedard & Krause 2007). Therefore, the employment of the hydrogen peroxide-sensing Amplex Red dye offers a robust measurement of ROS produced directly by DUOX and indirectly by NOX enzymes.

### 4.2.1.3  ROS levels in relation to different immune stimuli in bivalves

In addition to the detailed study of time- and dose dependent ROS generation in hemocytes discussed above (4.2.1.2), ROS production was further monitored in stimulation experiments together with the expression analysis of immune genes in *M. edulis* (see 4.2.3). In these experiments *L. anguillarum*, zymosan A and further MAMPs were employed. Applied stimuli belonging to the class of MAMPs, despite zymosan A, were the TLR5 agonist flagellin and the TLR4 ligand LPS. From these stimuli, only zymosan A and *L. anguillarum* were able to elicit a significant increase in extracellular ROS production. This is partly in agreement with other studies showing that, even though LPS increased ROS levels in some bivalves (Nakayama & Maruyama 1998; Bettencourt *et al.* 2007), it failed to induce a response in various studies involving *Mytilus* sp. (Arumugam *et al.* 2000; Ordás *et al.* 2000; Costa *et al.* 2009). On the other hand, opposing to the present study, flagellin led to elevated ROS levels in the Antarctic bivalve *L. elliptica* (Husmann *et al.* 2011). Yet, information about ROS generation upon flagellin stimulation in other molluscs is very limited. Nevertheless, in most bivalve studies examined so far zymosan A was among the strongest elicitors of ROS production (e.g. Costa *et al.* 2009; Husmann *et al.* 2011), which is in agreement with the present study, even though *L. anguillarum* also increased ROS levels significantly.

In contrast to mussels of the genus *Mytilus* sp., *Listonella anguillarum* was not able to elicit a significant increase in ROS levels in oysters and clams (Bramble & Anderson 1997; Bramble & Anderson 1998; Lambert & Nicolas 1998; Lambert *et al.* 2001). This is particularly interesting with regard to a study from Hariharan *et al.* (1995) observing a much higher number of culturable *L. anguillarum* bacteria isolates in the oyster *Crassostrea virginica* than in the blue mussel *M. edulis*,

both collected from similar sampling sites. Furthermore, *L. anguillarum* was even the most abundant bacteria species in oysters; whereas *V. alginolyticus* was the major bacteria species in *M. edulis.* In addition, low abundance of *L. anguillarum* in comparison to highly abundant *V. alginolyticus* in *Mytilus* sp. has been determined in studies by Ortigosa *et al.* (1989) and Cavallo & Stabili (2002). It can be hypothesized that the clearance of *L. anguillarum* in *M. edulis* is more efficient than in the investigated oyster species. Hence, one reason for this might be the stronger response in ROS production in *M. edulis.*

### 4.2.1.4   *Phagocytosis and ROS production are closely coupled in M. edulis hemocytes*

Sites of intracellular ROS production could be clearly co-located to ingested zymosan A particles and bacteria providing further evidence that the stimuli are directly connected to ROS production. This was also already postulated in 1991 by Adema *et al.* (1991), who observed that the events during phagocytosis go hand in hand with intracellular ROS levels in hemocytes of the snail *Lymnea stagnalis.* In mammalian neutrophils ROS production was clearly connected to the internalization of zymosan A particles (Dewitt *et al.* 2003) or bacteria (Bernardo *et al.* 2010) into the phagosome. Furthermore, phagocytosis of foreign particles and the resulting oxidative burst were directly associated with the assembly and activation of subunits of the phagocytic NADPH oxidase (NOX2) (DeLeo *et al.* 1999; Li *et al.* 2009; Nüsse 2011). Even though it has to be noted that the process of phagocytosis alone does not seem to be solely responsible for the generation of ROS, since an uptake of inert latex beads in absence of any immune stimulus was not sufficient to trigger ROS production during phagocytosis in *M. edulis* hemocytes, as will be discussed in section 4.2.3.

### 4.2.1.5   *NADPH oxidase activators and inhibitors influence ROS production in marine invertebrates*

NADPH oxidase orthologs in humans (Brown & Borutaite 2012), flies (Ha *et al.* 2005) and even in plants (Torres *et al.* 2002) were identified as being among the most significant sources of reactive oxygen species, especially during cellular defense responses. Therefore, evidence for the involvement of NADPH oxidases in ROS production of marine invertebrates have been obtained in several studies with the use of chemical compounds acting as more or less specific inhibitors or activators of NADPH oxidases.

In the present study, significantly enhanced ROS levels were determined in hemocytes in response to PMA stimulation, which is assumed to activate the protein kinase C (PKC), an enzyme needed for the induction of NADPH oxidases. On the other hand, ROS production was distinctly reduced by DPI, a known inhibitor of NADPH oxidases. Similarly, PMA and DPI were employed successfully in various marine molluscs including the bivalves *Bathymodiolus azoricus* (Bettencourt *et al.* 2007) and

*Crassostrea virginica* (Goedken & De Guise 2004); the gastropods *Biomphalaria glabrata* (Bender *et al.* 2005), *Haliotis discus discus* and *Turbo cornutus* (Donaghy *et al.* 2010). Furthermore, BAPTA-AM, an intracellular calcium chelator, also significantly reduced ROS production of *M. edulis* hemocytes in the present study, which hints towards a major participation of calcium-inducible NADPH oxidase family members, namely DUOX and NOX5 orthologs, in the generation of ROS in *M. edulis*. A conforming result was obtained in hemocytes of the ascidian *Halocynthia roretzi* (Azumi *et al.* 2002). Interestingly, inhibition assays in the present study revealed a decrease in ROS levels of unstimulated cells, leading to the conclusion that hemocytes produce ROS even in the absence of an immune stimulus, which might be evoked by handling stress due to the experimental procedure.

Although many authors such as Adema *et al.* (1993) and Arumugam *et al.* (2000) deduced an involvement of NADPH oxidases in bivalve ROS production from experiments employing these chemicals and other compounds, these findings should be considered with care due to the weak specificity of these pharmacological inhibitors and activators. Even though PMA is assumed to be highly specific for PKC due to its resemblance to its natural activator diacylglycerol (Blumberg 1988), PKC can phosphorylate and regulate various other enzymes apart from NADPH-oxidases (Nishizuka 1986). Furthermore, the PKC is also influenced by intracellular calcium levels (Ananthanarayanan *et al.* 2003) and can, therefore, also be constricted by BAPTA-AM. In addition, BAPTA-AM has been identified to impede the translocation of the NADPH oxidase activator NOXA1 in human airway cells as depicted by immunoblot analysis and, therefore, also directly affects ROS production (Pacquelet *et al.* 2008). Moreover, it has to be noted that calcium acts as a second messenger, thereby regulating many diverse signaling pathways as well (Vig & Kinet 2009). The inhibitory compound DPI can not only interfere with ROS production of all NADPH oxidase orthologs, but also inhibits other ROS generating enzymes like mitochondrial complex I (Li & Trush 1998), xanthine oxidases (Doussiére & Vignais 1992) and others (as summarized by Bedard & Krause (2007)). Therefore, the results obtained in the present study can only be considered as a hint for the contribution of NADPH oxidases in ROS production, especially if taken together with other studies also pointing in that direction.

As discussed in the last sections, there is a large amount of studies dealing with immune-stimulated ROS production in marine invertebrates and especially bivalves available. Furthermore, various studies already addressed the possible involvement of NADPH oxidase family members in the "oxidative burst" of marine invertebrates. However, due to the missing specificity of the applied activators and inhibitors of NOX and DUOX enzymes, it is surprising that only very few molecular analyses of these enzymes have been conducted so far. Hence, it was interesting to prove the existence of NOX and DUOX at transcriptome level and carry out further functional analysis during the work of this thesis.

### 4.2.2 The presence of ROS-producing NADPH- and dual oxidases in Lophotrochozoa

#### *4.2.2.1 Lophotrochozoa possess NOX2, NOX5 and DUOX transcripts*

Orthologs of the NADPH oxidase family of enzymes are highly conserved at sequence level in most eukaryotes ranging from the cellular slime mold *Dictyostelium discoideum* over the sea urchin *Strongylocentrotus purpuratus* to humans (Kawahara *et al.* 2007). Their existence since the early onsets of the evolution of eukaryotes is taken as an indication for their importance not only in the immune system but also in other major cellular processes (Lalucque & Silar 2003). Despite the high amount of studies dealing with ROS production, only little is known about the existence of these ROS-producing enzymes in molluscs or even in the whole superphylum of the Lophotrochozoa. So far the only known full length transcripts of NOX and DUOX orthologs in Lophotrochozoa have been identified in the genome of the snail *Lottia gigantea* (as already described by Kawahara & Lambeth (2007)) and the polychaete *Capitella teleta* (partly mentioned by Sumimoto (2008)). In the transcriptome analyses of Mitta *et al.* (2005); Hou *et al.* (2011) and Moreira *et al.* (2012), NOX and DUOX fragments were mentioned, but barely investigated in more depth. Therefore, the present study is not only the first specific investigation of NOX and DUOX orthologs in relation to ROS production at transcript level in bivalves, but also provides the first detailed overview of the presence of NADPH oxidase family members in the whole superphylum Lophotrochozoa.

The existence of various Lophotrochozoan orthologs of NOX and DUOX enzymes was confirmed at transcriptome level. In *M. edulis* full-length open reading frames were obtained for two DUOX orthologs; one NOX2 ortholog; the minor subunits p22$^{phox}$ and DUOXA; as well as RAC. In addition, only a fragment of NOX5 was identified lacking the EF hand and ferric reductase domains. Further analysis via BLAST depicted a putative high conservation of these orthologs. Moreover, transcripts of the same kinds of NADPH oxidase family members were identified in the in-house transcriptome databases of *Arctica islandica* and *Laternula elliptica* as well, comprising NOX2, NOX5 and DUOX orthologs. Furthermore, these kinds of orthologs were found throughout the Lophotrochozoa, including other bivalves, gastropods and polychaetes. Even though only nucleotide sequence fragments of NOX5 were obtained in bivalves, the existence of full-length NOX5 orthologs was depicted in the genomes of a gastropod and a polychaete. In addition, the NOX5 ortholog of the snail *Lottia gigantea* was further validated by protein alignment in Kawahara & Lambeth (2008). These findings together with the significant BLAST results of the NOX5 fragments support the existence of NOX5 orthologs in bivalves, despite the missing information about the full-length open reading frame. Taken together, the high conservation of the obtained NOX/DUOX sequences and their seemingly ubiquitous presence in the investigated species belonging to the superphylum Lophotrochozoa might indicate the importance of the encoded enzymes throughout evolution.

### 4.2.2.2  E. scolopes is so far the only Lophotrochozoan organism exhibiting a putative NOX4 ortholog

Remarkably, no NOX4 sequence was detected in the investigated Lophotrochozoan species, except in the Cephalopod *Euprymna scolopes* (Figure 4-1; in cooperation with Prof. Dr. Margaret McFall-Ngai, UW-Madison, USA), which is well known for its symbiosis with bioluminescent bacteria of the species *Vibrio fischeri*. Interestingly, in contrast to the present study, Kawahara *et al.* (2007) discovered the appearance of NOX4 orthologs not before the emergence of the urochordates.

**a)** *Es* NOX4 SMART domain architecture



**b)** Alignment of NAD domains



**c)** UniProt/Swiss-Prot BLAST results

| Organism | Accession Number | Id. (%) | Score | E value | Ortholog |
|---|---|---|---|---|---|
| *M. musculus* | Q9JHI8 | 38 | 486 | $10^{-54}$ | |
| *P. abellii* | Q5R5C5 | 36 | 473 | $10^{-52}$ | NOX 4 |
| *H. sapiens* | Q9NPH5 | 35 | 468 | $10^{-51}$ | |
| *R. norvegicus* | Q924V1 | 37 | 467 | $10^{-51}$ | |
| *H. sapiens* | P04839 | 31 | 307 | $10^{-28}$ | NOX2 |
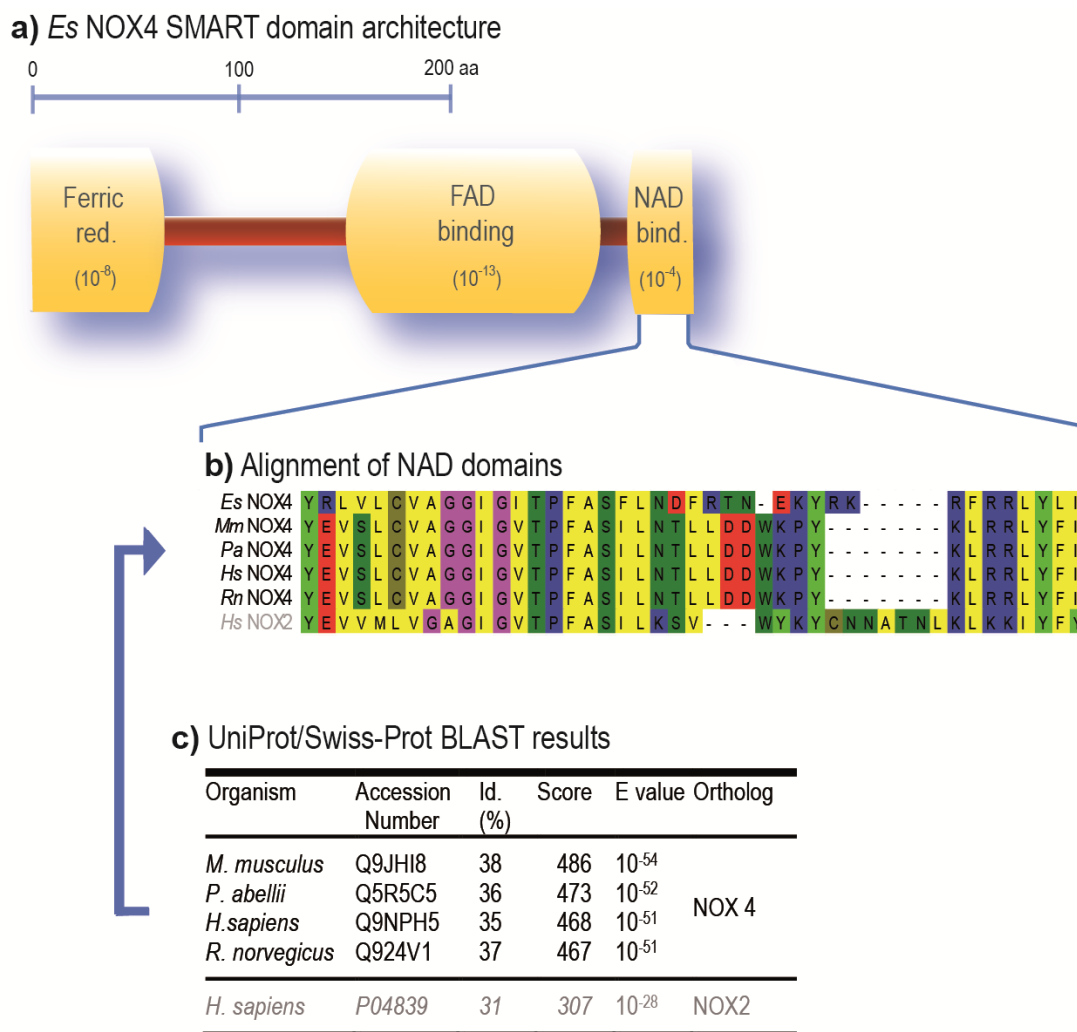
**Figure 4-1: Analysis of a NOX4 mRNA sequence in the squid *Euprymna scolopes* (*Es* NOX4).** Three different analyses are depicted: **a**) The SMART domain architecture search results are shown including their corresponding E values (in brackets); **b**) NAD domain mRNA sequences of the four organisms containing the most significant BLAST hits in the UniProt/Swiss-Prot database as well as a human NOX2 sequence for comparison are aligned; their corresponding BLASTp results are listed in **c**) including accession numbers, identities (Id.), scores and E values. *Mm = Mus musculus (M. musculus), Pa = Pongo abellii (P. abellii), Hs = Homo sapiens (H. sapiens), Rn = Rattus norvegicus (R. norvegicus). Es* NOX4 obtained from transcriptome datasets established in cooperation with Prof. Dr. Margaret McFall-Ngai, UW-Madison, USA.

In humans, NOX4 is thought to be responsible for sensing oxygen and, subsequently, regulating oxygen-dependent gene expression in renal cells (Geiszt *et al.* 2000). Further, NOX4 is also involved in the hypoxia-induced production of cytokines (Fitzgerald *et al.* 2012). The symbiotic relationship in the light organ of the squid *E. scolopes* has been postulated to be influenced by ROS levels and other oxygen-related processes in the host as well as in the microbe (Ruby & McFall-Ngai 1999). Therefore, it is particularly interesting to investigate why a NOX4 ortholog seems to be merely present in *E. scolopes* in contrast to all other Lophotrochozoa. But since so far only a fragment of a NOX4 transcript was obtained, more detailed analyses are highly recommended and are an interesting topic for future work.

### 4.2.2.3  New insights into the evolution of NOX and DUOX orthologs

The investigation of the evolutionary relationship between deduced amino acid sequences of NOX/DUOX orthologs in various eukaryotes via phylogenetic tree analysis depicted some surprises. Mainly, the succession of species on the tree, the absence of specific orthologs in some species as well as the distinct differences in orthologs of plants, amoeba and fungi, which were therefore used as an out-group in the present study, matched the observations made by Kawahara *et al.* (2007). By investigating a higher number of species and especially more members of the Lophotrochozoa new insights into the phylogeny of NOX and DUOX orthologs were obtained extending the findings of the previous study. First of all, it was shown that DUOX orthologs of popular model organisms from the Ecdysozoa, as for example *Caenorhabditis elegans* and *Drosophila melanogaster*, are not as closely related to basal deuterostomes than orthologs of bivalves and other Lophotrochozoa are. In addition, various studies already suggested that nematodes are lacking NOX5 orthologs, while NOX2 orthologs are even absent from all Ecdysozoa. In members of the Lophotrochozoa, however, these orthologs exist, thereby corroborating the suggested closer relationship of Lophotrochozoa to the earliest common ancestor of deuterostomes and protostomes. Findings are consistent with recent phylogenetic analysis suggesting a major gene loss during the evolution of the Ecdysozoa in comparison to the more basal Lophotrochozoa (Raible & Arendt 2004). This was also supported by transcriptome analysis of the Lophotrochozoans *M. edulis* (Philipp *et al.* 2012a) and *Pomatoceros lamarckii* (Takahashi *et al.* 2009), as well as the Cnidarian *Acropora millepora* (Kortschak *et al.* 2003). The evolutionary relationship and high conservation of the obtained NOX and DUOX orthologs in Lophotrochozoa support the suitability of bivalves as model organisms for the investigation of conserved immune pathways and proteins. Furthermore, this even may indicate that at least in some cases bivalves present a more suitable model to investigate the innate immune system from an evolutionary perspective than model organisms of the Ecdysozoan clade.

Kawahara *et al.* (2007) already investigated NOX5 orthologs of invertebrate deuterostomes in phylogenetic tree analysis, namely two NOX5 isoforms of the sea urchin *Strongylocentrotus purpuratus.* In the present study, a higher number of NOX5 orthologs of other basal deuterostomes were included in the phylogenetic analysis, consisting of two isoforms of the acorn worm *Saccoglossus kowalevskii* and one ortholog of the lancelet *Branchiostoma floridae,* next to the Lophotrochozoan orthologs. As a result, basal deuterostomes depicted two differently evolved NOX5 isoforms in the present study, one clustering with orthologs of the Lophotrochozoa and the other one with orthologs of the Ecdysozoa. The phylogenetic tree of Kawahara *et al.* (2007) and Inada *et al.* (2012) also depicted the divergent evolution of two NOX5 isoforms in basal deuterostomes. Even though the authors did not go into any detail about this finding, it further confirmed the observation made in the present study.

Phylogenetic analysis of NOX2 orthologs yielded no significant results for the identification of distinct evolutionary relationships between lower deuterostomes and protostomes. Reasons for this may be that sequences are either too similar or too different to provide appropriate sequences to resolve their relationships (Yang 1998). Therefore, taken their highly significant BLAST parameters into consideration, sequences most probably share a too great resemblance to conduct phylogenetic analysis using the employed methods. This observation further stresses the high conservation of NOX2 orthologs in Lophotrochozoa.

Even though, the present study demonstrated that NOX2 orthologs are highly conserved in various Lophotrochozoa, EF hand containing NOX5 and DUOX orthologs are thought to be the most widely distributed NADPH oxidase family members throughout the eukaryotes (Bedard *et al.* 2007; Kawahara *et al.* 2007; Aguirre & Lambeth 2010), existing also in arthropods, nematodes and plants (Torres *et al.* 2002), which otherwise even lack NOX2 orthologs. Therefore, together with the inhibition of ROS production upon incubation with the intracellular calcium chelator BAPTA-AM (4.2.1.5) and the discovery of more than one DUOX isoform in bivalves (4.2.2.1), this might hint towards an important role of particularly EF hand containing orthologs in innate immune responses in molluscs.

Furthermore, bivalve, and possibly even molluscan, DUOX orthologs seem to cluster into three distinct groups, namely DUOX-a, -b and -c rather than species-specific groups, similar to the differentiation of DUOX1 and 2 in mammals. A bivalve DUOX-c ortholog was obtained exclusively from the transcriptome of *Laternula elliptica*, but it significantly clustered with the DUOX-c ortholog of *Lottia gigantea* and a putative DUOX-c ortholog of *Capitella teleta*. From the phylogenetic tree it could be inferred that each kind of ortholog may also fulfill a different function in bivalves. This is additionally underpinned by the similarities in tissue-specific expression patterns of the different ortholog cluster, as outlined in the following section (4.2.2.4).

*4.2.2.4   NOX/ DUOX encoding genes display a high expression in immune-relevant tissues of bivalves*

Phylogenetic analysis suggested the existence of three distinct DUOX orthologs in bivalves, clustering together in the phylogenetic tree. Tissue panel analysis further revealed that the members of each cluster also showed a similar mRNA expression pattern amongst tissues. In this manner, genes encoding DUOX-b orthologs possessed an extraordinarily high expression in hemocytes in tissue panels of all three investigated bivalves, comprising *M. edulis*, *L. elliptica* and *A. islandica.* DUOX-a displayed an elevated expression level in gill tissue of all three bivalves and also DUOX-c was strongly expressed in the gill tissue of *L. elliptica* at transcript level.

In *M. edulis*, NOX5 transcripts were increased in gill tissue, while NOX2 transcripts seemed highly present in hemocytes. The mRNA expression of NOX2 and DUOX-a, however, was not always as markedly elevated in comparison to the other tissues as was shown for NOX5, DUOX-b or -c. A high expression of NOX and DUOX orthologs in other tissues than phagocytic hemocytes is not surprising, since in humans it was verified that the activity and mRNA expression of NOX and DUOX orthologs is not restricted to the phagocyte membrane, where it was discovered at first (Bokoch & Knaus 2003). In addition to the hemocytes, the bivalves' immune cells, the gill tissue can also be considered a highly immune-relevant barrier organ, since various beneficial but also potentially pathogenic microorganisms get trapped in the mucus layer of the gills due to the filter-feeding behavior of bivalves, imposing a constant threat to the immune system. In this manner, many potential immune gene orthologs exhibit very high transcript levels in immune-relevant tissues, such as hemocytes and gill tissue, in comparison to other tissues of *M. edulis* (Philipp *et al.* 2012a). Therefore, the high expression in these immune-relevant tissues might additionally underline a putative important role of NOX and DUOX orthologs in the defense response of bivalves.

## 4.2.3   The function of NOX and DUOX orthologs in bivalves

The function of NOX and DUOX orthologs in marine invertebrates still needs to be elucidated. The only functional study carried out in molluscs before depicted an increase in the transcript levels of a DUOX fragment in the snail *Biomphalaria glabrata* after exposure to the parasite *Echinostoma caproni* (Mitta *et al.* 2005), even though this result was only obtained in snails susceptible to parasitic infections in comparison to resistant snails. In a marine crustacean, the kuruma shrimp *Marsupenaeus japonicas,* a putative NOX encoding gene was up-regulated after *Vibrio penaeicida* and poly I:C stimulation (Inada *et al.* 2012). However, ROS production in these studies was not assessed simultaneously.

In other invertebrates, functions of NOX and DUOX enzymes have already been verified employing specific antibodies or by RNA interference. In this manner, the sea urchin DUOX ortholog Udx1 could be directly connected to tyrosine cross-linking during fertilization (Wong *et al.* 2004) and was shown to play an important part during early embryonic development (Wong & Wessel 2005) at protein level. Using RNAi assays in the non-marine invertebrate *Caenorhabditis elegans*, DUOX orthologs have been shown to be involved in tyrosine cross-linking to support cuticle stabilization (Edens *et al.* 2001). In addition, they were also linked to immune responses such as antimicrobial activity and pathogen resistance particularly in the hypodermis and the intestine of *C. elegans* (Chávez *et al.* 2009). DUOX orthologs have also been identified to play an important part in gut immunity of other Ecdysozoa such as *Drosophila melanogaster* (Ha *et al.* 2005) and *Anopheles gambiae* (Kumar *et al.* 2010). But due to missing similar studies especially in the Lophotrochozoa, the functions of NOX and DUOX orthologs of invertebrates, particularly in the marine environment, are still obscure.

The present study provides a unique insight into the expression of putative NOX and DUOX transcripts concomitantly measured with ROS production in hemocytes of a marine invertebrate. In some cases the expression of NOX and DUOX orthologs was even significantly reduced upon stimulation with LPS or *L. anguillarum*. Because the pattern of down-regulation was similar in all investigated orthologs, it is, therefore, regarded as a putative side effect of the stimulation, potentially to save energy for other more important immune processes at that time.

The mRNA expression of the bivalve antimicrobial peptide myticin C was investigated next to NOX and DUOX orthologs in the present study, since antimicrobial peptides are thought to be putative downstream effectors of NOX/DUOX enzymes. In addition, myticin C has already been proposed to possess immune-modulatory properties and to respond to various immune stimuli in hemocytes of *Mytilus galloprovincialis* (Costa *et al.* 2009; Balseiro *et al.* 2011). In the present study, *Me* Myticin C depicted a significant increase at transcript level only after 24 hours of *L. anguillarum* challenge, being independent of any changes in NOX/DUOX expression. This was consistent with *in vivo* findings in *Mytilus galloprovincialis* by Costa *et al.* (2009), who also observed an increase in myticin C expression not before 24 hours upon injection with *L. anguillarum*. Therefore, the amount of time was probably not sufficient to trigger a transcriptional response of myticin C in flagellin or zymosan A treated cells incubated only for up to 8 hours.

Surprisingly, there was a large discrepancy between ROS generation and NOX/DUOX transcript levels. The stimuli, which were clearly able to alter ROS production in *M. edulis*, namely zymosan A and *L. anguillarum* (see also 4.2.1.3), were not the same stimuli leading to elevated transcript levels. In this manner, only flagellin was able to increase the expression of transcripts coding for NADPH oxidase family members, such as *Me* NOX2, *Me* NOX5, *Me* DUOXA and especially DUOX orthologs. Due to the

limited amount of studies dealing with NADPH oxidases in marine invertebrates, the results of the present study in terms of NOX/DUOX expression cannot be related to findings in other bivalves and, therefore, provide exciting new insights. In mammals, however, DUOX2 has been identified to play an important role in TLR5-mediated immune responses, since increasing DUOX2 transcript levels and DUOX2-mediated ROS production upon flagellin stimulation in cells of the airway mucosa were observed (Gattas *et al.* 2009; Joo *et al.* 2012). In TLR5-expressing colon cells, flagellin has been shown to trigger NOX1 mRNA expression and NOX1-dependent ROS production (after NOXO and NOXA transfection in the study by Kawahara *et al.* (2004)). Similarly, FLS2, a plant pattern recognition receptor with similarities to mammalian TLR5 (Gómez-Gómez & Boller 2002), is thought to activate the plant respiratory burst homolog RbohD upon flagellin binding (Zhang *et al.* 2007).

Indeed, it has been shown that TLR signaling and NOX/DUOX enzymes seem to be closely coupled (Ogier-Denis *et al.* 2008). Thus, a knock-out of MYD88, an important adaptor protein of most TLRs, led for instance to impaired NOX2 assembly and, hence, diminished ROS production in phagocytes (Laroux *et al.* 2005). Interactions between NOX/DUOX expression, ROS production and TLR signaling were already the topic of various studies in mammalian phagocytes. In this manner, an up-regulation of NOX2 mRNA and ROS production had been observed upon stimulation with LPS, a ligand for TLR4 (Kim *et al.* 2010) as well as upon TLR2 stimulation with zymosan A (Yang *et al.* 2012). As mentioned before, these observations could not be verified in hemocytes of *M. edulis,* since flagellin led only to an increase in transcript levels of NOX and DUOX orthologs but not to increased ROS levels.

It is very surprising that *L. anguillarum* was unable to increase NOX/DUOX transcript levels in contrast to flagellin, since flagellin plays an essential part in the pathogenicity of *L. anguillarum* (Milton *et al.* 1996). In the present study, however, flagellin of *Salmonella typhimurium* (strain 14028) was used and, therefore, results may not be directly comparable. On the other hand, transcript levels even decreased at some time points after *L. anguillarum* stimulation. In some cases it has already been shown that pathogens are able to evade the host's defense responses by altering immune system processes, as has been reviewed for marine bivalves by Canesi *et al.* (2002). ROS production was, for example, only triggered by heat-killed but not by living *L. anguillarum* bacteria in hemocytes of the oyster *Crassostrea virginica* (Bramble & Anderson 1997). In tobacco plants, the tobacco mosaic virus has been observed to decrease superoxide generation simultaneously with transcript levels of a NADPH oxidase ortholog (Király *et al.* 2008). However, in the present study heat-killed *L. anguillarum* bacteria did not evoke a different immune response in terms of NOX and DUOX expression in *M. edulis* hemocytes than did living bacteria. Therefore, the unaltered or even decreased NOX and DUOX mRNA expression in response to *L. anguillarum* was not a result of protective mechanisms in living bacteria interfering with the hemocytes' immune responses.

In mammalian immune cells, the production of ROS by the phagocyte NADPH oxidase seems to be tightly coupled to phagocytosis (Cross & Segal 2004; Minakami & Sumimotoa 2006). Furthermore, the oxidative burst by mammalian phagocytes is generally accepted to lead to the clearance of ingested microbes (see section 1.4). In bivalves the killing of bacteria by hemocytes seems to be related to phagocytosis as well (Canesi *et al.* 2002). In the present study, intracellular ROS production and phagocytosis of *L. anguillarum* and zymosan A particles were also shown to be co-localized in hemocytes of *M. edulis* (4.2.1.4). Since the soluble stimuli flagellin and LPS were not able to induce ROS production in hemocytes, they were linked to inert latex beads in order to trigger ROS production upon phagocytosis of MAMPs. Incubation of hemocytes with LPS- or flagellin-coated latex beads, however, did not result in an increased ROS production, indicating that phagocytosis of bacterial components alone is probably not sufficient for the generation of ROS in *M. edulis*. This was also concluded in the review by Donaghy *et al.* (2009), who depicted that ROS generation and phagocytosis in bivalves could not directly be linked so far, since an increase in ROS production by phagocytosis of microbes did not always lead to an increase in ROS production.

RNA interference studies were carried out in the present study to close the gap between ROS production and NOX/DUOX expression in marine invertebrates. Even though the injection of dsRNA had already been successfully conducted in a few studies in bivalves (Fabioux *et al.* 2009; Suzuki *et al.* 2009; Huvet *et al.* 2011; Wang *et al.* 2011), during the course of the present study, a successful knock-down of *Me* DUOX-b and *Me* DUOXA could not be achieved. Hence, the final evidence for the NOX/DUOX-mediated ROS production in hemocytes of marine invertebrates is still missing.

Although the exact function of NOX and DUOX enzymes and their putative role in the generation of ROS in hemocytes of the blue mussel *Mytilus edulis* still needs to be investigated in more detail in future studies, the present study clearly depicted that an increase of NOX and DUOX orthologs at transcript level is not coupled to ROS production in *M. edulis*, as has been shown for other organisms. Therefore, observations made in this study allow for two possibilities: Firstly, ROS may originate from other enzymes than the previously stated; or secondly, NOX and DUOX enzymes are regulated at protein level rather than at gene expression level.

## 4.3 Orthologs of IL-17-like cytokines: Phylogenetic ancient players in the innate immune system of bivalves?

### 4.3.1 Transcripts putatively coding for IL-17-like cytokines exist in various bivalves

Sequences with a high homology to IL-17 encoding transcripts were identified in transcriptome databases of *Mytilus edulis, Laternula elliptica* and *Arctica islandica*. In *A. islandica* only one ortholog was discovered opposing to two orthologs each in *M. edulis* and *L. elliptica*. However, the transcriptome database of *A. islandica* did not include MAMP-stimulated tissues or hemocytes (Philipp *et al.* 2012c). In addition, IL-17 orthologs displayed only a very low mRNA expression under unstimulated control conditions. Therefore, it is possible that *A. islandica* may also possess two orthologs of IL-17 encoding transcripts. The finding of two orthologs in *M. edulis* in the present study confirmed earlier observations in the *M. edulis* transcriptome database by Philipp *et al.* (2012a). However, the present study was far more detailed and successfully validated both nucleotide sequences via Sanger sequencing. The presence of transcripts putatively coding for IL-17 in a member of the Mytilidae, is quite noteworthy, since clearly no ortholog exists so far in the transcriptome database of *Mytilus galloprovincialis* as pointed out by Venier *et al.* (2011). Furthermore, only recently studies revealed that orthologs of vertebrate cytokines exist in invertebrates at molecular level at all (Malagoli 2010). Prior to this, the existence of cytokine orthologs was highly disputed for a long time. The sequencing of the complete sea urchin genome also confirmed that many vertebrate cytokine families are seemingly not present in invertebrates (Hibino *et al.* 2006). A major exception to this seems to be the family of interleukin-17-like cytokines, of which respective nucleotide sequences could not only be identified in the sea urchin but also in one bivalve species before the present study. In the oyster *Crassostrea gigas* a potential IL-17 ortholog was discovered at transcript level by random sequencing of cDNA libraries (Roberts *et al.* 2008). As pointed out by this previous study, sequences of IL-17 encoding genes from the invertebrates *Caenorhabditis elegans* (NP_505700) and *Ciona intestinalis* (BAD22762) are also present in the NCBI database. And only recently have genes presumably coding for IL-17 orthologs been identified at genome level in the amphioxus *Branchiostoma floridae* (Huang *et al.* 2008).

Even though invertebrates lack the complexity of cytokines which vertebrates possess, orthologs of IL-17-like cytokines seem to be present throughout various classes of invertebrates. This is particularly interesting, because, although IL-17 fulfills similar functions to other interleukins in vertebrates, it is structurally very unique in comparison to other cytokines (Aggarwal & Gurney 2002). Roberts *et al.* (2008) regarded this as another hint that IL-17 might have evolved long before the divergence of vertebrates and invertebrates, while the evolution of most other cytokines is coupled to the appearance of the vertebrate lineage. Interestingly, IL-17 can be produced by innate immune cells

as well as adaptive immune cells (Yu & Gaffen 2008; Cua & Tato 2010). Therefore, IL-17 orthologs can be regarded as evolutionary important cytokines, which connect adaptive and innate immune responses.

In vertebrates six different IL-17 family members exist: IL-17A to F. It was shown that on one hand IL-17 proteins seemed to be highly conserved throughout mammals; human IL-17 family members were, therefore, highly homologous to mouse IL-17 orthologs with 62-88 % homology (Moseley *et al.* 2003). On the other hand the different IL-17 family members within the same organism were only distantly related to each other. As a result, IL-17A and IL-17D depicted only 25 % homology to each other in humans (Kolls & Lindén 2004) and even only 16 % in mice (Weaver *et al.* 2007). The first mammalian IL-17 isoform to be identified was IL-17A in 1993 (Rouvier *et al.* 1993), but only with recent large-scale genomic and EST sequencing approaches other members were identified in the years 2000 to 2001 (Li *et al.* 2000; Lee *et al.* 2001; Starnes *et al.* 2001) and IL-17D was not even discovered until 2002 (Starnes *et al.* 2002). *Le1* IL-17 and the ortholog obtained from the oysters *C. gigas* (Roberts *et al.* 2008), which in turn displayed the highest similarity to orthologs in *M. edulis* and *Le2* IL-17 in the present study, all depicted the highest homology to human IL-17D. Interestingly, Kono *et al.* (2011) indicated that IL-17D is the family member with the highest degree of homology between various vertebrate species, and that it existed, for instance, even in lampreys (Tsutsui *et al.* 2007), an ancient vertebrate lineage, as well as in sea urchins (Hibino *et al.* 2006). Furthermore, it was particularly striking that IL-17 orthologs of invertebrates (nematode, sea urchin, oyster) and lampreys distinctly clustered together with IL-17B and IL-17D of vertebrates in the phylogenetic analysis pointing towards a close relationship of these orthologs (Kono *et al.* 2011).

So far no nucleotide sequences, displaying homologies to genes encoding receptors of IL-17 isoforms, were obtained in bivalves. Interestingly, in vertebrates IL-17D is also the only interleukin-17 family member, whose receptor has not been identified yet (Gaffen 2011), which might, in addition to the points mentioned before, indicate that vertebrate IL-17D isoforms are putatively closely related to invertebrate IL-17 orthologs.

Although the SMART domain architecture search and UniProt-Swiss-Prot BLAST results were specific and similarities to oyster and vertebrate IL-17 sequences were clearly depicted, BLASTp values were not as outstanding for deduced amino acid sequences of IL-17 as for NOX/DUOX subunits of about the same length, which could imply that IL-17 orthologs are probably far less conserved than DUOX orthologs. Together with the low abundance of transcripts encoding bivalve IL-17 in unstimulated control cells, the late discovery of IL-17D in vertebrates and the limited number of sequence information before the advent of affordable large-scale sequencing techniques, this probably led to the limited

knowledge about IL-17 orthologs in invertebrates so far. Therefore, the present study provided an important contribution to an advanced understanding of IL-17 orthologs not only in bivalves but also in invertebrates in general.

To learn more about the IL-17 family in bivalves, IL-17 mRNA expression was investigated in tissue panels of the three different bivalves. *Me1* IL-17 transcripts were highly variable expressed in all tissues of *M. edulis,* whereas *Le1* IL-17 transcripts were clearly more abundant in foot and gill tissue than in hemocytes of *L. elliptica.* Therefore, no unifying conclusion could be drawn from transcripts belonging to the first IL-17 ortholog in the two bivalves. The second ortholog on the other hand provided a much clearer picture: Transcript levels of *Me2* IL-17, *Le2* IL-17 and *Ai* IL-17 were distinctly elevated in gill tissue of the corresponding organisms. This is in accordance with the oyster IL-17 ortholog, which was also increased in gill tissue at mRNA level in comparison to other tissues such as for instance adductor muscle and hemocytes (Roberts *et al.* 2008). In humans, IL-17A and IL-17F seem to be restricted to some specialized lymphocytes, whereas the two orthologs clustering together with invertebrate IL-17 orthologs in the phylogenetic tree (Kono *et al.* 2011), namely IL-17B and IL-17D, exhibit a high mRNA expression in various other tissues. While IL-17B is highly expressed in the gastrointestinal tract, pancreas and neurons; IL-17D is present in muscles, brain, heart, pancreas and adipose tissue (Gaffen 2009b). The similarity of vertebrate IL-17B, IL-17D as well as invertebrate IL-17 orthologs, in that they are expressed in cells other than immune cells, seems to support the observation of the phylogenetic analysis by Kono *et al.* (2011).

As noted before (4.2.2.4), gill tissue is thought to be not only relevant for respiration and food ingestion; it is also highly immune-relevant. Therefore, increased mRNA expression in this tissue might nevertheless hint towards a possible immune function of these orthologs.

### 4.3.2  IL-17 encoding genes are up-regulated upon immune stress in *M. edulis*

Deeper analysis of transcripts potentially coding for IL-17-like cytokines in *Mytilus edulis* depicted significant increases in their expression level *in vitro* in hemocytes after immune stimulation with bacteria and MAMPs. In the case of hemocytes stimulated with bacteria, the highest expression level of *Me2* IL-17 was obtained between 4-6 hours. This is in accordance with results for oyster IL-17, which also depicted the strongest increase in expression after 6 hours upon injection with *Listonella anguillarum* amongst others (Roberts *et al.* 2008). Together with the high expression in gill tissue of these orthologs, this indicates that oyster IL-17 may be more closely related to *Me2* IL-17 rather than *Me1* IL-17. Even though the high expression in gill tissue may also be related to an

infiltration of activated, IL-17 expressing hemocytes into the gill, in humans a high expression of IL-17 not only in immune cells but also in barrier organs, such as the intestine and the lung, has also been shown (see section 1.5).

The mRNA expression of *Me2* IL-17 in hemocytes strongly increased until 4-6 hours of *L. anguillarum* stimulation, after which it slowly decreased again but remained significantly elevated above control levels for up to 24 hours in the present study, and even 48 hours in the oyster study. *Me1* IL-17, however, depicted a different expression pattern. Transcript levels of *Me1* IL-17 were also increased after 4 hours but then they remained more or less constant, thereby being only slightly elevated above control cells. Expression patterns upon flagellin incubation also depicted distinct differences between the two IL-17 orthologs. Even though mRNA levels of both orthologs were significantly increased in stimulated hemocytes at all times and both orthologs depicted a very strong induction of up to a 30 fold increase in their expression within the first two hours, only *Me1* IL-17 remained at a constantly high expression level afterwards, while *Me2* IL-17 significantly decreased at 4 and 8 hours of flagellin stimulation. Interestingly, LPS was the only stimulus, which led to a very similar response in both orthologs resulting in the same expression pattern with a significant increase after 24 hours. These results strongly suggest that *Me1* IL-17 and *Me2* IL-17 are distinctly different from each other not only in their sequence and tissue panel distribution, but also in their behavior upon immune challenge and, therefore, most likely even possess different functions in *M. edulis*.

Other, non-MAMP-related stimuli have not been observed to affect invertebrate IL-17 orthologs at transcript level so far, as depicted in the study by Mello *et al.* (2012), in which Brevetoxin, a toxin originating from dinoflagellates and known to cause shellfish poisoning, was unable to alter the mRNA expression of the oyster IL-17 ortholog. In vertebrates, expression of IL-17 encoding transcripts was also clearly induced upon MAMP incubation: for instance after flagellin stimulation in mice (Van Maele *et al.* 2010) or after LPS stimulation in fish (Tsutsui *et al.* 2007; Korenaga *et al.* 2010). The rapid increase in transcripts putatively coding for IL-17-like cytokines in the blue mussel upon stimulation with different TLR ligands or bacteria indicates that IL-17 family members may also be important in defenses against pathogens involving the upstream recognition of MAMPs in bivalves.

IL-17 family members are thought to possess mainly proinflammatory functions. Hence, they can induce the production of many other cytokines, chemokines and prostaglandins, thereby attracting other cells to the site of inflammation (Aggarwal & Gurney 2002; Gaffen 2009b). It has been shown in vertebrates that IL-17 is not only activated by NF-κB but also activates the classical NF-κB pathway (Barnes 1997; Sonder *et al.* 2011). Thereby, IL-17 induces many other genes as for instance the tissue inhibitor of metalloproteinase (TIMP) encoding gene (Qiu *et al.* 2009) amongst many others. In accordance with these studies, an increase in transcript levels of both IL-17 orthologs, NF-κB pathway

members as well as *Me1* TIMP was observed upon flagellin stimulation in hemocytes of *M. edulis* in the present study. Furthermore, an increase in the expression of related orthologs has also been shown upon *Vibrio* sp. challenge in gill tissue of the oyster *Crassostrea gigas* (Roberts *et al.* 2009). Similarly, transcripts of IL-17 (Roberts *et al.* 2008), NF-κB pathway members (Montagnani *et al.* 2004; Zhang *et al.* 2011) as well as TIMP (Montagnani *et al.* 2001) were also increased upon bacterial challenge in oyster hemocytes. Further studies could indicate if a functional relationship of these orthologs exists in bivalves as well.

## 4.4 Conclusion

The present study presented a unique insight into the immune system of *Mytilus edulis*, a member of the much overlooked superphylum of Lophotrochozoa. The newly established hemocyte transcriptome datasets generated by 454-pyrosequencing proved to be a successful tool for the identification of putative conserved proteins and pathways with relevance for the *M. edulis* immune system. Pathway analysis in 'resting' hemocytes compared to other tissues depicted an over-representation of immune-relevant pathways, which were even up-regulated upon immune challenge, and, therefore, supported the role of hemocytes as the immune cells of *M. edulis*. But due to the many drawbacks of the pathway analysis conducted, this method solely offered a rough overview of related-pathway groups in hemocytes, rather than a detailed insight into the single pathways themselves. Closer investigation of the time-dependent mRNA expression of potentially important receptors, regulators and effectors of immune pathways at individual gene level depicted early- (e.g. NF-κB pathway members) and late-inducible (e.g. Toll-like receptors) immune gene orthologs in response to flagellin stimulation. Results indicated that MAMP recognition by TLRs, such as LPS putatively binds to *Me1* & *Me2* TLR and flagellin to *Me3* & *Me4* TLR, may potentially activate the NF-κB pathway and, subsequently, induce the expression of further immune genes in *M. edulis*, such as *Me1* TIMP, *Me2* Ependymin and orthologs of IL-17, NOX and DUOX. Among immune gene orthologs up-regulated upon flagellin-challenge were also orthologs coding for LPS-inducible proteins, such as *Me1* LITAF and *Me1* LBP, which potentially prepare the hemocyte for further bacterial challenge. NF-κB activation in conjunction with MAMP binding by TLRs and a C-type lectin ortholog in *M. edulis* may also lead to the induction of the lectin pathway of the complement system. These results illustrated how interactions of MAMPs with PRRs may trigger inflammatory responses in *M. edulis* hemocytes in a similar manner as in mammals, which includes the NF-κB-dependent regulation of conserved immune gene orthologs and the activation of the complement system.

Two conserved families of immune gene orthologs with great significance for the human immune system were investigated in more detail. NOX/DUOX and their minor subunits encoding nucleotide sequences seemed to be present not only in the bivalves *M. edulis, A. islandica* and *L. elliptica* but throughout the Lophotrochozoa. Three different DUOX orthologs named DUOX-a, -b and –c were identified in bivalves based on similarities in the phylogenetic analysis and tissue-specific mRNA expression. Due to the high expression of DUOX-b transcripts in hemocytes of all three investigated bivalves, an immune function especially of this ortholog seemed possible. But even though hemocytes depicted a clear time- and dose-dependent ROS production upon bacteria and zymosan A stimulation, analysis at transcript level did not reveal an induction of any NOX or DUOX ortholog using these stimuli. Interestingly, only flagellin was able to elicit a significant increase at transcript level, but not in ROS levels. Therefore, evidence for the involvement of NOX/DUOX enzymes in bivalve ROS production was obtained solely via the employment of more or less specific inhibitors of NADPH-oxidases. Hence, this study demonstrated that a rise in NOX and DUOX transcript levels does not necessarily lead to an elevated ROS production in bivalves.

Furthermore, the present study complemented the knowledge of NOX and DUOX evolution in eukaryotes by depicting a closer relationship of DUOX orthologs from Deuterostomes to Lophotrochozoa than from Deuterostomes to Ecdysozoa. As shown in other studies NOX5 seems to be absent in nematodes and NOX2 even in all Ecdysozoa, whereas this study depicted that these orthologs seem to exist in Lophotrochozoans, such as bivalves. This highlights a putative higher suitability of bivalves as models for specific parts of the vertebrate innate immune system compared to model organisms from the Ecdysozoa, such as *D. melanogaster* and *C. elegans*. As a consequence, this may lead to a re-evaluation of findings obtained solely by the investigation of invertebrate organisms from the Ecdysozoa so far.

The present study not only examined the first orthologous sequences coding for potential IL-17-like cytokines in the genus *Mytilus* sp. and the species *L. elliptica* and *A. islandica* in more detail, it also depicted the existence of two different IL-17 orthologs in the first two. Furthermore, at least one ortholog in each bivalve possessed a high mRNA expression in gill tissue, a highly immune-relevant barrier organ in bivalves. While the expression of IL-17 transcripts was generally low in hemocytes in comparison to other tissues, it was highly inducible in hemocytes of *M. edulis* upon stimulation with various MAMPs and bacteria. The resulting expression profiles varied depending on the ortholog and stimulus applied. Hence, the present study demonstrated for the first time the presence of two distinctive IL-17 orthologs with potentially differing functions in *M. edulis*. Due to their high expression upon immune challenge, a putative relevance for the bivalve immune system may be inferred.

The findings obtained in the present study illustrate the suitability of *M. edulis* as a model organism to study conserved immune gene orthologs of vertebrates in a phylogenetic more basal animal. Insights into the evolution of conserved immune genes, in this case NOX and DUOX orthologs, were obtained. Furthermore, this study provides an important contribution to the understanding of the bivalve immune system at transcript level. Even though conserved orthologs may also fulfill conserved roles in the immune system of invertebrates, as has been suggested for NF-κB activation via MAMP-PRR interaction, some orthologs might display a different function, which could be possible for NOX/DUOX enzymes in bivalve hemocytes in contrast to human neutrophils. Since information in this study was mainly obtained at transcript level, further studies at protein level are highly desirable.

## 4.5 Future prospects

In the present study sequences of putative conserved proteins in bivalves were identified by transcriptome analysis and their transcriptional response upon immune challenge was investigated in hemocytes of *M. edulis*. Thereby, this study provides valuable implications for future studies elucidating the involvement of these conserved orthologs in the immune response of bivalves even further. Since work focusing solely on the molecular mechanisms at transcript level can only depict part of the picture (as seen for the discrepancy in NOX/DUOX expression and ROS production), studies in bivalves have to be taken to a more systemic level to obtain the "the full richness of invertebrate immunity" (Little *et al.* 2005). Hence, next to additional genomic and proteomic information, functional studies are utterly needed to link physiological and molecular findings to each other. The scarcity of such studies is mainly due to the fact that the number and functionality of available molecular tools for marine invertebrates is very limited so far. Therefore, the establishment of a successful gene knock-down in hemocytes as well as bivalve-specific antibodies to link immune gene orthologs to protein level is highly requested, as will be discussed in the following.

Since the knock-down of target genes using recent RNAi approaches (siRNA, 500 bp dsRNA) was not successful, the use of the more robust morpholino antisense oligomers (Heasman 2002) in hemocytes might provide an interesting topic for future work in *M. edulis*. The knock-down of specific genes is not only badly needed to establish a connection between transcript and protein levels, it would also provide an insight into the functional network the gene is part of.

Even long before interleukin orthologs were detected in bivalves at transcript level, hints for the existence of interleukin-1 orthologs were claimed using human recombinant proteins (Hughes *et al.* 1990) and human antibodies (Hughes *et al.* 1991). However, without the use of specific antibodies

against proteins in bivalves an unexpected cross reaction cannot be excluded. This may be underlined by the fact that no interleukin-1 ortholog was so far discovered in bivalve transcriptomes. Therefore, bivalve-specific antibodies are urgently demanded.

In *A. islandica* only one IL-17 ortholog in comparison to *M. edulis* and *L. elliptica* was identified, which is supposedly due to missing transcript information from immune-challenged hemocytes, which were not included in the generation of the *A. islandica* transcriptome dataset. Hence, sequence information from hemocytes upon immune stimulation could provide additional insights in the future. Furthermore, since IL-17 orthologs in hemocytes were highly inducible, a RACE-PCR of immune stimulated hemocytes might represent a more promising approach to obtain the open reading frame of all IL-17 orthologs in further studies. In line with this, the use of tissue panels from immune challenged bivalves might also offer more insights into the tissue-specific immune function of IL-17 orthologs. Studies in immune-challenged hemocytes demonstrated that IL-17 orthologs in *M. edulis* depict mostly divergent mRNA expression patterns. Whether these also resemble divergent protein levels could be addressed using specific antibodies in subsequent studies, which would also emphasize a putative different function for each ortholog. In addition, using specific antibodies in co-immunoprecipitation experiments the yet unknown IL-17 receptor in bivalves may be identified. In addition, the treatment of hemocytes with bivalve-specific, recombinant IL-17 protein would allow for the investigation of molecular interactions, e.g. the identification of downstream targets, and physiological parameters, e.g. cell migration. Taken together, these future studies might evaluate if IL-17 possesses a similar mode of action in bivalves than in mammals and would, therefore, connect knowledge obtained at transcript level to a more systemic level.

The importance to connect molecular studies and physiological studies becomes evident in regard to the observed discrepancy between ROS production and NOX/DUOX expression patterns. To identify if ROS in hemocytes are generated by other enzymes than the previously stated, additional sources of ROS should be considered in future bivalve studies. One possibility could be, for instance, a mainly mitochondrial origin of ROS, as has been recently suggested for gastropod hemocytes (Donaghy *et al.* 2010). Furthermore, in mammalian mast cells, which possess functions similar to basophil granulocytes, ROS production seems to be independent from NADPH-oxidases, but dependent on Lipoxygenases and Cyclooxygenases (Swindle *et al.* 2007). On the other hand, specific antibodies against NOX and DUOX enzymes as well as their knock-down might also be able to close the gap between NOX/DUOX enzymes and ROS production in hemocytes. Especially in respect to the chronic granulomatous disease (CGD) in humans, where even small mutations in one of the NADPH-oxidase subunits cause severe effects, this would be an interesting topic for future research.

The present study focused mainly on the immune response in bivalve immune cells. But during recent years the immunological importance of barrier organs, e.g. the gut and lungs, became also increasingly apparent (Schreiber *et al.* 2005). The gill epithelium of filter-feeding bivalves represents such a barrier organ. In addition, it also depicted the highest expression of various immune gene orthologs next to the hemocytes (Philipp *et al.* 2012a). Furthermore, in *Drosophila melanogaster* only a knock-down of DUOX in the gut and not in hemocytes led to a diminished ROS production (Ha *et al.* 2005). Therefore, studies focusing also on other immune-relevant tissues in addition to hemocytes might complement the knowledge about the innate immune system in bivalves obtained so far.

## 5. SUMMARY

Invertebrate and vertebrate organisms alike rely on efficient immune mechanisms to cope with potentially harmful microbes. Immune cells of invertebrates, e.g. hemocytes in bivalves, perform innate but not adaptive immune responses as found in lymphatic cells of jawed vertebrates. Since several genes and principles of innate immunity are highly conserved throughout the animal kingdom, invertebrates are sometimes even regarded as a simplified model of the vertebrate innate immune system. Most invertebrate animals belong to one of the three major bilaterian clades: Deuterostomia, Ecdysozoa or Lophotrochozoa. Whereas research on innate immunity was mainly conducted in the first two groups, information about molecular immune mechanisms in the Lophotrochozoa, including molluscs such as bivalves, is still scarce. In addition, marine, invertebrate filter feeders, such as bivalves, are especially suited to elucidate evolutionary conserved immune responses, since they are constantly in direct contact with the surrounding sea water and, hence, with the microbiota within. Therefore, this project aimed to identify and characterize putative conserved and important proteins and pathways of innate immune responses at molecular level in bivalves, including the ocean quahog, *Arctica islandica*, the Antarctic bivalve *Laternula elliptica* and especially the ecologically and economically important blue mussel *Mytilus edulis*.

To provide the molecular basis for subsequent investigations, transcriptome datasets of unstimulated and flagellin-challenged *M. edulis* hemocytes were generated using massively parallel sequencing techniques (Roche 454). Comparative analysis of putative conserved pathways in the generated and existing *M. edulis* transcriptome datasets displayed an enrichment of putative immune-relevant pathways in hemocytes. Furthermore, deeper insights into the time-dependent mRNA expression pattern of selected receptors, regulators and effectors of potential immune pathways in *M. edulis* revealed early- (e.g. NF-κB pathway members) and late-inducible (e.g. Toll-like receptors) immune gene orthologs in response to flagellin stimulation. The transcriptome datasets also offered the molecular background to detect and characterize phylogenetic ancient immune gene orthologs in bivalves possessing also a great relevance in the human immune system, such as genes potentially coding for NOX/DUOX enzymes and IL-17-like cytokines.

One important and phylogenetic conserved immune response investigated in this study was the production of reactive oxygen species (ROS). In humans and also lower animals, such as sea urchins and nematodes, enzymes of the NADPH oxidase (NOX) and dual oxidase (DUOX) family are mainly responsible for the production of ROS. Accordant to various other studies, hemocytes of *M. edulis* depicted a clear dose- and time-dependent ROS production in response to immune stimulation in the present study. But despite the large number of studies dealing with the generation of ROS in molluscs,

the present study was the first to identify putative NOX and DUOX orthologs as well as their subunits in bivalves and even presents one of the first studies in the whole superphylum of Lophotrochozoa. Phylogenetic analyses of these orthologs depicted a closer relationship of deuterostome DUOX orthologs to Lophotrochozoan than to Ecdysozoan orthologs, which underlines the suitability of Lophotrochozoan model organisms for the investigation of the innate immune system from an evolutionary perspective. Furthermore, DUOX orthologs clustered in three distinct groups in the phylogenetic analysis, which mostly coincide with their specific expression pattern among tissues. Orthologs comprising the DUOX-b cluster displayed a particularly high mRNA expression in hemocytes in contrast to other tissues and even to other major immune gene orthologs. On the other hand, the fast and high induction of DUOX expression upon immune stimulation did not correlate with ROS production in *M. edulis* hemocytes. Nevertheless, the high transcript levels of DUOX-b in hemocytes, its increased transcription in response to immune challenge and a reduced ROS production, when using the inhibitor BAPTA, provides strong evidence for a role of DUOX-b in the innate immune response of bivalves.

Mammals use a multitude of cytokine families to communicate within and between cells. Many of these families cannot be found in invertebrates; one major exception are proteins belonging to the interleukin-17 (IL-17) family of cytokines. In the present study, transcripts of two potential IL-17 orthologs were identified and characterized in *M. edulis* and *L. elliptica* as well as one ortholog in *A. islandica*. At least one ortholog in each bivalve depicted a high mRNA expression in gill tissue in comparison to other tissues and hemocytes. In hemocytes of *M. edulis*, however, transcription of both IL-17 orthologs was highly inducible using various immune stimulants. The resulting expression profiles varied depending on the ortholog and stimulus applied, supporting the presence of two distinctive orthologs with potentially differing functions in bivalves.

This study provided a deeper understanding of flagellin-mediated defense mechanisms in *M. edulis*. Additionally, it gave insights into the conservation and transcriptional regulation of two families of immune gene orthologs in a phylogenetic older group of animals. Thereby, the present study contributes to a more complete view on the evolution of the innate immune system itself.

## 6. ZUSAMMENFASSUNG

Evertebraten wie auch Vertebraten benötigen gleichermaßen effiziente Immunmechanismen, um potenziell schädliche Mikroben abzuwehren. Die Immunzellen der Evertebraten, wie z.B. Hämozyten in Muscheln, können angeborene aber nicht adaptive Immunantworten, wie sie in lymphatischen Zellen der kiefertragenden Wirbeltiere vorkommen, ausführen. Da mehrere Gene und Gesetzmäßigkeiten der angeborenen Immunität im Tierreich hoch konserviert sind, werden Evertebraten mitunter als vereinfachtes Modell des angeborenen Immunsystems der Wirbeltiere angesehen. Die meisten wirbellosen Tiere gehören einem der drei Hauptstämme der Bilateria an: den Deuterostomia, Ecdysozoa oder Lophotrochozoa. Bisher wurden hauptsächlich Untersuchungen in den ersten beiden Gruppen durchgeführt, wohingegen nur begrenzte Kenntnisse über die molekularen Immunmechanismen der Lophotrochozoa, zu denen auch Weichtiere wie z.B. Muscheln gehören, vorhanden sind. Hinzu kommt, dass wirbellose, marine Filtrierer, wie z.B. Muscheln, im Besonderen geeignet sind, um evolutionär konservierte Immunantworten zu untersuchen, da sie kontinuierlich dem umgebenden Seewasser und somit auch den darin enthaltenden Mikroorganismen ausgesetzt sind. Ziel dieser Studie war es daher, wichtige, putativ konservierte Proteine und Signalwege der angeborenen Immunantwort in Muscheln auf molekularer Ebene zu identifizieren und zu charakterisieren. Dies beinhaltete Untersuchungen in der Islandmuschel, *Arctica islandica*, der antarktischen Muschel *Laternula elliptica* und insbesondere der ökologisch und ökonomisch bedeutenden Miesmuschel, *Mytilus edulis*.

Die molekulare Grundlage für sich anschließende Analysen bildeten die mit Hilfe von moderner Hochdurchsatz-Sequenziermethoden (454 Roche) generierten Transkriptomdatensätze unstimulierter und Flagellin-stimulierter Hämozyten von *M. edulis*. Vergleichende Untersuchungen zu potenziell konservierten Signalwegen in den generierten und bereits vorhandenen *M. edulis* Transkriptomdatensätzen ergaben eine Anreicherung von putativ immunrelevanten Signalwegen in Hämozyten. Des Weiteren ließ eine detailierte Analyse zeitabhängiger mRNA Expressionsmuster ausgewählter Rezeptoren, Regulatoren und Effektoren von potenziell immunrelevanten Signalwegen in *M. edulis* nach Flagellinstimulation früh (z.B. Mitglieder des NF-κB Signalweges) und spät induzierte (z.B. Toll-ähnliche Rezeptoren) Orthologe von Immungenen erkennen. Zusätzlich boten Transkriptom-datensätze den molekularen Hintergrund, um phylogenetisch ursprüngliche Immungen-Orthologe zu ermitteln und zu charakterisieren, die auch von großer Bedeutung im humanen Immunsystem sind.

Eine wichtige und phylogenetisch konservierte Immunantwort ist die Produktion von reaktiven Sauerstoffspezies (ROS). Im Menschen wie auch in Niederen Tieren, wie z.B. Seeigel und Fadenwürmer, sind Enzyme der NADPH- (NOX) und Dualen Oxidasen (DUOX) maßgeblich für die

Produktion von ROS verantwortlich. In Übereinstimmung mit anderen Studien konnte in dieser Studie ebenfalls eine dosis- und zeitabhängige ROS Produktion in Hämozyten von *M. edulis* nach Immunstimulation gezeigt werden. Trotz der hohen Anzahl von Studien, die sich mit der Generierung von ROS in Weichtieren beschäftigen, ist dies die erste Studie, in der die Identifizierung von NOX und DUOX Orthologen sowie ihrer Untereinheiten in Muscheln erfolgte und damit eine der ersten Studien im gesamten Überstamm der Lophotrochozoa. Die durchgeführten phylogenetischen Analysen wiesen auf einen höheren Verwandtschaftsgrad von DUOX Orthologen der Deuterostomier zu denen der Lophotrochozoa als zu denen der Ecdysozoa hin, welches die Eignung von Lophotrochozoen als Modell zur Erforschung der Evolution des angeborenen Immunsystems unterstreicht. Des Weiteren wurden die DUOX Orthologe mithilfe der phylogenetischen Analyse in drei verschiedene Gruppen eingeteilt, die sich größtenteils mit ihrem individuellen, gewebespezifischen Expressionsmuster deckten. Orthologe der DUOX-b Gruppe besaßen eine besonders hohe mRNA Expression in Hämozyten verglichen mit anderen Geweben und besonders im Vergleich mit anderen, bedeutenden Immungenen. Im Gegensatz dazu steht, dass die schnelle und starke Induktion der DUOX Expression nach Immunstimulation sich nicht mit der ROS Produktion in Hämozyten von *M. edulis* deckte. Dennoch deuten die hohe basale Expression von DUOX-b Transkripten in Hämozyten, die erhöhte DUOX Transkription nach Immunstimulation und eine reduzierte ROS Produktion bei Einsatz des Inhibitors BAPTA verstärkt auf eine Rolle von DUOX-b im Immunsystem der Muscheln hin.

Säugetiere bedienen sich einer Vielzahl von Zytokin-Familien zur intra- und extrazellulären Kommunikation. Viele dieser Familien können jedoch nicht in Evertebraten vorgefunden werden; Eine große Ausnahme hierzu stellen Zytokine der Interleukin-17 (IL-17) Familie dar. In dieser Studie wurden Transkripte je zwei potenzieller IL-17 Orthologe für *M. edulis* und *L. elliptica* sowie ein Ortholog für *A. islandica* beschrieben. Mindestens ein Ortholog je Muschel wies, im Vergleich zu anderen Geweben sowie Hämozyten, sehr hohe Transkriptlevel im Kiemengewebe auf. Dennoch war die Transkription der IL-17 Orthologe in Hämozyten von *M. edulis* mit Hilfe von verschiedenen Immunstimuli stark induzierbar. Dabei war das resultierende Expressionsprofil stark vom betrachteten Ortholog und Stimulus abhängig, welches das Vorkommen von zwei differenten IL-17 Orthologen mit potenziell unterschiedlicher Funktion in Muscheln bekräftigt.

Erkenntnisse aus dieser Arbeit lieferten tiefere Einsichten in die Flagellin-vermittelte Abwehrreaktion in *M. edulis*. Zusätzlich wurden die Konservierung und transkriptionelle Regulation zweier orthologer Familien von Immungenen eines phylogenetisch ursprünglicheren Tierstammes genauer erläutert. Auf diese Weise konnte die Studie zu umfassenderen Kenntnissen über die Evolution des angeborenen Immunsystems selber beitragen.

## 7. REFERENCES

Adams M.D., Celniker S.E., Holt R.A., Evans C.A., Gocayne J.D., Amanatides P.G., Scherer S.E., Li P.W., Hoskins R.A. and Galle R.F. (2000). The genome sequence of *Drosophila melanogaster*. *Science*. **287**, 2185-2195.

Adema C.M., van Deutekom-Mulder E.C., van der Knaap W.P. and Sminia T. (1993). NADPH-oxidase activity: the probable source of reactive oxygen intermediate generation in hemocytes of the gastropod *Lymnaea stagnalis*. *Journal of Leukocyte Biology*. **54**, 379-383.

Adema C.M., van Deutekom-Mulder E.C., van der Knaap W.P.W., Meuleman E.A. and Sminia T. (1991). Generation of oxygen radicals in hemocytes of the snail *Lymnaea stagnalis* in relation to the rate of phagocytosis. *Developmental & Comparative Immunology*. **15**, 17-26.

Aderem A. and Underhill D.M. (1999). Mechanisms of phagocytosis in macrophages. *Annual Review of Immunology*. **17**, 593-623.

Aggarwal S. and Gurney A.L. (2002). IL-17: prototype member of an emerging cytokine family. *Journal of Leukocyte Biology*. **71**, 1-8.

Aguirre J. and Lambeth J.D. (2010). Nox enzymes from fungus to fly to fish and what they tell us about Nox function in mammals. *Free Radical Biology and Medicine*. **49**, 1342-1353.

Alberts B., Johnson A., Walter P. and Lewis J. (2007). The adaptive immune system. In *Molecular Biology of the Cell*. (B Alberts, ed). New York: Garland Science, pp. 1539-1600.

Altincicek B. and Vilcinskas A. (2007). Analysis of the immune-related transcriptome of a lophotrochozoan model, the marine annelid *Platynereis dumerilii*. *Frontiers in Zoology*. **4**, 18.

Altschul S.F., Gish W., Miller W., Meyers E.W. and Lipman D.J. (1990). Basic Local Alignment Search Tool. *Journal of Molecular Biology*. **215**, 403-410.

Ananthanarayanan B., Stahelin R.V., Digman M.A. and Cho W. (2003). Activation mechanisms of conventional protein kinase C isoforms are determined by the ligand affinity and conformational flexibility of their C1 Domains. *Journal of Biological Chemistry*. **278**, 46886-46894.

Anderson R.S., Mora L.M. and Thomson S.A. (1994). Modulation of oyster (*Crassostrea virginica*) hemocyte immune function by copper, as measured by luminol-enhanced chemiluminescence. *Comparative Biochemistry & Physiology Part C: Pharmacology, Toxicology & Endocrinology*. **108**, 215-220.

Anguiano-Beltrán C., Lizárraga-Partida M.L. and Searcy-Bernal R. (2004). Effect of *Vibrio alginolyticus* on larval survival of the blue mussel *Mytilus galloprovincialis*. *Diseases of Aquatic Organisms*. **59**, 119-123.

Anrather J., Racchumi G. and Iadecola C. (2006). NF-κB regulates phagocytic NADPH oxidase by inducing the expression of gp91phox. *Journal of Biological Chemistry*. **281**, 5657-5667.

Arumugam M., Romestand B., Torreilles J. and Roch P. (2000). *In vitro* production of superoxide and nitric oxide (as nitrite and nitrate) by *Mytilus galloprovincialis* haemocytes upon incubation with PMA or laminarin or during yeast phagocytosis. *European Journal of Cell Biology*. **79**, 513-519.

Ashburner M., Ball C.A., Blake J.A., Botstein D., Butler H., Cherry J.M., Davis A.P., Dolinski K., Dwight S.S., Eppig J.T., Harris M.A., Hill D.P., Issel-Tarver L., Kasarskis A., Lewis S., Matese J.C., Richardson J.E., Ringwald M., Rubin G.M. and Sherlock G. (2000). Gene ontology: tool for the unification of biology. The Gene Ontology Consortium. *Nature genetics*. **25**, 25-29.

Azumi K., Kuribayashi F., Kanegasaki S. and Yokosawa H. (2002). Zymosan induces production of superoxide anions by hemocytes of the solitary ascidian *Halocynthia roretzi*. *Comparative Biochemistry & Physiology Part C: Toxicology & Pharmacology*. **133**, 567-574.

Bach J.-F. (2002). The effect of infections on susceptibility to autoimmune and allergic diseases. *New England Journal of Medicine*. **347**, 911-920.

Balseiro P., Falcó A., Romero A., Dios S., Martínez-López A., Figueras A., Estepa A. and Novoa B. (2011). *Mytilus galloprovincialis* Myticin C: A chemotactic molecule with antiviral activity and immunoregulatory properties. *PLoS ONE*. **6**, e23140.

Bánfi B., Tirone F., Durussel I., Knisz J., Moskwa P., Molnar G.Z., Krause K.-H. and Cox J.A. (2004). Mechanism of $Ca^{2+}$ activation of the NADPH oxidase NOX5. *Journal of Biological Chemistry*. **279**, 18583-18591.

Barnes P.J. (1997). Nuclear factor-κB. *The International Journal of Biochemistry & Cell Biology*. **29**, 867-870.

Baumgart D.C. and Carding S.R. (2007). Inflammatory bowel disease: cause and immunobiology. *The Lancet*. **369**, 1627-1640.

Bedard K., Jaquet V. and Krause K.-H. (2012). NOX5: from basic biology to signaling and disease. *Free Radical Biology and Medicine*. **52**, 725-734.

Bedard K. and Krause K.-H. (2007). The NOX family of ROS-generating NADPH oxidases: Physiology and pathophysiology. *Physiological Reviews*. **87**, 245-313.

Bedard K., Lardy B. and Krause K.-H. (2007). NOX family NADPH oxidases: Not just in mammals. *Biochimie*. **89**, 1107-1112.

Bender R.C., Broderick E.J., Goodall C.P. and Bayne C.J. (2005). Respiratory burst of *Biomphalaria glabrata* hemocytes: *Schistosoma mansoni*-resistant snails produce more extracellular $H_2O_2$ than susceptible snails. *Journal of Parasitology*. **91**, 275-279.

Bernardo J., Long H.J. and Simons E.R. (2010). Initial cytoplasmic and phagosomal consequences of human neutrophil exposure to *Staphylococcus epidermidis*. *Cytometry Part A*. **77A**, 243-252.

Bettencourt R., Roch P., Stefanni S., Rosa D., Colaço A. and Serrão Santos R. (2007). Deep sea immunity: Unveiling immune constituents from the hydrothermal vent mussel *Bathymodiolus azoricus*. *Marine Environmental Research*. **64**, 108-127.

Blumberg P.M. (1988). Protein kinase C as the receptor for the phorbol ester tumor promoters: Sixth Rhoads Memorial Award Lecture. *Cancer Research*. **48**, 1-8.

Boehm T. (2012). Evolution of vertebrate immunity. *Current Biology*. **22**, R722-R732.

Bokoch G.M. and Knaus U.G. (2003). NADPH oxidases: not just for leukocytes anymore! *Trends in Biochemical Sciences*. **28**, 502-508.

Bonardi V., Cherkis K., Nishimura M.T. and Dangl J.L. (2012). A new eye on NLR proteins: focused on clarity or diffused by complexity? *Current Opinion in Immunology*. **24**, 41-50.

Bozym Rebecca A., Delorme-Axford E., Harris K., Morosky S., Ikizler M., Dermody Terence S., Sarkar Saumendra N. and Coyne Carolyn B. (2012). Focal adhesion kinase is a component of antiviral RIG-I-like receptor signaling. *Cell Host & Microbe*. **11**, 153-166.

Bramble L. and Anderson R.S. (1997). Modulation of *Crassostrea virginica* hemocyte reactive oxygen species production by *Listonella anguillarum*. *Developmental & Comparative Immunology*. **21**, 337-348.

Bramble L.H. and Anderson R.S. (1998). A comparison of the chemiluminescent response of *Crassostrea virginica* and *Morone saxatilis* phagocytes to zymosan and viable *Listonella anguillarum*. *Developmental & Comparative Immunology*. **22**, 55-61.

Bray S.J. (2006). Notch signalling: a simple pathway becomes complex. *Nature Reviews Molecular Cell Biology*. **7**, 678-689.

Brereton J.D. and Alderman D.J. (1979). Wound healing in the European oyster, *Ostrea edulis* L. *Aquaculture*. **16**, 147-151.

Brew K., Dinakarpandian D. and Nagase H. (2000). Tissue inhibitors of metalloproteinases: evolution, structure and function. *Biochimica et Biophysica Acta (BBA) - Protein Structure and Molecular Enzymology*. **1477**, 267-283.

Brinkmann H. and Philippe H. (2008). Animal phylogeny and large-scale sequencing: progress and pitfalls. *Journal of Systematics and Evolution*. **46**, 274-286.

Brocker C., Thompson D., Matsumoto A., Nebert D.W. and Vasiliou V. (2010). Evolutionary divergence and functions of the human interleukin (IL) gene family. *Human genomics*. **5**, 30-55.

Brown G.C. and Borutaite V. (2012). There is no evidence that mitochondria are the main source of reactive oxygen species in mammalian cells. *Mitochondrion*. **12**, 1-4.

Buggé D.M., Hégaret H., Wikfors G.H. and Allam B. (2007). Oxidative burst in hard clam (*Mercenaria mercenaria*) haemocytes. *Fish & Shellfish Immunology*. **23**, 188-196.

Buttgereit F., Burmester G.-R. and Brand M.D. (2000). Bioenergetics of immune functions: fundamental and therapeutic aspects. *Immunology Today*. **21**, 194-199.

Cajaraville M.P. and Pal S.G. (1995). Morphofunctional study of the haemocytes of the bivalve mollusc *Mytilus galloprovincialis* with emphasis on the endolysosomal compartment. *Cell Structure & Function*. **20**, 355-367.

Cambi A., Koopman M. and Figdor C.G. (2005). How C-type lectins detect pathogens. *Cellular Microbiology*. **7**, 481-488.

Canesi L., Gallo G., Gavioli M. and Pruzzo C. (2002). Bacteria–hemocyte interactions and phagocytosis in marine bivalves. *Microscopy Research and Technique*. **57**, 469-476.

Casadevall A. and Pirofski L.A. (2002). What is a pathogen? *Annals of medicine*. **34**, 2-4.

Cavallo R.A. and Stabili L. (2002). Presence of vibrios in seawater and *Mytilus galloprovincialis* (Lam.) from the Mar Piccolo of Taranto (Ionian Sea). *Water Research*. **36**, 3719-3726.

Chapman J.A., Kirkness E.F., Simakov O., Hampson S.E., Mitros T., Weinmaier T., Rattei T., Balasubramanian P.G., Borman J., Busam D., Disbennett K., Pfannkoch C., Sumin N., Sutton G.G., Viswanathan L.D., Walenz B., Goodstein D.M., Hellsten U., Kawashima T., Prochnik S.E., Putnam N.H., Shu S., Blumberg B., Dana C.E., Gee L., Kibler D.F., Law L., Lindgens D., Martinez D.E., Peng J., Wigge P.A., Bertulat B., Guder C., Nakamura Y., Ozbek S., Watanabe H., Khalturin K., Hemmrich G., Franke A., Augustin R., Fraune S., Hayakawa E., Hayakawa S., Hirose M., Hwang J.S., Ikeo K., Nishimiya-Fujisawa C., Ogura A., Takahashi T., Steinmetz P.R., Zhang X., Aufschnaiter R., Eder M.K., Gorny A.K., Salvenmoser W., Heimberg A.M., Wheeler B.M., Peterson K.J., Bottger A., Tischler P., Wolf A., Gojobori T., Remington K.A., Strausberg R.L., Venter J.C., Technau U., Hobmayer B., Bosch T.C., Holstein T.W., Fujisawa T., Bode H.R., David C.N., Rokhsar D.S. and Steele R.E. (2010). The dynamic genome of *Hydra*. *Nature*. **464**, 592-596.

Chávez V., Mohri-Shiomi A. and Garsin D.A. (2009). Ce-Duox1/BLI-3 generates reactive oxygen species as a protective innate immune mechanism in *Caenorhabditis elegans. Infection and Immunity*. **77**, 4983-4989.

Cheng W., Juang F.-M. and Chen J.-C. (2004). The immune response of Taiwan abalone *Haliotis diversicolor supertexta* and its susceptibility to *Vibrio parahaemolyticus* at different salinity levels. *Fish & Shellfish Immunology*. **16**, 295-306.

Ciacci C., Betti M., Canonico B., Citterio B., Roch P. and Canesi L. (2010). Specificity of anti-*Vibrio* immune response through p38 MAPK and PKC activation in the hemocytes of the mussel *Mytilus galloprovincialis*. *Journal of Invertebrate Pathology*. **105**, 49-55.

Clark I.M., Swingler T.E., Sampieri C.L. and Edwards D.R. (2008). The regulation of matrix metalloproteinases and their inhibitors. *The International Journal of Biochemistry & Cell Biology*. **40**, 1362-1378.

Clark M.S., Thorne M.A.S., Vieira F.A., Cardoso J.C.R., Power D.M. and Peck L.S. (2010). Insights into shell deposition in the Antarctic bivalve *Laternula elliptica*: gene discovery in the mantle transcriptome using 454 pyrosequencing. *BMC Genomics*. **11**, 362.

Comesaña P., Casas S.M., Cao A., Abollo E., Arzul I., Morga B. and Villalba A. (2012). Comparison of haemocytic parameters among flat oyster *Ostrea edulis* stocks with different susceptibility to bonamiosis and the Pacific oyster *Crassostrea gigas*. *Journal of Invertebrate Pathology*. **109**, 274-286.

Cooper M.D. and Alder M.N. (2006). The Evolution of Adaptive Immune Systems. *Cell*. **124**, 815-822.

Costa M.M., Prado-Alvarez M., Gestal C., Li H., Roch P., Novoa B. and Figueras A. (2009). Functional and molecular immune response of Mediterranean mussel (*Mytilus galloprovincialis*) haemocytes against pathogen-associated molecular patterns and bacteria. *Fish & Shellfish Immunology*. **26**, 515-523.

Coteur G., Danis B., Fowler S.W., Teyssié J.L., Dubois P. and Warnau M. (2001). Effects of PCBs on reactive oxygen species (ROS) production by the immune cells of *Paracentrotus lividus* (Echinodermata). *Marine Pollution Bulletin*. **42**, 667-672.

Coteur G., Warnau M., Jangoux M. and Dubois P. (2002). Reactive oxygen species (ROS) production by amoebocytes of *Asterias rubens* (Echinodermata). *Fish & Shellfish immunology*. **12**, 187-200.

Cross A.R. and Segal A.W. (2004). The NADPH oxidase of professional phagocytes—prototype of the NOX electron transport chain systems. *Biochimica et Biophysica Acta (BBA) - Bioenergetics*. **1657**, 1-22.

Cua D.J. and Tato C.M. (2010). Innate IL-17-producing cells: the sentinels of the immune system. *Nature Reviews Immunology*. **10**, 479-489.

Damiano S., Fusco R., Morano A., De Mizio M., Paternò R., De Rosa A., Spinelli R., Amente S., Frunzio R., Mondola P., Miot F., Laccetti P., Santillo M. and Avvedimento E.V. (2012). Reactive oxygen species regulate the levels of dual oxidase (Duox1-2) in human neuroblastoma cells. *PLoS ONE*. **7**, e34405.

de Lorgeril J., Zenagui R., Rosa R.D., Piquemal D. and Bachère E. (2011). Whole transcriptome profiling of successful immune response to *Vibrio* infections in the oyster *Crassostrea gigas* by digital gene expression analysis. *PLoS ONE*. **6**, e23142.

De Zoysa M., Jung S. and Lee J. (2009). First molluscan TNF-α homologue of the TNF superfamily in disk abalone: Molecular characterization and expression analysis. *Fish & Shellfish Immunology*. **26**, 625-631.

De Zoysa M., Nikapitiya C., Oh C., Whang I., Lee J.-S., Jung S.-J., Choi C.Y. and Lee J. (2010). Molecular evidence for the existence of lipopolysaccharide-induced TNF-α factor (LITAF) and Rel/NF-kB pathways in disk abalone (*Haliotis discus discus*). *Fish & Shellfish Immunology*. **28**, 754-763.

de Zwaan A. and Mathieu M. (1992). Cellular biochemistry and endocrinology In *The mussel Mytilus: ecology, physiology, genetics and culture.* (E Gosling, ed). Amsterdam: Elsevier, pp. 223-308.

Dehal P., Satou Y., Campbell R.K., Chapman J., Degnan B., De Tomaso A., Davidson B., Di Gregorio A., Gelpke M., Goodstein D.M., Harafuji N., Hastings K.E.M., Ho I., Hotta K., Huang W., Kawashima T., Lemaire P., Martinez D., Meinertzhagen I.A., Necula S., Nonaka M., Putnam N., Rash S., Saiga H., Satake M., Terry A., Yamada L., Wang H.-G., Awazu S., Azumi K., Boore J., Branno M., Chin-bow S., DeSantis R., Doyle S., Francino P., Keys D.N., Haga S., Hayashi H., Hino K., Imai K.S., Inaba K., Kano S., Kobayashi K., Kobayashi M., Lee B.-I., Makabe K.W., Manohar C., Matassi G., Medina M., Mochizuki Y., Mount S., Morishita T., Miura S., Nakayama A., Nishizaka S., Nomoto H., Ohta F., Oishi K., Rigoutsos I., Sano M., Sasaki A., Sasakura Y., Shoguchi E., Shin-i T., Spagnuolo A., Stainier D., Suzuki M.M., Tassy O., Takatori N., Tokuoka M., Yagi K., Yoshizaki F., Wada S., Zhang C., Hyatt P.D., Larimer F., Detter C., Doggett N., Glavina T., Hawkins T., Richardson P., Lucas S., Kohara Y., Levine M., Satoh N. and Rokhsar D.S. (2002). The draft genome of *Ciona intestinalis*: Insights into chordate and vertebrate origins. *Science*. **298**, 2157-2167.

DeLeo F.R., Allen L.-A.H., Apicella M. and Nauseef W.M. (1999). NADPH oxidase activation and assembly during phagocytosis. *The Journal of Immunology*. **163**, 6732-6740.

Deslous-Paoli J.M. (1986). Feeding and digestion with Bivalves. In *Nutrition in marine aquaculture, FAO-MEDRAP*. (A Bruno, ed). Lisbon, pp. 145-198.

DesVoigne D.M. and Sparks A.K. (1968). The process of wound healing in the Pacific oyster, *Crassostrea gigas*. *Journal of Invertebrate Pathology*. **12**, 53-65.

Dewitt S., Laffafian I. and Hallett M.B. (2003). Phagosomal oxidative activity during β2 integrin (CR3)-mediated phagocytosis by neutrophils is triggered by a non-restricted $Ca^{2+}$ signal: $Ca^{2+}$ controls time not space. *Journal of Cell Science*. **116**, 2857-2865.

Dikkeboom R., Tijnagel J.M.G.H., Mulder E.C. and van der Knaap W.P.W. (1987). Hemocytes of the pond snail *Lymnaea stagnalis* generate reactive forms of oxygen. *Journal of Invertebrate Pathology*. **49**, 321-331.

Dishaw L.J., Haire R.N. and Litman G.W. (2012). The amphioxus genome provides unique insight into the evolution of immunity. *Briefings in Functional Genomics*. **11**, 167-176.

Dodds A.W. (2008). The evolution of complement system. In *Molecular Aspects of Innate and Adaptive Immunity*. (KBM Reid , RB Sim, eds). Cambridge: Royal Society of Chemistry, pp. 27-48.

Dodds A.W. and Matsushita M. (2007). The phylogeny of the complement system and the origins of the classical pathway. *Immunobiology*. **212**, 233-243.

Donaghy L., Hong H.-K., Lambert C., Park H.-S., Shim W.J. and Choi K.-S. (2010). First characterisation of the populations and immune-related activities of hemocytes from two edible gastropod species, the disk abalone, *Haliotis discus discus* and the spiny top shell, *Turbo cornutus*. *Fish & Shellfish Immunology*. **28**, 87-97.

Donaghy L., Lambert C., Choi K.-S. and Soudant P. (2009). Hemocytes of the carpet shell clam (*Ruditapes decussatus*) and the Manila clam (*Ruditapes philippinarum*): Current knowledge and future prospects. *Aquaculture*. **297**, 10-24.

Doussiére J., Gaillard J. and Vignais P.V. (1999). The heme component of the neutrophil NADPH oxidase complex is a target for aryliodonium compounds. *Biochemistry*. **38**, 3694-3703.

Doussiére J. and Vignais P.V. (1992). Diphenylene iodonium as an inhibitor of the NADPH oxidase complex of bovine neutrophils. *European Journal of Biochemistry*. **208**, 61-71.

Drickamer K. (1999). C-type lectin-like domains. *Current Opinion in Structural Biology*. **9**, 585-590.

Dunn C.W., Hejnol A., Matus D.Q., Pang K., Browne W.E., Smith S.A., Seaver E., Rouse G.W., Obst M., Edgecombe G.D., Sorensen M.V., Haddock S.H.D., Schmidt-Rhaesa A., Okusu A., Kristensen R.M., Wheeler W.C., Martindale M.Q. and Giribet G. (2008). Broad phylogenomic sampling improves resolution of the animal tree of life. *Nature*. **452**, 745-749.

Edens W.A., Sharling L., Cheng G., Shapira R., Kinkade J.M., Lee T., Edens H.A., Tang X., Sullards C., Flaherty D.B., Benian G.M. and Lambeth J.D. (2001). Tyrosine cross-linking of extracellular matrix is catalyzed by Duox, a multidomain oxidase/peroxidase with homology to the phagocyte oxidase subunit gp91phox. *The Journal of Cell Biology*. **154**, 879-892.

Edgar R. (2004). MUSCLE: a multiple sequence alignment method with reduced time and space complexity. *BMC Bioinformatics*. **5**, 113.

Eiler A., Johansson M. and Bertilsson S. (2006). Environmental influences on *Vibrio* populations in northern temperate and boreal coastal waters (Baltic and Skagerrak Seas). *Applied and Environmental Microbiology*. **72**, 6004-6011.

Emmert-Streib F. and Glazko G.V. (2011). Pathway analysis of expression data: Deciphering functional building blocks of complex diseases. *PLoS Computational Biology*. **7**, e1002053.

Fabioux C., Corporeau C., Quillien V., Favrel P. and Huvet A. (2009). *In vivo* RNA interference in oyster -*vasa* silencing inhibits germ cell development. *FEBS Journal*. **276**, 2566-2573.

FAO (2012). Fisheries and Aquaculture Information and Statistics Service, assessed 7th September, 2012 *Food and Agriculture Organization of the United Nations*, http://www.fao.org.

Fedders H. (2008). Charakterisierung von Effektormolekülen der antimikrobiellen Abwehr von *Ciona intestinalis*. *Dissertation, Uni-Kiel*.

Felsenstein J. (1985). Confidence limits on phylogenies: an approach using the bootstrap. *Evolution*. **39**, 783-791.

Fensterl V. and Sen G.C. (2009). Interferons and viral infections. *BioFactors*. **35**, 14-20.

Fire A., Xu S., Montgomery M.K., Kostas S.A., Driver S.E. and Mello C.C. (1998). Potent and specific genetic interference by double-stranded RNA in *Caenorhabditis elegans*. *Nature*. **391**, 806-811.

Fitzgerald J.P., Nayak B., Shanmugasundaram K., Friedrichs W., Sudarshan S., Eid A.A., DeNapoli T., Parekh D.J., Gorin Y. and Block K. (2012). Nox4 mediates renal cell carcinoma cell invasion through hypoxia-induced interleukin 6- and 8- production. *PLoS ONE*. **7**, e30712.

Flajnik M.F. and Du Pasquier L. (2004). Evolution of innate and adaptive immunity: can we draw a line? *Trends in Immunology*. **25**, 640-644.

Flajnik M.F. and Kasahara M. (2001). Comparative genomics of the MHC: Glimpses into the evolution of the adaptive immune system. *Immunity*. **15**, 351-362.

Flannagan R.S., Cosio G. and Grinstein S. (2009). Antimicrobial mechanisms of phagocytes and bacterial evasion strategies. *Nature Reviews Microbiology*. **7**, 355-366.

Foldi J., Chung A.Y., Xu H., Zhu J., Outtz H.H., Kitajewski J., Li Y., Hu X. and Ivashkiv L.B. (2010). Autoamplification of Notch signaling in macrophages by TLR-induced and RBP-J-dependent induction of Jagged1. *The Journal of Immunology*. **185**, 5023-5031.

Fujino S., Andoh A., Bamba S., Ogawa A., Hata K., Araki Y., Bamba T. and Fujiyama Y. (2003). Increased expression of interleukin 17 in inflammatory bowel disease. *Gut*. **52**, 65-70.

Fujita T. (2002). Evolution of the lectin-complement pathway and its role in innate immunity. *Nature Reviews Immunology*. **2**, 346-353.

Gabbott P.A. and Peek K. (1991). Cellular biochemistry of the mantle tissue of the mussel *Mytilus edulis* L. *Aquaculture*. **94**, 165-176.

Gaffen S.L. (2009a). The role of interleukin-17 in the pathogenesis of rheumatoid arthritis. *Current rheumatology reports*. **11**, 365-370.

Gaffen S.L. (2009b). Structure and signalling in the IL-17 receptor family. *Nature Reviews Immunology*. **9**, 556-567.

Gaffen S.L. (2011). Recent advances in the IL-17 cytokine family. *Current Opinion in Immunology*. **23**, 613-619.

Garneau J.E., Dupuis M.-E., Villion M., Romero D.A., Barrangou R., Boyaval P., Fremaux C., Horvath P., Magadan A.H. and Moineau S. (2010). The CRISPR/Cas bacterial immune system cleaves bacteriophage and plasmid DNA. *Nature*. **468**, 67-71.

Gattas M.V., Forteza R., Fragoso M.A., Fregien N., Salas P., Salathe M. and Conner G.E. (2009). Oxidative epithelial host defense is regulated by infectious and inflammatory stimuli. *Free radical biology & medicine*. **47**, 1450-1458.

Gauss K.A., Nelson-Overton L.K., Siemsen D.W., Gao Y., DeLeo F.R. and Quinn M.T. (2007). Role of NF-κB in transcriptional regulation of the phagocyte NADPH oxidase by tumor necrosis factor-α. *Journal of Leukocyte Biology*. **82**, 729-741.

Geijtenbeek T.B.H. and Gringhuis S.I. (2009). Signalling through C-type lectin receptors: Shaping immune responses. *Nature Reviews Immunology*. **9**, 465-479.

Geiszt M., Kopp J.B., Várnai P. and Leto T.L. (2000). Identification of Renox, an NAD(P)H oxidase in kidney. *Proceedings of the National Academy of Sciences*. **97**, 8010-8014.

Gilmore T.D. (2006). Introduction to NF-κB: players, pathways, perspectives. *Oncogene*. **25**, 6680-6684.

Goedken M. and De Guise S. (2004). Flow cytometry as a tool to quantify oyster defence mechanisms. *Fish & Shellfish Immunology*. **16**, 539-552.

Gómez-Gómez L. and Boller T. (2002). Flagellin perception: a paradigm for innate immunity. *Trends in plant science*. **7**, 251-256.

Gonzalez M., Gueguen Y., Destoumieux-Garzón D., Romestand B., Fievet J., Pugnière M., Roquet F., Escoubas J.-M., Vandenbulcke F., Levy O., Sauné L., Bulet P. and Bachère E. (2007). Evidence of a bactericidal permeability increasing protein in an invertebrate, the *Crassostrea gigas Cg*-BPI. *Proceedings of the National Academy of Sciences*. **104**, 17759-17764.

Gosling E. (1992). *The mussel Mytilus: ecology, physiology, genetics and culture*. Amsterdam: Elsevier.

Grasberger H. and Refetoff S. (2006). Identification of the maturation factor for dual oxidase. *Journal of Biological Chemistry*. **281**, 18269-18272.

Greger E.A., Drum A.S. and Elston R.A. (1995). Measurement of oxidative activity in hemocytes of the Pacific razor clam, *Siliqua patula*, and the oyster, *Crassostrea gigas*, using lucigenin- and luminol-dependent chemiluminescence. *Journal of Invertebrate Pathology*. **65**, 48-60.

Gupta P.K. and Sirover M.A. (1980). Sequential stimulation of DNA repair and DNA replication in normal human cells. *Mutation Research/Fundamental and Molecular Mechanisms of Mutagenesis*. **72**, 273-284.

Gutiérrez J.L., Jones C.G., Strayer D.L. and Iribarne O.O. (2003). Mollusks as ecosystem engineers: the role of shell production in aquatic habitats. *Oikos*. **101**, 79-90.

Ha E.-M., Oh C.-T., Bae Y.S. and Lee W.-J. (2005). A direct role for dual oxidase in *Drosophila* gut immunity. *Science*. **310**, 847-850.

Hahn U.K., Bender R.C. and Bayne C.J. (2000). Production of reactive oxygen species by hemocytes of *Biomphalaria glabrata*: carbohydrate-specific stimulation. *Developmental & Comparative Immunology*. **24**, 531-541.

Halanych K.M., Bacheller J.D., Aguinaldo A.M., Liva S.M., Hillis D.M. and Lake J.A. (1995). Evidence from 18S ribosomal DNA that the lophophorates are protostome animals. *Science*. **267**, 1641-1643.

Hamilton J.A. (2008). Colony-stimulating factors in inflammation and autoimmunity. *Nature Reviews Immunology*. **8**, 533-544.

Hanelt B., Lun C.M. and Adema C.M. (2008). Comparative ORESTES-sampling of transcriptomes of immune-challenged *Biomphalaria glabrata* snails. *Journal of Invertebrate Pathology*. **99**, 192-203.

Hariharan H., Giles J.S., Heaney S.B., Arsenault G., McNair N. and Rainnie D.J. (1995). Bacteriological studies on mussels and oysters from six river systems in Prince Edward Island, Canada. *Journal of Shellfish Research*. **14**, 527-532.

Harman D. (1956). Aging: a theory based on free radical and radiation chemistry. *Journal of Gerontology*. **11**, 298-300.

Hawlisch H. and Köhl J. (2006). Complement and Toll-like receptors: Key regulators of adaptive immune responses. *Molecular Immunology*. **43**, 13-21.

Hayashi F., Smith K.D., Ozinsky A., Hawn T.R., Yi E.C., Goodlett D.R., Eng J.K., Akira S., Underhill D.M. and Aderem A. (2001). The innate immune response to bacterial flagellin is mediated by Toll-like receptor 5. *Nature*. **410**, 1099-1103.

Hayden M.S. and Ghosh S. (2004). Signaling to NF-κB. *Genes & Development*. **18**, 2195-2224.

Hayden M.S. and Ghosh S. (2012). NF-κB, the first quarter-century: remarkable progress and outstanding questions. *Genes & Development*. **26**, 203-234.

Hayden M.S., West A.P. and Ghosh S. (2006). NF-κB and the immune response. *Oncogene*. **25**, 6758-6780.

Heasman J. (2002). Morpholino oligos: Making sense of antisense? *Developmental Biology*. **243**, 209-214.

Hégaret H., Wikfors G.H. and Soudant P. (2003). Flow cytometric analysis of haemocytes from eastern oysters, *Crassostrea virginica*, subjected to a sudden temperature elevation: II. Haemocyte functions: aggregation, viability, phagocytosis, and respiratory burst. *Journal of Experimental Marine Biology and Ecology*. **293**, 249-265.

Helmkampf M., Bruchhaus I. and Hausdorf B. (2008). Phylogenomic analyses of lophophorates (brachiopods, phoronids and bryozoans) confirm the Lophotrochozoa concept. *Proceedings of the Royal Society B: Biological Sciences*. **275**, 1927-1933.

Heyworth P.G. and Badwey J.A. (1990). Protein phosphorylation associated with the stimulation of neutrophils. Modulation of superoxide production by protein kinase C and calcium. *Journal of Bioenergetics and Biomembranes*. **22**, 1-26.

Heyworth P.G., Cross A.R. and Curnutte J.T. (2003). Chronic granulomatous disease. *Current Opinion in Immunology*. **15**, 578-584.

Hibino T., Loza-Coll M., Messier C., Majeske A.J., Cohen A.H., Terwilliger D.P., Buckley K.M., Brockton V., Nair S.V., Berney K., Fugmann S.D., Anderson M.K., Pancer Z., Cameron R.A., Smith L.C. and Rast J.P. (2006). The immune gene repertoire encoded in the purple sea urchin genome. *Developmental Biology*. **300**, 349-365.

Hily C. (1991). Is the activity of benthic suspension feeders a factor controlling water quality in the Bay of Brest? *Marine ecology progress series*. **69**, 179-188.

Hirota K., Ahlfors H., Duarte J.H. and Stockinger B. (2012). Regulation and function of innate and adaptive interleukin-17-producing cells. *EMBO Reports*. **13**, 113-120.

Hoebe K., Janssen E. and Beutler B. (2004). The interface between innate and adaptive immunity. *Nature immunology*. **5**, 971-974.

Hoffmann A. and Baltimore D. (2006). Circuitry of nuclear factor κB signaling. *Immunological Reviews*. **210**, 171-186.

Hoffmann A., Levchenko A., Scott M.L. and Baltimore D. (2002). The IκB-NF-κB signaling module: Temporal control and selective gene activation. *Science*. **298**, 1241-1245.

Hornef M.W., Wick M.J., Rhen M. and Normark S. (2002). Bacterial strategies for overcoming host innate and adaptive immune responses. *Nature immunology*. **3**, 1033-1040.

Hoskin D.W. and Ramamoorthy A. (2008). Studies on anticancer activities of antimicrobial peptides. *Biochimica et Biophysica Acta-Biomembranes*. **1778**, 357-375.

Hou R., Bao Z., Wang S., Su H., Li Y., Du H., Hu J., Wang S. and Hu X. (2011). Transcriptome sequencing and *de novo* analysis for yesso scallop (*Patinopecten yessoensis*) using 454 GS FLX. *PLoS ONE*. **6**, e21560.

Hu X., Chung A.Y., Wu I., Foldi J., Chen J., Ji J.D., Tateya T., Kang Y.J., Han J., Gessler M., Kageyama R. and Ivashkiv L.B. (2008). Integrated regulation of Toll-like receptor responses by Notch and Interferon-γ pathways. *Immunity*. **29**, 691-703.

Huang S., Yuan S., Guo L., Yu Y., Li J., Wu T., Liu T., Yang M., Wu K., Liu H., Ge J., Yu Y., Huang H., Dong M., Yu C., Chen S. and Xu A. (2008). Genomic analysis of the immune gene repertoire of amphioxus reveals extraordinary innate complexity and diversity. *Genome Research*. **18**, 1112-1126.

Hughes T.K., Smith E.M., Barnett J.A., Charles R. and Stefano G.B. (1991). LPS stimulated invertebrate hemocytes: A role for immunoreactive TNF and IL-1. *Developmental & Comparative Immunology*. **15**, 117-122.

Hughes T.K., Smith E.M., Chin R., Cadet P., Sinisterra J., Leung M.K., Shipp M.A., Scharrer B. and Stefano G.B. (1990). Interaction of immunoactive monokines (interleukin 1 and tumor necrosis factor) in the bivalve mollusc *Mytilus edulis*. *Proceedings of the National Academy of Sciences*. **87**, 4426-4429.

Humphries J.E. and Yoshino T.P. (2003). Cellular receptors and signal transduction in Molluscan hemocytes: Connections with the innate immune system of vertebrates. *Integrative and Comparative Biology*. **43**, 305-312.

Husmann G., Abele D., Rosenstiel P., Clark M.S., Kraemer L. and Philipp E.E.R. (in revision). Age dependent hemocyte and tissue gene expression response of the Antarctic bivalve *Laternula elliptica* upon injury and starvation. *Cell Stress and Chaperones*.

Husmann G., Philipp E.E.R., Rosenstiel P., Vazquez S. and Abele D. (2011). Immune response of the Antarctic bivalve Laternula elliptica to physical stress and microbial exposure. *Journal of Experimental Marine Biology and Ecology*. **398**, 83-90.

Huvet A., Fleury E., Corporeau C., Quillien V., Daniel J., Riviere G., Boudry P. and Fabioux C. (2011). *In vivo* RNA interference of a gonad-specific transforming growth factor-β in the Pacific oyster *Crassostrea gigas*. *Marine Biotechnology*, 1-9.

Hymowitz S.G., Filvaroff E.H., Yin J., Lee J., Cai L., Risser P., Maruoka M., Mao W., Foster J., Kelley R.F., Pan G., Gurney A.L., de Vos A.M. and Starovasnik M.A. (2001). IL-17s adopt a cystine knot fold: structure and activity of a novel cytokine, IL-17F, and implications for receptor binding. *EMBO Journal*. **20**, 5332-5341.

Inada M., Sudhakaran R., Kihara K., Nishi J., Yoshimine M., Mekata T., Kono T., Sakai M., Yoshida T. and Itami T. (2012). Molecular cloning and characterization of the NADPH oxidase from the kuruma shrimp, Marsupenaeus japonicus: Early gene up-regulation after Vibrio penaeicida and poly(I:C) stimulations in vitro. *Molecular and Cellular Probes*. **26**, 29-41.

Jones D.T., Taylor W.R. and Thornton J.M. (1992). The rapid generation of mutation data matrices from protein sequences. *Computer applications in the biosciences*. **8**, 275-282.

Jones R.M. and Petermann E. (2012). Replication fork dynamics and the DNA damage response. *Biochemical Journal*. **443**, 13-26.

Joo J.H., Ryu J.H., Kim C.H., Kim H.J., Suh M.S., Kim J.O., Chung S.Y., Lee S.N., Kim H.M., Bae Y.S. and Yoon J.H. (2012). Dual oxidase 2 is essential for the toll-like receptor 5-mediated inflammatory response in airway mucosa. *Antioxidants & Redox Signaling*. **16**, 57-70.

Karpala A.J., Doran T.J. and Bean A.G.D. (2005). Immune responses to dsRNA: Implications for gene silencing technologies. *Immunology & Cell Biology*. **83**, 211-216.

Katsuyama M. (2010). NOX/NADPH oxidase, the superoxide-generating enzyme: its transcriptional regulation and physiological roles. *Journal of pharmacological sciences*. **114**, 134-146.

Kaufmann S.H.E. (2008). Immunology's foundation: the 100-year anniversary of the Nobel Prize to Paul Ehrlich and Elie Metchnikoff. *Nature immunology*. **9**, 705-712.

Kautsky H. and Van der Maarel E. (1990). Multivariate approaches to the variation in phytobenthic communities and environmental vectors in the Baltic Sea. *Marine Ecology Progress Series*. **60**, 169-184.

Kautsky N. (1982). Growth and size structure in a baltic *Mytilus edulis* population. *Marine Biology*. **68**, 117-133.

Kautsky N. and Evans S. (1987). Role of biodeposition by *Mytilus edulis* in the circulation of matter and nutrients in a Baltic coastal ecosystem. *Marine Ecology Progress Series*. **38**, 201-212.

Kawahara T., Kuwano Y., Teshima-Kondo S., Takeya R., Sumimoto H., Kishi K., Tsunawaki S., Hirayama T. and Rokutan K. (2004). Role of nicotinamide adenine dinucleotide phosphate oxidase 1 in oxidative burst response to Toll-like receptor 5 signaling in large intestinal epithelial cells. *The Journal of Immunology*. **172**, 3051-3058.

Kawahara T. and Lambeth J.D. (2007). Molecular evolution of Phox-related regulatory subunits for NADPH oxidase enzymes. *BMC Evolutionary Biology*. **7**, 178.

Kawahara T. and Lambeth J.D. (2008). Phosphatidylinositol (4,5)-bisphosphate modulates Nox5 localization via an N-terminal polybasic region. *Molecular Biology of the Cell*. **19**, 4020-4031.

Kawahara T., Quinn M. and Lambeth J.D. (2007). Molecular evolution of the reactive oxygen-generating NADPH oxidase (Nox/Duox) family of enzymes. *BMC Evolutionary Biology*. **7**, 109.

Kawai T. and Akira S. (2010). The role of pattern-recognition receptors in innate immunity: update on Toll-like receptors. *Nature Immunology*. **11**, 373-384.

Kim S.Y., Lee J.G., Cho W.S., Cho K.H., Sakong J., Kim J.R., Chin B.R. and Baek S.H. (2010). Role of NADPH oxidase-2 in lipopolysaccharide-induced matrix metalloproteinase expression and cell migration. *Immunology and cell biology*. **88**, 197-204.

Kingeter L.M. and Lin X. (2012). C-type lectin receptor-induced NF-κB activation in innate immune and inflammatory responses. *Cellular & Molecular Immunology*. **9**, 105-112.

Király L., Hafez Y.M., Fodor J. and Király Z. (2008). Suppression of tobacco mosaic virus-induced hypersensitive-type necrotization in tobacco at high temperature is associated with downregulation of NADPH oxidase and superoxide and stimulation of dehydroascorbate reductase. *Journal of General Virology*. **89**, 799-808.

Kocot K.M., Cannon J.T., Todt C., Citarella M.R., Kohn A.B., Meyer A., Santos S.R., Schander C., Moroz L.L. and Lieb B. (2011). Phylogenomics reveals deep molluscan relationships. *Nature*. **477**, 452-456.

Kolls J.K. and Lindén A. (2004). Interleukin-17 family members and inflammation. *Immunity*. **21**, 467-476.

Kominsky D.J., Campbell E.L. and Colgan S.P. (2010). Metabolic shifts in immunity and inflammation. *The Journal of Immunology*. **184**, 4062-4068.

Kono T., Korenaga H. and Sakai M. (2011). Genomics of fish IL-17 ligand and receptors: A review. *Fish & Shellfish Immunology*. **31**, 635-643.

Korenaga H., Kono T. and Sakai M. (2010). Isolation of seven IL-17 family genes from the Japanese pufferfish *Takifugu rubripes*. *Fish & Shellfish Immunology*. **28**, 809-818.

Kortschak R.D., Samuel G., Saint R. and Miller D.J. (2003). EST analysis of the Cnidarian *Acropora millepora* reveals extensive gene loss and rapid sequence divergence in the model invertebrates. *Current biology* **13**, 2190-2195.

Krasity B.C., Troll J.V., Weiss J.P. and McFall-Ngai M.J. (2011). LBP/BPI proteins and their relatives: conservation over evolution and roles in mutualism. *Biochemical Society Transactions*. **39**, 1039.

Kufer T.A. and Sansonetti P.J. (2011). NLR functions beyond pathogen recognition. *Nature Immunology*. **12**, 121-128.

Kumar S., Molina-Cruz A., Gupta L., Rodrigues J. and Barillas-Mury C. (2010). A peroxidase/dual oxidase system modulates midgut epithelial immunity in *Anopheles gambiae*. *Science*. **327**, 1644-1648.

Lalucque H. and Silar P. (2003). NADPH oxidase: an enzyme for multicellularity? *Trends in microbiology*. **11**, 9-12.

Lambert C. and Nicolas J.-L. (1998). Specific inhibition of chemiluminescent activity by pathogenic Vibrios in hemocytes of two marine bivalves: *Pecten maximus* and *Crassostrea gigas*. *Journal of Invertebrate Pathology*. **71**, 53-63.

Lambert C., Nicolas J.-L. and Bultel V. (2001). Toxicity to bivalve hemocytes of pathogenic *Vibrio* cytoplasmic extract. *Journal of Invertebrate Pathology*. **77**, 165-172.

Lambeth J.D. (2004). NOX enzymes and the biology of reactive oxygen. *Nature Reviews Immunology*. **4**, 181-189.

Lambeth J.D., Kawahara T. and Diebold B. (2007). Regulation of Nox and Duox enzymatic activity and expression. *Free Radical Biology and Medicine*. **43**, 319-331.

Lane E. and Birkbeck T.H. (1999). Toxicity of bacteria towards haemocytes of *Mytilus edulis*. *Aquatic Living Resources*. **12**, 343-350.

Lange C., Hemmrich G., Klostermeier U.C., López--Quintero J.A., Miller D.J., Rahn T., Weiss Y., Bosch T.C.G. and Rosenstiel P. (2011). Defining the origins of the NOD-like receptor system at the base of animal evolution. *Molecular Biology and Evolution*. **28**, 1687-1702.

Laroux F.S., Romero X., Wetzler L., Engel P. and Terhorst C. (2005). Cutting edge: MyD88 controls phagocyte NADPH oxidase function and killing of gram-negative bacteria. *The Journal of Immunology*. **175**, 5596-5600.

Lee C.G., Link H., Baluk P., Homer R.J., Chapoval S., Bhandari V., Kang M.J., Cohn L., Kim Y.K., McDonald D.M. and Elias J.A. (2004). Vascular endothelial growth factor (VEGF) induces remodeling and enhances TH2-mediated sensitization and inflammation in the lung. *Nature Medicine*. **10**, 1095-1103.

Lee J., Ho W.H., Maruoka M., Corpuz R.T., Baldwin D.T., Foster J.S., Goddard A.D., Yansura D.G., Vandlen R.L. and Wood W.I. (2001). IL-17E, a novel proinflammatory ligand for the IL-17 receptor homolog IL-17Rh1. *Journal of Biological Chemistry*. **276**, 1660-1664.

Leipe D.D., Koonin E.V. and Aravind L. (2004). STAND, a class of P-Loop NTPases including animal and plant regulators of programmed cell death: Multiple, complex domain architectures, unusual phyletic patterns, and evolution by horizontal gene transfer. *Journal of Molecular Biology*. **343**, 1-28.

Leippe M. and Renwrantz L. (1985). On the capability of bivalve and gastropod hemocytes to secrete cytotoxic molecules. *Journal of Invertebrate Pathology*. **46**, 209-210.

Leippe M. and Renwrantz L. (1988). Release of cytotoxic and agglutinating molecules by *Mytilus* hemocytes. *Developmental & Comparative Immunology*. **12**, 297-308.

Li H., Chen J., Huang A., Stinson J., Heldens S., Foster J., Dowd P., Gurney A.L. and Wood W.I. (2000). Cloning and characterization of IL-17B and IL-17C, two new members of the IL-17 cytokine family. *Proceedings of the National Academy of Sciences*. **97**, 773.

Li H., Parisi M.G., Parrinello N., Cammarata M. and Roch P. (2011). Molluscan antimicrobial peptides, a review from activity-based evidences to computerassisted sequences. *Invertebrate Survival Journal*. **8**, 85-97.

Li X.J., Tian W., Stull N.D., Grinstein S., Atkinson S. and Dinauer M.C. (2009). A fluorescently tagged C-terminal fragment of p47phox detects NADPH oxidase dynamics during phagocytosis. *Molecular Biology of the Cell*. **20**, 1520-1532.

Li Y. and Trush M.A. (1998). Diphenyleneiodonium, an NAD(P)H oxidase inhibitor, also potently inhibits mitochondrial reactive oxygen species production. *Biochemical and Biophysical Research Communications*. **253**, 295-299.

Little T.J., Hultmark D. and Read A.F. (2005). Invertebrate immunity and the limits of mechanistic immunology. *Nature Immunology*. **6**, 651-654.

Livak K.J. and Schmittgen T.D. (2001). Analysis of relative gene expression data using Real-time quantitative PCR and the $2^{-\Delta\Delta C_T}$ Method. *Methods*. **25**, 402-408.

Locksley R.M., Killeen N. and Lenardo M.J. (2001). The TNF and TNF receptor superfamilies: integrating mammalian biology. *Cell*. **104**, 487.

Macagno E., Gaasterland T., Edsall L., Bafna V., Soares M., Scheetz T., Casavant T., Da Silva C., Wincker P., Tasiemski A. and Salzet M. (2010). Construction of a medicinal leech transcriptome database and its application to the identification of leech homologs of neural and innate immune genes. *BMC Genomics*. **11**, 407.

Malagoli D. (2010). Cytokine network in invertebrates: the very next phase of comparative immunology. *Invertebrate Survival Journal*. **7**, 146-148.

Malham S.K., Lacoste A., Gélébart F., Cueff A. and Poulet S.A. (2002). A first insight into stress-induced neuroendocrine and immune changes in the octopus *Eledone cirrhosa*. *Aquatic Living Resources*. **15**, 187-192.

Mallatt J., Craig C.W. and Yoder M.J. (2012). Nearly complete rRNA genes from 371 Animalia: Updated structure-based alignment and detailed phylogenetic analysis. *Molecular Phylogenetics and Evolution*. **64**, 603-617.

Mathieu M. and Lubet P. (1993). Storage tissue metabolism and reproduction in marine bivalves—a brief review. *Invertebrate Reproduction & Development*. **23**, 123-129.

McGee K., Hörstedt P. and Milton D.L. (1996). Identification and characterization of additional flagellin genes from *Vibrio anguillarum*. *Journal of Bacteriology*. **178**, 5188-5198.

McHenery J.G. and Birkbeck T.H. (1986). Inhibition of filtration in *Mytilus edulis* L. by marine vibrios. *Journal of Fish Diseases*. **9**, 257-261.

Medzhitov R. and Janeway Jr C.A. (1998). Innate immune recognition and control of adaptive immune responses. *Seminars in Immunology*. **10**, 351-353.

Mello D.F., de Oliveira E.S., Vieira R.C., Simoes E., Trevisan R., Dafre A.L. and Barracco M.A. (2012). Cellular and transcriptional responses of *Crassostrea gigas* hemocytes exposed *in vitro* to Brevetoxin (PbTx-2). *Marine Drugs*. **10**, 583-597.

Meyer H.A. and Möbius K.A. (1872). *Die Prosobranchia und Lamellibranchia der Kieler Bucht* Leipzig: Wilhelm Engelmann.

Miller D., Hemmrich G., Ball E., Hayward D., Khalturin K., Funayama N., Agata K. and Bosch T. (2007). The innate immune repertoire in Cnidaria - ancestral complexity and stochastic gene loss. *Genome Biology*. **8**, R59.

Milton D.L., O'Toole R., Horstedt P. and Wolf-Watz H. (1996). Flagellin A is essential for the virulence of *Vibrio anguillarum*. *Journal of Bacteriology*. **178**, 1310-1319.

Minakami R. and Sumimotoa H. (2006). Phagocytosis-coupled activation of the superoxide-producing phagocyte oxidase, a member of the NADPH oxidase (NOX) family. *International Journal of Hematology*. **84**, 193-198.

Mitta G., Galinier R., Tisseyre P., Allienne J.F., Girerd-Chambaz Y., Guillou F., Bouchut A. and Coustau C. (2005). Gene discovery and expression analysis of immune-relevant genes from *Biomphalaria glabrata* hemocytes. *Developmental & Comparative Immunology*. **29**, 393-407.

Mitta G., Vandenbulcke F., Hubert F., Salzet M. and Roch P. (2000a). Involvement of mytilins in mussel antimicrobial defense. *Journal of Biological Chemistry*. **275**, 12954-12962.

Mitta G., Vandenbulcke F. and Roch P. (2000b). Original involvement of antimicrobial peptides in mussel innate immunity. *FEBS Letters*. **486**, 185-190.

Mohanty J.G., Jaffe J.S., Schulman E.S. and Raible D.G. (1997). A highly sensitive fluorescent micro-assay of $H_2O_2$ release from activated human leukocytes using a dihydroxyphenoxazine derivative. *Journal of Immunological Methods*. **202**, 133-141.

Moné Y., Ribou A.-C., Cosseau C., Duval D., Théron A., Mitta G. and Gourbal B. (2011). An example of molecular co-evolution: Reactive oxygen species (ROS) and ROS scavenger levels in *Schistosoma mansoni/Biomphalaria glabrata* interactions. *International Journal for Parasitology*. **41**, 721-730.

Monie T.P., Bryant C.E. and Gay N.J. (2009). Activating immunity: lessons from the TLRs and NLRs. *Trends in Biochemical Sciences*. **34**, 553-561.

Montagnani C., Kappler C., Reichhart J.M. and Escoubas J.M. (2004). *Cg*-Rel, the first Rel/NF-κB homolog characterized in a mollusk, the Pacific oyster *Crassostrea gigas*. *FEBS Letters*. **561**, 75-82.

Montagnani C., Le Roux F., Berthe F. and Escoubas J.-M. (2001). *Cg*-TIMP, an inducible tissue inhibitor of metalloproteinase from the Pacific oyster *Crassostrea gigas* with a potential role in wound healing and defense mechanisms. *FEBS letters*. **500**, 64-70.

Montagnani C., Tirape A., Boulo V. and Escoubas J.-M. (2005). The two *Cg*-Timp mRNAs expressed in oyster hemocytes are generated by two gene families and differentially expressed during ontogenesis. *Developmental & Comparative Immunology*. **29**, 831-839.

Mootha V.K., Lindgren C.M., Eriksson K.F., Subramanian A., Sihag S., Lehar J., Puigserver P., Carlsson E., Ridderstrale M., Laurila E., Houstis N., Daly M.J., Patterson N., Mesirov J.P., Golub T.R., Tamayo P., Spiegelman B., Lander E.S., Hirschhorn J.N., Altshuler D. and Groop L.C. (2003). PGC-1alpha-responsive genes involved in oxidative phosphorylation are coordinately downregulated in human diabetes. *Nature genetics*. **34**, 267-273.

Moreira R., Balseiro P., Planas J.V., Fuste B., Beltran S., Novoa B. and Figueras A. (2012). Transcriptomics of *in vitro* immune-stimulated hemocytes from the Manila clam *Ruditapes philippinarum* using high-throughput sequencing. *PLoS ONE*. **7**, e35009.

Moseley T.A., Haudenschild D.R., Rose L. and Reddi A.H. (2003). Interleukin-17 family and IL-17 receptors. *Cytokine & Growth Factor Reviews*. **14**, 155-174.

Mullis K.B. and Faloona F.A. (1987). Specific synthesis of DNA *in vitro* via a polymerase-catalyzed chain reaction. *Methods in enzymology*. **155**, 335-350.

Murphy M.P., Holmgren A., Larsson N.-G., Halliwell B., Chang C.J., Kalyanaraman B., Rhee S.G., Thornalley P.J., Partridge L., Gems D., Nyström T., Belousov V., Schumacker P.T. and Winterbourn C.C. (2011). Unraveling the biological roles of reactive oxygen species. *Cell Metabolism*. **13**, 361-366.

Myokai F., Takashiba S., Lebo R. and Amar S. (1999). A novel lipopolysaccharide-induced transcription factor regulating tumor necrosis factor α gene expression: Molecular cloning, sequencing, characterization, and chromosomal assignment. *Proceedings of the National Academy of Sciences*. **96**, 4518-4523.

Nakayama K. and Maruyama T. (1998). Differential production of active oxygen species in photo-symbiotic and non-symbiotic bivalves. *Developmental & Comparative Immunology*. **22**, 151-159.

Nam D. and Kim S.-Y. (2008). Gene-set approach for expression pattern analysis. *Briefings in Bioinformatics*. **9**, 189-197.

Nathan C. (2006). Neutrophils and immunity: challenges and opportunities. *Nature Reviews Immunology*. **6**, 173-182.

Nelson D.E., Ihekwaba A.E.C., Elliott M., Johnson J.R., Gibney C.A., Foreman B.E., Nelson G., See V., Horton C.A., Spiller D.G., Edwards S.W., McDowell H.P., Unitt J.F., Sullivan E., Grimley R.,

Benson N., Broomhead D., Kell D.B. and White M.R.H. (2004). Oscillations in NF-κB signaling control the dynamics of gene expression. *Science.* **306**, 704-708.

Nishizuka Y. (1986). Studies and perspectives of protein kinase C. *Science.* **233**, 305-312.

Nöel D., Bachère E. and Mialhe E. (1993). Phagocytosis associated chemiluminescence of hemocytes in *Mytilus edulis* (Bivalvia). *Developmental & Comparative Immunology.* **17**, 483-493.

Nonaka M. (2011). The complement C3 protein family in invertebrates. *Invertebrate Survival Journal.* **8**, 21-32.

Nottage A.S. and Birkbeck T.H. (1986). Toxicity to marine bivalves of culture supernatant fluids of the bivalve-pathogenic Vibrio strain NCMB 1338 and other marine vibrios. *Journal of Fish Diseases.* **9**, 249-256.

Nüsse O. (2011). Biochemistry of the phagosome: The challenge to study a transient organelle. *The Scientific World Journal.* **11**, 18.

Officer C.B., Smayda T.J. and Mann R. (1982). Benthic filter feeding: a natural eutrophication control. *Marine Ecology Progress Series.* **9**, 203-210.

Ogata H., Goto S., Sato K., Fujibuchi W., Bono H. and Kanehisa M. (1999). KEGG: Kyoto Encyclopedia of Genes and Genomes. *Nucleic Acids Research.* **27**, 29-34.

Ogier-Denis E., Mkaddem S.B. and Vandewalle A. (2008). NOX enzymes and Toll-like receptor signaling. *Seminars in Immunopathology.* **30**, 291-300.

Ordás M.C., Novoa B. and Figueras A. (2000). Modulation of the chemiluminescence response of Mediterranean mussel (*Mytilus galloprovincialis*) haemocytes. *Fish & Shellfish Immunology.* **10**, 611-622.

Ortigosa M., Esteve C. and Pujalte M.-J. (1989). *Vibrio* species in seawater and mussels: Abundance and numerical taxonomy. *Systematic and Applied Microbiology.* **12**, 316-325.

Ottaviani E. (2006). Molluscan immunorecognition. *Invertebrate Survival Journal.* **3**, 50-63.

Pacquelet S., Lehmann M., Luxen S., Regazzoni K., Frausto M., Noack D. and Knaus U.G. (2008). Inhibitory action of NoxA1 on dual oxidase activity in airway cells. *Journal of Biological Chemistry.* **283**, 24649-24658.

Palaga T., Buranaruk C., Rengpipat S., Fauq A.H., Golde T.E., Kaufmann S.H.E. and Osborne B.A. (2008). Notch signaling is activated by TLR stimulation and regulates macrophage functions. *European Journal of Immunology.* **38**, 174-183.

Pan Z.K. (1998). Anaphylatoxins C5a and C3a induce nuclear factor IκB activation in human peripheral blood monocytes. *Biochimica et Biophysica Acta - Gene Structure and Expression.* **1443**, 90-98.

Pancer Z., Amemiya C.T., Ehrhardt G.R.A., Ceitlin J., Larry Gartland G. and Cooper M.D. (2004). Somatic diversification of variable lymphocyte receptors in the agnathan sea lamprey. *Nature.* **430**, 174-180.

Patel S.J., King K.R., Casali M. and Yarmush M.L. (2009). DNA-triggered innate immune responses are propagated by gap junction communication. *Proceedings of the National Academy of Sciences.* **106**, 12867-12872.

Philipp E.E.R., Kraemer L., Melzner F., Poustka A.J., Thieme S., Findeisen U., Schreiber S. and Rosenstiel P. (2012a). Massively parallel RNA sequencing identifies a complex immune gene repertoire in the Lophotrochozoan *Mytilus edulis*. *PLoS ONE.* **7**, e33091.

Philipp E.E.R., Kraemer L., Mountfort D., Schilhabel M., Schreiber S. and Rosenstiel P. (2012b). The Transcriptome Analysis and Comparison Explorer--T-ACE: a platform-independent, graphical tool to process large RNAseq datasets of non-model organisms. *Bioinformatics.* **28**, 777-783.

Philipp E.E.R., Lipinski S., Rast J. and Rosenstiel P. (2011). Immune defense of marine invertebrates: The role of reactive oxygen and nitrogen species. In *Oxidative Stress in Aquatic Ecosystems.* (D Abele, JP Vázquez-Medina , T Zenteno-Savín, eds). Chichester: John Wiley & Sons, Ltd, pp. 236-246.

Philipp E.E.R., Wessels W., Gruber H., Strahl J., Wagner A.E., Ernst I.M.A., Rimbach G., Kraemer L., Schreiber S., Abele D. and Rosenstiel P. (2012c). Gene expression and physiological changes

of different populations of the long-lived bivalve *Arctica islandica* under low oxygen conditions. *PLoS ONE*. **7**, e44621.

Philippe H., Lartillot N. and Brinkmann H. (2005). Multigene analyses of bilaterian animals corroborate the monophyly of Ecdysozoa, Lophotrochozoa, and Protostomia. *Molecular Biology and Evolution*. **22**, 1246-1253.

Pipe R.K. (1992). Generation of reactive oxygen metabolites by the haemocytes of the mussel *Mytilus edulis*. *Developmental & Comparative Immunology*. **16**, 111-122.

Pipe R.K. and Coles J.A. (1995). Environmental contaminants influencing immunefunction in marine bivalve molluscs. *Fish & Shellfish Immunology*. **5**, 581-595.

Pipe R.K., Coles J.A., Carissan F.M.M. and Ramanathan K. (1999). Copper induced immunomodulation in the marine mussel, *Mytilus edulis*. *Aquatic Toxicology*. **46**, 43-54.

Poinar H.N., Schwarz C., Qi J., Shapiro B., MacPhee R.D.E., Buigues B., Tikhonov A., Huson D.H., Tomsho L.P., Auch A., Rampp M., Miller W. and Schuster S.C. (2006). Metagenomics to paleogenomics: Large-scale sequencing of mammoth DNA. *Science*. **311**, 392-394.

Poltorak A., He X., Smirnova I., Liu M.Y., Van Huffel C., Du X., Birdwell D., Alejos E., Silva M., Galanos C., Freudenberg M., Ricciardi-Castagnoli P., Layton B. and Beutler B. (1998). Defective LPS signaling in C3H/HeJ and C57BL/10ScCr mice: mutations in Tlr4 gene. *Science*. **282**, 2085-2088.

Ponder W.F. and Lindberg D.R. (2008). *Phylogeny and Evolution of the Mollusca*. Berkeley: University of California Press.

Powolny-Budnicka I., Riemann M., Tanzer S., Schmid R.M., Hehlgans T. and Weih F. (2011). RelA and RelB transcription factors in distinct thymocyte populations control lymphotoxin-dependent interleukin-17 production in γδ T cells. *Immunity*. **34**, 364-374.

Prins T.C., Smaal A.C. and Dame R.F. (1997). A review of the feedbacks between bivalve grazing and ecosystem processes. *Aquatic Ecology*. **31**, 349-359.

Putnam N.H., Butts T., Ferrier D.E.K., Furlong R.F., Hellsten U., Kawashima T., Robinson-Rechavi M., Shoguchi E. and Yu A.T.J.K. (2008). The amphioxus genome and the evolution of the chordate karyotype. *Nature*. **453**, 1064-1071.

Qiu Z., Dillen C., Hu J., Verbeke H., Struyf S., Van Damme J. and Opdenakker G. (2009). Interleukin-17 regulates chemokine and gelatinase B expression in fibroblasts to recruit both neutrophils and monocytes. *Immunobiology*. **214**, 835-842.

Rada B. and Leto T. (2008). Oxidative innate immune defenses by Nox/Duox family NADPH oxidases. *Contributions to Microbiology*. **15**, 164–187.

Ragnarsson S.Á. and Raffaelli D. (1999). Effects of the mussel *Mytilus edulis* on the invertebrate fauna of sediments. *Journal of Experimental Marine Biology and Ecology*. **241**, 31-43.

Raible F. and Arendt D. (2004). Metazoan evolution: Some animals are more equal than others. *Current Biology*. **14**, R106-R108.

Ramos H.C., Rumbo M. and Sirard J.-C. (2004). Bacterial flagellins: mediators of pathogenicity and host immune responses in mucosa. *Trends in microbiology*. **12**, 509-517.

Rast J.P., Smith L.C., Loza-Coll M., Hibino T. and Litman G.W. (2006). Genomic insights into the immune system of the sea urchin. *Science*. **314**, 952-956.

Ridley A.J., Schwartz M.A., Burridge K., Firtel R.A., Ginsberg M.H., Borisy G., Parsons J.T. and Horwitz A.R. (2003). Cell migration: Integrating signals from front to back. *Science*. **302**, 1704-1709.

Rigutto S., Hoste C., Grasberger H., Milenkovic M., Communi D., Dumont J.E., Corvilain B., Miot F.o. and De Deken X. (2009). Activation of dual oxidases Duox1 and Duox2. *Journal of Biological Chemistry*. **284**, 6725-6734.

Rinaldi M., Moroni P., Paape M.J. and Bannerman D.D. (2007). Evaluation of assays for the measurement of bovine neutrophil reactive oxygen species. *Veterinary Immunology and Immunopathology*. **115**, 107-125.

Roberts S., Goetz G., White S. and Goetz F. (2009). Analysis of genes isolated from plated hemocytes of the Pacific oyster, *Crassostreas gigas*. *Marine Biotechnology*. **11**, 24-44.

Roberts S., Gueguen Y., de Lorgeril J. and Goetz F. (2008). Rapid accumulation of an interleukin 17 homolog transcript in *Crassostrea gigas* hemocytes following bacterial exposure. *Developmental & Comparative Immunology*. **32**, 1099-1104.

Roch P. (1999). Defense mechanisms and disease prevention in farmed marine invertebrates. *Aquaculture*. **172**, 125-145.

Rosenstiel P., Jacobs G., Till A. and Schreiber S. (2008). NOD-like receptors: Ancient sentinels of the innate immune system. *Cellular and Molecular Life Sciences*. **65**, 1361-1377.

Rosenstiel P., Philipp E.E.R., Schreiber S. and Bosch T.C.G. (2009). Evolution and function of innate immune receptors -- Insights from marine invertebrates. *Journal of Innate Immunity*. **1**, 291-300.

Rot A. and von Andrian U.H. (2004). Chemokines in innate and adaptive host defense: Basic chemokinese grammar for immune cells. *Annual Review of Immunology*. **22**, 891-928.

Rouvier E., Luciani M.F., Mattei M.G., Denizot F. and Golstein P. (1993). CTLA-8, cloned from an activated T cell, bearing AU-rich messenger RNA instability sequences, and homologous to a herpesvirus saimiri gene. *Journal of Immunology*. **150**, 5445-5456.

Rozental R., Campos-de-Carvalho A. and Spray D. (2000). Gap junctions in the cardiovascular and immune systems. *Brazilian Journal of Medical and Biological Research*. **33**, 365-368.

Ruby E.G. and McFall-Ngai M.J. (1999). Oxygen-utilizing reactions and symbiotic colonization of the squid light organ by *Vibrio fischeri*. *Trends in microbiology*. **7**, 414-420.

Saiki R.K., Scharf S., Faloona F., Mullis K.B., Horn G.T., Erlich H.A. and Arnheim N. (1985). Enzymatic amplification of β-globin genomic sequences and restriction site analysis for diagnosis of sickle cell anemia. *Science*. **230**, 1350-1354.

Sanger F., Nicklen S. and Coulson A.R. (1977). DNA sequencing with chain-terminating inhibitors. *Proceedings of the National Academy of Sciences*. **74**, 5463-5467.

Sarma J. and Ward P. (2011). The complement system. *Cell and Tissue Research*. **343**, 227-235.

Sato M., Sano H., Iwaki D., Kudo K., Konishi M., Takahashi H., Takahashi T., Imaizumi H., Asai Y. and Kuroki Y. (2003). Direct binding of Toll-like receptor 2 to Zymosan, and Zymosan-induced NF-κB activation and TNF-α secretion are down-regulated by lung collectin surfactant protein A. *The Journal of Immunology*. **171**, 417-425.

Satoh T., Kato H., Kumagai Y., Yoneyama M., Sato S., Matsushita K., Tsujimura T., Fujita T., Akira S. and Takeuchi O. (2010). LGP2 is a positive regulator of RIG-I– and MDA5-mediated antiviral responses. *Proceedings of the National Academy of Sciences*. **107**, 1512-1517.

Scheidereit C. (2006). IκB kinase complexes: gateways to NF-κB activation and transcription. *Oncogene*. **25**, 6685-6705.

Schmitt P., Lorgeril J.d., Gueguen Y., Destoumieux-Garzón D. and Bachère E. (2012). Expression, tissue localization and synergy of antimicrobial peptides and proteins in the immune response of the oyster *Crassostrea gigas*. *Developmental & Comparative Immunology*. **37**, 363-370.

Schneeweiß H. and Renwrantz L. (1993). Analysis of the attraction of haemocytes from *Mytilus edulis* by molecules of bacterial origin. *Developmental & Comparative Immunology*. **17**, 377-387.

Schreiber S., Rosenstiel P., Albrecht M., Hampe J. and Krawczak M. (2005). Genetics of Crohn disease, an archetypal inflammatory barrier disease. *Nature Reviews Genetics*. **6**, 376-388.

Schuster S.C. (2008). Next-generation sequencing transforms today's biology. *Nature*. **200**.

Sea Urchin Genome Sequencing Consortium, Sodergren E., Weinstock G.M., Davidson E.H., Cameron R.A., Gibbs R.A., Angerer R.C., Angerer L.M., Arnone M.I., Burgess D.R., Burke R.D., Coffman J.A., Dean M., Elphick M.R., Ettensohn C.A., Foltz K.R., Hamdoun A., Hynes R.O., Klein W.H., Marzluff W., McClay D.R., Morris R.L., Mushegian A., Rast J.P., Smith L.C., Thorndyke M.C., Vacquier V.D., Wessel G.M., Wray G., Zhang L., Elsik C.G., Ermolaeva O., Hlavina W., Hofmann G., Kitts P., Landrum M.J., Mackey A.J., Maglott D., Panopoulou G., Poustka A.J., Pruitt K., Sapojnikov V., Song X., Souvorov A., Solovyev V., Wei Z., Whittaker C.A., Worley K., Durbin K.J., Shen Y., Fedrigo O., Garfield D., Haygood R., Primus A., Satija R., Severson T., Gonzalez-Garay M.L., Jackson A.R., Milosavljevic A., Tong M., Killian C.E., Livingston B.T., Wilt F.H., Adams N., Bellé R., Carbonneau S., Cheung R., Cormier P., Cosson B., Croce J.,

Fernandez-Guerra A., Geneviĕre A.-M., Goel M., Kelkar H., Morales J., Mulner-Lorillon O., Robertson A.J., Goldstone J.V., Cole B., Epel D., Gold B., Hahn M.E., Howard-Ashby M., Scally M., Stegeman J.J., Allgood E.L., Cool J., Judkins K.M., McCafferty S.S., Musante A.M., Obar R.A., Rawson A.P., Rossetti B.J., Gibbons I.R., Hoffman M.P., Leone A., Istrail S., Materna S.C., Samanta M.P., Stolc V., Tongprasit W., Tu Q., Bergeron K.-F., Brandhorst B.P., Whittle J., Berney K., Bottjer D.J., Calestani C., Peterson K., Chow E., Yuan Q.A., Elhaik E., Graur D., Reese J.T., Bosdet I., Heesun S., Marra M.A., Schein J., Anderson M.K., Brockton V., Buckley K.M., Cohen A.H., Fugmann S.D., Hibino T., Loza-Coll M., Majeske A.J., Messier C., Nair S.V., Pancer Z., Terwilliger D.P., Agca C., Arboleda E., Chen N., Churcher A.M., Hallbȶĸ F., Humphrey G.W., Idris M.M., Kiyama T., Liang S., Mellott D., Mu X., Murray G., Olinski R.P., Raible F., Rowe M., Taylor J.S., Tessmar-Raible K., Wang D., Wilson K.H., Yaguchi S., Gaasterland T., Galindo B.E., Gunaratne H.J., Juliano C., Kinukawa M., Moy G.W., Neill A.T., Nomura M., Raisch M., Reade A., Roux M.M., Song J.L., Su Y.-H., Townley I.K., Voronina E., Wong J.L., Amore G., Branno M., Brown E.R., Cavalieri V., Duboc V.r., Duloquin L., Flytzanis C., Gache C., Lapraz F.o., Lepage T., Locascio A., Martinez P., Matassi G., Matranga V., Range R., Rizzo F., Röttinger E., Beane W., Bradham C., Byrum C., Glenn T., Hussain S., Manning G., Miranda E., Thomason R., Walton K., Wikramanayke A., Wu S.-Y., Xu R., Brown C.T., Chen L., Gray R.F., Lee P.Y., Nam J., Oliveri P., Smith J., Muzny D., Bell S., Chacko J., Cree A., Curry S., Davis C., Dinh H., Dugan-Rocha S., Fowler J., Gill R., Hamilton C., Hernandez J., Hines S., Hume J., Jackson L., Jolivet A., Kovar C., Lee S., Lewis L., Miner G., Morgan M., Nazareth L.V., Okwuonu G., Parker D., Pu L.-L., Thorn R. and Wright R. (2006). The genome of the sea urchin *Strongylocentrotus purpuratus*. *Science*. **314**, 941-952.

Serrander L., Jaquet V., Bedard K., Plastre O., Hartley O., Arnaudeau S., Demaurex N., Schlegel W. and Krause K.-H. (2007). NOX5 is expressed at the plasma membrane and generates superoxide in response to protein kinase C activation. *Biochimie*. **89**, 1159-1167.

Sharma P.P., González V.L., Kawauchi G.Y., Andrade S.C.S., Guzmán A., Collins T.M., Glover E.A., Harper E.M., Healy J.M., Mikkelsen P.M., Taylor J.D., Bieler R. and Giribet G. (2012). Phylogenetic analysis of four nuclear protein-encoding genes largely corroborates the traditional classification of Bivalvia (Mollusca). *Molecular Phylogenetics and Evolution*. **65**, 64-74.

Shen F., Hu Z., Goswami J. and Gaffen S.L. (2006). Identification of common transcriptional regulatory elements in Interleukin-17 target genes. *Journal of Biological Chemistry*. **281**, 24138-24148.

Smith S.A., Wilson N.G., Goetz F.E., Feehery C., Andrade S.C.S., Rouse G.W., Giribet G. and Dunn C.W. (2011). Resolving the evolutionary relationships of molluscs with phylogenomic tools. *Nature*. **480**, 364-367.

Sonder S.U., Saret S., Tang W., Sturdevant D.E., Porcella S.F. and Siebenlist U. (2011). IL-17-induced NF-κB activation via CIKS/Act1: Physiologic significance and signaling mechanisms. *Journal of Biological Chemistry*. **286**, 12881-12890.

Song L., Wang L., Qiu L. and Zhang H. (2010). Bivalve Immunity. In *Invertebrate Immunity*. (K Söderhäll, ed). New York: Springer, pp. 44-65.

Song Y.L. and Hsieh Y.T. (1994). Immunostimulation of tiger shrimp (*Penaeus monodon*) hemocytes for generation of microbicidal substances: Analysis of reactive oxygen species. *Developmental & Comparative Immunology*. **18**, 201-209.

Sperstad S.V., Haug T., Blencke H.-M., Styrvold O.B., Li C. and Stensvåg K. (2011). Antimicrobial peptides from marine invertebrates: Challenges and perspectives in marine antimicrobial peptide discovery. *Biotechnology Advances*. **29**, 519-530.

Starnes T., Broxmeyer H.E., Robertson M.J. and Hromas R. (2002). Cutting edge: IL-17D, a novel member of the IL-17 family, stimulates cytokine production and inhibits hemopoiesis. *The Journal of Immunology*. **169**, 642-646.

Starnes T., Robertson M.J., Sledge G., Kelich S., Nakshatri H., Broxmeyer H.E. and Hromas R. (2001). Cutting edge: IL-17F, a novel cytokine selectively expressed in activated T cells and

monocytes, regulates angiogenesis and endothelial cell cytokine production. *The Journal of Immunology*. **167**, 4137-4140.

Suárez-Castillo E. and Garcia-Arraras J. (2007). Molecular evolution of the ependymin protein family: a necessary update. *BMC Evolutionary Biology*. **7**, 23.

Suárez-Castillo E.C., Medina-Ortíz W.E., Roig-López J.L. and García-Arrarás J.E. (2004). Ependymin, a gene involved in regeneration and neuroplasticity in vertebrates, is overexpressed during regeneration in the echinoderm *Holothuria glaberrima*. *Gene*. **334**, 133-143.

Subramanian A., Tamayo P., Mootha V.K., Mukherjee S., Ebert B.L., Gillette M.A., Paulovich A., Pomeroy S.L., Golub T.R., Lander E.S. and Mesirov J.P. (2005). Gene set enrichment analysis: A knowledge-based approach for interpreting genome-wide expression profiles. *Proceedings of the National Academy of Sciences*. **102**, 15545-15550.

Sumimoto H. (2008). Structure, regulation and evolution of Nox-family NADPH oxidases that produce reactive oxygen species. *FEBS Journal*. **275**, 3249-3277.

Sun S.C., Ganchi P.A., Ballard D.W. and Greene W.C. (1993). NF-κB controls expression of inhibitor IκBα: Evidence for an inducible autoregulatory pathway. *Science*. **259**, 1912-1915.

Suzuki M., Saruwatari K., Kogure T., Yamamoto Y., Nishimura T., Kato T. and Nagasawa H. (2009). An acidic matrix protein, Pif, is a key macromolecule for nacre formation. *Science*. **325**, 1388-1390.

Swindle E.J., Coleman J.W., DeLeo F.R. and Metcalfe D.D. (2007). FcεRI- and Fcγ Receptor-mediated production of reactive oxygen species by mast cells is Lipoxygenase- and Cyclooxygenase-dependent and NADPH oxidase-independent. *The Journal of Immunology*. **179**, 7059-7071.

Takahashi T., McDougall C., Troscianko J., Chen W.-C., Jayaraman-Nagarajan A., Shimeld S. and Ferrier D. (2009). An EST screen from the annelid Pomatoceros lamarckii reveals patterns of gene loss and gain in animals. *BMC Evolutionary Biology*. **9**, 240.

Takeuchi O. and Akira S. (2010). Pattern recognition receptors and inflammation. *Cell*. **140**, 805-820.

Tamura K., Peterson D., Peterson N., Stecher G., Nei M. and Kumar S. (2011). MEGA5: Molecular Evolutionary Genetics Analysis using Maximum Likelihood, Evolutionary Distance, and Maximum Parsimony methods. *Molecular Biology and Evolution*. **28**, 2731-2739.

Terahara K. and Takahashi K.G. (2008). Mechanisms and immunological roles of apoptosis in molluscs. *Current Pharmaceutical Design*. **14**, 131-137.

Thelen M. (2001). Dancing to the tune of chemokines. *Nature Immunology*. **2**, 129-134.

Timmons L., Court D.L. and Fire A. (2001). Ingestion of bacterially expressed dsRNAs can produce specific and potent genetic interference in *Caenorhabditis elegans*. *Gene*. **263**, 103-112.

Timmons L. and Fire A. (1998). Specific interference by ingested dsRNA. *Nature*. **395**, 854-854.

Ting J.P., Lovering R.C., Alnemri E.S., Bertin J., Boss J.M., Davis B.K., Flavell R.A., Girardin S.E., Godzik A. and Harton J.A. (2008). The NLR gene family: a standard nomenclature. *Immunity*. **28**, 285-287.

Tiscar P. and Mosca F. (2004). Defense mechanisms in farmed marine molluscs. *Veterinary research communications*. **28**, 57-62.

Tisoncik J.R., Korth M.J., Simmons C.P., Farrar J., Martin T.R. and Katze M.G. (2012). Into the Eye of the Cytokine Storm. *Microbiology and Molecular Biology Reviews*. **76**, 16-32.

Torreilles J. and Guérin M.-C. (1999). Production of peroxynitrite by zymosan stimulation of *Mytilus galloprovincialis* haemocytes *in vitro*. *Fish & Shellfish Immunology*. **9**, 509-518.

Torres M.A., Dangl J.L. and Jones J.D.G. (2002). *Arabidopsis* gp91phox homologues *AtrbohD* and *AtrbohF* are required for accumulation of reactive oxygen intermediates in the plant defense response. *Proceedings of the National Academy of Sciences*. **99**, 517-522.

Tsoi S.C.M., Ewart K.V., Penny S., Melville K., Liebscher R.S., Brown L.L. and Douglas S.E. (2004). Identification of immune-relevant genes from Atlantic salmon using suppression subtractive hybridization. *Marine Biotechnology*. **6**, 199-214.

Tsutsui S., Nakamura O. and Watanabe T. (2007). Lamprey (*Lethenteron japonicum*) IL-17 upregulated by LPS-stimulation in the skin cells. *Immunogenetics*. **59**, 873-882.

Underhill D.M., Ozinsky A., Hajjar A.M., Stevens A., Wilson C.B., Bassetti M. and Aderem A. (1999). The Toll-like receptor 2 is recruited to macrophage phagosomes and discriminates between pathogens. *Nature*. **401**, 811-815.

Van Maele L., Carnoy C., Cayet D., Songhet P., Dumoutier L., Ferrero I., Janot L., Erard F., Bertout J., Leger H., Sebbane F., Benecke A., Renauld J.C., Hardt W.D., Ryffel B. and Sirard J.C. (2010). TLR5 signaling stimulates the innate production of IL-17 and IL-22 by $CD3^{neg}CD127^+$ immune cells in spleen and mucosa. *Journal of Immunology*. **185**, 1177-1185.

Vander Heiden M.G., Cantley L.C. and Thompson C.B. (2009). Understanding the Warburg effect: The metabolic requirements of cell proliferation. *Science*. **324**, 1029-1033.

Vega J.A., Garcia-Suarez O., Hannestad J., Perez-Perez M. and Germana A. (2003). Neurotrophins and the immune system. *Journal of anatomy*. **203**, 1-19.

Velculescu V.E., Zhang L., Zhou W., Vogelstein J., Basrai M.A., Bassett D.E., Hieter P., Vogelstein B. and Kinzler K.W. (1997). Characterization of the yeast transcriptome. *Cell*. **88**, 243-252.

Venier P., Varotto L., Rosani U., Millino C., Celegato B., Bernante F., Lanfranchi G., Novoa B., Roch P., Figueras A. and Pallavicini A. (2011). Insights into the innate immunity of the Mediterranean mussel *Mytilus galloprovincialis*. *BMC Genomics*. **12**, 69.

Vicente-Manzanares M. and Sanchez-Madrid F. (2004). Role of the cytoskeleton during leukocyte responses. *Nature Reviews Immunology*. **4**, 110-122.

Vig M. and Kinet J.-P. (2009). Calcium signaling in immune cells. *Nature Immunology*. **10**, 21-27.

Vignais P.V. (2002). The superoxide-generating NADPH oxidase: structural aspects and activation mechanism. *Cellular and Molecular Life Sciences*. **59**, 1428-1459.

Vijay-Kumar M. and Gewirtz A.T. (2009). Flagellin: key target of mucosal innate immunity. *Mucosal Immunology*. **2**, 197-205.

Wanamaker Jr A.D., Heinemeier J., Scourse J.D., Richardson C.A., Butler P.G., Eiriksson J. and Knudsen K.L. (2008). Very long-lived Mollusks confirm 17th Century AD tephra-based radiocarbon reservoir ages for North Icelandic shelf waters. *Radiocarbon*. **50**, 399-412.

Wang M., Yang J., Zhou Z., Qiu L., Wang L., Zhang H., Gao Y., Wang X., Zhang L., Zhao J. and Song L. (2011). A primitive Toll-like receptor signaling pathway in mollusk Zhikong scallop *Chlamys farreri*. *Developmental & Comparative Immunology*. **35**, 511-520.

Weaver C.T., Hatton R.D., Mangan P.R. and Harrington L.E. (2007). IL-17 family cytokines and the expanding diversity of effector T cell lineages. *Annual Reviews of Immunology*. **25**, 821-852.

Wehrle-Haller B. (2012). Structure and function of focal adhesions. *Current opinion in cell biology*. **24**, 116-124.

Weis W.I., Taylor M.E. and Drickamer K. (1998). The C-type lectin superfamily in the immune system. *Immunological Reviews*. **163**, 19-34.

Whelan S. and Goldman N. (2001). A general empirical model of protein evolution derived from multiple protein families using a Maximum-Likelihood approach. *Molecular Biology and Evolution*. **18**, 691-699.

Widdows J. and Brinsley M. (2002). Impact of biotic and abiotic processes on sediment dynamics and the consequences to the structure and functioning of the intertidal zone. *Journal of Sea Research*. **48**, 143-156.

Winston G.W., Moore M.N., Kirchin M.A. and Soverchia C. (1996). Production of reactive oxygen species by hemocytes from the marine mussel, *Mytilus edulis*: lysosomal localization and effect of xenobiotics. *Comparative Biochemistry & Physiology Part C: Pharmacology, Toxicology & Endocrinology*. **113**, 221-229.

Wong J.L., Créton R. and Wessel G.M. (2004). The oxidative burst at fertilization is dependent upon activation of the dual oxidase Udx1. *Developmental Cell*. **7**, 801-814.

Wong J.L. and Wessel G.M. (2005). Reactive oxygen species and Udx1 during early sea urchin development. *Developmental Biology*. **288**, 317-333.

Woods Hole Oceanographic Institution and United States Navy's Bureau of Ships (1952). *Marine fouling and its prevention*. Annapolis: United States Naval Institute.

Wootton E.C. and Pipe R.K. (2003). Structural and functional characterisation of the blood cells of the bivalve mollusc, *Scrobicularia plana*. *Fish & Shellfish Immunology*. **15**, 249-262.

Wu B., Jin M., Gong J., Du X. and Bai Z. (2011). Dynamic evolution of CIKS (TRAF3IP2/Act1) in metazoans. *Developmental & Comparative Immunology*. **35**, 1186-1192.

Yang C.-S., Lee J.-S., Rodgers M., Min C.-K., Lee J.-Y., Kim Hee J., Lee K.-H., Kim C.-J., Oh B., Zandi E., Yue Z., Kramnik I., Liang C. and Jung Jae U. (2012). Autophagy protein Rubicon mediates phagocytic NADPH oxidase activation in response to microbial infection or TLR stimulation. *Cell Host & Microbe*. **11**, 264-276.

Yang Z. (1998). On the best evolutionary rate for phylogenetic analysis. *Systematic Biology*. **47**, 125-133.

Yoneyama M. and Fujita T. (2012). Cytoplasmic sensing of viral double-stranded RNA and activation of innate immunity by RIG-I-like receptors. *Innate Immune Regulation and Cancer Immunotherapy*, 51-60.

Yu J. and Gaffen S.L. (2008). Interleukin-17: a novel inflammatory cytokine that bridges innate and adaptive immunity. *Frontiers in Bioscience*. **13**, 170.

Zandee D.I., Kluytmans J.H., Zurburg W. and Pieters H. (1980). Seasonal variations in biochemical composition of *Mytilus edulis* with reference to energy metabolism and gametogenesis. *Netherlands Journal of Sea Research*. **14**, 1-29.

Zänker K.S. (2001). Immunology of invertebrates: Humoral. *eLS*, John Wiley & Sons, Ltd.

Zasloff M. (2002). Antimicrobial peptides of multicellular organisms. *Nature*. **415**, 389-395.

Zelensky A.N. and Gready J.E. (2005). The C-type lectin-like domain superfamily. *FEBS Journal*. **272**, 6179-6217.

Zhang G., Fang X., Guo X., Li L., Luo R., Xu F., Yang P., Zhang L., Wang X., Qi H., Xiong Z., Que H., Xie Y., Holland P.W.H., Paps J., Zhu Y., Wu F., Chen Y., Wang J., Peng C., Meng J., Yang L., Liu J., Wen B., Zhang N., Huang Z., Zhu Q., Feng Y., Mount A., Hedgecock D., Xu Z., Liu Y., Domazet-Loso T., Du Y., Sun X., Zhang S., Liu B., Cheng P., Jiang X., Li J., Fan D., Wang W., Fu W., Wang T., Wang B., Zhang J., Peng Z., Li Y., Li N., Wang J., Chen M., He Y., Tan F., Song X., Zheng Q., Huang R., Yang H., Du X., Chen L., Yang M., Gaffney P.M., Wang S., Luo L., She Z., Ming Y., Huang W., Zhang S., Huang B., Zhang Y., Qu T., Ni P., Miao G., Wang J., Wang Q., Steinberg C.E.W., Wang H., Li N., Qian L., Zhang G., Li Y., Yang H., Liu X., Wang J., Yin Y. and Wang J. (2012). The oyster genome reveals stress adaptation and complexity of shell formation. *Nature*. **490**, 49-54.

Zhang J., Shao F., Li Y., Cui H., Chen L., Li H., Zou Y., Long C., Lan L., Chai J., Chen S., Tang X. and Zhou J.-M. (2007). A *Pseudomonas syringae* effector inactivates MAPKs to suppress PAMP-induced immunity in plants. *Cell Host & Microbe*. **1**, 175-185.

Zhang X., Luan W., Jin S. and Xiang J. (2008). A novel tumor necrosis factor ligand superfamily member (CsTL) from *Ciona savignyi*: Molecular identification and expression analysis. *Developmental & Comparative Immunology*. **32**, 1362-1373.

Zhang Y., He X. and Yu Z. (2011). Two homologues of inhibitor of NF-κB (IκB) are involved in the immune defense of the Pacific oyster, *Crassostrea gigas*. *Fish & Shellfish Immunology*. **30**, 1354-1361.

# 8. MATERIALS

## 8.1 Aquaria equipment

| | |
|---|---|
| Air pumps | SCHEGO ideal, REBIE Germany |
| Air stones | Hobby, REBIE |
| Heating elements | JBL ProTemp 150 Watt, REBIE |
| Maintenance tanks (Stack and nest bins (60x40x35 cm)) | Transoplast |
| Plastic aquaria (6 l) | SAVIC, REBIE, Germanx |
| Water and air tubing | SAVIC, REBIE |

## 8.2 Chemicals

| | |
|---|---|
| 2-Mercaptoethanol | Merck |
| Agarose SeaKem LE | Biozym |
| Ammonium nitrate ($NH_4NO_3$) | Sigma-Aldrich |
| Ampicillin | Sigma-Aldrich |
| Amplex Red reagent | Invitrogen |
| Artificial sea salt | Preis, REBIE |
| Biotin | Sigma-Aldrich |
| Boric acid ($H_3BO_3$) | Sigma-Aldrich |
| Bromophenol blue | Sigma-Aldrich |
| Carboxylated latex beads (1 µm) | Polysciences |
| Chloroform ($CHCl_3$) | Sigma-Aldrich |
| Cobalt sulphate, heptahydrate ($CoSO_4\,7H_2O$) | Merck |
| DCFH-DA (2', 7'-dichlorfluorescein-diacetate) | Sigma-Aldrich |
| DEPC | Sigma-Aldrich |
| Dimethylformamid (DMF) | Sigma-Aldrich |
| Dimethylsulfoxid (DMSO) | Sigma-Aldrich |
| Ferrous ammonium sulphate, hexahydrate ($Fe(NH_4)_2(SO_4)_2\,6H_2O$) | Merck |
| Glycerol | Roth |
| HEPES | Sigma-Aldrich |
| Horse radish peroxidase, Type II | Sigma-Aldrich |
| Hydrochloric acid (HCl) | Roth |
| Hydrogen peroxide ($H_2O_2$) | Sigma-Aldrich |
| Iron chloride, heptahydrate ($FeCl_3\,6H_2O$) | Merck |

| | |
|---|---|
| Isopropanol ($C_3H_8O$) | Merck |
| Manganese sulphate, monohydrate ($MnSO_4\ H_2O$) | Merck |
| Meat extract | Sigma-Aldrich |
| Peptone | Sigma-Aldrich |
| Phenol/Chloroform/Isoamyl alcohol ($C_6H_6O/CHCl_3/C_5H_{12}O$) | Sigma-Aldrich |
| Quant-iT PicoGreen dsDNA reagent | Invitrogen |
| Potassium dihydrogen phosphate ($KH_2PO_4$) | Merck |
| RLT buffer (RNeasy Lysis Buffer) | Quiagen |
| RNase-free water | Qiagen |
| Sodium chloride (NaCl) | Merck |
| SYBR safe | Invitrogen |
| TAE buffer Rotiphorese, 10x | Roth |
| Thiamine | Sigma-Aldrich |
| Titriplex III ($Na_2EDTA$) | Sigma-Aldrich |
| TRI reagent | Sigma-Aldrich |
| TRIS | Merck |
| Tryptone | Becton Dickson |
| Vitamin $B_{12}$ | Merck |
| X-gal (5-Brom-4-chlor-3-indolyl-β-D-galactopyranosid) | Roth |
| Xylene cyanol | Sigma-Aldrich |
| Yeast extract | Becton Dickson |
| Zinc sulphate, heptahydrate ($ZnSO_4\ 7H_2O$) | Sigma-Aldrich |

## 8.3   Media and Buffers

| | |
|---|---|
| Medium 101 | 5 g peptone, 3 g meat extract *ad.* 1 l distilled water, autoclave |
| Provasolis medium | 1. Fe-solution: 315 mg of $Fe(NH_4)_2(SO_4)_2\ 6H_2O$, 300 mg of $Na_2EDTA$ (Titriplex III) *ad.* 500 ml distilled water |
| | 2. Metal solution: 500 mg $Na_2EDTA$ (Titriplex III), 570 mg $H_3BO_3$, 24.5 g $FeCl_3\ 6H_2O$, 82 mg $MnSO_4\ H_2O$, 11 mg $ZnSO_4\ 7H_2O$, 2.4 g $CoSO_4\ 7H_2O$, *ad.* 1 l distilled water |
| | 3. Vitamin solution: 0.2 mg vitamin $B_{12}$, 10 mg thiamine, 0.1 mg biotin, 5 g TRIS, *ad.* 1 l distilled water |
| | Mix solutions and adjust to pH 7.8, *ad.* 3 l, autoclave and store in aliquots at 10°C. |
| LB-medium | 10 g NaCl, 10 g tryptone, 5 g yeast extract, *ad.* 1 l distilled water, autoclave |

| | |
|---|---|
| LB-agar plates w/ ampicillin | 10 g NaCl, 10 g tryptone, 5 g yeast extract, 15 g agar, *ad.* 1 l distilled water, autoclave, add 100 mg ampicillin |
| 1x TAE buffer | 10x TAE buffer diluted 1:10 in distilled water |
| DNA-loading-buffer | 50 % (v/v) glycerol, 50 % (v/v) distilled water, 0.025 % (w/v) bromophenol blue (for DNA fragments <100 bp) or xylene cyanol (>100 bp), pH 8.0 |
| S.O.C. medium | Invitrogen |
| DPBS | PAA, GE Healthcare |

## 8.4 Stimulants and Inhibitors

| Substance | Supplier | Catalogue # | Lot # | Stock solution | Final concentration |
|---|---|---|---|---|---|
| Flagellin | Enzo Life Science | ALX-522-058 | L25312 | 100 µg ml$^{-1}$ | 2.5 µg ml$^{-1}$ |
| Zymosan | Sigma-Aldrich | Z4250 | 1421649 | 1 mg ml$^{-1}$ | 25, 50 or 100 µg ml$^{-1}$ |
| LPS | Sigma-Aldrich | L3024 | 089K4074 | 1 mg ml$^{-1}$ | 50 µg ml$^{-1}$ |
| PMA | Sigma-Aldrich | 79346 | BCBG3079V | 1 mg ml$^{-1}$ | 10 µg ml$^{-1}$ |
| DPI | Sigma-Aldrich | D2926 | 046K4021 | 150 µM | 10 µM |
| BAPTA/AM | Calbiochem | 196419 | D00104065 | 13 mM | 1 mM |

## 8.5 Oligonucleotides

Oligonucleotides (Primers), supplied by Microsynth, were designed using Primer3 v.0.4.0 (http://frodo.wi.mit.edu/) and checked for annealing temperatures ($T_{anneal}$), hairpin structures, self and cross dimers via NetPrimer (http://www.premierbiosoft.com/netprimer/).

### 8.5.1 RACE-PCR oligonucleotides

Gene-specific oligonucleotides were designed according to the following criteria:
- 23–28 nt long
- 50–70% GC content
- $T_{anneal} \geq 65°C$
- no or only small possibility of cross dimers with the universal primer mix (UPM) or nested primer

  (NSP) supplied by Clontech (see section 2.5 for further detail)

*Me = Mytilus edulis*; *Le = Laternula elliptica*; *Ai = Arctica islandica*; N = A, C, G, or T; V = A, G, or C.

| Name/Gene | Step | Sequence (5'→3') | T$_{anneal}$ (°C) | t$_{elong}$ (min) |
|---|---|---|---|---|
| **General RACE oligonucleotides provided by Clontech** | | | | |
| SMART II™ Oligonucleotide | 5' RACE - ready cDNA generation | AAGCAGTGGTATCAACGCAGAGTACGCGGG | 70.0 | 90.0 |
| 5'-RACE CDS Primer A | 5' RACE - ready cDNA generation | (T)25V N | 70.0 | 90.0 |
| 3' SMART™ CDS Primer II A | 3' RACE - ready cDNA generation | AAGCAGTGGTATCAACGCAGAGTACT(30)VN | 70.0 | 90.0 |
| Universal Primer Mix (UPM) | 3' and 5' RACE-PCR | CTAATACGACTCACTATAGCAAGCAGTGGTATCAACG CAGAGT & CTAATACGACTCACTATAGC | see gene-specific oligonucleotides | |
| Nested Primer (NSP) | 3' and 5' RACE-PCR | AAGCAGTGGTATCAACGCAGAGT | see gene-specific oligonucleotides | |
| **Gene-specific oligonucleotides** | | | | |
| *Me* DUOX-a | 5' RACE-PCR | CTGACAAATGGCATGGCGAACACA | 72.0 | 5.0 |
| *Me* DUOX-a | 5' nested PCR | AGTAGTGGAAAGATGCAAGCACGTCTGT | 67.0 | 5.0 |
| *Me* DUOX-a | 3' RACE-PCR | GGCGGCAAAGACACATTTTGGACGAC | 72.0 | 5.0 |
| *Me* DUOX-a | 3' nested PCR | AGCTGTGGTCCTCCACCAATGAC | 67.0 | 5.0 |
| *Me* DUOX-b | 3' RACE-PCR | CCCCTCCCCTGAATAGGACCAGA | 68.0 | 5.0 |
| *Me* DUOX-b | 3' nested PCR | TACCCCCATTACGACCATCATCCTTG | 69.0 | 5.0 |
| *Me* DUOXA | 5' RACE-PCR | CGGCGGTGATCTCAAAACATCCTGAC | 72.0 | 5.0 |
| *Me* DUOXA | 5' nested PCR | CGTCTCCTCGGTGCCTGTAGTCC | 68.0 | 5.0 |
| *Me* DUOXA | 3' RACE-PCR | TGGAGATGGGAACAAGGCAGATTTGG | 72.0 | 5.0 |
| *Me* DUOXA | 3' nested PCR | CCGTGAGTACAGAGAAGCACAGTTCC | 68.0 | 5.0 |

## 8.5.2   qRT-PCR oligonucleotides

Oligonucleotides annealed at 60°C. ENA accession numbers are stated, if available.
*Me = Mytilus edulis*, *Le = Laternula elliptica*, *Ai = Arctica islandica*.
If the efficiency was not assessed (n/a), a theoretical efficiency of 2 was used.

| Target transcript (Accession number) | Orientation | Sequence (5'→3') | Amplicon length (bp) | Efficiency |
|---|---|---|---|---|
| *Reference genes* | | | | |
| *Me* 18S rRNA | sense antisense | TCAACACGGGAAAACTCACC GCTCACTAAAACGCCCAATC | 468 | 2.0 |
| *Me* 28S rRNA | sense antisense | AAGCGGAGGAAAAGAAACTAAC TTTACCTCTAAGCGGTTTCAC | 376 | 2.4 |

| | | | | |
|---|---|---|---|---|
| *Me* GAPDH | sense<br>antisense | CATCAAAAATGCTGCTCCTG<br>GCAATGACCGCTACACAAAA | 352 | 2.0 |
| *Me* RPS18 | sense<br>antisense | CGTCTTCCTGTGGTCTTTGTT<br>CTGCCATCAAGGGTATTGG | 338 | n/a |
| *Me* EI-1-alpha | sense<br>antisense | TGTCGGAGTCAACAAGATGG<br>TGGAGTGGGAGACGGAGA | 306 | n/a |
| *Le* 18S rRNA | sense<br>antisense | CACCACCAACCACCGA<br>AAGACGAACGACAGCGAAAG | 352 | 2.2 |
| *Le* β-Actin | sense<br>antisense | GCCAAATCCAGACGAAGG<br>TGAAGCCCAGAGTAAGAGAGG | 375 | 2.1 |
| *Ai* 18S rRNA | sense<br>antisense | TGGTGCTCTTGACTGAGTGTCTCG<br>GGCAAATGCTTTCGCTGTAGTTC | 247 | 1.9 |
| *Ai* GAPDH | sense<br>antisense | CGTCTGCCTTTGTGTATTTTTC<br>CCGTATTGGTCGTCTGGTG | 398 | 1.7 |

### General putative immune-relevant transcripts

| | | | | |
|---|---|---|---|---|
| *Me*1 TLR<br>(HE609238) | sense<br>antisense | TTGTCGTCATAATGTCTCCAAAC<br>CCCAGAAAACTGTGTCTCCA | 228 | 1.7 |
| *Me*2 TLR<br>(HE609227) | sense<br>antisense | TGGGTTTGTGTGTCTCTCGT<br>TTGGCATTTGTGAAGGAGAA | 277 | 1.6 |
| *Me*3 TLR<br>(HE609225) | sense<br>antisense | CCCGAGGAGAACAAAATGTATG<br>CTGGCAAAGCAAACTCTAACTT | 421 | 1.9 |
| *Me*4 TLR<br>(HE609242) | sense<br>antisense | AAATCCGCCCAACCTTAGTG<br>TCAAGCCATCCTTTCATCCAT | 462 | 1.6 |
| *Me*1 LBP/BPI<br>(HE609065) | sense<br>antisense | ATTGTGTTTGTGTGCCTGGT<br>GAGGTGGTTTGGCTTGGATA | 380 | 1.5 |
| *Me*2 LBP/BPI<br>(HE609068) | sense<br>antisense | CGGTTCAGTTTTCAGGGATG<br>TCTTGCTGTCTGTGATTGGTG | 435 | 1.9 |
| *Me* C-type lectin | sense<br>antisense | TCGCCGTAGTTCTTGCTCGT<br>TGCTTGTCACTGGCTTTCTGG | 401 | 1.7 |
| *Me*1 C3a receptor | sense<br>antisense | AAGTCGTTTTTGGCGTTGTAGG<br>ATGGACGGTGGGCGTGTAA | 401 | 1.5 |
| *Me2* C3a receptor | sense<br>antisense | CTGCGTCTTGTTGATTTTTGGA<br>CAGCGGTTATAGGACAGATGTGA | 450 | 2.2 |
| *Me1* IκBα<br>(HE609059) | sense<br>antisense | GAGACACACCCTTACACATCG<br>TCCCACATTTACCATCCTTGA | 258 | 2.3 |
| *Me2* IκBα<br>(HE609060) | sense<br>antisense | GCCGCAATAAAACTGAAACC<br>GGAAAAGACGAGGATGGTGA | 292 | 2.4 |

| | | | | |
|---|---|---|---|---|
| *Me2* LITAF (HE609139) | sense antisense | GCCAACATCCAACAATACACAAA CCCACCACCACCCTATCCA | 380 | 1.6 |
| *Me3* NF-κB p50 | sense antisense | CCACCTTGTTCTCAGCCATCA CTCAGCCACCATTCTTCTTGC | 393 | 1.6 |
| *Me1* TIMP | sense antisense | GCTCTCACCTACATCATCCGAAA TCTAACTCTCCAACCCCGCTAC | 393 | 1.6 |
| *Me2* TIMP | sense antisense | AGTGGATGTCGGTGCTTTGC ATCGTTCCTGTTGTGTTACTCCTG | 273 | 1.6 |
| *Me1* Ependymin | sense antisense | ACTTGAGGGACAGATTGGGATG GCTCGCCATTATTTTATCAGAAGG | 292 | 1.5 |
| *Me2* Ependymin | sense antisense | ACTTGGAGATGGTGTATTGACTGTG ACTTGGTTCCGTTGCCTTGT | 203 | 1.6 |
| *Me* OAS | sense antisense | CGTCTCATACATCAACACCCAAT CGGCAGAAAGTCTACATCAAACC | 311 | n/a |
| *Me* RIG1 | sense antisense | CTGAACAGCAGGCAGAGAGATG CACCTACAGATGCAGTCAAACCAA | 342 | n/a |

**Antimicrobial/Antifungal peptides**

| | | | | |
|---|---|---|---|---|
| *Me1* Defensin (HE609174) | sense antisense | CATCATTTATCTACTGTGTGCGTCTG TCCATTCACCCTTAGCAACCA | 297 | 1.6 |
| *Me1* Myticin A | sense antisense | CCTTTGCTTTCATTCTCACTGC TTGGGCGAAATGTCTCTTGTT | 215 | 1.5 |
| *Me1* Myticin C (HE609163) | sense antisense | GCATAACAAGTGAGGGAAAACA TGAACGACAAGAACAACGAGA | 328 | 2.2 |
| *Me1* Mytilin C (HE609176) | sense antisense | TATCCTAGCCATCGCCCTTG CCTTGTTCGGTTTCTCCTTTC | 270 | 2.2 |
| *Me1* Mytilin D (HE609180) | sense antisense | GGGGACATCCTGCTGACTTG TCGTCTTCCAAAACTGGCTGA | 210 | 1.5 |
| *Me1* Mytimycin (HE610032) | sense antisense | TCGTTGTGTTGTCTGTTATGTCC CGCTTTTGTTTGTTGTTTGTT | 358 | 2.0 |

**DUOX and NOX**

| | | | | |
|---|---|---|---|---|
| *Me* NOX2 | sense antisense | TCGGGAAGTAGGAGAAATCG GCAAACAGGAAGTAAAATAAGCAT | 339 | 2.2 |
| *Me* NOX5 | sense antisense | TTTTCTCCTTGAACCTACAGCA CCTGCAATAGCTGAACACGA | 228 | 1.9 |
| *Me* DUOX-a | sense antisense | TTGAAGTAAAACAGGCAGAAC GCCACCACCAACTAATACA | 344 | 2.1 |

| | | | | |
|---|---|---|---|---|
| *Me* DUOX-b | sense<br>antisense | TTCTTGGATTTCTTTGTTGTTTTG<br>CGTATGAGCGTATTCTTTTGAGG | 279 | 2.0 |
| *Me* DUOXA | sense<br>antisense | TGATGTGGTTGGCTCTTCC<br>CGCTCTTTGGTGTGCTTGT | 397 | 2.1 |
| *Me* p22phox | sense<br>antisense | CTTGGAGTGGCTGGATTTTT<br>GAGGGGGCATCTTTGGTT | 370 | 2.2 |
| *Le* DUOX-a | sense<br>antisense | AGCAAGCACCGAGAAAGAAA<br>GCGAACCTCAAAACCAAATC | 265 | 1.8 |
| *Le* DUOX-b | sense<br>antisense | ACCAATCTACGGCGGGTCT<br>TCGTGTCTTTACTCTCCACATCTC | 302 | 1.8 |
| *Le* DUOX-c | sense<br>antisense | CAGGACACAACCAGAGAAACTACAAA<br>GATAAGACCAAAGGAAGCCCAAA | 450 | 2.1 |
| *Ai* DUOX-a | sense<br>antisense | AAGTCGGCGTATTCAGTTGTG<br>GCTTTGGCTTCCGTTAGTTG | 361 | 1.7 |
| *Ai* DUOX-b | sense<br>antisense | GAGGTGTCCGTTTTGATTGG<br>CTTGCCCGCTATCTTCTGG | 305 | 1.7 |
| **IL-17** | | | | |
| *Me1* IL17 | sense<br>antisense | AGTCAATGAAACAGGGTTGTATTTGT<br>AGGTTCTCTCCTGCTGTTTATGAAT | 337 | 1.9 |
| *Me2* IL17 | sense<br>antisense | GACGGCTGGAAACAAGACACA<br>GCAGGGGTTATTGGAACATCA | 395 | 1.8 |
| *Le1* IL17 | sense<br>antisense | GGTAGAAAATGAGGACAACCACAGA<br>CACCCGATCAATCACCGACT | 368 | 2.3 |
| *Le2* IL17 | sense<br>antisense | GCATTGTGGGAATGTTTCAGAG<br>ATAGATCGACTTGTCCGTGGTTT | 377 | 2.2 |
| *Ai* IL17 | sense<br>antisense | TTCCACCTGTCCTTGGCATT<br>GACAGTTATTCTCTCCATTGTTTTCC | 226 | 2.1 |

### 8.5.3   Oligonucleotides for Sanger DNA sequencing

| Name | Sequence (5'→3') | Supplier |
|---|---|---|
| M13 forward | GTAAAACGACGGCCAG | Metabion |
| M13 reverse | CAGGAAACAGCTATGAC | Metabion |

## 8.6 DNA Ladders
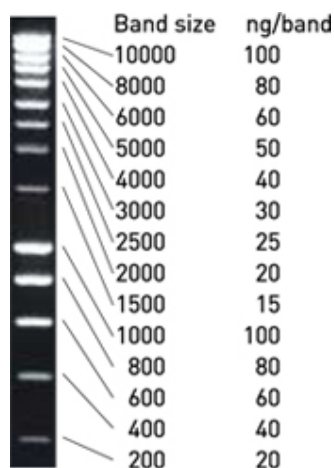


1kb SmartLadder, Eurogentec
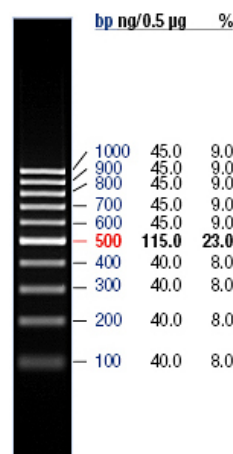


GeneRuler 100 bp DNA Ladder, Fermentas

## 8.7 Kits

| | |
|---|---|
| Advantage 2 PCR Kit | Clontech |
| Advantage RT-for-PCR Kit | Clontech |
| BigDye Terminator v1.1.Cycle Sequencing Kit | Applied Biosystems |
| DNA 1000 LabChip Kit | Agilent |
| GeneJet Plasmid Miniprep Kit | Fermentas |
| GS FLX Titanium SV emPCR Kit (Lib-L) | Roche |
| MEGAscript High Yield Transcription Kit | Applied Biosystems |
| $NH_4$-Ammonium-Test-Set | JBL |
| $NO_2$-Nitrite-Test-Set | JBL |
| Oligotex mRNA Mini Kit | Qiagen |
| Power SYBR Green PCR Master Mix | Applied Biosystems |
| Premium First Strand cDNA Synthesis Kit | Fermentas |
| QIAquick PCR Purification Kit | Qiagen |
| QIAshredder | Qiagen |
| Rapid Library Preparation Kit | Roche |
| RNA 6000 Nano LabChip Kit | Agilent |
| RNase-free DNase Set | Qiagen |
| RNeasy Kit | Qiagen |
| SMARTer cDNA Synthesis Kit | Clontech |
| SMARTer RACE Kit | Clontech |
| TA Cloning Kit including the pCR2.1-TOPO vector | Invitrogen |
| TOP10 chemically competent *E. coli* | Invitrogen |
| Wizard SV Gel and PCR Clean-Up system | Promega |

## 8.8 Devices

### 8.8.1 Incubators

| | |
|---|---|
| Incubator used for *M. edulis*: | MIR-154, Sanyo Biomedical |
| Incubator used for *L. anguillarum*: | Shaking incubator 3033, GFL |
| Incubator used for *E. coli* on agar plates: | Incucell 111, MMM Group |
| Incubator used for *E. coli* in media: | Orbital Incubator SI50,Stuart Scientific |

### 8.8.2 Centrifuges

| | |
|---|---|
| Centrifuge for Eppendorf tubes at RT: | Centrifuge 5415D, Eppendorf |
| Centrifuge for Eppendorf tubes below RT: | Sigma 3K30, Braun Biotech International |
| Centrifuge for Falcon tubes: | Varifuge 3.0R Heraeus |

### 8.8.3 Thermocycler and Sequencer

| | |
|---|---|
| Gene Amp, PCR System 9700 | Applied Biosystems |
| Veriti, 96 Well Fast Thermal Cycler | Applied Biosystems |
| Veriti, 96 Well Cycler | Applied Biosystems |
| 2720 Thermal Cycler | Applied Biosystems |
| 7900HT Fast Real-Time PCR System | Applied Biosystems |
| SpeedVac, centrifugal vacuum concentrator | Thermo Scientific |
| ABI PRISM 3700 Genetic Analyzer | Applied Biosystems |
| GS FLX | Roche |

### 8.8.4 Electrophoresis devices and power supplies

| | |
|---|---|
| Gel caster, trays and combs | Bio-Rad |
| Wide Mini-Sub Cell GT, horizontal gel chamber | Bio-Rad |
| Mini-Sub Cell GT, horizontal gel chamber | Bio-Rad |
| Power Pac 300 | Bio-Rad |
| ChemiDoc XRS | Bio-Rad |

### 8.8.5 Microscopes

| | |
|---|---|
| TCS SP5, confocal microscope | Leica |
| Inverted Microscope Willovert H500 | Helmut Hund GmbH |
| EVOS fl, inverted fluorescence microscope | PeqLab |

### 8.8.6 Other devices

| | |
|---|---|
| BioAnalyzer 2100 | Agilent |
| Certomat MV, vortex mixer | B. Braun Biotech Internat. |
| Concentrator 5301 | Eppendorf |
| Electronic pipet filler | Eppendorf |
| Electronic pipette | Proline, Biohit |
| Eppendorf Research®, adjustable-volume pipette | Eppendorf |
| GeniosPro Plate reader | Tecan |
| NanoDrop ND-1000 spectrophotometer | Thermo Scientific |
| NanoDrop ND-3300 fluorospectrometer | Thermo Scientific |
| Cellometer Auto T4 | Nexcelom |
| Osmomat 030 | Gonotec |
| PH/COND Instrument 340i Set with SenTix P41-3 and TetraCon C325-3 | WTW, VWR |
| Thermomixer compact 5350 | Eppendorf |
| Water purification system „Ultra Clear UV plus TM", (ISO 3696) | SG |

### 8.9 Consumables

| | |
|---|---|
| 26G needles | Sterican, Braun |
| 0.5 ml, 1.5 ml and 2 ml micro tubes | Sarstedt |
| 1 ml syringes, BD Plastipak | Becton Dickson |
| 100 ml culture flasks | Duran, Schott |
| 15 ml and 50 ml tubes | Sarstedt |
| 5 l Erlenmeyer flasks | Duran, Schott |
| Black 96-well plates | Becton Dickson |
| MicroAmp Optical 384-Well Reaction Plates | Applied Biosystems |
| Nitratex nitrile gloves | Ansell |
| Paper towels | Satino Comfort |
| Peha-soft nitrile gloves | Hartmann |
| Pipette tips and filter tips | Sarstedt |

| | |
|---|---|
| Pipette tips for electronic pipette | Biohit |
| Rotilabo 0.22 µm syringe filter | Roth |
| Serological pipettes | Sarstedt |
| Surgical disposable scalpels | Braun |
| Tissue culture dishes 96-, 24- and 12-well | Sarstedt |

## 8.10 Software and Tools

| | |
|---|---|
| 454 Sequencing Data Analysis software | Roche |
| AMOScmp | AMOS consortium (Open source) |
| Grubb's outlier detection test | http://graphpad.com/quickcalcs/Grubbs1.cfm |
| GS De novo Assembler 2.3/NEWBLER | Roche |
| Image J | National Institutes of Health (Open source) |
| Microsoft Excel 2007 | Microsoft |
| MEGA 5.05 | http://www.megasoftware.net/mega.php (Open source) |
| NetPrimer | PREMIER, Biosoft (Open source) |
| ORF Finder | NCBI (http://www.ncbi.nlm.nih.gov/projects/gorf/) |
| Primer3 | http://frodo.wi.mit.edu/ |
| Prism 5.03 | Graph Pad software Inc. |
| Quantity One 4.6.8. | Bio-Rad |
| SeqClean | TGI (Open source) |
| Sequencher version 4.5 | GeneCodes |
| T-ACE | ICMB, CAU-Kiel (http://www.ikmb.uni-kiel.de/tace/) |
| TGICL/CAP3 | TGI (Open source) |

## 8.11 Databases

| | |
|---|---|
| DBGET, KEGG | http://www.genome.jp/dbget/ |
| ENA | http://www.ebi.ac.uk/ena/ |
| InterPro | http://www.ebi.ac.uk/interpro/ |
| JGI Database | http://genome.jgi-psf.org/ |
| KEGG | http://www.genome.jp/kegg/ |
| Mollusc DB, Mark Blaxter | http://www.nematodes.org/NeglectedGenomes/MOLLUSCA/ |
| MytiBase | http://mussel.cribi.unipd.it/?p=search |
| NCBI nt database | http://www.ncbi.nlm.nih.gov |
| SMART domain database | http://smart.embl-heidelberg.de/ |
| UniProt Knowledgebase (UniProt/Swiss-Prot) | http://www.uniprot.org |

The nucleotide sequence of each contig can be found on the CD under "**File_1_Hemocyte transcriptome contigs.fasta**".

**Table S 1: Hemocyte transcriptome contigs selected for qRT-PCR analysis.** Hemocytes dataset reads in comparison to reads from other tissue datasets are denoted. Furthermore, sequence length (in bp) and ORF length (in amino acids (aa)) of each ortholog are depicted. The protein length (aa), Id. (Identity in %), score, E value and accession number of the best BLASTp hit in UniProt/Swiss-Prot are shown.

| Ortholog | Reads Hemocytes | Reads Other tissues | Length (bp) | ORF (aa) | Protein (aa) | Id. (%) | Score | E value | UniProt/Swiss-Prot (BLASTp) Organism | Accession Number |
|---|---|---|---|---|---|---|---|---|---|---|
| *Me1* TLR | 6 | 14 | 1687 | 527 | 991 | 26 | 348 | $10^{-31}$ | *Mus musculus* | Q6R5N8 |
| *Me2* TLR | 1 | 10 | 1000 | 326 | 785 | 28 | 324 | $10^{-30}$ | *Canis familiaris* | Q689D1 |
| *Me3* TLR | 106 | 30 | 3744 | 964 | 1198* | 33* | 1408* | $10^{-174*}$ | *Chlamys farreri** | A2SVB4* |
| *Me4* TLR | 111 | 75 | 2477 | 479 | 1097 | 23 | 255 | $10^{-20}$ | *Drosophila melanogaster* | P08953 |
| *Me1* LBP/BPI | 47 | 53 | 1798 | 494 | 481 | 26 | 492 | $10^{-53}$ | *Homo sapiens* | P18428 |
| *Me1* C-type lectin | 248 | 17 | 1373 | 194 | 156 | 29 | 156 | $10^{-10}$ | *Mytilus galloprovincialis* | P86854 |
| *Me1* C3a-receptor | 87 | 2 | 1812 | 344 | 361 | 24 | 209 | $10^{-15}$ | *Danio rerio* | P0C7U4 |
| *Me2* C3a-receptor | 32 | 2 | 1829 | 334 | 361 | 26 | 243 | $10^{-20}$ | *Danio rerio* | P0C7U4 |
| *Me1* IκB | 58 | 108 | 1840 | 355 | 482 | 35 | 377 | $10^{-38}$ | *Drosophila melanogaster* | Q03017-2 |
| *Me2* IκB | 245 | 294 | 1663 | 392 | 318 | 39 | 360 | $10^{-36}$ | *Gallus gallus* | Q91974 |
| *Me2* LITAF | 32 | 81 | 2565 | 161 | 181 | 42 | 327 | $10^{-36}$ | *Dictyostelium discoideum* | Q54HX8 |
| *Me3* NF-κB p50 | 56 | 134 | 4622 | 767 | 983 | 28 | 157 | $10^{-9}$ | *Gallus gallus* | Q04861-3 |
| *Me1* TIMP | 685 | 183 | 1707 | 221 | 214 | 26 | 204 | $10^{-18}$ | *Scyliorhinus torazame* | Q9W6B4 |
| *Me2* TIMP | 158 | 14 | 801 | 153 | 207 | 26 | 111 | $10^{-6}$ | *Bos taurus* | P20414 |
| *Me1* Ependymin | 2119 | 221 | 2079 | 212 | 236 | 29 | 95 | $10^{-3}$ | *Bos taurus* | A6QLI0 |
| *Me2* Ependymin | 1218 | 57 | 938 | 192 | 200 | 25 | 162 | $10^{-11}$ | *Haliotis asinina* | P86734 |
| *Me1* Defensin | 833 | 55 | 962 | 61 | 38 | 50 | 109 | $10^{-7}$ | *Crassostrea virginica* | P85008 |
| *Me1* Myticin A | 350 | 21 | 436 | 50 | 96 | 89 | 272 | $10^{-33}$ | *Mytilus galloprovincialis* | P82103 |
| *Me1* Mytilin D | 106 | 168 | 494 | 97 | 97* | 90* | 473* | $10^{-60*}$ | *Mytilus galloprovincialis** | B3VT96* |

*no Swiss-Prot hit

## 9.2 Contigs involved in pathway analysis

Information about contigs comprising KEGG terms used for pathway analysis as shown in Figure 3-1 and Figure 3-2 can be found on CD. For Excel file see "**File_2_Contigs involved in pathway analysis.xls**". For interactive T-ACE RunCompare files see "**File_3_Pathway analysis_HemoTissue.rc**" and "**File_4_Pathway_analysis_UpDown.rc**".

## 9.3 Filtering of immune-relevant contigs

Screening for putative immune-relevant contigs for hemocyte transcriptome dataset analysis according to section 2.11.2 and Figure 2-1 is depicted on CD in "**File_5_Filtering of immune-relevant contigs.xls**".

## 9.4 Identified NOX and DUOX sequences and domains

The nucleotide and amino acid sequence of each contig as well as the corresponding domain structure of the SMART domain architecture search can be found in detail on the CD under "**File_6_NOX and DUOX sequences and domains.pdf**".

## 9.5 Phylogenetic analysis of NOX and DUOX orthologs

**Table S 2. Sequences used for phylogenetic tree analysis.** Protein sequences involved in phylogenetic tree construction are depicted by their corresponding accession numbers in their respective database, as well as UniProt accession numbers if available.

| Organism | Accession number (database see left) | UniProt accession number | Swiss-Prot hit? | Database |
|---|---|---|---|---|
| **DUOX orthologs** | | | | |
| *Dictyostelium discoideum(NOX C)* | | Q54F44.1 | Yes | NCBI |
| *Dictyostelium purpureum(NOX C)* | EGC28364.1 | | No | NCBI |
| *Arabidopsis thaliana (RBOHD)* | | Q9FIJ0.1 | Yes | NCBI |
| *Oryza sativa (RbohB)* | | Q6J2K5.1 | Yes | NCBI |
| *Nicotiana tabacum (RbohD)* | ABN58915.1 | Q8LRN5 | No | NCBI |
| *Hydra magnipapillata (DUOX-like)* | XP_002157441.1 | | No | NCBI |
| *Lottia gigantea (DUOX a)* | 71226 | | No | JGI |
| *Lottia gigantea (DUOX b)* | 112284 | | No | JGI |
| *Lottia gigantea (DUOX c)* | 71249 | | No | JGI |
| *Arctica islandica (DUOX a)* | *Ai* DUOX-a | | No | ICMB |
| *Arctica islandica (DUOX b)* | *Ai* DUOX-b | | No | ICMB |
| *Laternula elliptica (DUOX a)* | *Le*DUOX-a | | No | ICMB |
| *Laternula elliptica (DUOX b Fragment)* | *Le*DUOX-b | | No | ICMB |
| *Laternula elliptica (DUOX c Fragment)* | *Le*DUOX-c | | No | ICMB |

| | | | | |
|---|---|---|---|---|
| *Mytilus edulis (DUOX a)* | *Me* DUOX-a | | No | ICMB |
| *Mytilus edulis (DUOX b)* | *Me* DUOX-b | | No | ICMB |
| *Capitella teleta (DUOX)* | 191097 | | No | JGI |
| *Caenorhabditis elegans (DUOX)* | | O61213.2 | Yes | NCBI |
| *Brugia malayi (DUOX)* | EDP30805.1 | A8Q7P3 | No | NCBI |
| *Meloidogyne incognita (DUOX)* | AAY84711.2 | Q4JJA9 | No | NCBI |
| *Drosophila melanogaster (DUOX)* | NP_608715.2 | Q9VQH2 | Yes | NCBI |
| *Camponotus floridanus(DUOX)* | EFN74201.1 | E1ZXB1 | No | NCBI |
| *Tribolium castaneum (DUOX)* | XP_970848.2 | | No | NCBI |
| *Daphnia pulex (DUOX )* | EFX69361.1 | E9HFQ7 | No | NCBI |
| *Ixodes scapularis (DUOX)* | EEC10543.1 | B7PVC0 | No | NCBI |
| *Lytechinus variegatus(DUOX)* | AAU95793.1 | Q5XMJ0 | No | NCBI |
| *Strongylocentrotus purpuratus (DUOX a)* | NP_001118237.1 | | No | NCBI |
| *Strongylocentrotus purpuratus (DUOX b)* | XP_001176563.1 | | No | NCBI |
| *Branchiostoma floridae (DUOX a)* | EEN51030.1 | C3Z8T1 | No | NCBI |
| *Branchiostoma floridae (DUOX b)* | EEN62449.1 | C3YBU2 | No | NCBI |
| *Ciona intestinalis (DUOX-A)* | FAA00328.1 | A7E3J9 | No | NCBI |
| *Ciona intestinalis (DUOX-B)* | FAA00329.1 | A7E3K0 | No | NCBI |
| *Ciona intestinalis (DUOX-C)* | FAA00330.1 | A7E3K1 | No | NCBI |
| *Ciona intestinalis (DUOX-D)* | FAA00331.1 | A7E3K2 | No | NCBI |
| *Ciona savignyi (DUOX)* | SINCSAVP00000010931 | | No | Ensembl |
| *Danio rerio (DUOX)* | BAF33370.1 | Q08JS2 | No | NCBI |
| *Takifugu rubripes (DUOX)* | FAA00350.1 | A7E3M1 | No | NCBI |
| *Tetraodon nigroviridis (DUOX)* | FAA00349.1 | A7E3M0 | No | NCBI |
| *Xenopus tropicalis(DUOX1)* | XP_002937936.1 | | No | NCBI |
| *Xenopus tropicalis(DUOX2)* | XP_002937935.1 | | No | NCBI |
| *Anolis carolinensis (DUOX2)* | XP_003227541.1 | | No | NCBI |
| *Gallus gallus (DUOX2)* | XP_425053.2 | | No | NCBI |
| *Meleagris gallopavo (DUOX2)* | XP_003209351.1 | | No | NCBI |
| *Taeniopygia guttata(DUOX2)* | XP_002193556.1 | | No | NCBI |
| *Ornithorhynchus anatinus (DUOX2)* | XP_001518643.1 | | No | NCBI |
| *Monodelphis domestica (DUOX1)* | XP_001367209.1 | | No | NCBI |
| *Homo sapiens (DUOX1)* | | Q9NRD9.1 | Yes | NCBI |
| *Homo sapiens (DUOX2)* | | Q9NRD8.2 | Yes | NCBI |
| *Mus musculus (DUOX1)* | CAM16331.1 | A2AQ92 | No | NCBI |
| *Mus musculus (DUOX2)* | CAM16338.1 | A2AQ99 | No | NCBI |
| *Rattus norvegicus (DUOX1)* | AAN33120.1 | Q8CIY2 | Yes | NCBI |
| *Rattus norvegicus (DUOX2)* | | Q9ES45.2 | Yes | NCBI |
| *Bos taurus (DUOX1)* | XP_002690987.1 | E1BMK1 | No | NCBI |
| *Bos taurus (DUOX2)* | XP_002690988.1 | | No | NCBI |
| *Sus scrofa (DUOX1)* | | Q8HZK3.1 | Yes | NCBI |
| *Sus scrofa (DUOX2)* | | Q8HZK2.2 | Yes | NCBI |
| *Oryctolagus cuniculus (DUOX1)* | XP_002717948.1 | | No | NCBI |
| *Oryctolagus cuniculus (DUOX2)* | XP_002717951.1 | | No | NCBI |
| *Canis lupus familiaris (DUOX1)* | | Q9MZF4.1 | Yes | NCBI |
| *Equus caballus (DUOX1)* | XP_001502729.1 | | No | NCBI |
| *Equus caballus (DUOX2)* | XP_001500280.2 | | No | NCBI |

**NOX5 orthologs**

| | | | | |
|---|---|---|---|---|
| *Magnaporthe grisea (NOXC)* | EAA57330.1 | | No | NCBI |
| *Gibberella zeae (NOXC)* | XP_391371.1 | | No | NCBI |
| *Dictyostelium discoideum (NOX C)* | | Q54F44.1 | Yes | NCBI |
| *Polysphondylium pallidum (NOX C)* | EFA86586.1 | D3AWB3 | No | NCBI |
| *Dictyostelium purpureum (NOX  C)* | EGC28364.1 | | No | NCBI |
| *Chondrus crispus (NOXD)* | AAZ73480.1 | Q2FA46 | No | NCBI |
| *Porphyra yezoensis (NOXD)* | ABA18724 | Q2F9N3 | No | NCBI |
| *Arabidopsis thaliana (RBOHD)* | | Q9FIJ0.1 | Yes | NCBI |
| *Oryza sativa (RbohB)* | | Q6J2K5.1 | Yes | NCBI |
| *Nicotiana tabacum(RbohD)* | ABN58915.1 | Q8LRN5 | No | NCBI |
| *Trichoplax adhaerens(NOX5)* | EDV22281.1 | B3S4X0 | No | NCBI |
| *Lottia gigantea (NOX5 a)* | 159226 | | No | JGI |
| *Lottia gigantea (NOX5 b)* | 179958 | | No | JGI |
| *Arctica islandica (NOX5 Fragment)* | *Ai* NOX5 | | No | ICMB |
| *Laternula elliptica (NOX5 Fragment)* | *Le2* NOX5 | | No | ICMB |
| *Mytilus edulis (NOX5 Fragment)* | *Me* NOX5 | | No | ICMB |
| *Capitella teleta (NOX5 a)* | 147619 | | No | JGI |
| *Capitella teleta (NOX5 b)* | 147607 | | No | JGI |
| *Drosophila melanogaster (NOX5)* | ABV53818.1 | A8DWJ8 | No | NCBI |
| *Camponotus floridanus(NOX5)* | EFN67259.1 | E2AH28 | No | NCBI |
| *Harpegnathos saltator (NOX5)* | EFN89636.1 | E2B3W7 | No | NCBI |
| *Apis mellifera (NOX5)* | XP_391999.3 | | No | NCBI |
| *Strongylocentrotus purpuratus (NOX5 a)* | XP_001177608.1 | | No | NCBI |
| *Strongylocentrotus purpuratus (NOX5 b)* | XP_786060.2 | | No | NCBI |
| *Saccoglossus kowalevskii (NOX5 a)* | XP_002740169.1 | | No | NCBI |
| *Saccoglossus kowalevskii (NOX5 b)* | XP_002731084.1 | | No | NCBI |
| *Branchiostoma floridae (NOX5 Fragments)* | XP_002611039.1 | C3XXZ5 | No | NCBI |
| *Danio rerio (NOX5)* | XP_001921894.1 | | No | NCBI |
| *Takifugu rubripes (NOX5)* | FAA00346.1 | A7E3L7 | No | NCBI |
| *Tetraodon nigroviridis (NOX5 Fragment)* | GSTENP00000868001 | Q4TGY3 | No | Ensembl |
| *Xenopus tropicalis (NOX5)* | XP_002933005.1 | | No | NCBI |
| *Anolis carolinensis (NOX5)* | XP_003225935.1 | | No | NCBI |
| *Gallus gallus (NOX2)* | NP_001093755.1 | A7E3L6 | No | NCBI |
| *Meleagris gallopavo (NOX5)* | XP_003209648.1 | | No | NCBI |
| *Ornithorhynchus anatinus (NOX5)* | XP_001512259.1 | | No | NCBI |
| *Monodelphis domestica (NOX5)* | FAA00371.1 | A7E3P2 | No | NCBI |
| *Homo sapiens (NOX5)* | NP_078781.3 | Q96PH1-1 | Yes | NCBI |
| *Bos taurus (NOX5)* | NP_001094607.1 | A7E3L4 | No | NCBI |
| *Sus scrofa (NOX5)* | XP_001925437 | | No | NCBI |
| *Oryctolagus cuniculus (NOX5)* | XP_002722428.1 | | No | NCBI |
| *Canis lupus familiaris (NOX5)* | NP_001096688.1 | A7E3L5 | No | NCBI |
| *Equus caballus (NOX5)* | XP_001495715.2 | | No | NCBI |

**NOX2 orthologs**

| | | | | |
|---|---|---|---|---|
| *Dictyostelium discoideum(NOX A)* | | Q9XYS3.1 | Yes | NCBI |
| *Dictyostelium discoideum (NOX B)* | | Q86GL4.1 | Yes | NCBI |
| *Dictyostelium purpureum (NOX A)* | EGC36287.1 | | No | NCBI |
| *Dictyostelium purpureum (NOX B)* | EGC30582.1 | | No | NCBI |
| *Arabidopsis thaliana (RbohD)* | | Q9FIJ0.1 | Yes | NCBI |
| *Oryza sativa (RbohB)* | | Q6J2K5.1 | Yes | NCBI |
| *Nicotiana tabacum(RbohD)* | ABN58915.1 | Q8LRN5 | No | NCBI |
| *Nematostella vectensis (NOX2a)* | 168974 | | No | JGI |
| *Nematostella vectensis (NOX2b)* | 113989 | | No | JGI |
| *Trichoplax adhaerens (NOX2)* | 25818 | | No | JGI |
| *Lottia gigantea (NOX2)* | 175333 | | No | JGI |
| *Arctica islandica (NOX2 Fragment)* | *Ai* NOX2 | | No | ICMB |
| *Laternula elliptica (NOX2 Fragment)* | *Le* NOX2 | | No | ICMB |
| *Mytilus edulis (NOX2)* | *Me* NOX2 | | No | ICMB |
| *Euprymna scolopes (NOX2)* | *Es* NOX2 | | No | ICMB |
| *Capitella teleta (NOX2)* | 223007 | | No | JGI |
| *Helobdella robusta (NOX2)* | 66368 | | No | JGI |
| *Strongylocentrotus purpuratus (NOX2a)* | 765886 und 757329 | | No | DB GET, KEGG |
| *Strongylocentrotus purpuratus (NOX2b)* | 594258 | | No | DB GET, KEGG |
| *Strongylocentrotus purpuratus (NOX2c)* | 751832 | Q2TPT8 | No | DB GET, KEGG |
| *Branchiostoma floridae (NOX2)* | EEN68240.1 | C3XUP1 | No | NCBI |
| *Ciona intestinalis (NOX2)* | 100169685 | A7E3L0 | No | DB GET, KEGG |
| *Ciona savignyi (NOX2)* | SINCSAVP00000004515 | | No | Ensembl |
| *Oikopleura dioica (NOX2 a)* | CBY17896.1 | E4X2P3 | No | NCBI |
| *Oikopleura dioica (NOX2 b)* | CBY17894.1 | E4X2P1 | No | NCBI |
| *Danio rerio (NOX2 a)* | NP_956708.1 | Q7T2A7 | No | NCBI |
| *Danio rerio (NOX2 b)* | XP_003199995.1 | | No | NCBI |
| *Danio rerio (NOX2 c)* | XP_003199994.1 | | No | NCBI |
| *Salmo salar (NOX2)* | NP_001138891.1 | B8YQA0 | No | NCBI |
| *Takifugu rubripes(NOX2)* | NP_001027904.1 | Q7T1Q1 | No | NCBI |
| *Tetraodon nigroviridis(NOX2)* | FAA00338.1 | Q4SEQ8 | No | NCBI |
| *Xenopus tropicalis(NOX2)* | NP_001025689.1 | Q505H9 | No | NCBI |
| *Xenopus laevis (NOX2)* | NP_001085924.1 | Q6GNG7 | No | NCBI |
| *Anolis carolinensis(NOX2)* | XP_003218977.1 | | No | NCBI |
| *Gallus gallus (NOX2)* | NP_001093756.1 | A7E3K8 | No | NCBI |
| *Meleagris gallopavo (NOX2)* | XP_003203060.1 | | No | NCBI |
| *Taeniopygia guttata(NOX2)* | XP_002193334.1 | | No | NCBI |
| *Ornithorhynchus anatinus (NOX2)* | XP_001514075.1 | | No | NCBI |
| *Monodelphis domestica (NOX2 a)* | XP_001367055.1 | | No | NCBI |
| *Monodelphis domestica (NOX2 b)* | XP_001381338.1 | | No | NCBI |
| *Homo sapiens (NOX2)* | | P04839.2 | Yes | NCBI |
| *Mus musculus (NOX2)* | NP_031833.3 | Q61093 | Yes | NCBI |
| *Rattus norvegicus (NOX2)* | NP_076455.1 | Q9ER28 | No | NCBI |
| *Bos taurus (NOX2)* | NP_776460.1 | O46522 | Yes | NCBI |
| *Sus scrofa (NOX2)* | NP_999208.1 | P52649 | Yes | NCBI |

| | | | | |
|---|---|---|---|---|
| *Oryctolagus cuniculus (NOX2)* | NP_001075569.1 | Q95MN3 | No | NCBI |
| *Canis lupus familiaris (NOX2)* | NP_001093761.1 | A7E3K7 | No | NCBI |
| *Equus caballus (NOX2)* | ENSECAP00000015910 | | No | Ensembl |

Public databases:
> http://www.ncbi.nlm.nih.gov/
> http://genome.jgi.doe.gov/
> http://www.ensembl.org/index.html
> http://www.genome.jp/dbget/

For phylip alignment files of DUOX, NOX5 and NOX2 see CD:

"**File_7_DUOX alignment.phy**"

"**File_8_NOX5 alignment.phy**"

"**File_9_NOX2 alignment.phy**"

## 9.6 Identified IL-17 sequences

The nucleotide and amino acid sequence of each contig as well as the corresponding domain structure of the SMART domain architecture search can be found in detail on the CD under "**File_10_IL-17 sequences and domains.pdf**".

## 9.7 TLR and LPS Paper

For a draft of the "Materials and Methods" as well as the "Results" section of the currently in progress paper: "Characterization and expression analysis of Toll-like receptors and constituents of the TLR pathway in *Mytilus edulis*" see CD "**File_11_TLR Paper DRAFT.pdf**"

## 10. LIST OF FIGURES

## 11. LIST OF TABLES

## 12. PUBLICATIONS

Parts of this thesis are currently being prepared for publication or have already been presented at scientific conferences and symposia.

**Talks:**

Saphörster, J., Kraemer, L., Leippe, M., Schreiber, S., Rosenstiel, P. and Philipp, E.E.R. (2010): "The immune system in the blue mussel *Mytilus edulis*: A model for innate immunity", *North German Immunologists (NGI) Meeting*, Borstel, Germany

Saphörster, J., Kraemer, L., Leippe, M., Schreiber, S., Rosenstiel, P. and Philipp, E.E.R. (2010): "Molecular mechanisms of cellular immune responses in marine invertebrates", *First Student Meeting for Biotechnology and Medicine,* NORGENTA, Kiel, Germany

**Poster:**

Saphörster, J., Kraemer, L., Leippe, M., Schreiber, S., Rosenstiel, P. and Philipp, E.E.R. (2010): "NADPH oxidases in *Mytilus edulis* and their role in ROS generation and innate immune responses", *North Cluster PhD Conference*, Hamburg, Germany

Saphörster, J., Kraemer, L., Leippe, M., Schreiber, S., Rosenstiel, P. and Philipp, E.E.R. (2010): "Insights into innate immunity from marine invertebrates: Molecular and functional analysis of NOX-family NADPH oxidases in the blue mussel *Mytilus edulis"*, *German Zoologists (DZG) Annual Main Meeting*, Hamburg, Germany

Saphörster, J., Kraemer, L., Leippe, M., Schreiber, S., Rosenstiel, P. and Philipp, E.E.R. (2010): "Insights into innate immunity from marine invertebrates: Molecular and functional analysis of NOX-family NADPH oxidases in the blue mussel *Mytilus edulis"*, *Annual Main Meeting of the Society for Experimental Biology (SEB)*, Prag, Czech Republic

**Awards:**

Best presentation, First Student Meeting for Biotechnology and Medicine, 2010, NORGENTA, Kiel, Germany

## 13. CURRICULUM VITAE

## PERSONAL DATA

**Dipl.-Biol. Julia Saphörster**

born 1st December, 1983
in Münster, Germany
German

## RESEARCH EXPERIENCE

| | | |
|---|---|---|
| Since Jul. 2009 | **ICMB – Institute for Clinical Molecular Biology, CAU-Kiel**<br>*Supervisors: E.Philipp, M. Leippe, P. Rosenstiel (Head: S. Schreiber)*<br>*Cluster of Excellence "The future ocean" B2 - marine medicine*<br>*Cluster of Excellence "Inflammation at interfaces"*<br><br>PhD thesis: "Molecular mechanisms of cellular immune responses in marine invertebrates" | Kiel<br>Germany |
| Jan.-Jun. 2009 | **IFM-GEOMAR – Leibniz Institute of Marine Sciences**<br>*Cluster of Excellence "The future ocean" JRG A1 - ocean acidification*<br><br>Research assistant | Kiel,<br>Germany |
| Jan -Dec. 2008 | **IFM-GEOMAR – Leibniz Institute of Marine Sciences**<br>*Cluster of Excellence "The future ocean" JRG A1 - ocean acidification*<br>*Supervisor: F. Melzner*<br><br>Diplom thesis: "Physiology of *M. edulis* in relation to ocean acidification" | Kiel<br>Germany |
| Jan.-Mar. 2007 | **Alfred-Wegener-Institute for Polar- and Marine Research**<br>*Marine Ecophysiology (Head: H.O. Pörtner)*<br><br>Student assistant | Bremerhaven<br>Germany |
| Jul. –Oct. 2006 | **Alfred-Wegener-Institute for Polar- and Marine Research**<br>*Marine Ecophysiology, Supervisor: M. Schröer (Head: H.O. Pörtner)*<br><br>Semester thesis: "Temperature-dependent burrowing acitivity of *A. marina* and correlated pressure oscillations in the extracellular fluid" | Bremerhaven<br>Germany |
| Feb.-Mar. 2006 | **German Helmholtz Research Center for Environmental Health**<br>*Institute of Groundwater Ecology, Supervisor: M. Jahn (Head: R. Meckenstock)*<br><br>Internship | Munic<br>Germany |

## EDUCATION

| | | |
|---|---|---|
| 2003 - 2008 | University of Rostock<br>*Biology, Degree: Diplom (German equivalent to Master of Science)* | Rostock<br>Germany |
| 2000 - 2001 | Montgomery High School<br>*Exchange student* | Texas<br>USA |
| 1994 - 2003 | Joseph-Haydn-Grammar School<br>*Abitur (German equivalent to A-levels)* | Senden<br>Germany |

## 14. ACKNOWLEDGMENTS/DANKSAGUNG

## 15. EIDESSTATTLICHE ERKLÄRUNG

Hiermit versichere ich, Julia Saphörster, an Eides statt, dass ich die vorliegende Dissertation mit dem Titel „Molecular mechanisms of cellular immune responses in marine invertebrates" (Molekulare Mechanismen der zellulären Immunantwort in marinen Evertebraten) selbständig und unter Einhaltung der Regeln guter wissenschaftlicher Praxis der Deutschen Forschungsgemeinschaft verfasst habe.

Ich habe dabei keine anderen als die angegebenen Hilfsmittel und Quellen verwendet und keine weitere Hilfe, außer der Beratung durch meine wissenschaftlichen Betreuer Dr. Eva Philipp, Prof. Dr. Matthias Leippe und Prof. Dr. Philip Rosenstiel, in Anspruch genommen.

Die Arbeit wurde bis jetzt weder vollständig noch in Teilen einer anderen Stelle im Rahmen eines Prüfungsverfahren vorgelegt. Zudem erkläre ich, keine früheren Promotionsversuche unternommen zu haben.

Kiel, den 17.04.2013

Julia Saphörster